SCHOOL OF CIVIL ENGINEERING

JOINT HIGHWAY RESEARCH PROJECT

JHRP-12-75

LIMITING STRAIN AS A FAILURE CRITERION FOR BITUMINOUS MIXTURES

Raymond D. Pavlovich

PURDUE UNIVERSITY
INDIANA STATE HIGHWAY COMMISSION

75-12

Final Report

LIMITING STRAIN AS A FAILURE CRITERION FOR BITUMINOUS MIXTURES

TO: J. F. McLaughlin, Director
Joint Highway Research Project

June 4, 1975

Project: C-36-6Y

FROM: H. L. Michael, Associate Director
Joint Highway Research Project

File: 2-4-25

The attached Final Report titled "Limiting Strain as a Failure Criterion for Bituminous Mixtures" is for Phase II of the HPR Part II Research Study titled "Cracking in Bituminous Mixtures". The author is the principal investigator on this Phase of the Study, Raymond D. Pavlovich, with Professor W. H. Goetz of our staff as director.

The most significant parameter affecting strain is temperature with strain rate and gradation having some effects. This research also included development of a precision temperature control device and an extensometer to measure specimen deformations. Acoustic emission experiments were also included in the study and the results indicate usefulness of this tool in detecting micro-cracking long before visual observation indicates its occurrence.

This Final Report is submitted to the sponsoring agencies for acceptance as fulfillment of the objectives of Phase II and the total Study.

Respectfully submitted,

Harold L. Michael

Harold L. Michael
Associate Director

HLM:mf

cc: W. L. Dolch
R. L. Eskew
G. D. Gibson
W. H. Goetz
M. J. Gutzwiller
G. K. Hallock
M. L. Hayes
C. W. Lovell
G. W. Marks
R. F. Marsh
R. D. Miles
G. T. Satterly
C. F. Scholer
M. B. Scott
K. C. Sinha
H. R. J. Walsh
L. E. Wood
E. J. Yoder
S. R. Yoder

TECHNICAL REPORT STANDARD TITLE PAGE

1. Report No.	2. Government Accession No.	3. Recipient's Catalog No.

4. Title and Subtitle

LIMITING STRAIN AS A FAILURE CRITERION FOR BITUMINOUS MIXTURES

5. Report Date

June 1975

6. Performing Organization Code

C-36-6Y

7. Author(s)

Raymond D. Pavlovich

8. Performing Organization Report No.

JHRP-12-75

9. Performing Organization Name and Address

Joint Highway Research Project
Civil Engineering Building, Purdue University
West Lafayette, Indiana 47907

10. Work Unit No.

11. Contract or Grant No.

HPR-1(12) Part II

12. Sponsoring Agency Name and Address

Indiana State Highway Commission
100 North Senate Avenue
Indianapolis, Indiana 46204

13. Type of Report and Period Covered

Final Report

14. Sponsoring Agency Code

CA 371

15. Supplementary Notes

Conducted in cooperation with the U.S. Dept. of Transportation, Federal Highway Administration, Research Study titled "Cracking in Bituminous Mixtures".

16. Abstract

Experiments were conducted to measure strain at failure (limiting strain) for bituminous concretes. A secondary study was included to evaluate the possibilities of using acoustic emission techniques to detect and monitor cracking in portland cement and bituminous concretes.

Parameters for the limiting strain experiment included asphalt type, aggregate gradation, temperature, and strain rate analysis of variance was used to evaluate the effect of each of the parameters and regression equations are presented that relate significant independent variables to limiting strain.

The most significant parameter affecting limiting strain is temperature; strain rate and gradation do show some effects, but these are minor when compared to temperature. There was no measurable effect, in this experiment, due to asphalt type within a range which included a high and low viscosity material in each of three penetration grades (60-70, 85-100, 120-150).

Acoustic emission experiments showed that this technique is effective for detecting micro-cracking long before visual observation indicates the occurrence. Emission counts and count rate increases dramatically before visual manifestations occur for portland cement concrete and for bituminous concretes below room temperature. The Kaiser or memory effect for loads in excess of a proof load is demonstrated for both materials.

17. Key Words

Bituminous Concrete; Limiting Strain; Acoustic Emissions; Micro-crack Detection

18. Distribution Statement

19. Security Classif. (of this report)	20. Security Classif. (of this page)	21. No. of Pages	22. Price
Unclassified	Unclassified	340	

Form DOT F 1700.7 (8-69)

Final Report

LIMITING STRAIN AS A FAILURE CRITERION FOR BITUMINOUS MIXTURES

by

Raymond D. Pavlovich
Graduate Instructor in Research

Joint Highway Research Project

Project No.: C-36-6Y

File No.: 2-4-25

Prepared as Part of an Investigation

Conducted by

Joint Highway Research Project
Engineering Experiment Station
Purdue University

in cooperation with the

Indiana State Highway Commission

and the

U.S. Department of Transportation
Federal Highway Administration

Purdue University
West Lafayette, Indiana
June 4, 1975

ACKNOWLEDGMENTS

The author expresses his sincere gratitude to his major professor, Professor W. H. Goetz, for the advice and constructive criticism offered through the course of this study.

The interest and advice of the other members of the committee, Dr. M. E. Harr, Dr. E. C. Ting and especially the time and effort of Dr. V. L. Anderson are gratefully appreciated.

Particular thanks are extended to Nick Coburn, for unselfishly taking time, effort and patience to design and construct electronic components, supply equipment, and repair the many electrical malfunctions that occurred during the course of this study; thanks are also due Fred Glossic and Robert Williams for expediting the numerous machine shop items that always seemed necessary.

Additional thanks are extended to Mr. James Evans of AMOCO Oil Company for providing asphalts used for the project and to Mr. James Wood of R. D. P. and Associates for the loan of acoustic emission equipment.

Sincere thanks are extended to the authorities of the Joint Highway Research Project, Engineering Experiment

Station, Purdue University in cooperation with the Indiana State Highway Commission, Federal Highway Administration, U. S. Department of Transportation for making available the funds needed for this research.

Finally, special thanks also go to the author's wife and family whose patience and understanding greatly aided the successful completion of this investigation.

TABLE OF CONTENTS

Page

LIST OF TABLES

LIST OF FIGURES

LIST OF SYMBOLS

S	Stiffness
S_{bit}	Bitumen stiffness
S_{mix}	Mixture stiffness
$\sigma(t,T)$	Stress at loading time t and temperature T
σ_f	Stress at failure
$\varepsilon(t,T)$	Strain at loading time t and temperature T
ε_f	Limiting strain (strain at failure)
$\bar{\varepsilon}$	Average strain
$\dot{\varepsilon}$	Strain rate
$\bar{\dot{\varepsilon}}$	Average strain rate
C_v	Volume concentration of aggregate
Σ_{10}	Acoustic emission counts at a stress ratio of 10%
$\dot{c}$	Acoustic emission count rate
ϕ	Aggregate sphericity
μ	Kinematic viscosity in centistokes
ν	Absolute viscosity in poises
A	Volume coefficient of expansion
ΔV	Volume change
V	Original volume
V_i	Volume at temperature i
ΔT	Temperature change
r	Coefficient of correlation

MII	Microstrain in millionths of an inch per inch
BTUH	British thermal units per hour
kip	One thousand pounds
G_{mb}	Bulk specific gravity
L	Lower statistical limit
U	Upper statistical limit
T'_F	Shifted temperature
T_F	Actual test temperature
β_i	Regression coefficient
B_i	Estimated regression coefficient

ABSTRACT

Pavlovich, Raymond Doran. Ph.D., Purdue University, August 1975. Limiting Strain as a Failure Criterion for Bituminous Mixtures. Major Professor: Prof. W. H. Goetz.

Experiments were conducted to measure strain at failure (limiting strain) for bituminous concrete in direct tension and to evaluate the possibilities of using acoustic emission techniques to detect cracking in portland cement and bituminous concretes.

Parameters for the limiting strain experiment included type of asphalt, aggregate gradation, temperature, and strain rate. Regression equations are presented that relate significant independent variables to limiting strain.

The most significant parameter affecting limiting strain is temperature; strain rate and gradation do show some effects, but these are minor when compared to temperature. There was no measurable effect, in this experiment, due to asphalt type within a range which included a high and low viscosity material in each of three penetration grades, 60-70, 85-100 and 120-150.

Included as a part of the experiment was the development of a precision temperature control device and an extensometer to measure specimen deformations in direct tension that eliminates testing system compliance errors.

Acoustic emission experiments showed that this technique is very effective in detecting micro-cracking long before visual observation would indicate the occurrence; the technique is regarded as quasi-quantitative but can provide the researcher with a tool that has hitherto not been exploited. These experiments showed that acoustic emission counts and hence count rate increase substantially when fracture occurs. It is demonstrated that the Kaiser or memory effect is quite pronounced in portland cement concrete and in bituminous concrete when they are below room temperature. Signals could not be detected in bituminous mixtures at temperatures above room temperature, possible reasons for this are postulated to be that the viscous nature of bitumen at these temperatures attenuates elastic waves to an energy level below that necessary to activate transducers or that the failure mechanism is viscous flow and cracking is not taking place.

INTRODUCTION

Cracking of bituminous mixtures in service has long been recognized as a source of decreased pavement serviceability and increased maintenance effort and cost. Cracking may produce only minor functional failure as manifested by user discomfort, or cracking can be the mechanism that allows water to weaken moisture susceptible layers in the pavement system. The importance of this problem is demonstrated by studies in Canada [1, 2, 3] and the United States [4, 5, 6]. Further testimony to the seriousness of the problem is shown by presentations of symposiums to attempt to define the problem [7, 8] and construction of test roads to attempt to observe and correlate factors that may be involved [9].

Failure by cracking will occur when strains within the bituminous concrete exceed some limiting value for simple loading or when fatigue capacity of the material is exceeded [6]. Considerable information is available that enables prediction of stress fields within the system from imposed external loads as applied either by traffic or environmental conditions. Using stiffness values generated by Van der Poel [10, 11], strain response to imposed loads can be calculated for the bituminous mixture by means analogous to the familiar

elastic analysis, i.e.,

$$s = \frac{\sigma(t,T)}{\varepsilon(t,T)} = \frac{\text{tensile stress}}{\text{tensile strain}}$$

where s = stiffness modulus and σ and ε are time and temperature dependent.

This stiffness modulus will depend on loading procedure (quasi-static or dynamic), time of loading or frequency, and temperature.

Thermally induced stresses have been considered and partially evaluated [6, 12] and deformations under load have been calculated [13, 14, 15]. The methods previously mentioned that predict stress or deformation in service provide the technologist with information that can be refined and used for developing more workable and rational design procedures. The next step in the development of such a design procedure is to establish failure criteria that will allow reasonable safety factors and limits to be placed on in-service strains and thus prevent, or at least mitigate, the problem of premature cracking and related failures of flexible pavements.

The purpose of this study was to establish failure criteria (limiting strain) for several bituminous mixtures when subjected to direct tension. Statistical inference space included ordinary conditions of loading times (strain rates) within the limitations of available test equipment,

temperatures, and common mix variables of asphalt type and mixture gradation. A secondary purpose of the project was to evaluate acoustic emission techniques and their ability to detect and monitor crack initiation and propagation.

LITERATURE REVIEW

Consideration of cracking of bituminous mixtures in pavements occurs in the literature since about 1930. Ledus [18] noted that overheating of asphalts at the plant was probably the cause of much cracking in pavements. Later in the 1930's other publications began to appear that considered low temperature effects. Rader [19] and Brown and Steinbaugh [20] and others concluded that moduli of elasticity and rupture at low temperature should be considered in the design process. It was also noted that other properties such as loss of penetration and durability are probably causative factors in cracking. Abson [21] reported that mixtures using softer asphalts appeared to exhibit less cracking than did those using harder asphalts.

Laboratory tests of asphalts to determine deformation as related to asphalt types was begun in 1950 by Hughes and Faris [22]. An asphalt specimen in the form of a simple beam was failed in flexure and it was concluded that, for fast rates of loading, asphalt source, asphalt penetration and temperature (below 32°F) have little effect on deformation or strain at failure. Slow rate of loading tests, however, showed that source, penetration and temperature have an effect. Van der Poel's work [10, 11] generally

supported these findings but it was not until later that mixtures were considered.

Work continued in this area but was primarily concerned with the effects of environmental factors such as air, moisture and temperature; Vallerga [23] stated concern for relating properties of bituminous mixtures to performance.

Additional concern for cracking as a direct cause of failure began to appear after the first sections of the Interstate System were in service and evaluation of high capacity systems was made. Chipperfield and Welch [24] correlated field performance and properties of bitumen and concluded that hardening with age has an influence on performance. Lamb, Pavlovich and Scott [4] considered lateral cracking to be the mechanism that allowed surface water to enter and weaken a moisture susceptible subgrade. It was further postulated that temperature and not applied traffic was the source of the causative factor that initiated cracking.

In an AAPT Symposium, Marker [7] proposed several qualitative factors that could induce cracking. Among those submitted were: changes in moisture and consequent shrinkage of subgrade soils accompanied by reflection cracking of the bituminous surface; temperature changes that affect subgrade shrinkage; shrinkage of base or subbase courses and the pavement itself as well as shrinkage due to selective absorption of aggregate. Anderson, Shields and

Bacyszyn [2] postulated that temperature gradients are the cause of non-load associated cracking. In a discussion for the symposium, Hills and O'Brien provided theoretical equations to predict the temperature at which cracking will occur for a bituminous mixture of given tensile strength and bitumen stiffness modulus. Additional work on thermal shrinkage cracking has been presented by Haas [6] whereby laboratory tests have been correlated with field observations. This work concluded that production methods as well as undetermined subgrade factors are causes of cracking.

The literature is replete with suggestions that the cause of lateral cracking may be a single load, non-load (temperature) input, or a combination. Methods have been developed that provide stress from which strain can be calculated. Ashton and Moavenzadeh [13] analyzed displacements in a three-layered viscoelastic system for a uniform static circular load. Perloff and Moavenzadeh [14] provided predictive equations for deflections of a viscoelastic medium due to a moving load. Barksdale and Leonards [15] developed a viscoelastic theory that will predict tensile strains in a pavement system due to a stationary repeated load. These studies provide methods or at least first approximations that will predict stress fields within the system due to traffic loads.

Temperature gradients and thermally induced stress have been considered by Haas [6]. Tuckett, Jones and

Littlefield [25] have shown the effect of film thickness and aggregate type on thermally induced stress.

Fatigue aspects of bituminous mixtures have been extensively researched by Saal and Pell [26] and Pell [27]. Pell proposed a generalized equation for the number of repetitions or loading cycles for failure. The relationship is:

$$N = K \frac{\alpha (B_V)^n}{\varepsilon_m}$$

where N = number of cycles of applied load to cause crack initiation,

ε_m = amplitude of applied tensile strain in the mix,

B_V = proportion of bitumen present in the total volume of mix,

K and n = factors which are constants for a particular grade of bitumen, and

α = factor depending on amount of filler or voids present in the mix, or both.

Pell postulated that the probable relationship between strain in the mix (ε_m) and bitumen strain (ε_B) is

$$\varepsilon_B = \frac{\varepsilon_m}{\alpha\ B_V}.$$

Therefore it is possible, by applying a limiting strain parameter (ε_L), to determine fatigue life of a pavement.

Mixture stiffness as a function of bitumen stiffness has been investigated by Heukelom and Klomp [30] and Heukelom [31]. A set of curves, based on a large series

of tests, have been prepared which relate asphalt stiffness as determined from Van der Poel's nomograph to mixture stiffness. These curves are provided for various volume concentrations of aggregates (C_v) and relate stiffness by:

$$\frac{S_{mix}}{S_{bit}} = \left[1 + \frac{2.5}{n} \frac{C_v}{(1 - C_v)}\right]^n$$

where S_{mix} = mixture stiffness,

S_{bit} = bitumen stiffness from Van der Poel's nomograph,

C_v = volume concentration of aggregate

$= \frac{\text{volume of aggregate}}{\text{volume of (aggregate + asphalt)}}$, and

$$n = 0.83 \left[\log_{10} \left(\frac{4\ (10)^5}{S_{bit}}\right)\right]$$

This relationship was developed for well-compacted mixtures (approximately 3% air voids and C_v values between 0.7 and 0.9). Van Draat and Sommer [32] provided a correction for mixtures with air voids other than 3%.

Thus, the work done to date provides a basis on which to predict mixture strains that are imposed by the several types of loads; i.e., traffic, thermal gradients and fatigue situations. However, failure criteria have not been fully considered and the effects of mixture and loading variables have not been evaluated.

ACOUSTIC EMISSION EVALUATION

The objective of this phase of the study was to evaluate the feasibility of using acoustic emission techniques to detect cracking in non-ferrous materials such as portland cement and bituminous concrete.

It has been shown by Schofield [48] and others [16, 49] that one form of measurable energy associated with a plastic deformation process is the emission of acoustic signals or shock waves. Considerable work in the field of metals substantiates the validity of the concept [16, 50] and equipment is available from several suppliers that will monitor these signals and electronically amplify and record them. However, with one exception [51] the writer is not aware of any attempts to use the equipment in studies on portland cement or bituminous concretes.

Principles of the technique are quite simple in that energy released by breaking molecular bonds creates a wave in the media under consideration. This wave is detected by a lead-zirconate-titanate (PZT) transducer that exhibits a piezoelectric effect in that deformation of the crystal causes the emission of an electrical impulse. The impulse (the transducer conversion of mechanical to electrical energy) is conditioned and amplified and then fed to a pair

of counters that record the rate of emissions (counts per time unit) and cumulative or total counts. The plastic limit or yield point is accompanied by a peaking of count rate followed by immediate decay. Failure by fracture of a crystalline material is indicated by a sharp increase in total or cumulative counts.

The so-called Kaiser effect of fracture or progressive failure of a material can be monitored using acoustic emission techniques. This principle states that if a load, less than the ultimate capacity of the material but great enough to cause some micro-cracking, is applied and subsequently released, other loads less than the applied proof load will not cause additional micro fracture and existing micro cracks will not advance nor propagate. This says that if counts are recorded during a proof test, no further emissions will occur until loads (or cumulative fatigue damage) are applied that exceed the original proof test. If counts resulting from proof loading are recorded and later testing shows loads in excess of proof are required to produce emissions, it can be concluded that loads in excess of proof (overload or fatigue damage) have not previously been applied. If loads much less than the original proof load cause emissions it can be concluded that healing of the original micro fractures has occurred or that something has occurred in the structural system to cause a realignment of load distribution within the structure.

For this project, specimens of portland cement concrete in compression and bituminous concrete in tension were studied.

I. Portland Cement Concrete

Portland cement concrete specimens consisted of river sand and gravel obtained from Western Indiana Aggregates, Inc. of Lafayette, Indiana. Cement was a type III (high early strength). Concrete for three inch diameter by six inch high cylinders was mixed and cast in steel molds according to ASTM C 192. Fresh molds were covered and stored in the laboratory for twenty-four hours. The molds were then removed and the cylinders were stored for six days in a moist room. Capping was done on the day of the compression test.

Compression testing was performed by a MTS closed-loop electrohydraulic system. The Dunegan Research Corp. acoustic emission equipment consisted of the following pieces: S140B transducer, S/D-60P preamplifier, PP-2 power module preamplifier, N5-1 totalizer, BC-677 audio monitor, CP-10 reset clock and a CR-11 ramp generator. This equipment is compatible with and was fitted into the Purdue MTS Console. Emission counts were recorded on the x-y recorder of the MTS. The y axis of the recorder was used for acoustic emissions (cumulative) and the x axis of the recorder was hard-wired to the stroke output of the MTS. Since stroke and load output appear on a two-channel strip recorder of

the MTS, and the equipment was operated in stroke control, load vs cumulative counts could be related using the two recorder outputs.

An experiment was designed to produce controlled variability of strengths. Each of the cylinders in the experiment was compression loaded to failure with cumulative counts being recorded and count rate calculated from cumulative counts and the time base as shown on the MTS strip chart for stroke and load.

Three levels of water cement ratio (0.40, 0.45 and 0.50), and three levels of coarse aggregate percentage (0.42, 0.52 and 0.62), were investigated with three replications for each combination of water cement ratio and coarse aggregate percentage for a total of 27 specimens. Cylinder preparation and testing were completely randomized by affixing serial numbers to each proposed cylinder and selecting the test sequence from a table of random numbers.

Mixes were designed according to ACI 211-1-70 with the normal mix consisting of 62 percent coarse aggregate and a water cement ratio of 0.40. Other percentages of coarse aggregate and water cement ratios were arbitrarily selected to provide for orthogonal polynomials if later desired.

Strengths and a two-way classification ANOVA are shown in Tables 1 and 2.

Figure 1 shows a typical curve for acoustic emission counts versus stress ratio where stress ratio is the stress

TABLE 1

Concrete Cylinder Strengths

7 Day Strengths in psi

Water-Cement Ratio	Per Cent Coarse Aggregate 42		52		62	
0.40	1	2650	10	2020	19	2910
	2	2700	11	2530	20	3010
	3	2600	12	3350	21	3060
0.45	4	2500	13	2110	22	2330
	5	1420	14	1670	23	1630
	6	2250	15	2240	24	2290
0.50	7	1700	16	1400	25	1780
	8	1510	17	1300	26	1920
	9	1540	18	1640	27	722

q test for homogeneity (Foster and Burr [51]):

q = 0.234

q (critical) (2, 9) (0.99) = 0.371

q (critical) (2, 9) (0.999) = 0.481

TABLE 2

ANOVA, Cylinder Strengths

ANOVA (strengths reduced to ksi)

Source	SS	df	MS	F	F(crit) (0.05)
Water-cement	7.16	2	3.58	21.6	3.55
% Coarse Agg.	0.11	2	0.05	0.32	3.55
Interaction	0.18	4	0.05	0.27	2.93
Subtotal	7.45	8			
Within Treatment	2.99	18	0.17		
Total	10.44	26			

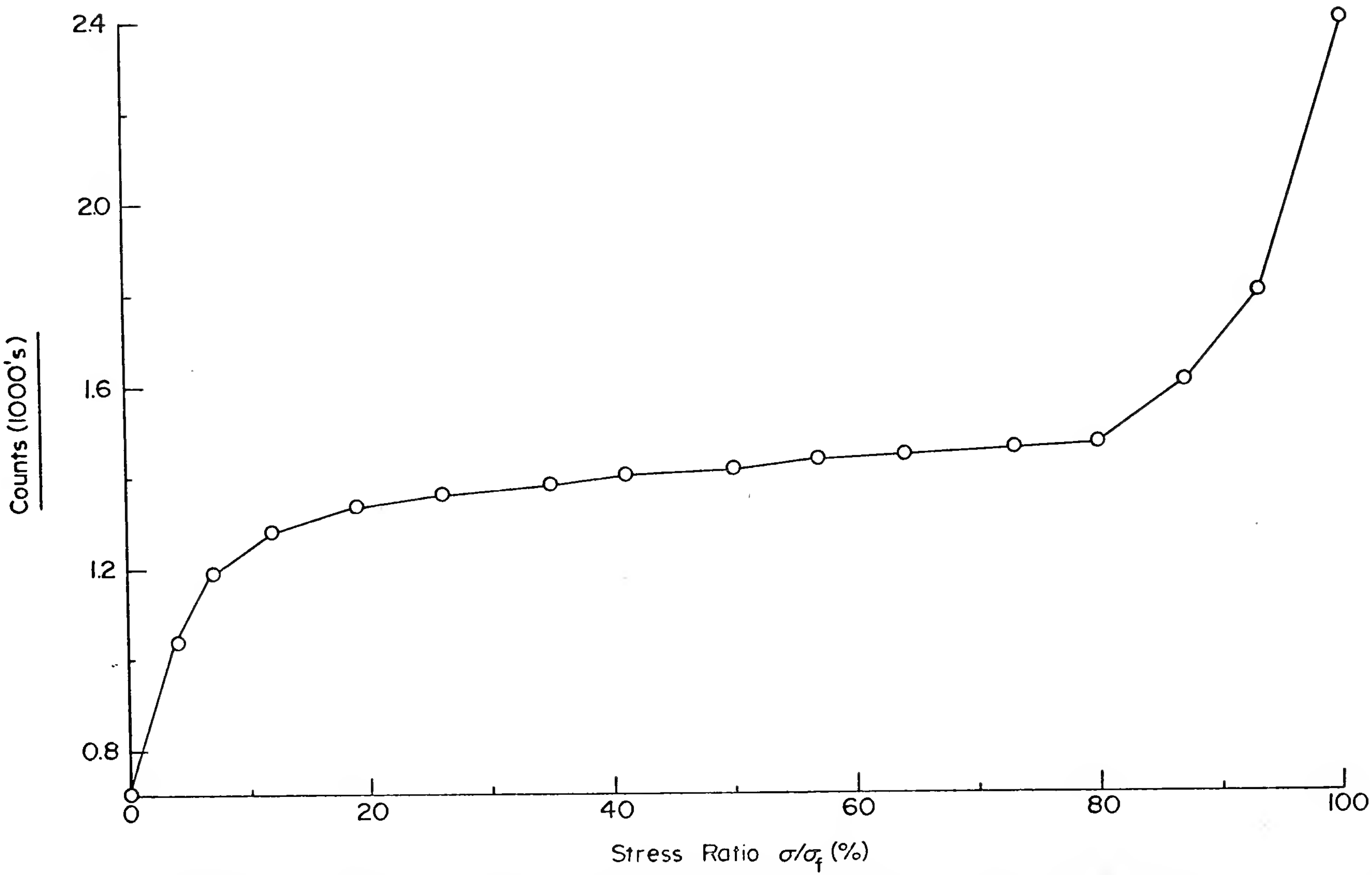

FIGURE I TOTAL COUNTS VS. STRESS RATIO, CYLINDER 23.

at a given instant expressed as a percentage of the ultimate strength. Typically, there will be a relatively large amount of noise produced up to a stress ratio of approximately ten per cent that is presumably due to seating effects such as loading device settlement on the cylinder cap or minor irregularities at the bottom of the cylinder reaching equilibrium. Cumulative counts (and hence count rate) begin to increase at about 80 per cent of ultimate strength and later, at about 95 per cent of ultimate strength there is a dramatic increase in cumulative counts and count rate. These patterns of acoustic emission output are in agreement with observations of fracture and micro fracture as described by Newman [53] and others [54, 55, 56, 57].

Figure 2 is a plot of normalized cumulative counts for each of the three water cement ratios used in the experiment. Count was normalized by subtracting the number of counts at a stress ratio of 10 per cent to remove the effect of seating and each point on each curve is the average of nine tests for the particular water cement ratio. Appendix B shows normalized counts and normalized count rates for each of the 27 test cylinders and are grouped according to their respective cell in the analysis of variance of ultimate strength. A typical set of calculations to reduce the data is shown in Appendix A.

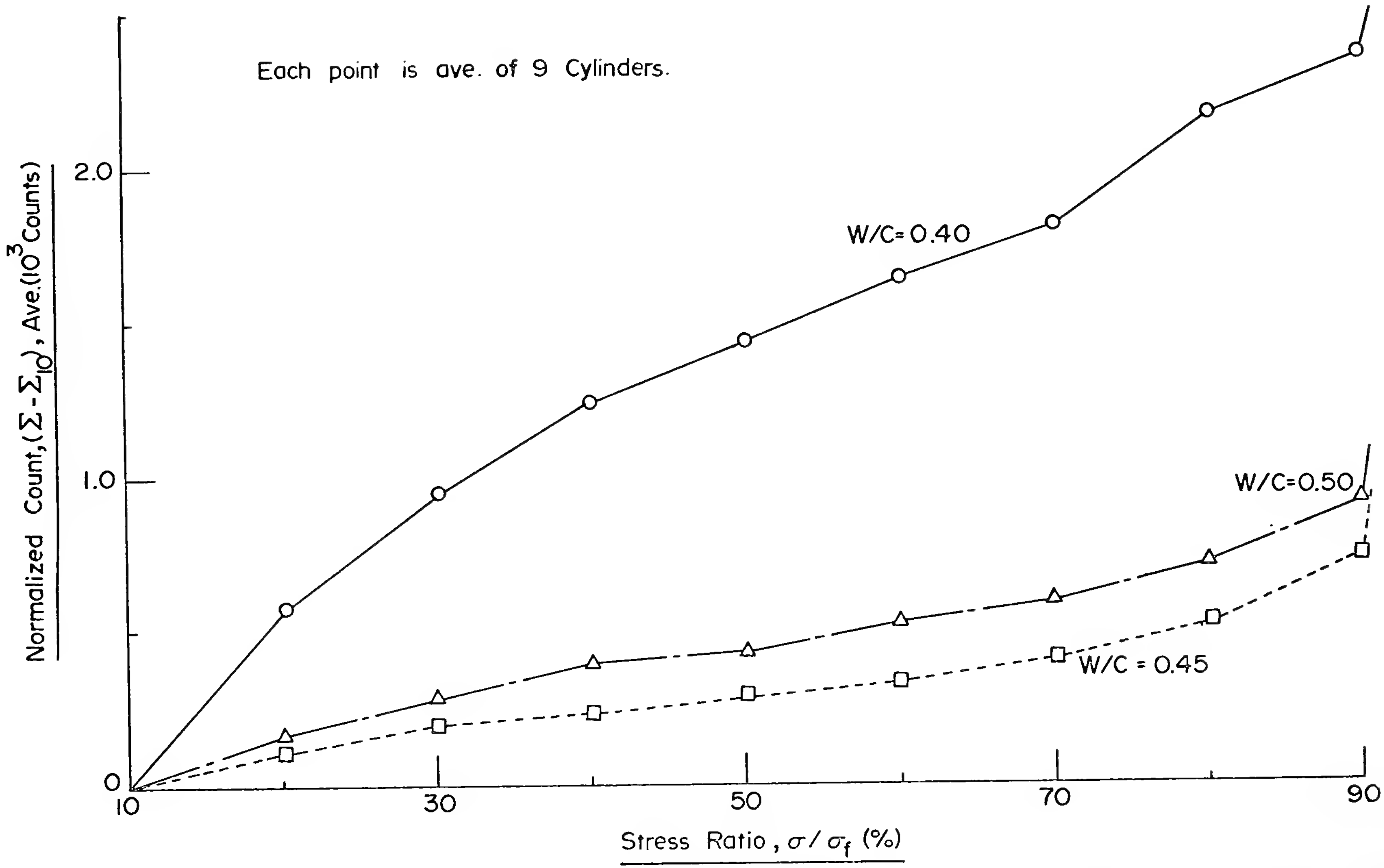

FIGURE 2 NORMALIZED COUNTS VS. STRESS RATIO AS A FUNCTION OF WATER CEMENT RATIO.

The Kaiser or memory effect for portland cement concrete is shown in Figures 3, 4, and 5 where time, load and cumulative counts are shown. These curves are somewhat idealized inasmuch as only peak points are shown.

II. Asphalt Concrete

It was intended to have acoustic emission output for the entire bituminous mixture limiting strain experiment and thus be able to report the effect of mixture and temperature variables on these signals. However, the equipment used for this study was on loan from a commercial supplier and, due to circumstances beyond the supplier's control, the equipment had to be removed from the laboratory during the period while most of the tension experiment was being conducted. Approximately twenty-five tests were conducted throughout the temperature and mix spectrum and valid conclusions can be made from these limited data.

In general, at temperatures below normal room temperature, the same trends and the same type of output appear for asphalt concretes as was observed for portland cement concretes. Figure 6 shows total counts and load as a function of time for a test at 45.5°F. The Kaiser effect is pronounced at lower temperatures as is shown in Figures 7 through 9 for tests conducted at 14 and 30°F.

At temperatures above room temperature, count sensitivity is quickly lost and output is totally due to background noise. When output gain is increased to full

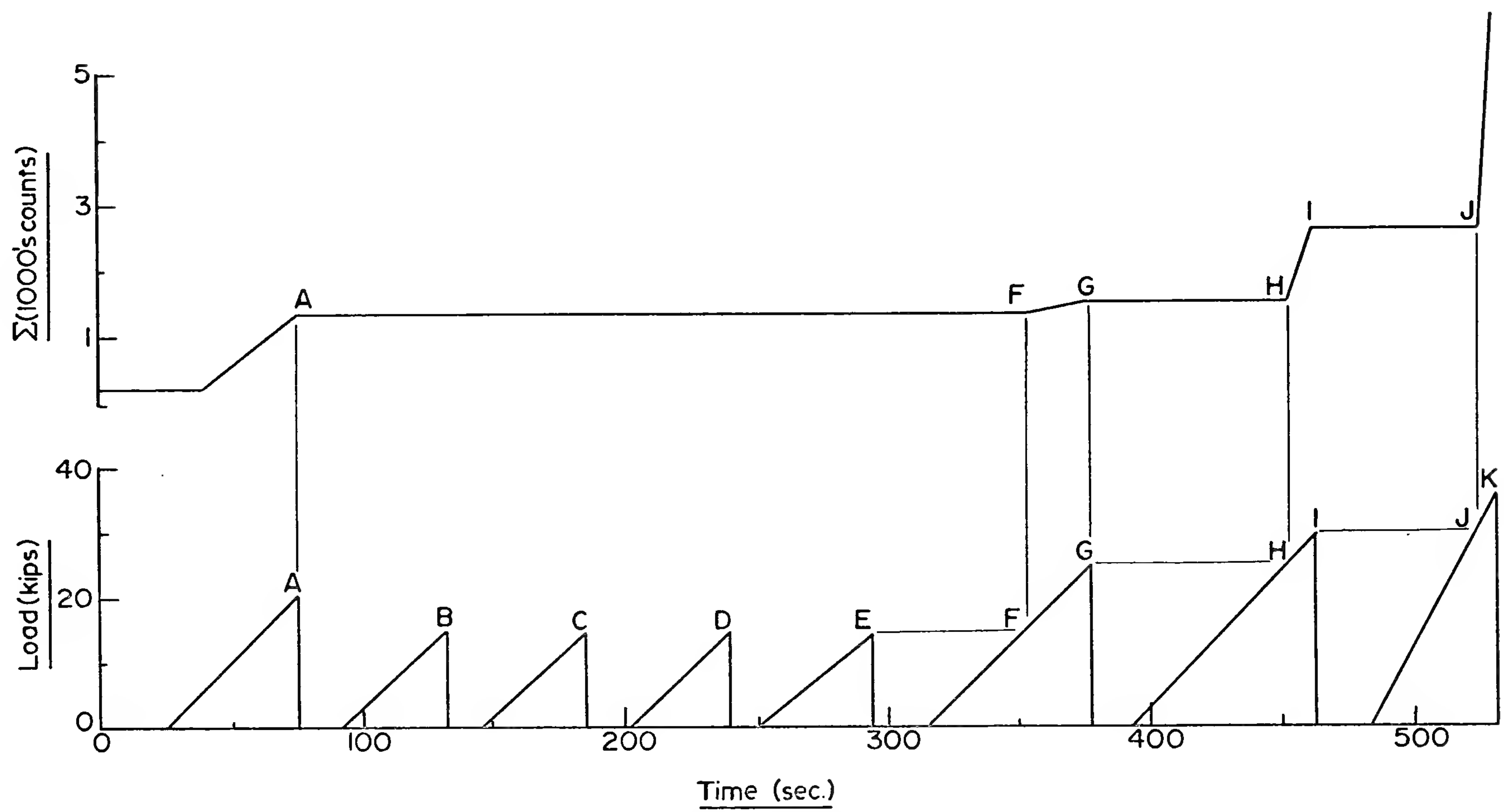

FIGURE 3 KAISER EFFECT, SERIAL 206.

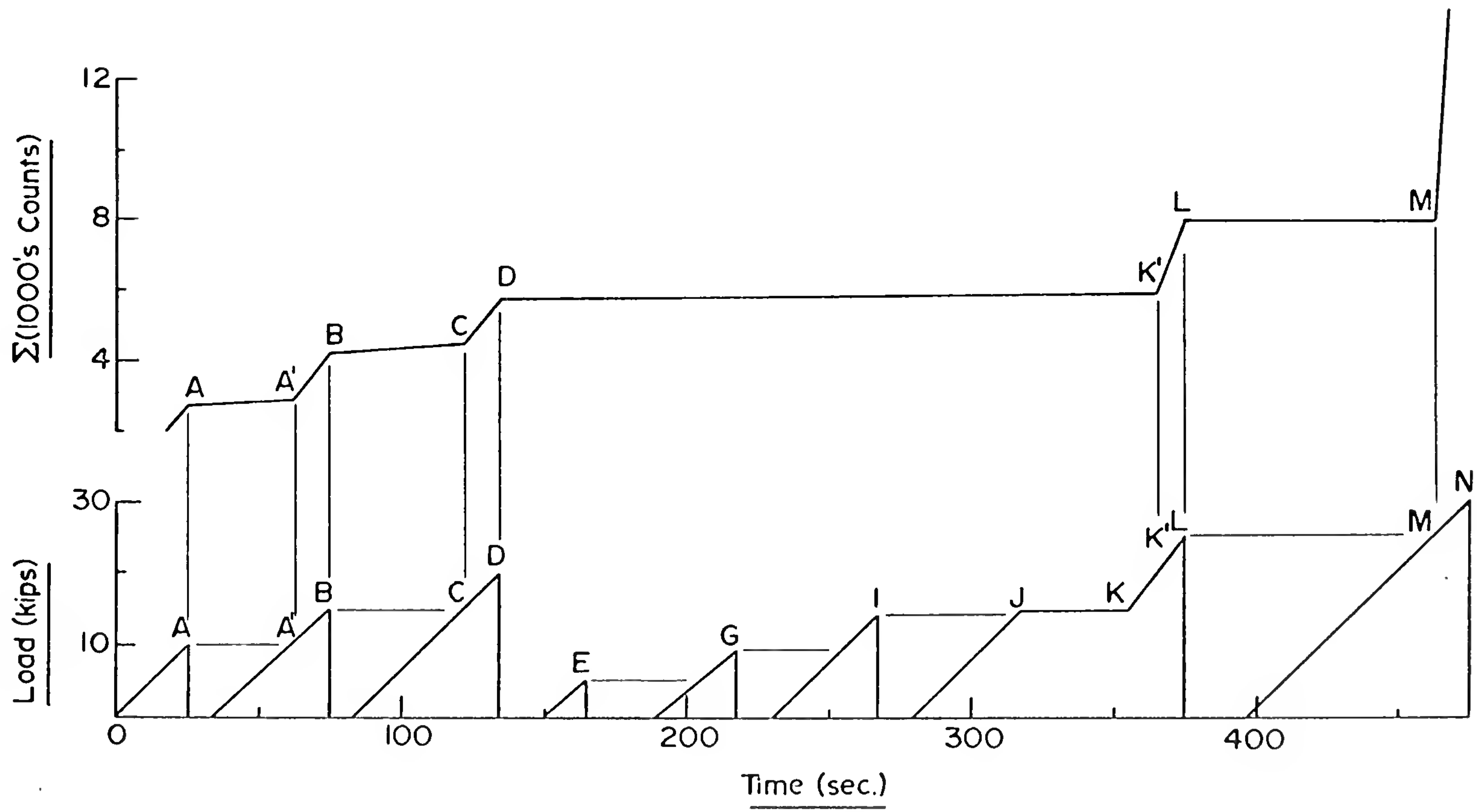

FIGURE 4 KAISER EFFECT, SERIAL 207.

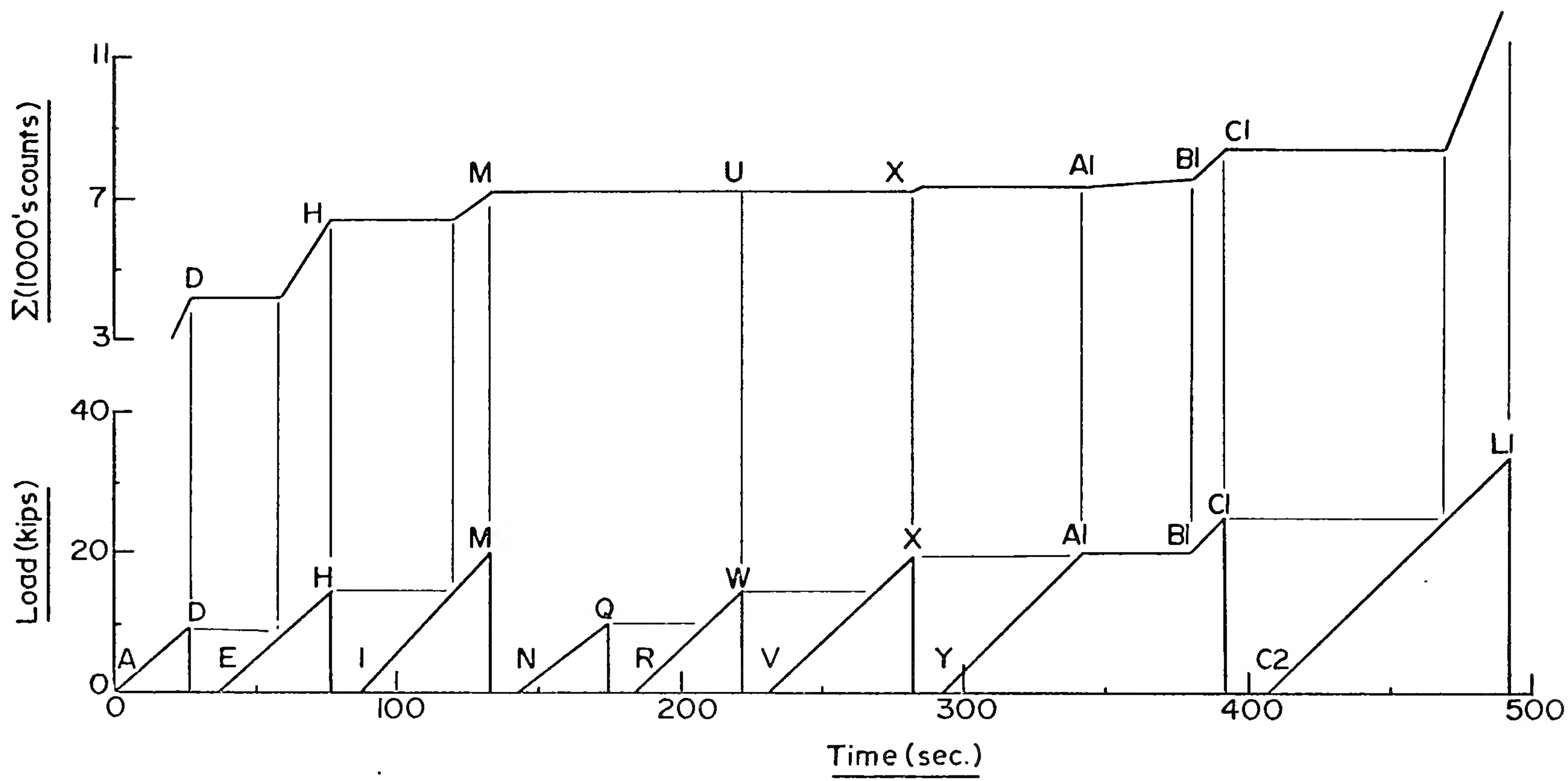

FIGURE 5 KAISER EFFECT, SERIAL 208.

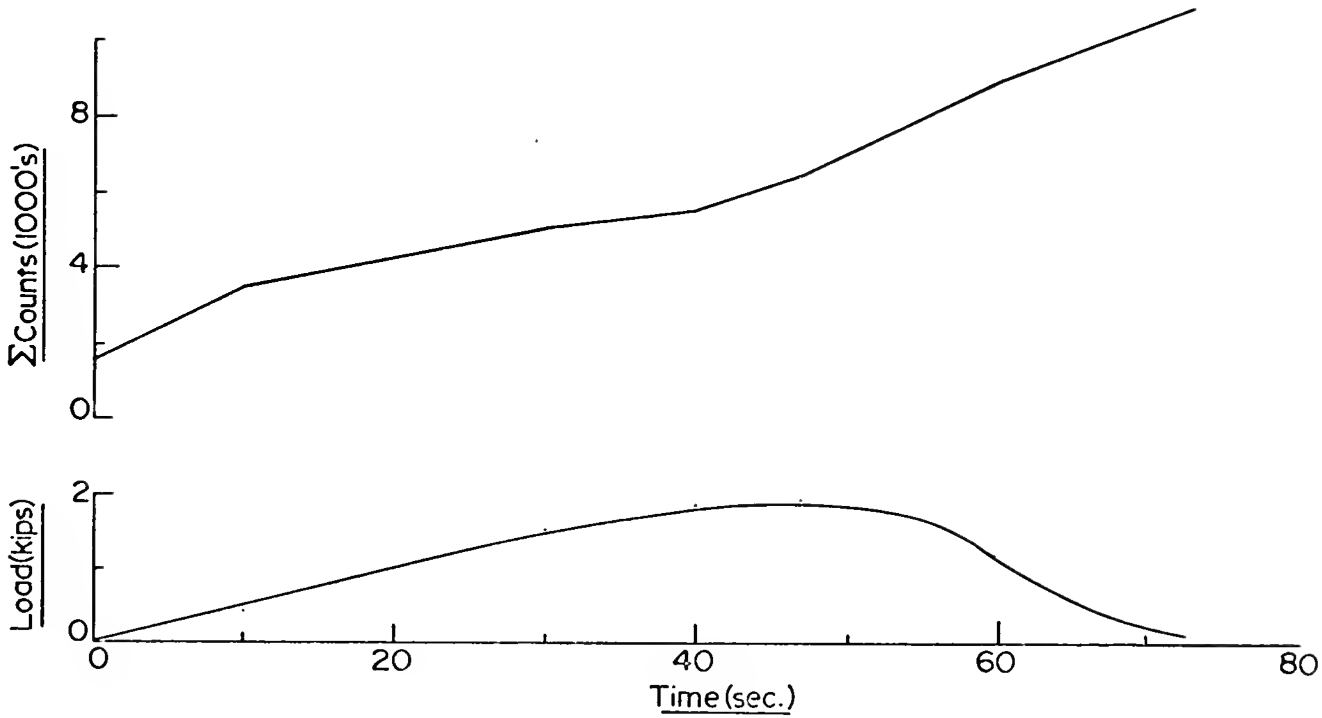

FIGURE 6 TOTAL COUNTS, SERIAL 369, G=30D3, 12HD, 45.5°F.

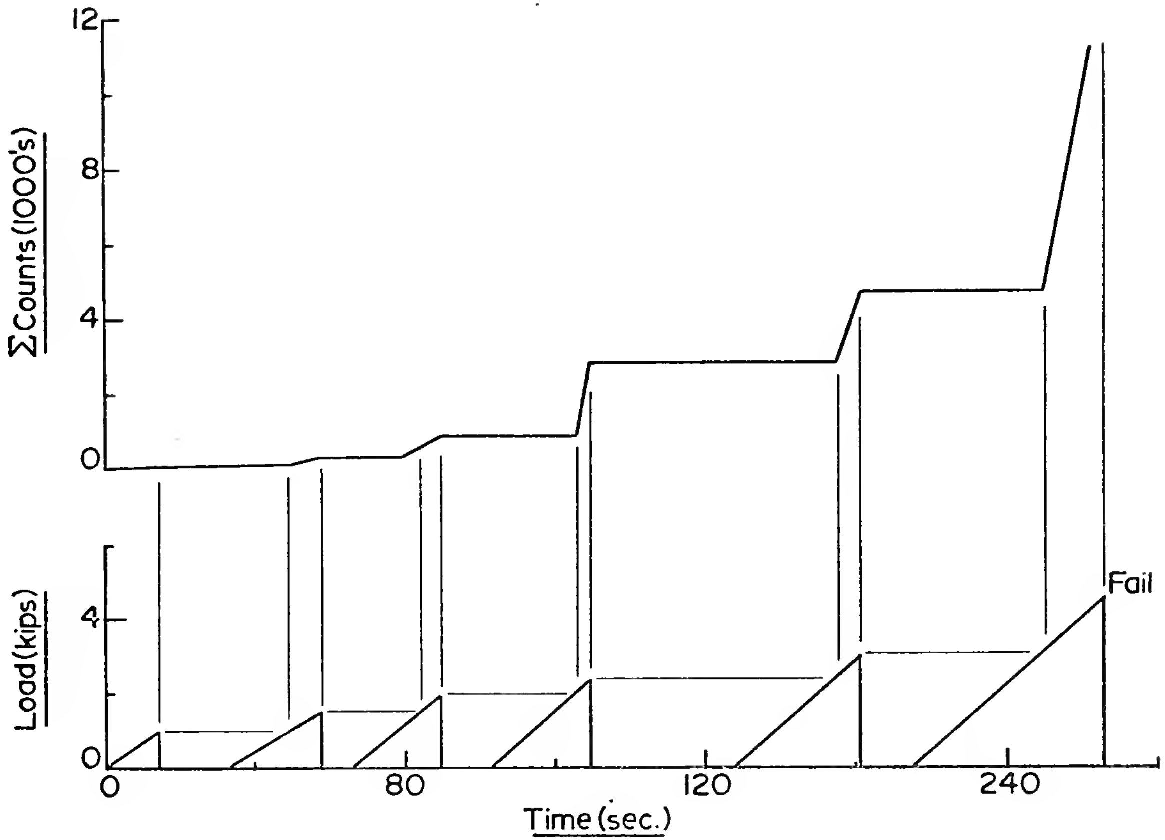

FIGURE 7 KAISER EFFECT, SERIAL 361, G=20DB, 8LD, 14°F.

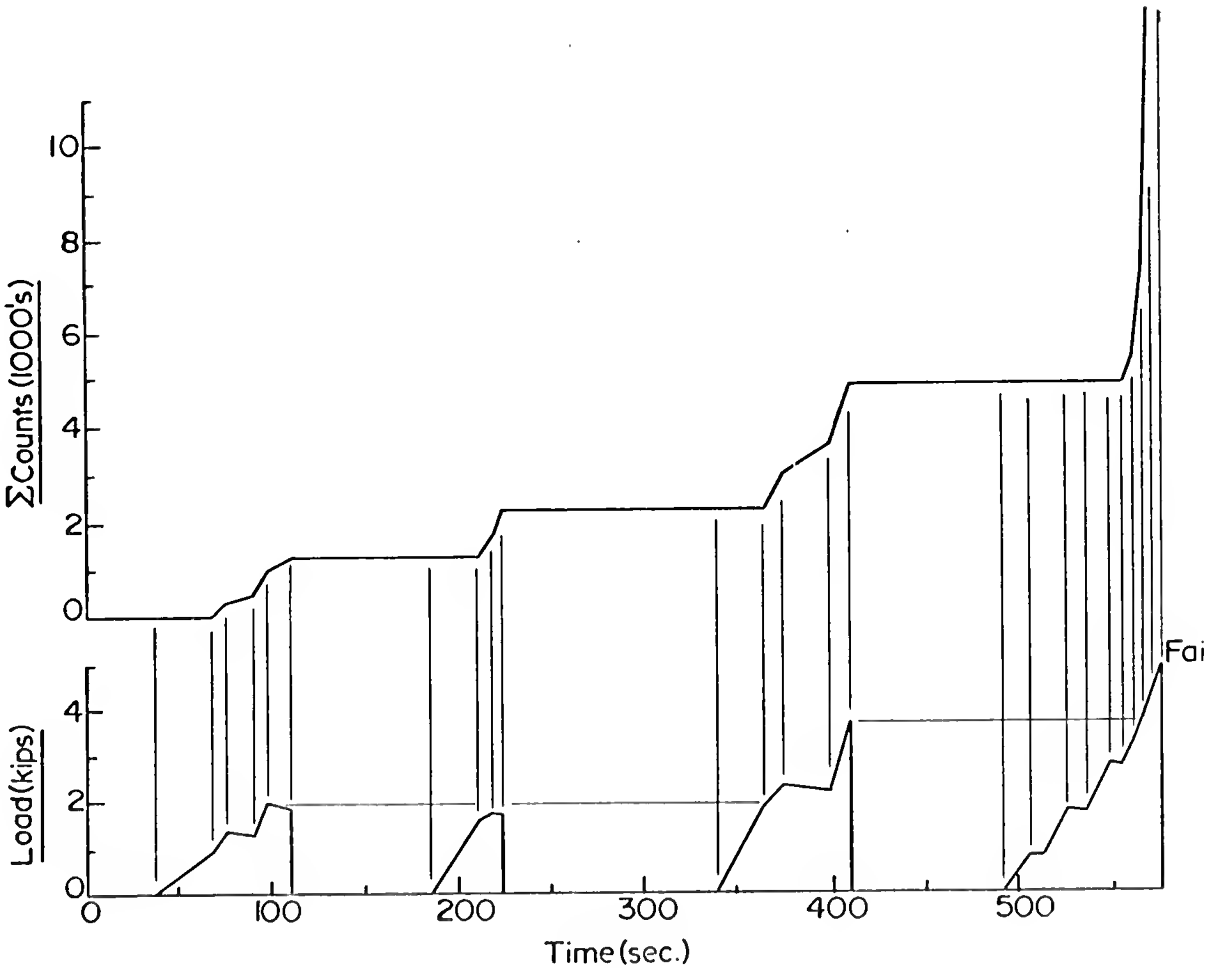

FIGURE 8 KAISER EFFECT, SERIAL 367, G=20DB, 12HD, 14°F.

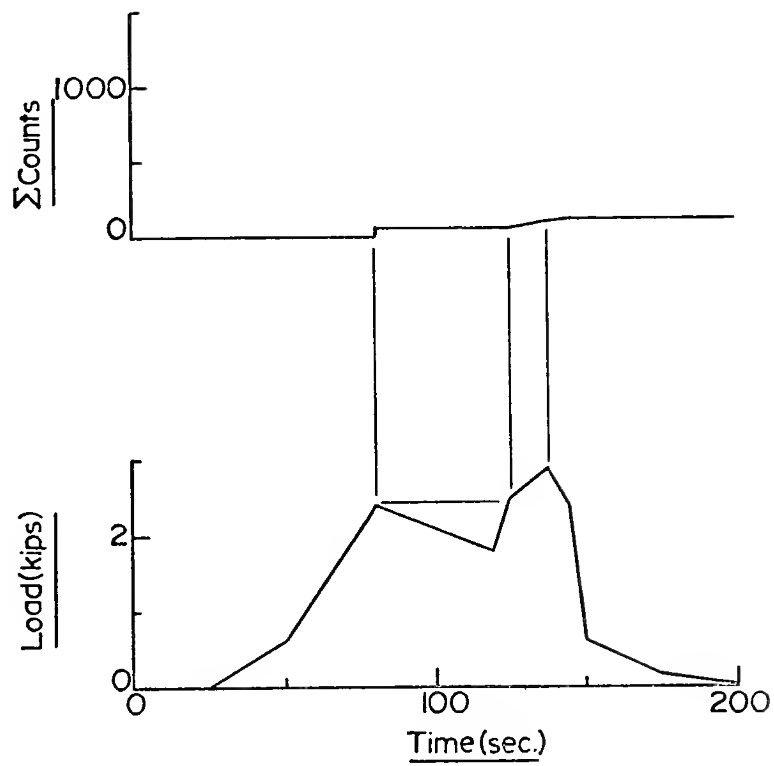

FIGURE 9 TOTAL COUNTS, SERIAL 368, G=20DB, 12 HD, 30°F.

equipment capacity (40 lb for this particular equipment) and sensitivity increased to provide for fewer counts per unit scale, recorder flutter is so great that output becomes meaningless.

It is possible that either of the following or some combination may be occurring: Fracture may be taking place in the aggregate and perhaps even to some degree in the asphalt binder, but at these elevated temperatures the binder is more viscous and less brittle than at low temperature and cannot transmit an elastic wave; or perhaps this transmitted wave is of so low a strength that it cannot activate the transducer. If low strength waves are noted, it may be possible to use a combination of more sensitive transducers and electronic filters to remove background noise and thus monitor these lower strength emissions. On the other hand, if at these temperatures the failure mechanism is predominantly extensive viscous flow and not fracture there should be no elastic waves produced and hence no acoustic emissions.

Since failure mechanisms are not within the scope of this study, no further experiments were conducted to investigate reasons for loss of signal output at higher temperatures.

Based on limited observations, the technique shows good promise for detecting crack initiation and propagation at low temperatures and may be quite useful in studies that investigate failure mechanisms at higher temperatures.

III. General

The experiment showed that acoustic emissions from portland cement concrete and bituminous concrete at lower temperatures are of similar type and character as those reported for metals. The output is probably best viewed as qualitative at this point in its development, but it does show dramatic increase in counts that can be detected before a decrease in load or other manifestations of failure such as cracks in the specimen are observed.

Since count rate increase at failure and existence of the Kaiser effect is observed in the materials of this experiment just as other research shows these effects in metals, it can be reasonably concluded that other applications made in the field of metals also can be applied to concretes and other civil engineering materials. Techniques are available to measure fatigue behavior, non-load associated failure and crack healing. Also, triangulation procedures have been developed that can locate the point in a structure where cracking is occurring. Each of these uses can be applied to both research and routine civil engineering problems.

Applications of this technique as a research tool are practically endless in the fields of both metallic and nonmetallic civil engineering materials. Some possibilities are, stress corrosion and embrittlement studies in metal structural components, reinforcement debonding in reinforced

concrete, autogeneous healing of portland cement and bituminous concretes, fatigue and remaining life studies of both types of concretes. In addition, it is clear that techniques used in other fields of engineering, such as multiple transducer triangulation to locate and follow crack propagation in structures and the use of the Kaiser effect for proof loading of structural components, can be conveniently and economically used.

AGGREGATES

I. Source and Type

Aggregates for this study consisted of 100 per cent crushed limestone obtained from the Erie Stone Company of Huntington, Indiana. This producer is listed as quarry number 58 by the Indiana State Highway Commission [33, 34].

Geologic setting for this material is the Louisville limestone formation of the Silurian period [35]. A typical section of this formation in northeastern Indiana consists of blue-gray to brown mottled dolomite in which chert nodules and argillaceous laminae are commonly present [36, 37].

II. Preparation

Material for this study originated from quarry stockpiles accepted by the Indiana State Highway Commission Bureau of Materials and Tests. These sources were designated as size numbers 9 and 14-2. Filler was minus No. 200 screenings from the 14-2 portion. Exact ledge location of the source was not known to quarry personnel at the time that the material was obtained.

Aggregates were transported to the Purdue Bituminous Materials Laboratories where they were resized to logarithmitic sieve series and washed.

III. Summary of Specification Tests and Physical Properties

Unless otherwise stated or required by standard methods all tests were performed on each sieve size fraction of aggregate.

1. Los Angeles Abrasion (per cent wear), (ASTM C131)

Grading	Wear after 100 rev., %	Wear after 500 rev., %
B	9.9	39.4
C	9.7	37.5
D	9.9	35.0

2. Deleterious Materials

A. Friable particles, ocher, and shells by visual inspection of hand specimens: None

B. Soft or nondurable particles (AASHTO T189):

Size	Sample wt. (g)	Number of Particles	% by wt. Soft Particles
3/4 - 1/2	600.5	124	0
1/2 - 3/8	202.1	95	0

C. Chert (less than 2.45 specific gravity). Test methods by visual count and heavy media separation. Heavy liquid consisted of 1,1,2,2-Tetrabromoethane (acetylene Tetrabromide) and carbon tetrachloride in proportions to provide specific gravity by hydrometer of 2.450 ± 0.002. Proportions were continually adjusted to make up evaporation losses [38, 39].

Size	Sample wt. (g)	Wt. particles less than 2.45 S.G.	No. particles less than 2.45 S.G.	% by wt. less than 2.45 S.G.
3/4 - 1/2	867.6	15.5	3	1.79
1/2 - 3/8	515.9	0	0	0
3/8 - 4	315.1	0	0	0
4 - 8	279.5	0	0	0

3. Soundness; five cycles, sodium sulfate (AASHTO T104).

Three gradations were selected as being representative of the final project mixtures. These gradations follow the mid-specification for dense (IVb), coarse (IIIc) and fine (Vb) as shown by The Asphalt Institute [40].

Gradation	Coarse Agg. (+ No. 4) % Loss	Fine Agg. (- No. 4) % Loss
Coarse	9.0	4.7
Dense	11.0	4.6
Fine	8.3	4.0

4. Specific Gravity and Absorption (ASTM C127, C128, D854).

Size Fraction	G_{BULK}	G_{BSSD}	G_{APP}	% ABS
3/4 - 1/2	2.543	2.598	2.689	2.135
1/2 - 3/8	2.497	2.564	2.678	2.707
3/8 - 4	2.514	2.586	2.708	2.852
4 - 8	2.569	2.643	2.772	2.849
8 - 16	2.599	2.672	2.802	2.798
16 - 30	2.692	2.729	2.795	1.358
30 - 50	2.753	2.775	2.816	0.806
50 - 100	2.671	2.699	2.747	1.024
100 - 200	2.778	2.793	2.822	0.570
Filler	—	—	2.860	—

Values shown are averages based on multiple measurements; following table shows the number of observations and standard deviation based on the range of values [41]. Test sequence for coarse and fine aggregates was determined by application of random numbers to each sample of each fraction. All values were checked for outliers according to ASTM E178 and in some cases data were rejected when necessary.

Size	No. Tests	Standard Deviations			
		G_B	G_{BSSD}	G_{APP}	% ABS
3/4 - 1/2	2	0	0	0.004	0.048
1/2 - 3/8	2	0	0	0.004	0.087
3/8 - 4	3	0.012	0.007	0.007	0.250
4 - 8	3	0.007	0.005	0.002	0.079
8 - 16	4	0.010	0.010	0.014	0.105
16 - 30	4	0.021	0.022	0.023	0
30 - 50	3	0.002	0.001	0.001	0.024
50 - 100	5	0.007	0.078	0.083	0.501
100 - 200	3	0.002	0.002	0.003	0.048
Filler	4	—	—	0.006	—

5. Flakiness Index and Sphericity

Flakiness index and sphericity are not specification tests but the measured values are included for future reference and comparison. Flakiness Index is as defined by The Asphalt Institute [42]. Sphericity is as defined by Krumbein and Pettijohn [43] except that particle volume was determined using weight and

apparent specific gravity instead of direct volume measurement. Sphericity is defined as:

$$\phi = \frac{d_n}{D_s}.$$

where ϕ = sphericity

d_n = diameter of a sphere of the same volume as the particle.

D_s = diameter of a sphere that would enclose the particle.

Size	No. Particles	Flakiness Index	Sphericity		
			No. Particles	Avg.	Std. Dev.
3/4 - 1/2	300	15.2	50	0.634	0.072
1/2 - 3/8	300	11.3	50	0.639	0.071
3/8 - 4	300	25.8	50	0.585	0.086

ASPHALTS

I. General

Six asphalt cements were used for this study. These materials include three specific penetration grades and two viscosity grades within each penetration grade. This may be viewed as three pairs matched by penetration at 77°F (25°C).

Test asphalts were provided by the American Oil Company of Whiting, Indiana. All test asphalts were stored after arrival until use in the experiment in a walk-in refrigerator at a temperature of approximately 17°F (-8.3°C). Asphalt required for testing or specimen fabrication was chipped from the container at this temperature without removal from the refrigerator.

Identification of materials will be by a number and letter combination whereby the number designates a nominal penetration and the letter designates relative viscosity, i.e., 6 H is a nominal 60-70 penetration asphalt with a relatively high viscosity and 6 L is a 60-70 penetration material with low viscosity. Some later identifications are made by laboratory test number.

ASPHALT IDENTIFICATION

Project Identification	Laboratory Number	Nominal Penetration (77°F)	Nominal Viscosity (Poises, 140°F)
6 H	102	60 - 70	4000
6 L	108	60 - 70	2000
8 H	116	85 - 100	2500
8 L	122	85 - 100	1200
12 H	127	120 - 150	1300
12 L	132	120 - 150	700

II. Tests for Physical Properties

The following physical properties were measured in strict conformance with applicable ASTM Standards:

a. Penetrations; 100g., 5 seconds at 77°F (25.0°C), 60°F (15.6°C), and 32°F (0.0°C); and 200 g., 60 seconds at 32°F (0.0°C).

b. Viscosity; absolute (poises), 30 cm. Hg. at 100°F (37.8°C), 140°F (60.0°C), and 180°F (82.2°C); kinematic (centistokes) at 205°F (96.1°C), 275°F (135.0°C) and 350°F (176.7°C).

c. Softening Point.

d. Thin Film Oven Test. Asphalts were tested for retained penetration at 77°F (25.0°C) and absolute viscosity increase at 140°F (60.0°C) and kinematic viscosity increase at 275°F (135.0°C).

e. Solubility in carbon tetrachloride.

f. Ductility; 5 cm. per min. at 77°F (25.0°C).

Randomization procedure for testing was as follows. For tests involving controlled constant temperature such as penetration, viscosity, and tests on the thin film heated materials, temperature sequence was determined by assigning random numbers to each temperature and using the smallest number as the first test temperature and the proceeding to the next number until the temperature sequence for the property was completed. All asphalts for a given property such as penetration, etc. were tested at the given temperature level before proceeding to the next temperature. At each temperature, sample testing sequence was developed in the same random manner, i.e., random numbers were assigned to each sample and samples were then tested in this predetermined sequence. After testing was completed for the entire temperature and sample spectrum the procedure was repeated for replicate testing.

Results of these tests are tabulated in Table 3.

III. Temperature Susceptibility

1. Penetration

The following tabulation provides parameters for a least squares fit of $\log_{10}$ penetration versus temperature that can be transformed to the following:

$$P = M(10)^{MT}$$

TABLE 3

Asphalt Physical Properties and Specification Compliance Results

Penetration (ASTM D5)

Sample	100g., 5 Sec.			200g., 60 Sec.
	77°F (25°C)	60°F (15.6°C)	32°F (0°C)	32°F (0°C)
6H	60	23	6	18
6L	54	18	1	11
8H	73	34	6	23
8L	86	31	5	16
12H	104	50	10	34
12L	119	43	6	23

Viscosity (ASTM D2171)

Sample	(Absolute (30cm. Hg.) (Poises)			Kinematic (Centistokes)		
	100°F (37.8°C)	140°F (60.0°C)	180°F (82.2°C)	205°F (96.1°C)	275°F (135°C)	350°F (176.7°C)
6H	177,000	3970	244	6680	500	89.0
6L	101,000	2060	146	3830	373	67.0
8H	93,500	2550	184	4780	492	89.4
8L	43,700	1200	86.8	2700	276	54.6
12H	36,400	1330	115	3300	361	71.2
12L	23,100	734	59.3	1960	226	48.1

Softening Point (ASTM D2398)

Sample	Softening Point	
	°C	°F
6H	51.0	124
6L	50.0	122
8H	49.5	121
8L	46.0	115
12H	46.0	115
12L	44.0	111

TABLE 3 (continued)

Thin Film Oven Test (ASTM D1754)

Sample	Penetration, % of Original	Loss of Wt. (%)	Viscosity (% Increase)	
			140°F (60.0°C)	275°F (135.0°C)
6H	55.5	0.02	125	54.4
6L	55.8	0.10	171	60.8
8H	66.3	0.51	253	79.3
8L	64.8	0.04	275	50.6
12H	61.7	0.52	273	91.3
12L	68.5	0.42	257	14.5

Solubility in CCL_4 (ASTM D2042)

Sample	% Soluble
6H	99.8
6L	99.7
8H	99.5
8L	99.5
12H	99.5
12L	99.3

Ductility (ASTM D113)

77°F (25.0°C)

All materials exceed 150 cm.

where P = penetration, 100 g. 5 sec.

T = temperature in degrees Fahrenheit

K and M are regression coefficients and

r is the correlation coefficient for the three data points.

TABLE 4

Regression Coefficients for Penetration Temperature Susceptibility

Sample	K	M	r
6H	1.153	0.02209	1.000
6L	0.0619	0.03913	0.950
8H	1.040	0.0244	1.000
8L	0.6661	0.02754	0.999
12H	1.930	0.02284	0.998
12L	0.7277	0.0290	1.000

A plot of these regression lines is shown in Figure 10.

2. Penetration Index

Penetration Index of the test asphalts was calculated according to Pfeiffer and Van Doormal [47]. They define the index as:

$$PI = \frac{30}{1 + 90\ PTS} - 10$$

where PI = penetration index

PTS = penetration temperature susceptibility

$$= \frac{\log_{10} 800 - \log_{10} P}{T_{R\&B} - T_p}$$

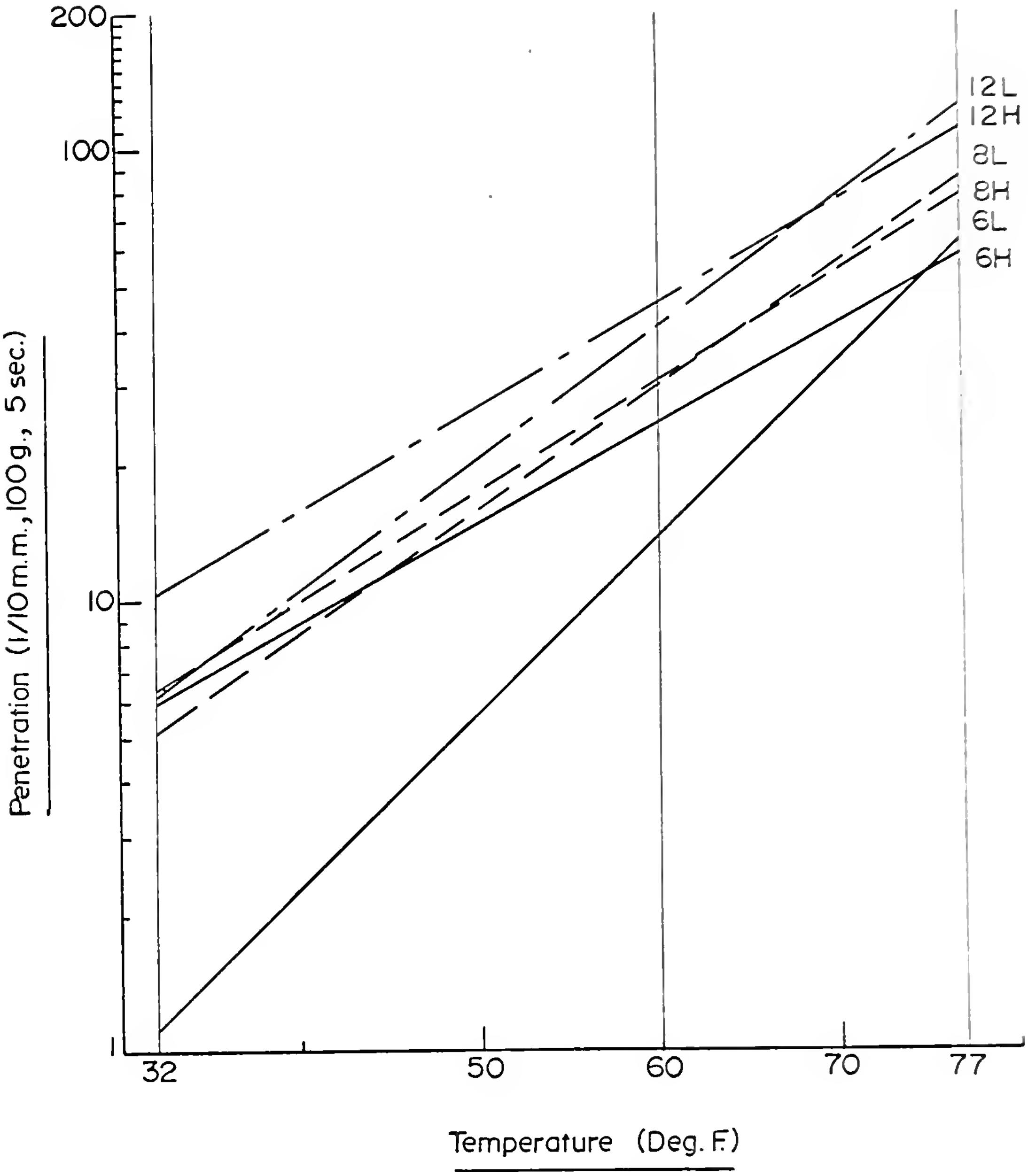

FIGURE 10 LOG. PENETRATION VS. TEMPERATURE.

where P = penetration at 77°F (25.0°C) 100 g., 5 seconds.

$T_{R\&B}$ = ring and ball softening point in °C.

T_p = temperature where penetration is determined, 25°C for this case.

Penetration indices of -2.0 to +2.0 correspond with "normal" residual asphalts whereas indices of less than -2.0 indicate highly temperature susceptible pitch types and indices above +2.0 are found for low susceptibility blown materials.

Penetration indices for the study asphalts are shown in the following table:

TABLE 5

Penetration Indices

Sample	Pen.	ΔT (°C)	P.I.
6H	60	26.0	-0.5
6L	54	25.0	-1.0
8H	73	24.5	-0.4
8L	86	21.0	-0.9
12H	104	21.0	-0.4
12L	119	19.0	-0.6

3. Viscosity

Another method used to describe temperature dependence is to consider the slope of a line that relates some function of viscosity to temperature. A difficulty in applying this method of characterization occurs in the measurement of

viscosity with commonly available equipment and even with the definition of units for viscosity.

The most common and probably the most practical device used to measure viscosity of asphalts is the capillary tube viscometer such as was used for this study. In this method, a standard amount of asphalt is allowed, or forced, to flow through a calibrated tube and the time for the material to flow (flow rate) is used to determine viscosity by comparing flow times of the material in question with standards of known viscosity. Lighter or less viscous materials exhibit faster flow times than the heavier. Due to the very wide range of viscosities for a given asphalt and the range of viscosities between various asphalt products (from practically solid at room temperature to just slightly more viscous than water at temperatures elevated to allow adequate mixing with aggregates), two capillary viscometry techniques are used. For the heavier materials a vacuum is used to pull material through the tube; the force produced by the vacuum greatly exceeds the weight or fluid head of the material and hence flow times are not significantly affected by the density of the material. Tube constants for this method are used to calculate absolute viscosity in poises where units are dyne-seconds per square centimeter. For the lighter materials where a vacuum would pull the material through the tube too fast to allow precise timing in determining flow rate, a simple tube such as the Zeitfuchs cross-arm

viscometer is used where flow is induced by the weight or fluid head of the material. Tube constants for this method are used to calculate kinematic viscosity in stokes or centistokes. Stoke units are grams per second-centimeter and kinematic viscosity is defined as absolute viscosity per unit density or

$$\nu = \frac{\mu}{\rho}$$

where ν = kinematic viscosity,

μ = absolute viscosity

ρ = density.

For this study, absolute viscosities were measured at 100°F (37.8°C), 140°F (60.0°C) and 180°F (82.2°C) and kinematic viscosities were measured at 205°F (96.1°C), 275°F (135.0°C) and 350°F (176.7°C).

In order to make a plot of kinematic viscosity versus temperature, absolute viscosities were converted to kinematic by using densities at the temperature under consideration. Since direct measurement of density at temperatures of 100, 140 and 180°F was impractical it was decided to calculate density at these temperatures based on measured specific gravity at 77 and 60°F (25.0 and 15.6°C) and the coefficient of volume expansion as follows:

$$P_i = \frac{W_i}{V_i}$$

where P_i = density at i°F

W_i = weight at i°F

V_i = volume at i°F

Now, consider the definition of volume coefficient of expansion:

$$A = \frac{\Delta V/V}{\Delta T}.$$

where A = volume coefficient of expansion

ΔV = change in volume = $V_i - V$

V = original volume

ΔT = change in temperature

For a constant weight and for i > 77°F

$$\Delta V = V_i - V_{77} = A\ \Delta T\ V_{77}$$

$$V_i = V_{77}\ [1 + A\ (i - 77)] \qquad \text{(I)}$$

Since

$$V_{77} = \frac{W_{77}}{G_{77}\ \gamma_{W77}}.$$

where G_{77} = specific gravity at 77°F

γ_{W77} = density of water at 77°F.

Equation (I) becomes

$$V_i = \frac{W_i}{G_{77}\gamma_{W77}}\ [1 + A(i - 77)]$$

Hence

$$P_i = \frac{W_i}{V_i} = \frac{G_{77}\ \gamma_{W77}}{1 + A(i - 77)}. \qquad \text{(II)}$$

To evaluate the volume coefficient of expansion, A:

$$A = \frac{\Delta V/V}{\Delta T} = \frac{V_H - V_L}{V_L(T_H - T_L)}.$$

where the subscript H indicates the higher and L indicates the lower temperature.

Since

$$V_i = \frac{W_i}{G_i \gamma_{Wi}}.$$

$$A = \frac{G_L \gamma_{WL} - G_H \gamma_{WH}}{G_H \gamma_{WH} \Delta T}.$$

Test temperatures of 60 and 77°F (15.6 and 25.0°C) were used for specific gravity determinations of the asphalt. Based on published density of water at these temperatures the coefficients of volume expansion were calculated and are shown in Table 6.

TABLE 6

Coefficients of Volume Expansion

Sample	G_{60}	G_{77}	Coeff. of Volume Expansion, A
6H	1.029	1.028	$1.726(10)^{-4}$
6L	1.029	1.028	$1.726(10)^{-4}$
8H	1.038	1.031	$5.154(10)^{-4}$
8L	1.028	1.027	$1.726(10)^{-4}$
12H	1.030	1.027	$2.874(10)^{-4}$
12L	1.028	1.026	$2.308(10)^{-4}$

These volume coefficients are in reasonable agreement with values of approximately $3(10)^{-4}$ per degree Fahrenheit as published by Traxler [58].

Using density values calculated from equation (II) and the measured absolute viscosities, kinematic viscosities for each of the test asphalts were calculated. These values are shown in Table 7.

Several methods of curve fitting were attempted in order to establish temperature susceptibility parameters. With the exception of the first method outlined below, all fits were obtained by the method of least squares. It should be noted that each point on each curve is the arithmetic mean of all replicates used in determining that particular value for viscosity. These techniques include:

a. Plot of kinematic viscosity versus temperature on the standard ASTM D341 scale which is a modified log log viscosity versus log temperature scale (see Figure 11).

b. Exponential curve of the form:

$$\nu = ae^{bT}$$

where ν = kinematic viscosity in centistokes

T = temperature in degrees Fahrenheit

a and b = material constants such that a is the intercept and b is the slope of a line with $\ln \nu$ versus T as axes.

c. Exponential curve of the form:

$$\nu = a(10)^{bT}$$

TABLE 7

Temperature vs. Kinematic Viscosity
[Values for 100, 140 and 180°F (37.8, 60.0 and 82.2°C) calculated from absolute viscosity and density at those temperatures]

	Kinematic Viscosity (Centistokes)					
Sample	100°F (37.8°C)	140°F (60.0°C)	180°F (82.2°C)	205°F (96.1°C)	275°F (135.0°C)	350°F (176.7°C)
6H	$1.74(10)^{7}$	$3.96(10)^{5}$	$2.47(10)^{4}$	$6.68(10)^{3}$	$5.00(10)^{2}$	$8.90(10)^{1}$
6L	$9.97(10)^{6}$	$2.05(10)^{5}$	$1.47(10)^{4}$	$3.83(10)^{3}$	$3.73(10)^{2}$	$6.70(10)^{1}$
8H	$9.17(10)^{6}$	$2.54(10)^{5}$	$1.86(10)^{4}$	$4.78(10)^{3}$	$4.92(10)^{2}$	$8.94(10)^{1}$
8L	$4.30(10)^{6}$	$1.19(10)^{5}$	$8.77(10)^{3}$	$2.70(10)^{3}$	$2.76(10)^{2}$	$5.46(10)^{1}$
12H	$3.59(10)^{6}$	$1.32(10)^{5}$	$1.16(10)^{4}$	$3.30(10)^{3}$	$3.61(10)^{2}$	$7.12(10)^{1}$
12L	$2.27(10)^{6}$	$7.33(10)^{4}$	$6.00(10)^{3}$	$1.96(10)^{3}$	$2.26(10)^{2}$	$4.81(10)^{1}$

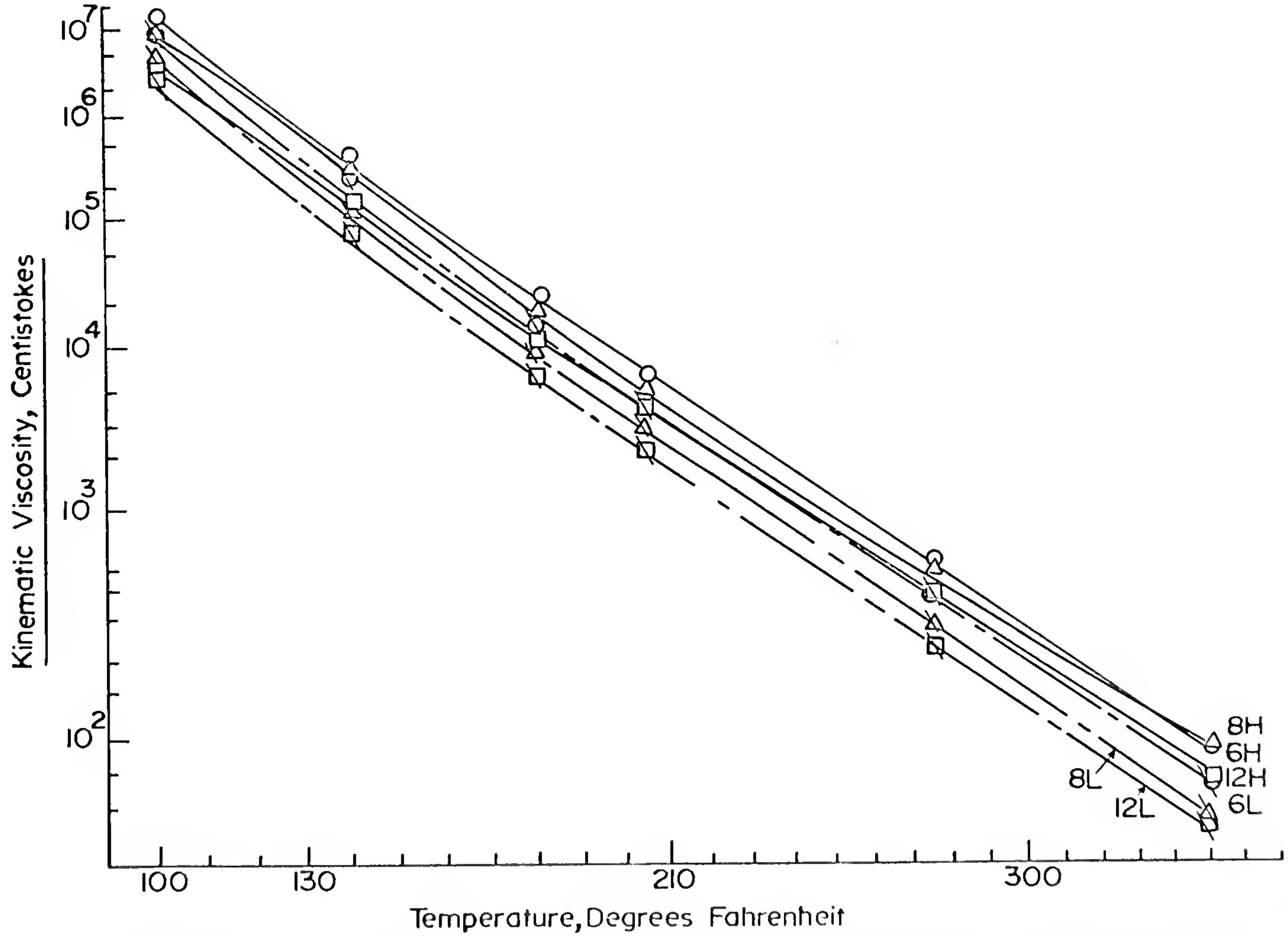

FIGURE 11 ASTM D341 STANDARD VISCOSITY - TEMPERATURE CHART FOR LIQUID PETROLEUM PRODUCTS.

where a is the intercept and b is slope of a line with $\log_{10} \nu$ versus T as axes.

d. Logarithmic curve of the form:

$$\nu = a + b \ln T$$

e. Logarithmic curve of the form:

$$\nu = a + b \log_{10} T$$

f. Power curve of the form:

$$\nu = a^{TB}$$

where a is the intercept and b the slope of a curve with ln ν versus ln T as axes.

g. Power curve of the form:

$$\nu = aT^{B}$$

where a is the intercept and b the slope of a curve with $\log_{10} \nu$ versus $\log_{10}$ T as axes.

h. log log viscosity versus log temperature.

In addition, fits were attempted using a shifted temperature, u such that $u = T - T_0$, according to the method as presented by Mandel [46]. This procedure shifts the axis of curves that are hyperbolic or asymptotic in nature, such as the typical arithmetic plot of kinematic viscosity versus temperature shown on Figure 12, and allows a linear fit of the transformed data. The procedure as presented by Mandel is essentially as follows:

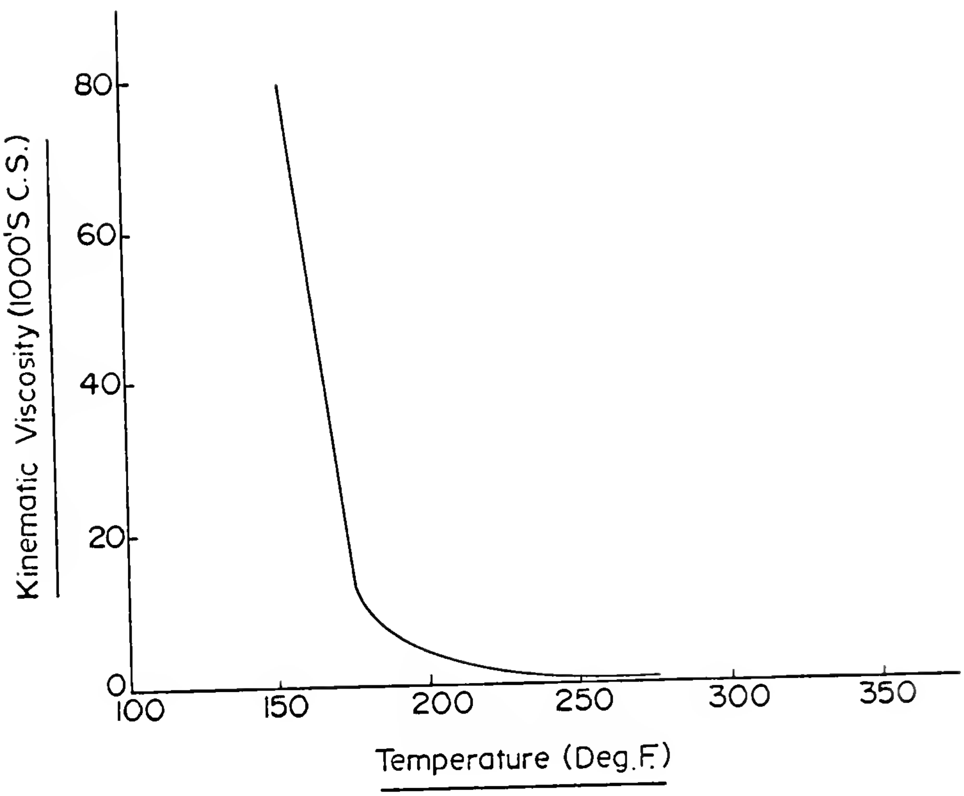

FIGURE 12 KINEMATIC VISCOSITY VS. TEMPERATURE.

a. Plot the data on rectangular coordinates.

b. Draw a smooth curve through the plotted points.

c. Select two values T_1 and T_2, near the opposite extremes of the data range, and read the corresponding values ν_1 and ν_2 from the smooth curve.

d. Calculate the quantity $\nu_3 = \sqrt{\nu_1 \ \nu_2}$ and locate it on the axis; read the corresponding value T_3 from the smooth curve and obtain the estimate:

$$T_0 = \frac{T_1 T_2 - T_3^2}{T_1 + T_2 - 2T_3}$$

Then compute the corresponding quantity:

$$U = T - T_0$$

This is the shifted temperature that replaces T in the preceding six curve functions.

This procedure was modified slightly inasmuch as 100°F and 300°F were selected for T_1 and T_2 for all asphalts. Calculated values for T_0 for each of the materials are as follows:

Sample	T_0
6H	21.81
6L	28.89
8H	28.89
8L	25.44
12H	25.89
12L	25.44

Parameters for each of the methods of fitting are included in the following table along with r (coefficient

of correlation) values and limits on r as shown by Ostle [41]. Calculation of the upper and lower limits of r are as follows; upper limit of r is given by:

$$U = z_r + z_{(1+\gamma)/2}\ \sigma_z \tag{A}$$

and the lower limit of r is given by"

$$L = z_r - z_{(1+\gamma)/2}\ \sigma_z \tag{B}$$

and

$$\sigma = \left[\frac{1}{n - 3}\right]^{\frac{1}{2}}$$

where n = number of observations (six per curve).

An approximate equation for z_r is given by:

$$z_r = \frac{1}{2} \ln (1 + r) - \ln (1 - r) \tag{C}$$

Upper and lower limits for r are determined by calculating upper limits from equations (A) or (B) and inserting this value into equation (C). Rearrangement of equation (C) gives

$$r = \frac{\exp(2zr_1) - 1}{\exp(2zr_1) + 1}.$$

Table 8 shows the calculated parameters for all of the techniques and Figure 13 is a typical plot of the calculated regression lines for log log ν versus log U.

TABLE 8

Regression Coefficients, Correlation Coefficients, and Limits on Correlation Coefficients for Kinematic Viscosity as a Function for Shifted Temperature

Case 2	Function, $\nu = ae^{bT}$		Exponential		
Sample	a	b	r	r_U	r_L
6H	3.29E08	-4.68E-02	0.96	0.98	0.90
6L	1.50E08	-4.53E-02	0.96	0.98	0.90
8H	1.89E10	-6.21E-02	0.86	0.94	0.67
8L	5.88E07	-4.30E-02	0.96	0.98	0.90
12H	5.11E07	-4.16E-02	0.96	0.98	0.90
12L	2.72E07	-4.10E-02	0.96	0.98	0.90

Case 3	Function, $\nu = a(10)^{bT}$		Exponential		
Sample	a	b	r	r_U	r_L
6H	3.29E08	-2.03E-02	0.96	0.98	0.90
6L	1.50E08	-1.97E-02	0.96	0.98	0.90
8H	1.44E08	-1.92E-02	0.96	0.98	0.90
8L	5.88E07	-1.87E-02	0.96	0.98	0.90
12H	5.11E07	-1.81E-02	0.96	0.98	0.90
12L	2.72E07	-1.78E-02	0.96	0.98	0.90

Case 4	Function, $\nu = a + b \ln T$		Logarithmic		
Sample	a	b	r	r_U	r_L
6H	6.18E07	-1.12E07	0.72	0.88	0.40
6L	3.54E07	-6.41E06	0.72	0.88	0.40
8H	3.27E07	-5.91E06	0.72	0.88	0.40
8L	1.53E07	-2.77E06	0.72	0.88	0.40
12H	1.28E07	-2.32E06	0.72	0.88	0.40
12L	8.10E06	-1.47E06	0.72	0.88	0.40

TABLE 8 (continued)

Case 5	Function, $\nu = a + b \log_{10} T$		Logarithmic		
Sample	a	b	r	r_U	r_L
6H	6.18E07	-2.58E07	0.72	0.88	0.40
6L	3.54E07	-1.48E07	0.72	0.88	0.40
8H	3.27E07	-1.36E07	0.72	0.88	0.40
8L	1.53E07	-6.38E06	0.72	0.88	0.40
12H	1.28E07	-5.35E06	0.72	0.88	0.40
12L	8.10E06	-3.38E06	0.72	0.99	0.40

Case 6	Function, $\nu = aT^b$		ln Power Curve		
Sample	a	b	r	r_U	r_L
6H	4.33E26	-9.79E00	1.00	1.00	1.00
6L	6.09E25	-9.51E00	1.00	1.00	1.00
8H	1.94E25	-9.26E00	1.00	1.00	1.00
8L	3.01E24	-9.02E00	1.00	1.00	1.00
12H	6.23E23	-8.70E00	1.00	1.00	1.00
12L	2.40E23	-8.61E00	1.00	1.00	1.00

Case 7	Function, $\nu = aT^b$		$\log_{10}$ Power Curve		
Sample	a	b	r	r_U	r_L
6H	4.33E26	-9.79E00	1.00	1.00	1.00
6L	6.09E25	-9.51E00	1.00	1.00	1.00
8H	1.94E25	-9.26E00	1.00	1.00	1.00
8L	3.01E24	-9.02E00	1.00	1.00	1.00
12H	6.23E23	-8.70E00	0.99	1.00	0.97
12L	2.40E23	-8.61E00	1.00	1.00	1.00

TABLE 8 (continued)

Case 8	Function, $\nu = ae^{bu}$		Exponential		
Sample	a	b	r	r_U	r_L
6H	1.19E08	-4.68E-02	0.96	0.98	0.90
6L	4.04E07	-4.53E-02	0.96	0.98	0.90
8H	4.01E07	-4.42E-02	0.96	0.98	0.90
8L	1.97E07	-4.30E-02	0.96	0.98	0.90
12H	1.74E07	-4.16E-02	0.96	0.98	0.90
12L	9.57E06	-4.10E-02	0.96	0.98	0.90

Case 9	Function, $\nu = a(10)^{bu}$		Exponential		
Sample	a	b	r	r_U	r_L
6H	1.19E08	-2.03E-02	0.96	0.98	0.90
6L	4.04E07	-1.97E-02	0.96	0.98	0.90
8H	4.01E07	-1.92E-02	0.96	0.98	0.90
8L	1.97E07	-1.87E-02	0.96	0.98	0.90
12H	1.74E07	-1.81E-02	0.96	0.98	0.90
12L	9.57E06	-1.78E-02	0.96	0.98	0.90

Case 10	Function, $\nu = a + b \ln U$		Logarithmic		
Sample	a	b	r	r_U	r_L
6H	5.44E07	-1.00E07	0.73	0.89	0.42
6L	3.54E07	-6.41E06	0.72	0.88	0.40
8H	2.74E07	-5.10E06	0.74	0.89	0.44
8L	1.32E07	-2.44E06	0.74	0.89	0.44
12H	1.10E07	-2.04E06	0.74	0.89	0.44
12L	-6.97E06	-1.29E06	0.74	0.89	0.44

TABLE 8 (continued)

Case 11	Function, $\nu = a + b \log_{10} U$		Logarithmic		
Sample	a	b	r	r_U	r_L
6H	5.44E07	-2.31E07	0.73	0.89	0.43
6L	2.97E07	-1.27E07	0.74	0.89	0.44
8H	2.74E07	-1.17E07	0.74	0.89	0.44
8L	1.32E07	-5.61E06	0.74	0.89	0.44
12H	1.10E07	-4.69E06	0.74	0.89	0.44
12L	6.97E06	-2.97E06	0.74	0.89	0.44

Case 12	Function, $\nu = aU^b$		ln Power Curve		
Sample	a	b	r	r_U	r_L
6H	2.42E23	-8.59E00	1.00	1.00	1.00
6L	3.92E21	-7.95E00	1.00	1.00	1.00
8H	1.58E21	-7.73E00	1.00	1.00	1.00
8L	9.57E20	-7.73E00	1.00	1.00	1.00
12H	2.25E20	-7.42E00	1.00	1.00	1.00
12L	1.11E20	-7.37E00	1.00	1.00	1.00

Case 13	Function, $\nu = aU_b$		$\log_{10}$ Power Curve		
Sample	a	b	r	r_U	r_L
6H	2.42E23	-8.59E00	1.00	1.00	1.00
6L	3.92E21	-7.95E00	1.00	1.00	1.00
8H	1.58E21	-7.73E00	1.00	1.00	1.00
8L	9.57E20	-7.73E00	1.00	1.00	1.00
12H	2.25E20	-7.42E00	1.00	1.00	1.00
12L	1.11E20	-7.37E00	1.00	1.00	1.00

TABLE 8 (continued)

Case 14	Function, $\ln \ln \nu = b \ln T + \ln \ln a$			$\ln \ln$
Sample	a	b	r	r_L
6H	7.72	-1.05	-0.99	-0.97
6L	7.77	-1.07	-1.00	-1.00
8H	7.52	-1.02	-1.00	-1.00
8L	7.71	-1.07	-0.99	-0.97
12H	7.43	-1.01	-0.99	-0.97
12L	7.63	-1.06	-1.00	-0.97

Case 15	Function, $\log_{10}\log_{10}\nu = b \log_{10} T + \log_{10}\log_{10} a$; log log			
Sample	a	b	r	r_L
6H	2.99	-1.05	-0.99	-0.97
6L	3.01	-1.07	-1.00	-1.00
8H	2.90	-1.02	-1.00	-1.00
8L	2.99	-1.07	-0.99	-0.97
12H	2.86	-1.01	-0.99	-0.97
12L	2.95	-1.06	-1.00	-1.00

Case 16	Function, $\ln \ln \nu = b \ln U + \ln \ln a$			$\ln \ln$
Sample	a	b	r	r_L
6H	6.89	-0.92	-0.99	-0.97
6L	6.65	-0.89	-0.99	-0.97
8H	6.45	-0.84	-0.99	-0.97
8L	6.73	-0.91	-0.99	-0.97
12H	6.48	-0.86	-0.99	-0.97
12L	6.65	-0.90	-0.99	-0.97

TABLE 8 (continued)

Case 17 Function, $\log_{10}\log_{10} \nu = b \log_{10}U + \log_{10}\log_{10}a$; log log

Sample	a	b	r	r_L
6H	2.63	-0.92	-0.99	-0.97
6L	2.52	-0.89	-0.99	-0.97
8H	2.44	-0.84	-0.99	-0.97
8L	2.56	-0.91	-0.99	-0.97
12H	2.45	-0.86	-0.99	-0.97
12L	2.53	-0.90	-0.99	-0.97

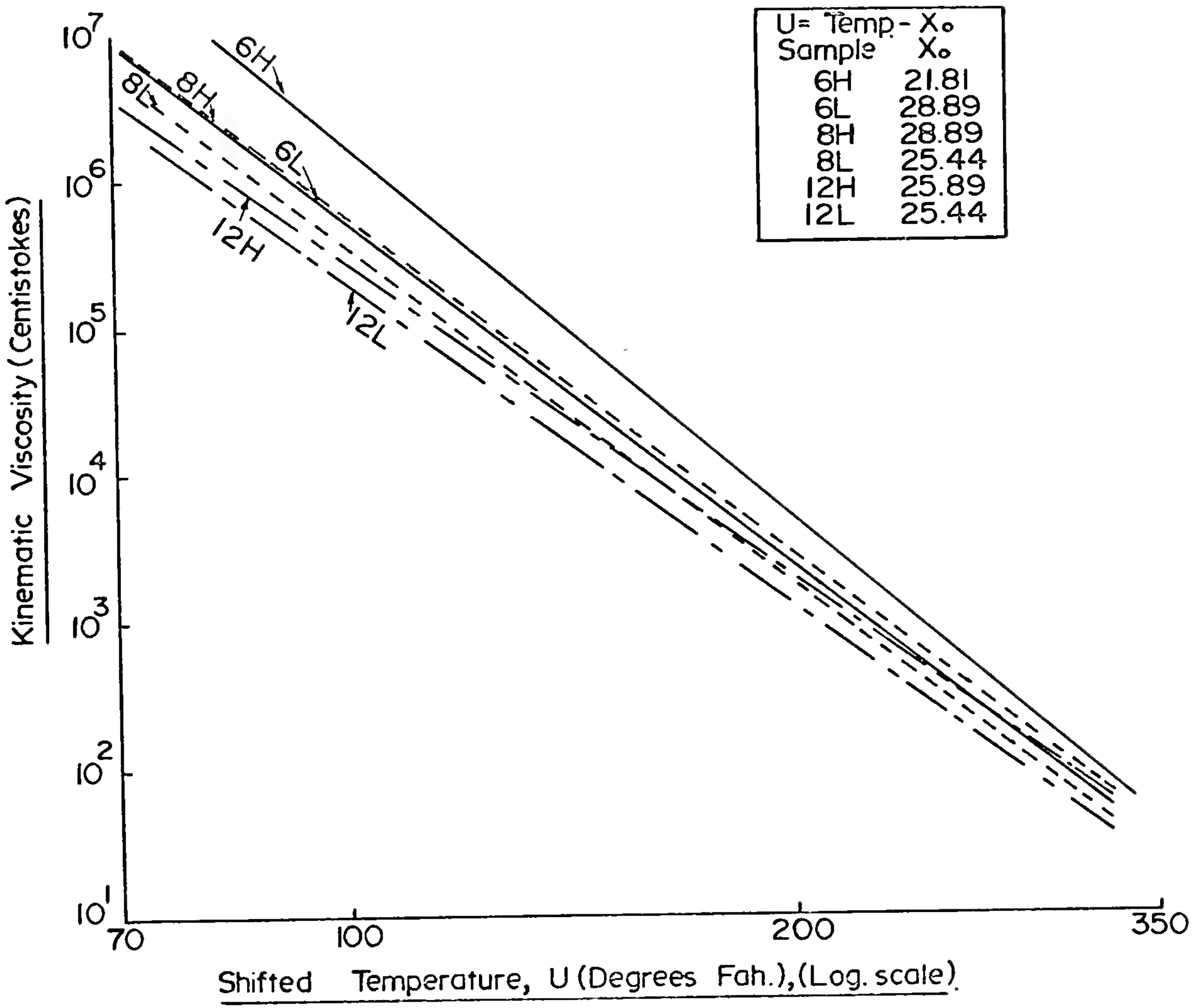

FIGURE 13 KINEMATIC VISCOSITY VS. SHIFTED TEMPERATURE ALL ASPHALTS.

IV. Fingerprinting of Study Asphalts

In order to catalog the test asphalts more accurately than is possible with the more common physical tests it was decided to fingerprint these materials according to the method presented by Rostler, et al. [44] and the Federal Highway Administration [45]. Laboratory testing for fingerprinting materials for this project was provided by Materials Research and Development of Oakland, California, under the direction of R. M. White. Fingerprint results as well as other physical properties for the test asphalts are included in the Federal Highway Administration Data Bank. Table 9 is a summary of fingerprint data.

TABLE 9

Fingerprint Data

Card Number	MR&D-5	MR&D-6	MR&D-7
Sample Identification	108	108	116
Project Identification	6H	6L	8H
Composition of asphalt, %			
Fraction A (asphaltenes)	25.3	21.3	27.9
Fraction N (nitrogen bases)	23.5	25.7	18.0
Fraction A_1 (first acidaffins)	17.0	19.6	17.7
Fraction A_2 (second acidaffins)	21.4	23.6	25.3
Fraction P (paraffins)	12.8	9.8	11.1
Wax	0.6	1.8	1.5
$(N + A_1)/(P + A_2)$	1.18	1.36	0.98
N/P	1.84	2.62	1.62
Refractive index of Fraction P (n_D^{25})	1.4861	1.4861	1.4817
Asphalt viscosity at 140°F, P	4122.	2472.	3114.
Penetration at 77°F, 100g, 5 sec.	63.	61.	80.
Maltenes viscosity at 77°F, P	4243.	17000.	1669.
at 140°F, P	41.16	76.48	16.02
at 275°F, cS	50.17	78.74	42.74
Molecular weight of Fraction A	6110.	4280.	5910.
Weight Loss in Thin Film Oven Test, %	0.52	0.04	0.29
Pellet abrasion loss at 77°F			
mg/revolution, unaged	0.108	2.030	0.155
aged 7 days	1.559	3.575	1.538
average of above	0.834	2.802	0.845
unaged	2.72	50.6	3.87
aged 7 days	39.1	89.4	39.0
average of above	20.9	70.0	21.4

TABLE 9 (continued)

Card Number	MR&D-8	MR&D-9	MR&D-10
Sample Identification	122	127	132
Project Identification	8H	12H	12L
Composition of asphalt, %			
Fraction A (asphaltenes)	20.7	26.4	19.8
Fraction N (nitrogen bases)	25.0	17.8	24.4
Fraction A_1 (first acidaffins)	19.6	117.1	19.7
Fraction A_2 (second acidaffins)	24.2	26.2	24.7
Fraction P (paraffins)	10.5	12.5	11.4
Wax	1.9	1.5	2.0
$(N + A_1)/(P + A_2)$	1.29	0.90	1.22
N/P	2.38	1.42	2.14
Refractive index of Fraction P (n_D^{25})	1.4809	1.4808	1.4803
Asphalt viscosity at 140°F, P	1089.	1476.	723.
Penetration at 77°F, 100g, 5 sec.	89.	116.	124.
Maltenes viscosity at 77°F, P	9366.	1202.	4920.
at 140°F, P	57.34	15.29	44.54
at 275°F, cS	67.60	36.34	60.23
Molecular weight of Fraction A	4160.	5850.	4350.
Weight Loss in Thin Film Oven Test, %	0.08	0.50	0.13
Pellet abrasion loss at 77°F			
mg/revolution, unaged	0.600	0.013	0.091
aged 7 days	2.638	0.200	1.062
average of above	1.619	0.106	0.576
unaged	15.0	0.33	2.28
aged 7 days	65.9	4.99	26.4
average of above	40.4	2.66	14.4

MIXTURE PROPERTIES

I. General

Three mixture gradations were used for each of the six asphalt cements previously discussed. Design asphalt content was determined by the Hveem (California) method as described by The Asphalt Institute [59].

II. Gradations

Mixture gradations for the experiment and typical Indiana State Highway Commission and Asphalt Institute Specifications for comparison are shown in Table 10; gradation curves are shown in Figure 14.

III. Mixture Designations

Gradations are designated as Coarse, Dense and Fine. In keeping with the designations for asphalt types as previously discussed, three letters are used to identify each mixture. The first number (6, 8 or 12) identifies the nominal asphalt penetration, the first letter (H or L) identifies the relative viscosity of the asphalt as high or low, and the second letter (C, D or F) identifies the mixture gradation as coarse, dense or fine. Hence a mixture designated as, say, 12LD consists of 120-150 nominal penetration grade asphalt cement of low relative viscosity and a dense gradation of aggregate.

TABLE 10

Mixture Gradations

Size	Percent Passing										
	Coarse					Dense			Fine		
	AI IIIC	ISHC #9 Binder	ISHC #9 Surface	ISHC #13 Base	Mix	AI IVb	ISHC #9 Surface	Mix	AI Vb	ISHC Curb Mix	Mix
3/4	100	100	100	90-100	100	100	100	100	100	—	100
1/2	75-100	73-91	76-96	60-90	90	80-100	76-92	91	85-100	100	93
3/8	60-85	40-73	46-77	—	72	70-90	46-77	76	—	85-92	90
4	30-50	24-46	32-53	35-60	45	50-70	32-53	54	65-80	60-80	80
8	20-35	18-39	24-47	—	34	35-50	24-47	46	50-65	55-70	65
16	—	12-34	17-40	—	27	—	16-40	37	37-52	35-55	51
30	5-20	5-22	6-26	12-30	19	18-29	6-26	25	25-40	20-40	39
50	3-12	1-14	2-17	—	11	13-23	2-17	16	18-30	10-25	24
100	2-8	0-6	0-7	—	6	8-16	0-7	7	10-20	5-15	14
200	0-4	0-4	0-4	0-5	4	4-10	0-4	4	3-10	2-8	8

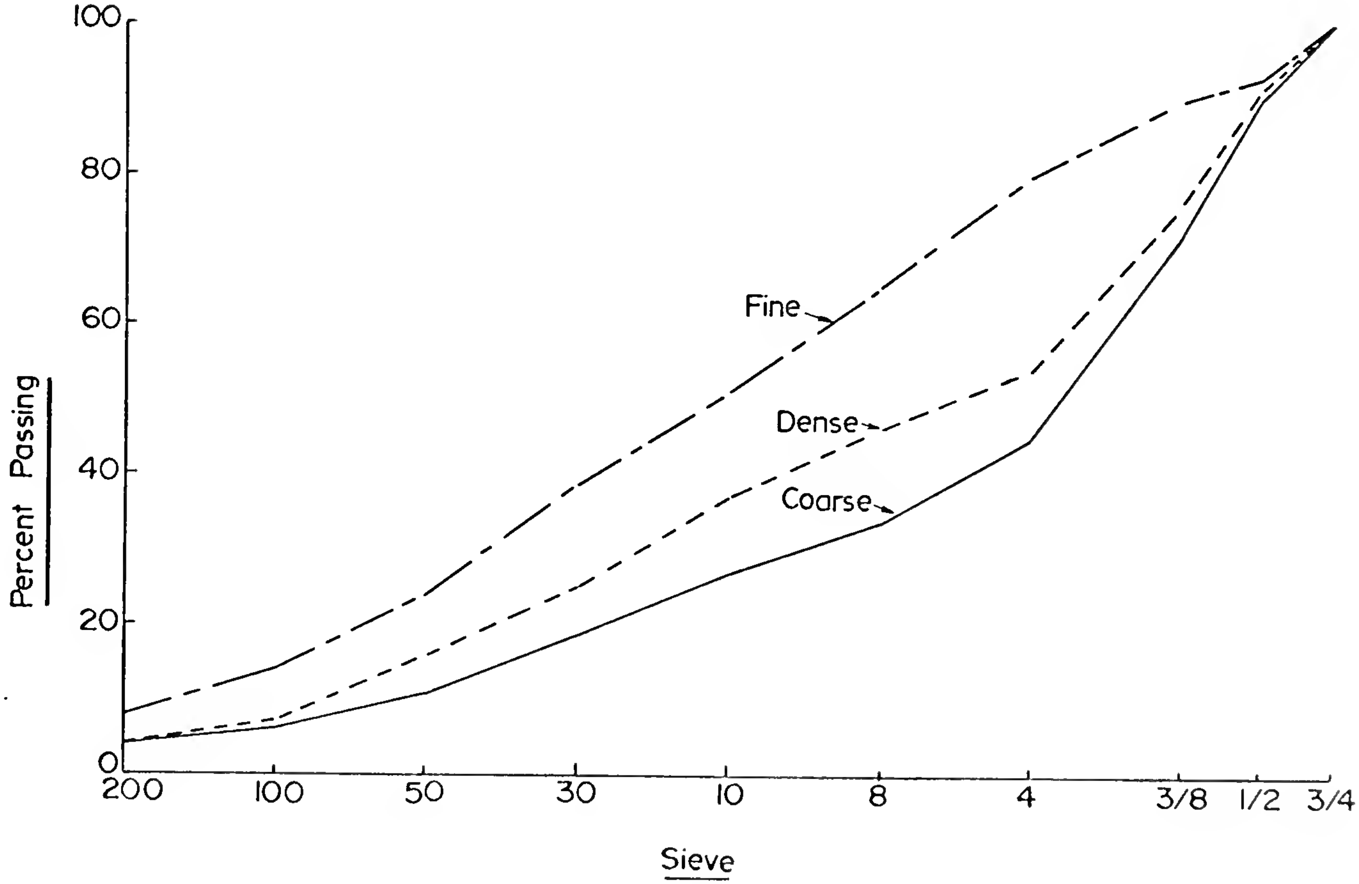

FIGURE 14 MIXTURE GRADATIONS.

IV. Specific Gravities and Water Absorption of Graded Aggregates

Specific gravities and absorption values of each aggregate fraction are given in the "aggregates" section. Specific gravity of the blended fractions that produce the mixture gradations were calculated from values obtained for the individual fractions. The reasons for using calculated values instead of direct measurement are twofold. First, many mixture combinations were used in designing the final gradations and asphalt combinations. This study required trials on approximately fifteen aggregate combinations before the final design would comply with nationally acceptable criteria. Determination of voids in the mixture is based partially on specific gravity of the aggregates, and each mixture trial requires that this property be evaluated. Time economy is greatly increased by using the calculated value rather than measuring the property for each trial. Secondly, in view of the inherent error in determining the saturated surface dry condition, as required by the standard test methods, it was decided that a large number of tests on fractions would provide greater precision than the same number of tests on a combined aggregate.

Specific gravities and absorptions were calculated for the coarse aggregate fraction (material retained on the No. 8 sieve) and the fine aggregate fraction (material passing the No. 8 and retained on the No. 200 sieve). These specific

gravities and absorptions were compared with values obtained by measuring these properties from replicated runs on the combined fractions. Replicate test results of the combined fractions comply with the ASTM precision requirement for specific gravity of a maximum difference of 0.020. These comparisons are included in Tables 11 and 12.

Values used for design and analysis are as follows:

Gradation	G_{BULK}	G_{APP}
Coarse	2.582	2.739
Dense	2.601	2.747
Fine	2.648	2.777

V. Surface Area of Aggregate

Surface areas of the aggregate were calculated using the California surface area factors [59]. This method multiplies a factor for each sieve size by the percentage by weight passing the sieve to give the surface in square feet per pound of material of that fraction. The sum of the surface areas of the fractions is the surface area of the blend of fractions used in the mixture. Surface areas of aggregates used for this study are as follows:

Gradation	Surface Area (ft^2/lb.)
Coarse	22.38
Dense	27.28
Fine	44.14

TABLE 11

Calculated vs. Measured Specific Gravity of Graded Coarse Aggregate

Gradation		Δ = Calc. - Meas.			
		G_B	G_{BSSD}	G_{APP}	% ABS
Coarse	Calc.	2.528	2.600	2.698	2.647
	Meas.	2.532	2.596	2.704	2.516
	Δ	-0.004	0.004	-0.006	0.131
Dense	Calc.	2.538	2.597	2.703	2.516
	Meas.	2.535	2.598	2.704	2.468
	Δ	0.003	-0.001	-0.001	0.902
Fine	Calc.	2.529	2.602	2.715	2.693
	Meas.	2.536	2.604	2.720	2.646
	Δ	-0.005	-0.002	-0.005	0.047

TABLE 12

Calculated vs. Measured Specific Gravity of Graded Fine Aggregate

Gradation		Δ = Calc. - Meas.			
		G_B	G_{BSSD}	G_{APP}	% ABS
Coarse	Calc.	2.674	2.720	2.800	1.671
	Meas.	2.738	2.762	2.808	0.918
	Δ	-0.064	-0.042	-0.008	0.753
Dense	Calc.	2.682	2.723	2.795	1.517
	Meas.	2.686	2.706	2.740	0.725
	Δ	-0.004	0.017	0.055	0.792
Fine	Calc.	2.685	2.726	2.796	1.491
	Meas.	2.756	2.774	2.806	0.644
	Δ	-0.071	-0.048	-0.010	0.847

VI. Hveem Mix Design

A. Trial Mixtures

Pertinent data for entering the mix design charts [59, 60] and design constants from the charts are shown in Table 13.

TABLE 13

Hveem Mixture Design Constants

Constant	Gradation		
	Coarse	Dense	Fine
Corr. CKE	2.58	2.64	2.83
K_f	1.00	1.03	1.00
Oil Ret.	4.3	4.3	4.3
Corr. K_c	1.86	1.92	1.87
K_m	1.16	1.19	0.97
Oil Ratio	3.51	4.00	4.15
Bit. Ratio	5.4	5.5	5.2

Mixtures were prepared using the estimated asphalt contents (bitumen ratio) from the design charts, and specimens were fabricated for stability and cohesiometer testing and density-voids analysis. For these asphalt contents, stability and cohesiometer values were adequate for heavy traffic (stabilities were 46, 50 and 48 for the coarse, dense and fine mixtures, respectively) but air voids in the compacted mixture exceeded the desirable level of 2-5 per

cent. Actual values were 7.3, 8.1 and 8.9 per cent for the coarse, dense and fine mixtures, respectively. Two alternatives are available to adjust mixture components to reduce air voids to an acceptable level; these are, (1) change aggregate gradation, usually by increasing the finer portions, or (2) increase the asphalt content.

Because calculated voids in the mineral aggregate are very close to minimum acceptable values and since the gradations as used in the trial mixtures is approaching the fine limit of the Indiana State Highway Commission Specifications for these types of mixtures, the first alternative was rejected and the second was chosen for trial. Calculations show, that to reduce voids in these mixtures by four per cent, approximately four additional grams of asphalt per 100 cc. of mix is necessary, hence three more sets of mixtures were fabricated and tested at these increased asphalt contents. Voids for both sets of preliminary mixtures were plotted and linear interpolation of these values was used to select the final mixture components.

B. Density - Voids Analysis

1. Absorbed asphalt was calculated using the technique outlined by The Asphalt Institute [59] which is based on the Rice method (ASTM D2041-64T, "Maximum Specific Gravity of Bituminous Paving Mixtures"). Tests were run for each asphalt-aggregate combination (18 tests) and, working under the supposition that absorption is a function of aggregate

characteristics and not asphalt, average maximum specific gravity for each of the gradations was calculated. This average includes all asphalt types for a given gradation of aggregates and since the method of measurement has some degree of error, ASTM E178 ("Standard Recommended Practice for Dealing With Outlying Observations") was used to reject values that did not belong to the population. Average values were used to calculate absorbed asphalt which, in turn, were later used to calculate air voids. A summary of measurements is given in Table 14.

TABLE 14

Absorbed Asphalt

Gradation	Coarse	Dense	Fine
No. Measurements	6	5	6
Rejected Specimen	12H	8L & 6L	8L
Avg. Absorbed Asph. (%)	2.339	1.972	1.452
Std. Deviation	0.050	0.043	0.072

For reference purposes, water absorption for each gradation was calculated from the measured values for each fraction and a regression was written for the three gradations. Results are:

$$A_{ac} = 1.905 \times A_w - 1.903$$

where A_{ac} = % asphalt absorbed

A_w = % water absorbed

and $$r = \frac{\Sigma xy}{\sqrt{(\Sigma x^2)(\Sigma y^2)}} = 0.996 \qquad \left\{\begin{matrix} r_U = 0.999 \\ r_L = 0.987 \end{matrix}\right\}$$ see p. 51.

2. Bulk Density

Bulk densities were run on the 18 test specimens prior to running measurements for absorbed asphalt. These tests were performed in strict accordance with ASTM D2726. Results are given in Table 15.

TABLE 15

Bulk Specific Gravity

		Gradation		
		C	D	F
Asphalt	6H	2.401	2.377	2.383
	6L	2.403	2.377	2.387
	8H	2.402	2.370	2.385
	8L	2.393	2.384	2.407
	12H	2.402	2.363	2.388
	12L	2.406	2.367	2.395

Since density would be used to evaluate fabrication techniques and specimen variability for the main experiment, it was decided that an analysis should be run to determine the effects of asphalt type and aggregate gradation on bulk density.

Homogeneity of variance was checked by Foster and Burr's q test [52] and no transformation was necessary.

Results of this analysis are shown in Table 16.

TABLE 16

ANOVA, Effect of Mixture Components on Bulk Density

ANOVA					
Source	SS	df	MS	F	F Crit (0.05)
Asphalt	1.99E-04	5	3.99E-05	0.68	3.33
Gradation	2.44E-03	2	1.22E-03	20.6	4.10
Residual	5.90E-04	10	5.90E-05		
Total	3.23E-03	17			

Analysis shows that asphalt type is not a significant factor and hence average bulk density can be determined for a given gradation by using all asphalt types within that gradation.

Average bulk specific gravities and the 95% confidence limits on upper and lower values are shown in Table 17.

TABLE 17

Average Bulk Densities

Gradation	Bulk Specific Gravity			Avg. Bulk Density (pcf)
	L	$\bar{X}$	U	
C	2.397	2.401	2.406	149.8
D	2.367	2.376	2.385	148.2
F	2.381	2.390	2.398	149.1

C. Summary of Mixture Properties

Summary of mixture properties is included in Table 18. Figure 15 shows mixture properties as functions of asphalt content.

VII. Hardening of Asphalt During Mixing and Curing

In order to determine the extent of hardening (loss of penetration) during mixing (approximately two minutes at 300°F (148.9°C)) and curing (fifteen hours in a 140°F (60.0°C) forced draft oven), replicate mixture specimens were made and tested. Two dense-graded mixtures were made with each of the six test asphalts. After curing at 140°F (60.0°C), the temperature of the mixture was increased to 235°F (112.8°C) in the same manner that was used to prepare both mix design and tension test specimens for compaction. Mixtures were then subjected to reflux extraction according to ASTM D2172, Method C ("Quantitative Extraction of Bitumen from Bituminous Paving Mixtures"). Asphalt was then separated from the trichloroethylene solvent by the Abson Method (ASTM D1856, "Recovery of Asphalt from Solution by Abson Method"). Penetration tests were made on the recovered asphalts.

To evaluate the effects of extraction and recovery on the asphalt in question, a blank sample was subjected to the process as follows:

1. A nominal 85-100 material (asphalt project number 116 which is classified as 8H) was subjected to the standard

TABLE 18

Summary of Mixture Properties

Property/Mixture	6HC	6HD	6HF	6LC	6LD	6LF
% Asph. by wt. agg.	6.8	6.8	6.9	6.8	6.8	6.9
% Agg. by wt. mix	6.37	6.37	6.45	6.37	6.37	6.45
% Agg.	93.63	93.63	93.55	93.63	93.63	93.55
Mix bulk sp. gr.	2.401	2.376	2.390	2.401	2.376	2.390
Absorbed Asph. (%)	2.339	1.972	1.452	2.339	1.972	1.452
Agg. bulk sp. gr.	2.582	2.601	2.648	2.582	2.601	2.648
Asph. sp. gr.	1.028	1.028	1.028	1.028	1.028	1.028
% Effective Asph.	4.180	4.524	5.092	4.180	4.524	5.092
VMA (%)	12.9	14.5	15.6	12.9	14.5	15.6
Air voids (%)	3.2	4.0	3.7	3.2	4.0	3.7
Stability	42.	46.	42.	45.	48.	45.
Cohesiometer	277.	390.	268.	335.	359.	303.

Property/Mixture	8HC	8HD	8HF	8LC	8LD	8LF
% Asph. by wt. agg.	6.8	6.8	6.9	6.8	6.8	6.9
% Agg. by wt. mix	6.37	6.37	6.45	6.37	6.37	6.45
% Agg.	93.63	93.63	93.55	93.63	93.63	93.55
Mix bulk sp. gr.	2.401	2.376	2.390	2.401	2.376	2.390
Absorbed Asph. (%)	2.339	1.972	1.452	2.339	1.972	1.452
Agg. bulk sp. gr.	2.582	2.601	2.648	2.582	2.601	2.648
Asph. sp. gr.	1.031	1.031	1.031	1.027	1.027	1.027
% Effective Asph.	4.180	4.524	5.092	4.180	4.524	5.092
VMA (%)	12.9	14.5	15.6	12.9	14.5	15.6
Air voids (%)	3.2	4.0	3.8	3.2	4.0	3.7
Stability	45.	47.	43.	47.	46.	45.
Cohesiometer	387.	435.	344.	334.	378.	351.

TABLE 18 (continued)

Property/Mixture	12HC	12HD	12HF	12LC	12LD	12LF
% Asph. by wt. agg.	6.8	6.8	6.9	6.8	6.8	6.9
% Agg. by wt. mix	6.37	6.37	6.45	6.37	6.37	6.45
% Agg.	93.63	93.63	93.55	93.63	93.63	93.55
Mix bulk sp. gr.	2.401	2.376	2.390	2.401	2.376	2.390
Absorbed Asph. (%)	2.339	1.972	1.452	2.339	1.972	1.452
Agg. bulk sp. gr.	2.582	2.601	2.648	2.582	2.601	2.648
Asph. sp. gr.	1.027	1.027	1.027	1.026	1.026	1.026
% Effective asph.	4.180	4.524	5.092	4.180	4.524	5.092
VMA (%)	12.9	14.5	15.6	12.9	14.5	15.6
Air voids (%)	3.2	4.0	3.7	3.2	4.0	3.7
Stability	41.	46.	40.	44.	43.	41.
Cohesiometer	413.	349.	405.	377.	323.	379.

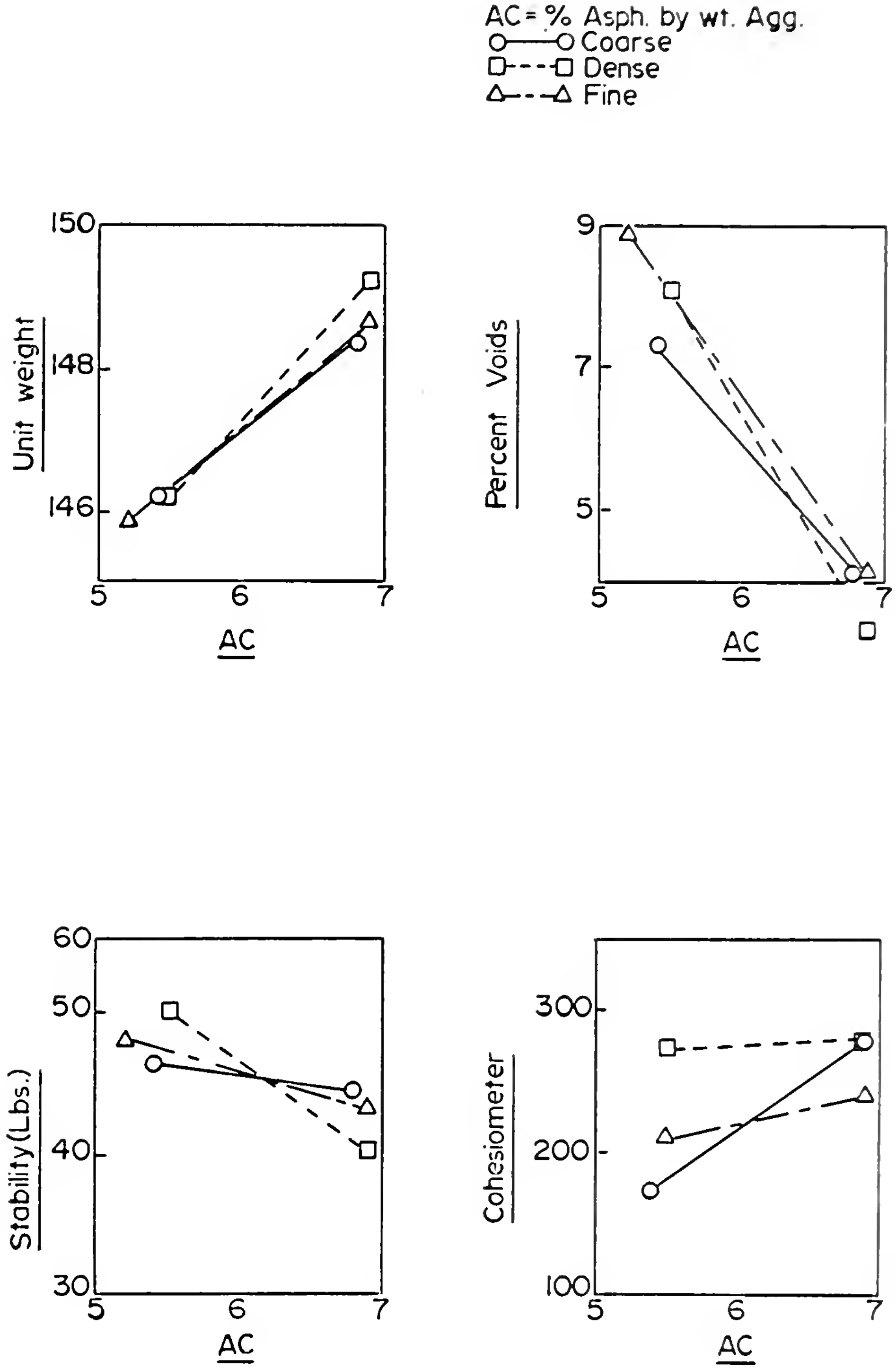

FIGURE 15 MIXTURE PROPERTIES.

thin film oven test (ASTM D1754, "Effect of Heat and Air on Asphaltic Materials"), to provide approximately the same degree of hardening as the mixing process, and penetration was determined before and after exposure to heat and air.

2. This material was then placed in the same amount of solvent and heated in the reflux extractor for the same amount of time as was used to extract asphalt from the mixtures.

3. Asphalt from the blank sample was then removed from the solvent by the Abson process.

4. Penetration tests were performed on the recovered asphalt.

Results of penetration testing of the blank are:

Penetration of asphalt before TFO = 75

Penetration after TFO and after being processed through recovery = 48

Penetration after TFO = 50

It was concluded from this set of tests on the blank specimen that there is no significant change in penetration due to the extraction and recovery process.

Results of penetration testing of materials before and after extraction and recovery are given in Table 19.

With the exception of the 6H material, penetration retained is practically a constant value of approximately 67 per cent of the original. This compares with an average of 62 percent penetration retained after the Thin Film Oven

Test. If 6H is removed, the average penetration retained is 63 per cent of the original.

TABLE 19

Asphalt Hardening Due to Mixing and Curing

Asphalt	Pen. Before Mixing	Pen. After Recovery			Pen. (after) / Pen. (before)
		#1	#2	Avg.	$P_A \div P_B$
6L	55	34	38	36	0.65
6H	56	51	45	48	0.86
8L	78	46	55	50	0.65
8H	75	50	49	50	0.66
12L	117	62	79	71	0.60
12H	112	70	65	68	0.60

DESIGN OF THE EXPERIMENT

I. Introduction

1. Response Variable

The primary response or dependent variable to be evaluated by this study was limiting strain. Limiting strain is defined as strain at failure or the strain that is associated with the maximum load carried when a specimen is loaded in direct uniaxial non-repeated tension. This definition may be redefined after the study and during application as working strain. Working strain is that strain associated with maximum allowable stress, usually failure stress modified by an appropriate safety factor.

2. Controlled or Independent Variables

Variables that were intended to be completely controlled during this study were:

A. Strain rate. This variable was intended to be controlled at four levels. The upper level was chosen to simulate high speed traffic, either a design tractor-trailer combination (WB-50) moving at 70 miles per hour in the highway case, or a design aircraft (DC-8) at a take-off rotation or landing speed of about 150 miles per hour in the case of airfields. The lower level was intended

to simulate contractions that occur during a six hour temperature change of approximately 100°F (55.6°C). Two intermediate levels were to be selected at uniform spacing to provide orthogonality for this factor of the experiment.

B. Mixture types. This variable was controlled at 18 levels. Three aggregate gradations, coarse, dense and fine and six asphalt types (6H, 6L, 8H, 8L, 12H, 12L) were to be considered for each of the gradations. Each mixture was tested at its single optimum asphalt content as determined by the Hveem method of mixture design.

C. Temperature. This variable was controlled at six levels. The upper level was 140°F (60.0°C) which is approximately the highest temperature that a pavement will experience in most of continental United States. This is also the standard test temperature for stability measurements that are used for mixture design. A lower limit was to be chosen that simulates a reasonably low temperature that would occur in the country and that would also place the asphalts in a glassy condition. Selection of this temperature will be discussed later. One intermediate temperature that must be considered is 77°F (25.0°C) which is commonly used in standard tests of asphalts.

II. Selection of Levels of Independent Variables

1. Load Induced Strains

Maximum strain rate was calculated for two pavement design situations, a typical heavy-duty (Interstate) highway and an airfield suitable for air carrier service.

Pavement sections were designed according to accepted practice [61, 62] and strains at the bottom fiber were calculated for each loading condition and pavement section by BISTRO [63] program on the Purdue CDC 6500 computer.

A. Highway design:

a. Subgrade, CBR = 10 (assumed).

b. Granular Base, CBR = 100 (assumed).

c. Traffic (4-lane interstate)

1) IDT = 10,800

2) 45% trucks in design lane, 19% heavy trucks with 42K average weight.

d. Design period = 25 years with 4% annual growth rate.

e. Alternative sections:

1) 9 inches A.C. (T_A) directly on subgrade.

2) 4 inch A.C. surface; 6½ inch hot mix sand base on subgrade.

3) 6½ inch A.C. surface, 5 inch granular base on subgrade.

f. For stress and strain calculations, the most severe case was shown by BISTRO to be the

standard AASHTO WB-50 tractor-trailer combination with 90 psi inflation pressures and loaded to the Indiana legal limit of 72K. Maximum tensile strain occurs in the extreme fiber of the section using granular base (case 3). Calculated maximum strain for this case amounted to 128 MII where MII is the standard abbreviation for microstrain or millionths of an inch per inch.

B. Air field design.

a. Subgrade, CBR = 10 (assumed).

b. Mean annual air temperature = 49.9°F (Lafayette, Indiana).

c. Traffic analysis used the same traffic as the example of the design manual [62].

d. Pavement section is 19 inches A.C. (T_A) directly on subgrade.

e. Strain calculations by BISTRO were based on the standard loaded DC-8 design vehicle. Maximum tensile strains at the extreme fiber for the airfield section were calculated by BISTRO to be 254 MII.

2. Maximum Strain Rate

BISTRO was used to calculate a strain influence line for each pavement situation by plotting strain contours and locating the points of maximum strain and the point where

strains approach zero for a static load. It was then assumed that strains for the dynamic and static case would be practically the same and times were calculated for the wheel to move from the point of essentially zero strain to the point of maximum strain for various speeds of the design vehicles. Maximum practical speeds used were 70 mph for the WB-50 truck and 150 mph for the DC-8 (which is approximate speed at rotation for take-off and also the approximate ground speed at landing touchdown). Strain rates as calculated by this method were 106 MII per second for the highway and 159 MII per second for the airfield. Maximum strain rate for the experiment was thus set at 159 MII per second.

3. Minimum Strain Rate

Lowest level strain rate is intended to simulate those contraction strains that occur due to temperature change over protracted periods of time. Haas [64] used a crosshead speed of 2×10^{-4} to 6×10^{-4} centimeters per minute for low temperature cracking studies which, for four inch specimens, amounts to approximately 0.3 MII per second. This is within the same order of magnitude as strain values resulting from calculations based on a 100°F (56.6°C) temperature change over a six hour period using a coefficient of linear expansion of 1.2×10^{-5} inches per inch per degree Fahrenheit as reported by Hooks and Goetz [65]. Accordingly, the lower limit was set at 0.3 MII per second.

4. Intermediate Strain Rates

In order to maintain orthogonality of the experiment, two intermediate strain rates equal spaced between upper and lower limits were chosen.

5. Summary of Strain Rates

The four levels of experimental strain rate selected are 159, 106, 53.2 and 0.321 MII per second.

6. Mixture Types

Mixture types as discussed in "Introduction."

7. Temperature

Six levels of temperature were selected using an upper limit of 140°F (60.0°C) and an intermediate temperature of 77°F (25.0°C). Since it was considered desirable to have a test temperature between 140 and 77 and also to include testing at temperatures where asphalts become glassy (or at least more glassy than viscous) while maintaining orthogonality in the experiment, a temperature increment of 31.5°F (17.5°C) was used to set test temperatures. This increment provided a low temperature limit of -17.5°F (-27.5°C) which would generally be regarded as placing most asphalts in the glassy behavior region.

Test temperatures were thus set at 140°F (60.0°C), 108.5°F (42.5°C), 77°F (25.0°C), 45.5°F (7.5°C), 14°F (-10.0°C), and -17.5°F (-27.5°C).

III. Ideal Replicated Full Factorial Experiment

Preliminary experiments indicated that at least three replications per cell were necessary to evaluate variability. Using levels of variables as outlined above, the number of tests required is calculated as follows:

Strain rates	4
Temperatures	6
Mixtures	18
Replications	3

Total = 4 × 6 × 18 × 3 = 1296

IV. Final Experiment Design

The amount of aggregate and asphalt available as well as the availability of fabrication and testing facilities make the number of tests required for a full factorial experiment impractical. Rather than arbitrarily reduce the replications or remove some levels of the independent variables, it was decided, after discussion, to proceed as follows: Perform an exploratory experiment at a single temperature near the middle of the temperature range (77°F (25.0°C) was selected) and include all mixture types to investigate the effect of mixture variables. After the first experiment was completed and analyzed, another was performed on a single mixture type (8LD) at all temperatures to determine the effects of temperature.

Information from the two exploratory experiments was used to partially evaluate the effects of all the independent variables and to evaluate variability for any given single set of conditions. These results were then used to determine which cells to proceed to for completion of the experiment.

It is realized that this type of procedure will somewhat limit complete randomization of the entire experiment in its final form and that the method is sequential in nature, but under the constraints of limited time and quantities of materials and no available previous data this method appeared to have reasonably good information efficiency.

Test values and sequential operations are reported in "Experimental Results and Analysis."

EXPERIMENTAL SET-UP

I. Temperature Control

Tension specimens were tested in a constant temperature chamber that was supplied with conditioned air from a larger conditioning box. Inside dimensions of the larger conditioning box are approximately five feet by five feet by three feet high. The structure consists of double-wall construction of 20 gage steel with two layers of two inch Styrofoam PR for insulation.

Two cooling units and one heating unit are used to condition air in the larger box. For low temperatures, cooling is provided by a Copeland Model CDAL 0200, 6200 BTUH, 2 h.p. condensing unit and a Bohn Model 650 EL, 6500 BTUH evaporator. Temperature control of this unit is achieved by manually adjusting an expansion valve located between the condenser and evaporator.

For temperatures only slightly below room temperature a smaller self-contained Copeland Model CSAS 0100, 1 h.p. condensing unit is used with approximately 60 feet of finned tubing forming a separate evaporator. This evaporator is mounted on the same frame and carriage as the larger evaporator in order to utilize the air circulation fan of the larger unit. Evaporator temperatures of this

unit are controlled by manually adjusting the expansion valve of the unit.

Separate units for very low and moderately low temperatures were used for two reasons. First, capacity of the large unit is so great that it was questionable that the unit could be shut down far enough to provide moderately low temperatures. Secondly, it was feared that even though the valving to the evaporator could be closed enough to prevent refirgerant flow that would cause lower temperatures than desired, amperage loads of the compressor motor would be high enough to damage the unit. After the conditioning box was constructed and the larger refrigeration unit was installed, tests were conducted and both conditions mentioned above did exist at moderate temperatures and the second refrigeration unit was installed.

A Chromalox Model CSF-220, 6824 BTUH, 2000 watt, 240 volts is used. Firing of the heater is by a 110 volt relay which is controlled automatically by a Research, Inc. Model 640B (IP-13)-DATR Process Controller. Temperature information is provided to the process controller by a Rosemount Model 104MA-35-A-A-C-A Platinum Resistance Temperature Sensor.

Temperatures only slightly above or below room temperature are provided by running the small compressor unit in conjunction with the automatically controlled electric heating system.

Inside dimensions of the test chamber are approximately two feet by two feet by three feet high. Construction is the same as for the larger box. Insulation and seals where actuator rods enter the top and bottom of the test chamber are flexible foam plastic.

Conditioned air is circulated from the larger control box to the smaller test chamber and returned to the box by six-inch round metal pipe ducts covered with two one-inch thicknesses of Armstrong Armaflex 22 flexible foam plastic insulation. Air is circulated by a foam insulated American-Standard Model 1-M, 300 cfm, 1/20 h.p. utility set. The system is designed so that ducts can be easily removed and replaced to allow flexibility in locating the test chamber remotely from the conditioning box.

Temperature readout for the conditioning box, temperature chamber, and both inlet and outlet ducts is by a Rosemount Model 2501 Digital Temperature Indicator with a ten position expandable switch. The temperature indicator is mounted on the testing machine control console. Sensors for the locations listed above are the same type of platinum units used to provide signals to the process controller.

Each sensor in the system was calibrated with a precision mercury thermometer throughout the range of test temperatures and applicable correction factors were applied during the experiment.

Brass cylindrical canisters with screened ends with approximate dimensions of five and one-half inch diameter by twelve inches long and partially filled with a moisture indicating commercial dehydrating agent were placed in each of the ducts to remove moisture from circulated air. These canisters were only used during low temperature testing and when laboratory relative humidity was high enough to produce frost or ice deposits when the system was opened to the atmosphere.

Tests of the system showed capabilities of maintaining plus or minus one degree Fahrenheit for extended periods (8 to 24 hours) and plus or minus one-half degree for shorter periods of approximately four hours. It should be noted that maintaining these temperature tolerances required continuous monitoring and adjustment to compensate for opening and closing of the system and for changes in laboratory room temperature.

Reasons for using a system involving a separate conditioning box and test chamber and for selecting the various system components are as follows. Several commercial temperature chambers were considered and investigated. Generally these systems are designed to provide either very low or very high temperatures far beyond the ranges necessary for this project or others that are presently anticipated. Furthermore, these low temperature systems employ liquid nitrogen or some similar non-reusable refrigerant with

consequent problems of availability, cost, transportation, handling and storage. Commercial units that provide both high and low temperatures have space capacities considerably less than the system used for this study and estimated costs were approximately three times greater than those incurred in providing the system.

Two distinct advantages of the system are that all components are shelf items and hence adjustments and repairs are readily available. However, it should be stated that there were no breakdowns or malfunctions during approximately one year of practically constant use. Another is that by using a large conditioning box with the smaller test chamber, thermal shock and small outside variations in temperature are relatively easy to accommodate due to the large volume of conditioned air in the system. Finally, a two-box system provides a degree of flexibility not inherent in commercial models in that control takes place in the conditioning box. The test chamber can be constructed to accommodate whatever specimen geometry is necessary. Design of the system was made by the author and fabrication and installation was by the Purdue University Physical Plant.

II. Temperature Monitoring of Specimens

A dummy specimen of the same size, shape and average composition as the test specimens was prepared and a calibrated thermistor was embedded in a drilled hole to sense temperature at its geometrical center. The drilled hole

was packed with insulation to prevent outside conditions from affecting the sensor. The dummy specimen was placed with the test specimens and temperature was monitored during conditioning and testing; it was assumed that the dummy and test specimens were at the same temperature.

III. Loading System

Loads for the experiment were applied by an MTS electro-hydraulic closed loop testing machine using a 30 kip actuator in stroke control with load read-out through a 50 kip load cell. Electrical and mechanical components of the system were calibrated and adjusted by a factory technician just prior to the experiment. Equipment operation for the experiment was conducted by the author.

Frequency control modules and hence strain rate control for this machine does not include a slow enough stroke rate to provide the lower strain rates necessary for this study. This is due to the existing combination of pump capacity and activator range available to apply loads of a necessary magnitude. As part of this project electronic additions were made to the frequency control module of the function generator to provide for the slower rate of ram movement. This controller was designed and built by a qualified electronics technician of the Joint Highway Research Project staff and was installed after consultation with the manufacturer of the testing machine. A schematic

diagram of this analog converter and a calibration curve for capacitance versus head speed is included in Figures 16 and 17.

IV. Frame Compliance

The original design of the experiment intended to use direct readout from the MTS machine to record load and ram displacement in tension and then to convert these values to stress and strain by dividing load by cross-sectional area to obtain stress and by dividing ram displacement by gage length to obtain strain. Experiments involving acoustic emissions of portland cement concrete in uniaxial compression showed spurious results when calculating Young's modulus based on values of strain obtained from measured stroke displacement and gage length. Strains based on stroke and those obtained from resistance strain gages attached to concrete specimens suggested that either movement of the frame was taking place or that incorrect displacements were being indicated by the displacement transducers (LVDT) of the testing machine actuator. Measurements by dial indicators showed that original machine calibration had not changed and hence some of the ram displacement was being taken up by the machine frame instead of the specimen.

In order to determine if tensile loads would cause a frame compliance error, and to evaluate the magnitude of this error along with measurement of deformation of proposed specimen attachment linkages, the following experiment was

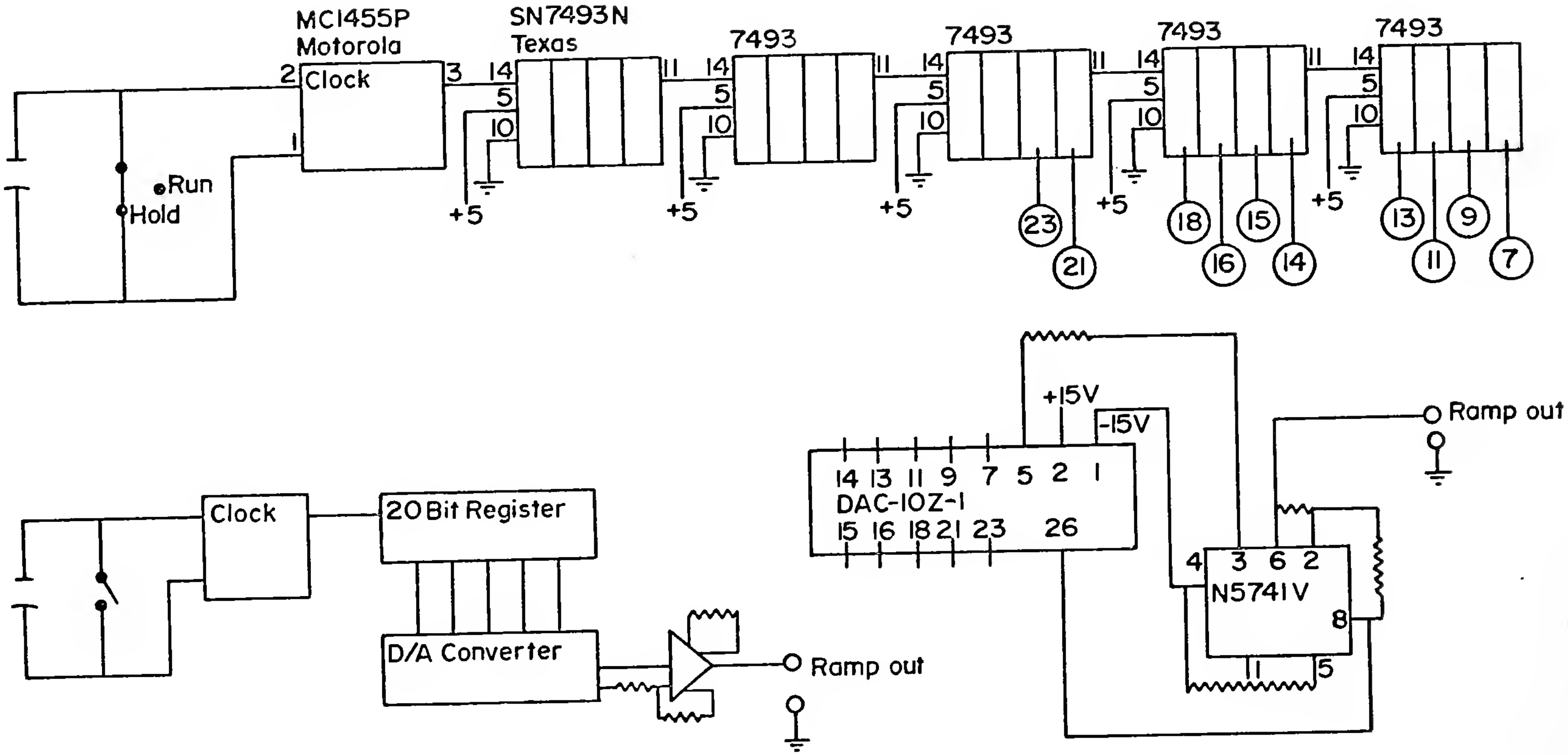

FIGURE 16 RAMP GENERATOR.

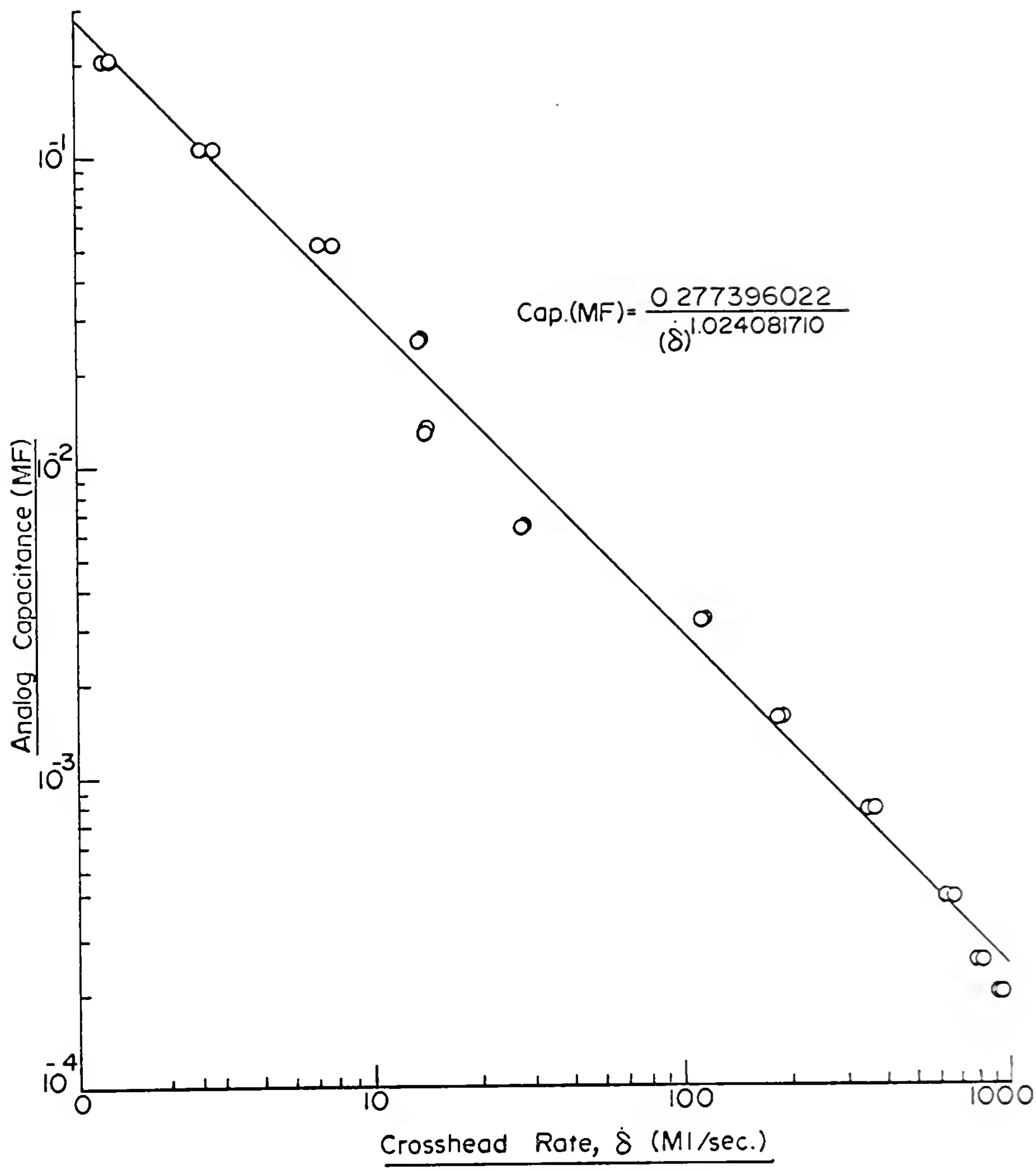

FIGURE 17 ANALOG CONTROLLER CALIBRATION.

performed. A four-inch diameter by four-inch high steel specimen was tested in direct tension. Attachment of the specimen to the testing machine was accomplished by fixing steel caps to each end of the specimen with a two-part epoxy adhesive. Two chain links between each cap and its actuator rod were installed to eliminate torque on either the specimen or actuators. Strain gages were attached to the specimen and an acoustic emission transducer was placed on one of the caps to monitor cracking and failure of the epoxy adhesive. Several specimens were loaded in tension and it was reasoned that the difference between specimen deformation as determined by strain gages, and checked theoretically, and the ram movement would be total system compliance that included frame, actuator rod, cap and adhesive movement. A correction factor could be applied to remove this system deformation from the subsequent measurements of asphalt concrete in tension.

Figure 18 shows results of several of these measurements. Examination of the data shows that total compliance variability is so large that realistic correction factors could very well mask or confound the effect that was to be investigated in the final experiment. It was deduced that other methods of strain measurement would have to be developed.

V. Strain Measurements

Two other methods of strain or displacement measurement are available; direct strain measurement with electrical

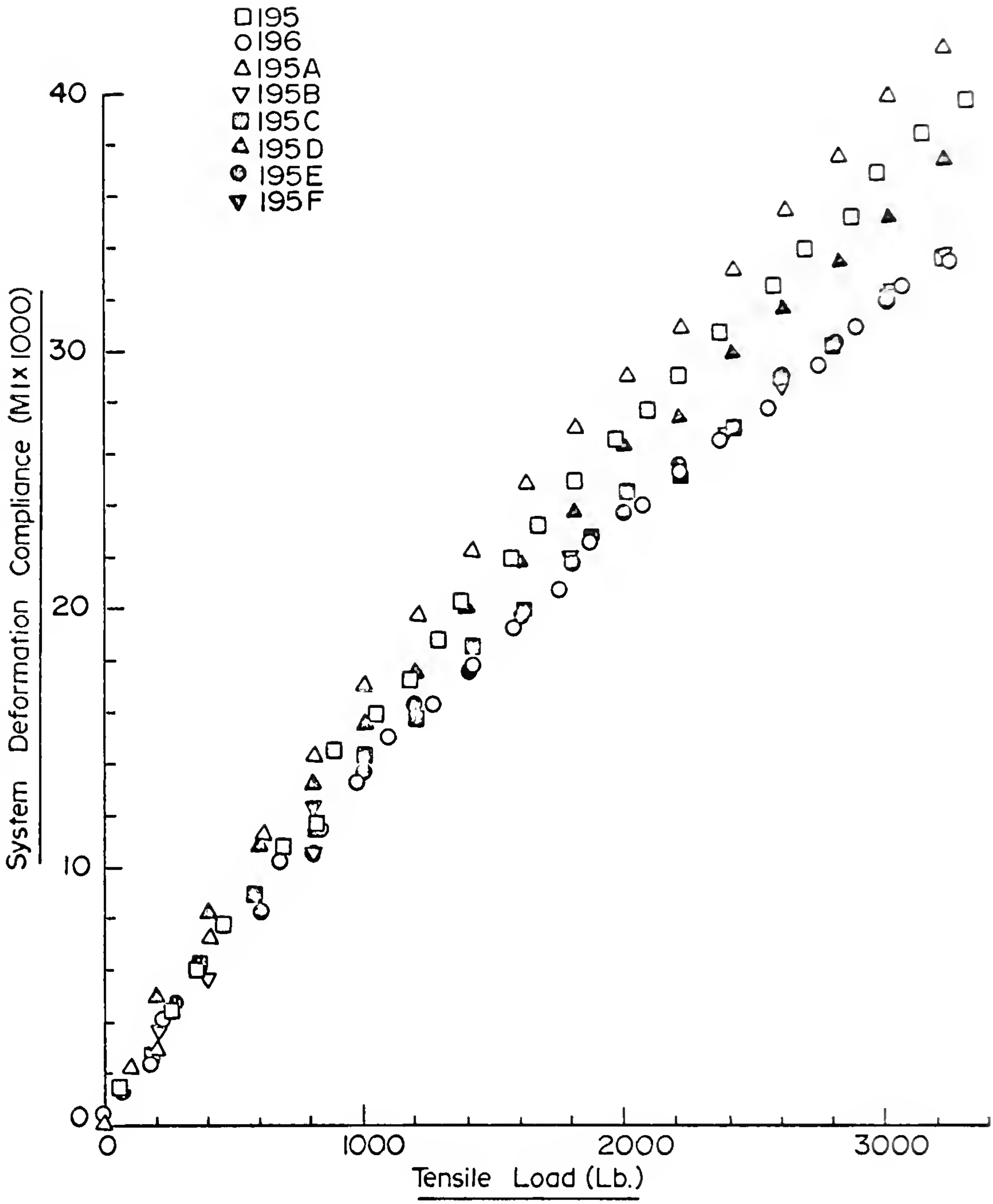

FIGURE 18 TESTING SYSTEM COMPLIANCE.

resistance strain gages and measurement with an extensometer. Either of these could be applied directly to the specimen and thus isolate specimen deformation from all other frame and connection movement.

Experiments with electrical resistance strain gages were performed to evaluate the technique. Several strain gage arrangements were evaluated that included foil micro-gages with gage lengths of approximately one-fourth of an inch, foil gages with gage lengths of one inch and SR-4 type gages. In all cases fixing the gages to asphalt concrete was extremely difficult. Recommended adhesives would either soften the asphalt or simply would not adhere, particularly at the extreme temperatures necessary for the test. Because of these difficulties in mounting, lack of reliability under conditions of the experiment, erratic results during the test and overall cost and time economy, direct measurement by strain gages was eliminated as a measuring technique.

Final selection of deformation measurement technique involved the use of an extensometer directly fastened to the specimen. This device consists of aluminum yokes at top and bottom of the specimen which hold a set of LVDT's (linear variable differential transformer). Theoretical and physical aspects of these devices are discussed in the references [66, 67]. LVDT's used for this project are Schaevitz model 100 HR-DC with serial numbers 1440 and 1441.

Both devices are direct current operated and are completely self contained inasmuch as microcircuitry necessary for signal conditioning, modulation and demodulation are encapsulated within the housing itself. The only external electronics necessary for operation of these devices is a 24 volt d.c. power supply and a device to measure and record output voltages that result from displacement of the LVDT core.

Calibration of these devices was substantially according to the manufacturer's recommendations. Each LVDT was fastened to a steel cylindrical specimen and approximately 200 measurements of output voltage versus displacement of a 0.0001 inch micrometer were made for each device. Measurements were made at room temperature and at the high and low temperature extremes. Least square fit of the data provided the following calibration:

SN 1440: 1.982 196 569 E02 10,000th inch per volt.

SN 1441: 2.022 157 978 E02 10,000th inch per volt.

Spot checks were made throughout the experiment and these calibration curves remained valid. Figures 19 and 20 detail the yokes and installation of extensometers.

VI. Readout Equipment

LVDT output leads and MTS load cell were hard wired to the Joint Highway Research Project Matrix Corporation Model 1700 data acquisition system. Maximum scan rate for this

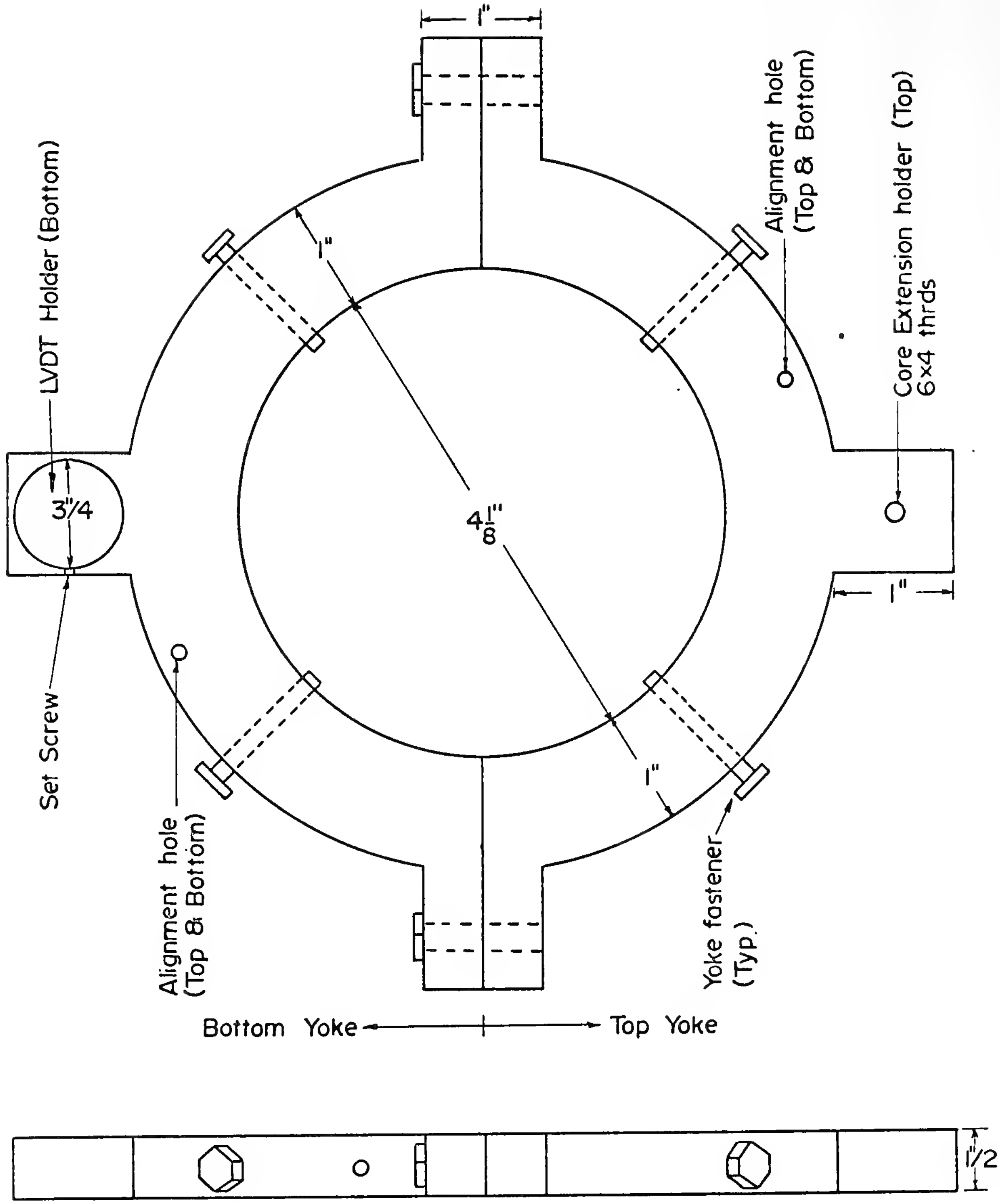

FIGURE 19 LVDT YOKES.

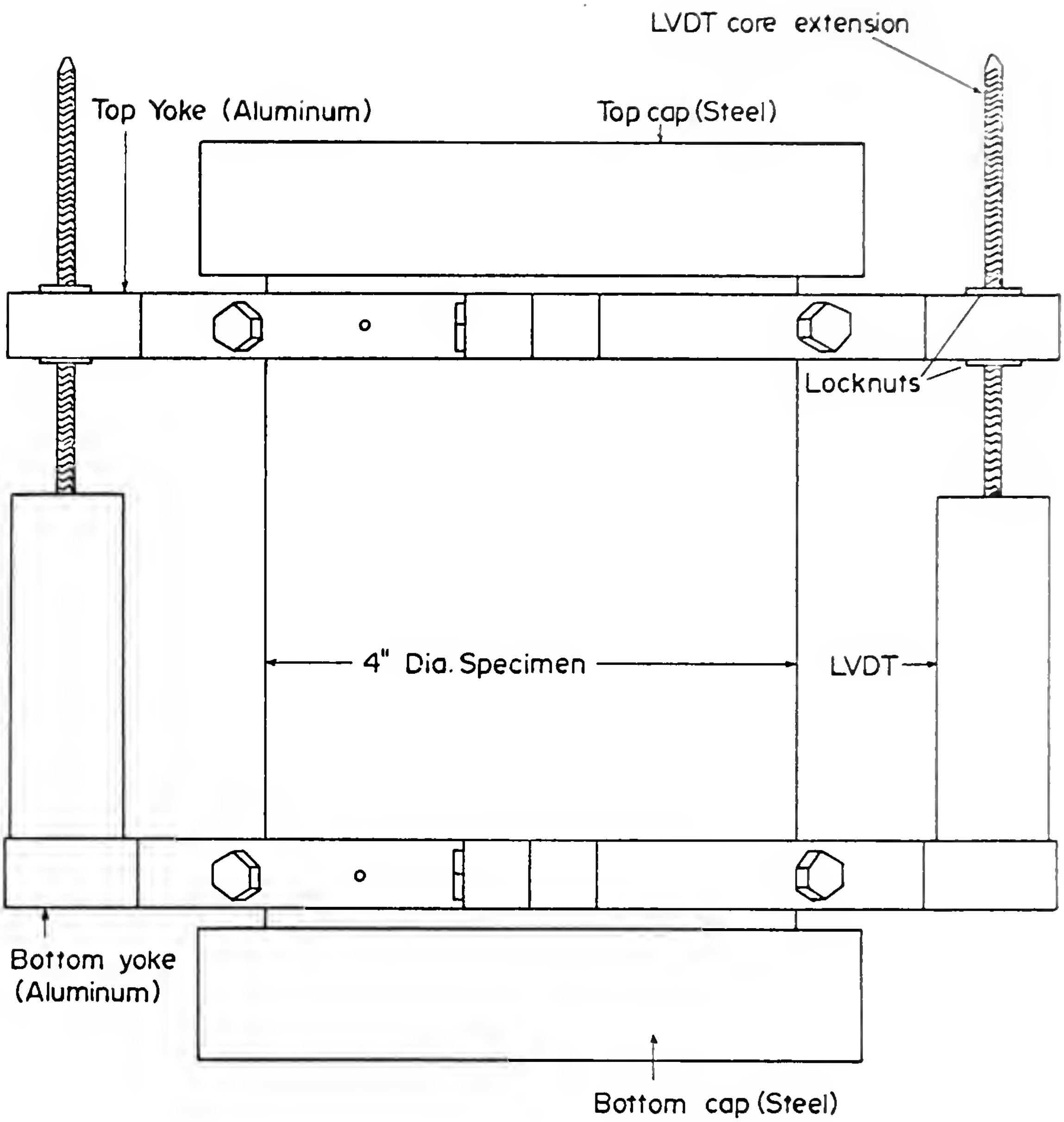

FIGURE 20 TEST SET UP.

device is limited by the tape printer to one scan of the three channels per second and this rate was used for the experiment. Output voltages are printed on tape and then reduced by appropriate calibration factors to displacements and load.

VII. Specimen Caps and Adhesive

In order to connect specimens to the testing machine actuator rods, steel caps were fastened to top and bottom of each specimen. The adhesive used was a two-part epoxy supplied by Thermoset Plastics, Inc. of Indianapolis, Indiana, and described as Thermoset 103 Variable Flexibility Epoxy Adhesive. For this project, a rigid bond formulation was used that consists of two parts resin to one part hardener by weight. Cap and specimen geometry is such that 18 grams of adhesive provide complete bond and just fill the annular space between the cap and specimen.

Caps were machined from steel and the interior surfaces roughened to improve bond at the specimen-adhesive-steel interface. Bolt holes in the center of the steel caps for clevis attachment to the testing machine presented minor problems inasmuch as bolts placed in the holes during adhesive application would become bonded to the cap by epoxy and were impossible to remove without damage to the specimen. This was solved by wrapping bolt threads with a single layer of teflon tape. Teflon provided an adequate

seal against epoxy migration into bolt or cap threads and did not bond to metal or epoxy.

Several tests were run to find the most effective method of bonding epoxy to the asphalt concrete. These included direct bonding of caps to the asphalt covered aggregate, sawing the specimen and bonding to the exposed untreated aggregate, acid etching of exposed aggregate and sand-blast etching of the exposed sawed aggregate. There were no bond failures (the joint is stronger in tension than the specimen) with any of the above situations as long as the bond surface was dry and free of loose material or dust before applying the adhesive. It should be noted that only very few bond failures occurred during the experiment and that these were at the low temperature extreme.

The following procedure for attaching caps to the specimen was adopted. To make the top plane as nearly perpendicular to the longitudinal axis of specimen as possible, specimen tops were sawed off with a diamond saw while the specimen was held in a jig. After drying, prepared caps and the specimen were placed in a vertical alignment jig. A spirit level was used to check that the longitudinal axis of the specimen was perpendicular to the exterior face of the end cap. If necessary, a single shim less than one-eighth inch square and less than one-sixteenth of an inch thick was used to establish perpendicularity of the face and the axis. The specimen was removed and the

correct amount of adhesive was weighed into the cap. The specimen was then firmly seated into the cap using the vertical alignment jig and a spirit level on the top surface to insure vertical and horizontal alignment. After at least 12 hours of curing, the other end of the specimen was capped by the same procedure. After an additional 24 hours of curing at room temperature, bolts were removed and the specimen was ready for temperature conditioning and testing.

After tension testing, failed specimens and caps were oven heated sufficiently to allow asphalt and aggregate to be scraped from the caps. Adhesive was removed from the caps with an oxyacetylene torch. After cooling, the caps were sand blasted to remove slag from interior surfaces and the threads were re-tapped. Toward the end of the experiment some of the caps were discarded because warping from the cleaning process prevented good alignment of the finished specimen.

Figure 21 shows shop details of the end caps.

VIII. Actuator Rod Connections to Specimen Caps

In order to make a moment-free hookup of the specimen to the testing machine actuator rods, a chain link and clevis arrangement was used at each end of the specimen. Each point of contact between the chain links and clevis pins was kept coated with silicone spray to eliminate as much friction as possible. Due to actuator rod geometry

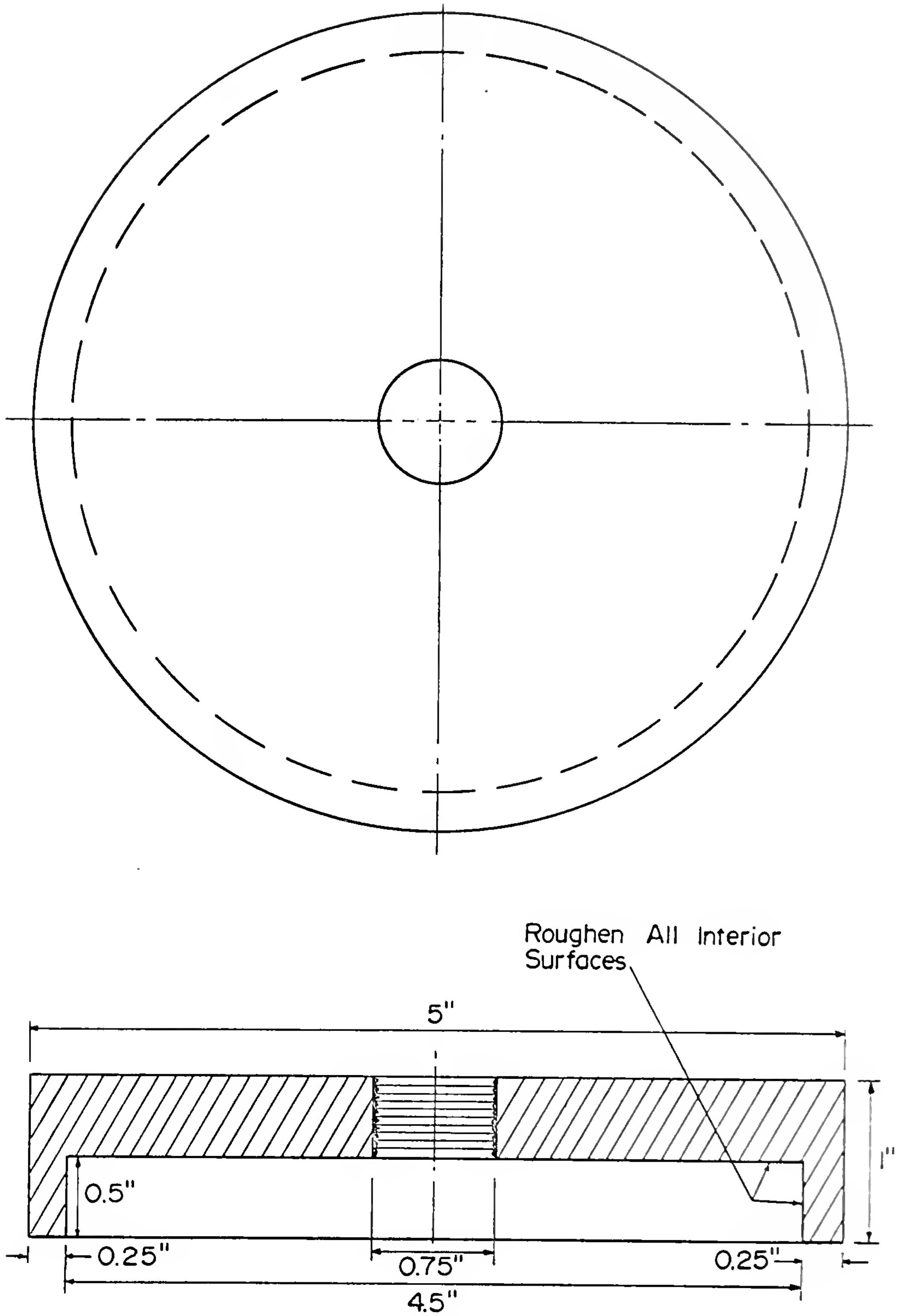

FIGURE 21 CAP DETAIL.

and piston characteristics, chain links were used for the top and bottom connections. Details of this hookup arrangement can be seen in Figure 22.

IX. Specimen Fabrication

Test specimens were prepared in groups of four of the same mixture type, i.e. the same gradation and asphalt type. Each specimen was fabricated from three 1200 gram batches of aggregate since this is the approximate volume that available mixing equipment can accommodate.

1. Mixing

1200 gram batches of aggregate were weighed into individual pans and heated to the mixing temperature in a forced-draft oven while asphalts were being heated in open beakers on electric hot-plates with constant stirring. Mixing temperatures were determined from temperature-viscosity relationships for each asphalt and were set to give mixing viscosities between 150 and 310 centistokes as recommended by the Asphalt Institute [68]. The weighed and heated aggregate was placed in a heated mixing bowl and placed on a balance where the required amount of asphalt was weighed into a crater in the aggregate.

Mixing was accomplished with a planetary action mechanical mixer using a wire beater. Coarse and dense mixtures were mixed for 20 seconds after which the bowl sides were scraped down with a hot spoon. Mixing was then continued for a total elapsed time of 60 seconds. Procedure

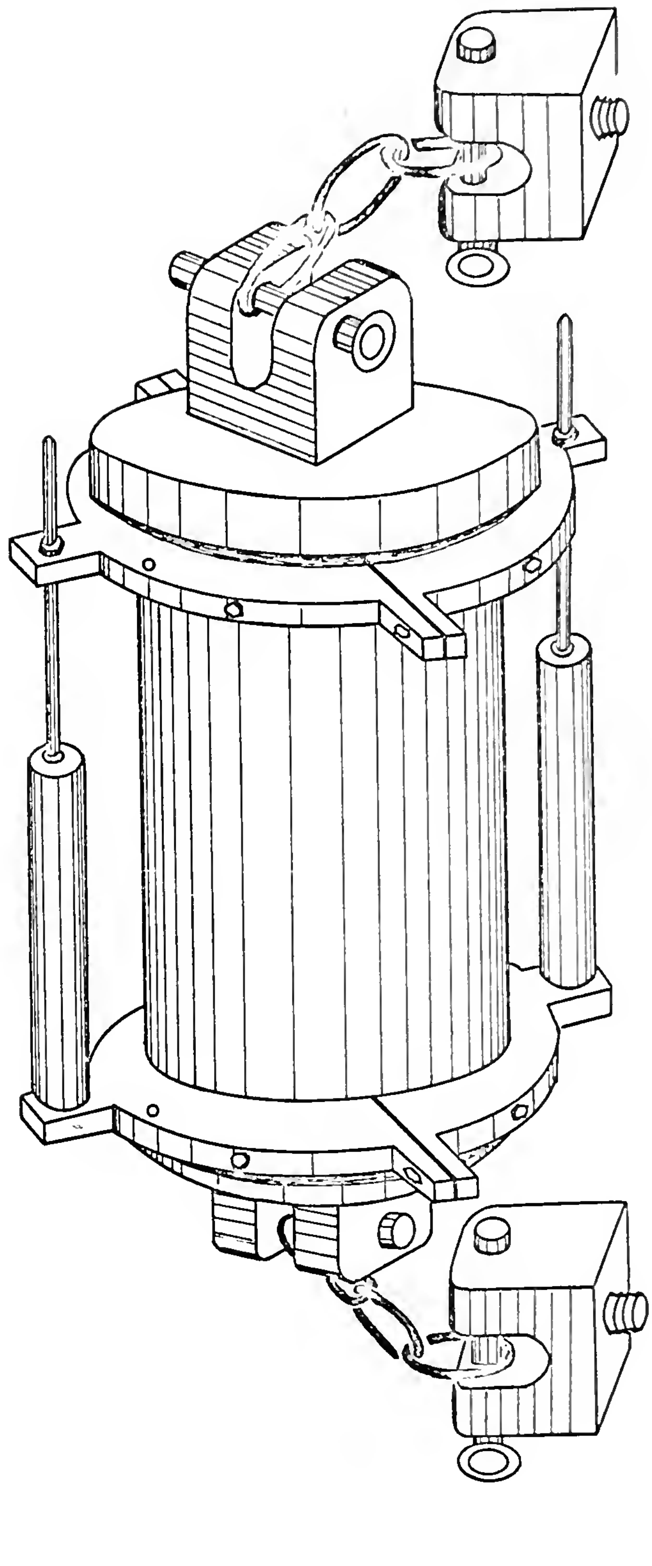

FIGURE 22 TEST SET-UP.

for fine-graded mixtures was the same except that total elapsed mixing time was 90 seconds. Examination of the fraction retained on a three-eighths inch screen showed that these procedures produced mixtures with at least 97 per cent of the particles totally coated. After mixing, each mixture was returned to the cleaned aggregate pan for curing.

2. Curing

Mixtures were cured at 140°F (60.0°C) for 15 hours in a forced draft oven prior to compaction.

3. Compaction

Molds were four-inch diameter by ten inches high and split longitudinally to comprise two half cylinders held together with six bolts. Compaction effort was provided by a California kneading compactor with the standard heated compacting foot. Mixtures and molds were brought to a temperature of 235°F (112.8°C) for specimen compaction.

A heated mold with no interior coating was placed in the kneading compactor carriage and fastened solid with no shims under the mold. The carriage was not loosened nor allowed to wobble during the compaction operation. A paper disc was placed in the bottom of the mold and the compacting foot was lowered completely.

Preliminary compaction was accomplished by introducing the first 1200 gram batch into the mold in a steady stream from a circular trough while the compacting foot was

applying 250 psi tamps. This first lift was subjected to 30 tamps during which the foot was allowed to "walk out" of the mixture. This procedure was repeated for each of two more lifts of approximately 1200 grams each. Finally, the specimen was subjected to 150 tamping blows at 500 psi foot pressure.

After kneading compaction the specimens were placed in a 140°F (60.0°C) oven and cured for 90 minutes. A 12,560 pound levelling load was applied by the double plunger method at a head speed of 0.05 inches per minute with a mechanical testing machine. After this final levelling load was applied, specimens were allowed to cool to room temperature.

4. Bulk Specific Gravity of Compacted Specimens and Uniformity of Test Specimens

After the specimens had reached room temperature (not less than six hours after application of the levelling load) molds were opened and specimens were removed and identified by specimen serial number.

Bulk specific gravity of the compacted mixture was determined in strict accordance with ASTM D2726 (section 4.1), "Bulk Specific Gravity of Compacted Bituminous Mixtures Using Saturated Surface-Dry Specimens."

Fabrication uniformity was checked by comparing specimen bulk specific gravity values with those obtained in the Hveem mixture design. Specimen bulk specific

gravity compared with Hveem design values is shown in Table 20. For all specimens, average percent of Hveem bulk specific gravity is 98.88 with a standard deviation of 0.503. Specific gravity values for all specimens can be found in Appendix C.

TABLE 20

Specimen Bulk Specific Gravity

Gradation	No. Obs.	Specimen G_{nb}			Spec. Avg. as % of Hveem
		Avg.	Std. Dev.		
C	16	2.370	0.009	2.401	98.1
D	132	2.351	0.012	2.376	98.9
F	20	2.352	0.010	2.390	98.4

X. Preparation of Specimen for Capping

After the specimens were fabricated and then bulk specific gravity determined, approximately one and one-half inches of material were removed from the top of the specimen with a diamond-bladed masonry saw. This procedure was followed for two principal reasons.

During compaction the bottom end of the specimen is forced to be perpendicular to the longitudinal axis due to the geometry of the mold, mold carriage and compaction foot. The top of the specimen, however, is not necessarily parallel with the bottom because aggregate particles at the top are disturbed by the compacting foot and the process

of levelling by double plunger does not provide end parallelism to tolerances necessary for this project. With the specimen held by a jig on the saw table in such a manner that the blade is parallel with the bottom end and perpendicular to the longitudinal axis, parallelism was insured, at least to a degree where only minor shimming was necessary in some isolated cases to have the caps of the finished specimen parallel to each other and perpendicular to and centered upon the longitudinal axis.

A second reason for removal was that some fracturing of aggregate occurs at the specimen top during final phases of compaction. Most of this fractured coarse aggregate is removed by sawing. The sawed portions were retained as a record for each specimen tested or used during the experiment.

XI. Capping

After drying the sawed specimens by blotting and then standing with the sawed surface exposed to air at room temperature for at least 24 hours, specimens were given a final visual inspection for dryness and fractured coarse aggregate and capped as discussed previously.

XII. Specimen Temperature Preconditioning

After the adhesive had cured for at least 24 hours, specimens were placed in the large conditioning box along with the dummy specimen and brought to temperature equilibrium.

After equilibrium had been reached, the specimen and dummy were removed from the conditioner and LVDT's were attached to the test specimen by the following procedure.

XIII. Attachment of LVDT's

LVDT housings were attached to the bottom yoke and the yoke was placed on the bottom of the specimen. A one-quarter inch shim was used to prevent contact between the yoke and cap and after levelling, the yoke was tightened onto the specimen by four bolts. The specimen was inverted and the top yoke was shimmed and aligned with the bottom yoke and fastened into place.

After installation of the yokes, LVDT cores were inserted and adjusted to approximate electrical zero by means of a spacer and two locknuts at the top yoke.

Gage length was determined by measurement of distance between gage marks on the yokes. Four sets of gage marks at 90 degrees were used and measurement was with a vernier caliper with a least reading of 0.001 inch. Gage length used for strain calculations was the arithmetic mean of the four measurements.

Specimen and dummy were then immediately transferred to the test chamber and again brought to test temperature equilibrium. The time was recorded for installation of LVDT's (time that the specimen was exposed to room temperature), and the time in the test chamber to reach equilibrium was determined. The next three specimens for the particular

test series were subjected to the same time exposure at room temperature. Time in the test chamber was the same as the monitored specimen plus an additional 20 minutes.

After temperature equilibrium was reached the LVDT connections were made and the cores adjusted by voltmeter and locked.

XIV. Tension Test

After the LVDT's were installed and adjusted, MTS system checks were performed and the scanner and printer were started. Then clevis connections between actuator rods and the specimen were made to close the testing system loop and the test deformations were applied through MTS stroke control. After the specimen had failed, it was removed from the test chamber and the yokes removed and cleaned if necessary. Later the caps were removed and cleaned for reuse.

LVDT's were then installed on the next specimen in the series for the particular test cell and the assembly placed in the test chamber. All data were reduced from voltage printouts to stress and strain. Strain rate and stiffness were calculated and checked while the next specimen was coming to test temperature equilibrium.

XV. Summary of Equipment Developments

Three pieces of equipment that were developed or utilized as a part of this study because they will be of

concern for use in future studies of this nature are summarized.

1. Extensometer with LVDT's.

The technique developed for measuring specimen deformation which uses an extensometer with LVDT's appears to be far superior to other methods known or tried for two reasons. First, the LVDT is mechanically fastened to the specimen and does not depend on adhesives. Adhesives can be a source of error when electrical resistance strain gages are used to measure strain or deformation. In addition, the LVDT is reusable, thus reducing equipment costs and the possibility of calibration errors. Secondly, an extensometer fastened directly to the specimen and independent from the testing frame and load actuators eliminates the effect of test system movement or compliance.

2. Analog Rate Controller for MTS.

An analog rate controller was developed for the MTS machine which extends the stroke rate on the slow end to produce a slow rate that approaches full ram movement in one million seconds. For the particular combination of fixed pump capacity and ram piston displacement of the machine, this device is necessary to produce ram movements slower than 0.05 inches per minute.

It should be noted that when this device is used ram movement is not continuous but results from a uniform series of step inputs. However, at rates used for this

study for all but the very slowest, step inputs are not distinguishable as such.

A calibration curve for variable capacitance input versus stroke rate is included in Figure 17.

3. Temperature Control System

A very efficient, highly reliable and relatively inexpensive temperature control system was developed as a part of this study that provides for precise temperature control in the range of -25°F (-31.7°C) to approximately 150°F (65.6°C). Plans for construction and instructions for operation are on file in the bituminous laboratory in the School of Civil Engineering at Purdue University.

EXPERIMENTAL RESULTS AND ANALYSIS

I. Introduction

All values for limiting strain (strain at failure) are in microstrain units (MII). Microstrain is defined as 1×10^{-6} inches per inch and was calculated as elongation at failure divided by original gage length.

Reduced data for each test specimen are contained in Appendix D and location of failure surfaces for each specimen is shown in Appendix E.

Cell designations, number of tests per cell and mean values of limiting strain for each cell (cell means) are shown in Table 21. A plot of mean cell value versus temperature is shown in Figure 23. Cell standard deviation values are shown in Table 22.

Serial numbers and limiting strain values for each specimen within each cell are shown in Table 23.

II. Effect of Strain Rate

Considerable effort was expended in the early phases of the study to control strain rate and to maintain the rates that were determined to be realistic for actual in-service application of loads as outlined in the design of the experiment. Original plans were to use a frequency

TABLE 21

Cell Designations, Number of Observations per Cell and Cell Means

		Temperature (°F)					
		-17.5	14	45.5	77	108.5	140
MIX TYPE	6LD	1 4 28			6 4 3770	6 4 4949	M 3 17,404
	6HD				I 4 4900		N 4 16,415
	8LD	A 4 51	B 8 274	C 4 2953	D 11 3640	E 3 5120	P 4 9,564
	8HD				F 4 4065		Q 3 14,371
	12LD	2 4 33			H 4 3252	7 4 5593	R 2 11,086
	12HD				J 4 4003		S 4 13,398
	8LF	8 4 44			K 4 5488	3 4 6200	T 3 17,675
	8LC	4 4 38			L 4 4097	5 4 5539	U 3 6,859

Cell → | 1 4 | ← No. obs.
| 28 | ← $\overline{\varepsilon}_f$ (MII)

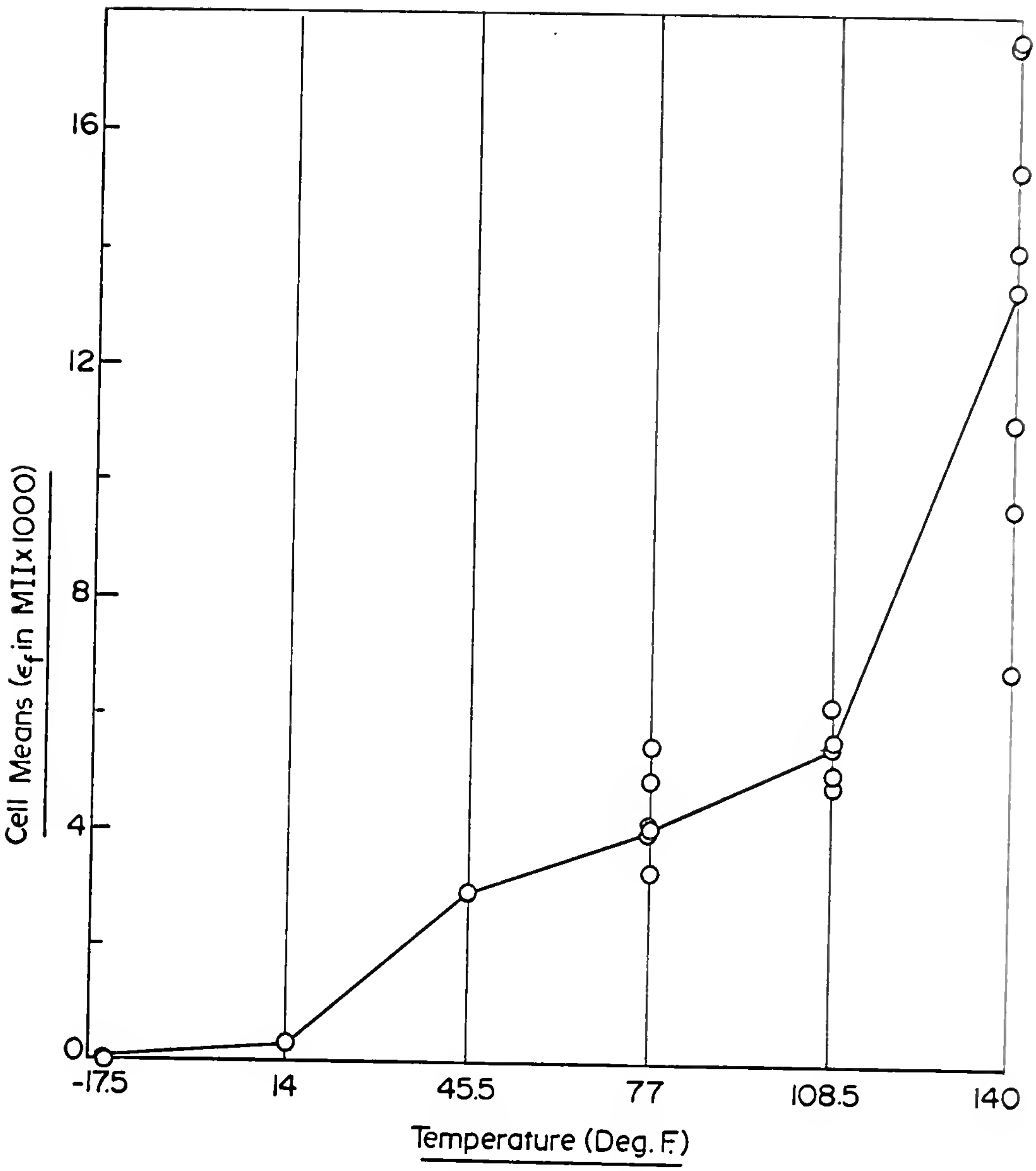

FIGURE 23 CELL MEANS (CURVE IS DRAWN THROUGH MEANS FOR EACH TEMPERATURE).

TABLE 22

Cell Standard Deviations in MII

		Temperature (°F)					
		-17.5	14	45.5	77	108.5	140
MIX TYPE	6LD	1 18			G 583	6 2331	M 5308
	6HD				I 1199		N 3768
	8LD	A 46	B 423	C 175	D 1060	E 1059	P 4069
	8HD				F 262		Q 5967
	12LD	2 21			H 972	7 1616	R 5784
	12HD				J 914		S 6515
	8LF	8 13			K 1017	3 1139	T 9157
	8LC	4 9			L 451	5 2776	4 4881

TABLE 23

Specimen Serials and Limiting Strain, ε_f, in MII for Each Cell

Cell	Mix	Temp (°F)	Serial	ε_f
1	6LD	-17.5	303	31
"	"	"	304	39
"	"	"	305	41
"	"	"	306	2
G	6LD	77	279	3134
"	"	"	280	3434
"	"	"	281	4228
"	"	"	282	4312
6	6LD	108.5	323	3847
"	"	"	325	8445
"	"	"	325	3810
"	"	"	326	3695
M	6LD	140	343	19,031
"	"	"	345	21,709
"	"	"	346	11,473
I	6HD	77	295	6061
"	"	"	296	4246
"	"	"	297	5744
"	"	"	298	3549
N	6HD	140	371	11,850
"	"	"	372	14,797
"	"	"	373	19,635
"	"	"	374	19,377
A	8LD	-17.5	264	6
"	"	"	265	45
"	"	"	266	115
"	"	"	267	39
B	8LD	14	262	109
"	"	"	255	164
"	"	"	256	106
"	"	"	257	127
"	"	"	258	129
"	"	"	254	164
"	"	"	261	75
"	"	"	260	1317
C	8LD	45.5	242	2748
"	"	"	244	3167
"	"	"	243	2995
"	"	"	247	2901

TABLE 23 (continued)

Cell	Mix	Temp (°F)	Serial	ϵ_f
D	8LD	77	268	4770
"	"	"	269	4591
"	"	"	271	3814
"	"	"	239	3971
"	"	"	272	3829
"	"	"	238	2698
"	"	"	274	4994
"	"	"	270	1713
"	"	"	273	3919
"	"	"	240	3632
"	"	"	241	2103
E	8LD	108.5	246	5652
"	"	"	248	5808
"	"	"	251	3900
P	8LD	140	339	15,414
"	"	"	340	7770
"	"	"	341	8954
"	"	"	342	6119
F	8HD	77	275	4244
"	"	"	276	4255
"	"	"	277	4067
"	"	"	278	3693
Q	8HD	140	375	20,572
"	"	"	377	13,871
"	"	"	378	8670
2	12LD	-17.5	307	61
"	"	"	308	16
"	"	"	309	36
"	"	"	310	19
H	12LD	77	283	3269
"	"	"	284	2600
"	"	"	285	4620
"	"	"	286	2517
7	12LD	108.5	327	4263
"	"	"	328	6059
"	"	"	329	4370
"	"	"	330	7679
R	12LD	140	349	6996
"	"	"	350	15,176

TABLE 23 (continued)

Cell	Mix	Temp (°F)	Serial	ε_f
J	12HD	77	299	3460
"	"	"	300	4694
"	"	"	301	3001
"	"	"	302	4857
S	12HD	140	379	22,679
"	"	"	380	8362
"	"	"	381	13,126
"	"	"	382	9426
8	8LF	-17.5	331	36
"	"	"	332	44
"	"	"	333	34
"	"	"	334	62
K	8LF	77	287	4340
"	"	"	288	6799
"	"	"	289	5245
"	"	"	290	5568
3	8LF	108.5	311	6259
"	"	"	312	7739
"	"	"	313	5746
"	"	"	314	5055
T	8LF	140	351	9540
"	"	"	352	27,592
"	"	"	353	15,893
4	8LC	-17.5	315	43
"	"	"	316	48
"	"	"	317	33
"	"	"	318	29
L	8LC	77	291	3519
"	"	"	292	4286
"	"	"	293	4578
"	"	"	294	4005
5	8LC	108.5	319	3798
"	"	"	320	4357
"	"	"	321	4316
"	"	"	322	9686
U	8LC	140	355	5458
"	"	"	356	12,287
"	"	"	357	2831

setting of the ramp function generator of the testing system that would produce the calculated deformation rate necessary for the desired strain rate. Two factors appear to make control of strain rate for a direct tension test with the present testing system impossible and estimated costs of equipment for this control were too high to consider their acquisition as part of this study.

First, due to frame and system compliance, which varies from test to test, a single predetermined setting of frequency for stroke rate will not necessarily provide repeatable rates of deformation for different test specimens (see "Experimental Set-Up: Frame Compliance"). Secondly, the nature of asphaltic concrete in tension is such that as loads are increased, the strain rate also increases. To control strain rate under this situation requires constant monitoring of deformation rate and adjustment of stroke rate to compensate for this increase. This compensation can be performed manually only if reduced strain data are produced as real time output during the test.

Both of the above problems can be conveniently handled by electronically comparing the output signal of the displacement transducer(s) with programmed external references; adjustment signals from this process controller then become the feedback for the existing function generator of the test system. Since output signals originate at the specimen instead of the external ram, effects of frame compliance of

reasonably large magnitude and high variability can be completely isolated from response of the system. Units that perform these functions are recently commercially available, but as was mentioned before, costs prohibited incorporation into this study.

A third source of difficulty in strain rate control occurs at the high temperature extreme of 140°F. At elevated temperatures with the specimen hook-up configuration used for this study, deformation is primarily due to the dead load of the specimen itself and not movement of the loading ram. This problem could be resolved by removing the bottom flexible connection and substituting a rigid connection and operating in load rather than stroke control. This technique was evaluated but was not subsequently used because of inconvenience involved in equipment switch-over. Also, later analysis of the effect showed strain rate to be relatively insignificant when compared with normal variability and other effects.

Average strain rates for each specimen are shown in Table 24. These values are the arithmetic mean of strain rates calculated from each time increment of each test.

Figures 24 through 29 show plots of strain rate versus limiting strain for each test temperature. Least square fits were made in an attempt to quantify the effect. As is shown by the figures, strain rate has little if any effect, when compared subjectively at least, with normal data

TABLE 24

Average Strain Rate, $\bar{\dot{\varepsilon}}$, in MII/sec for Each Test Specimen

Cell	Temp	Ser.	$\bar{\dot{\varepsilon}}$	Cell	Temp	Ser.	$\bar{\dot{\varepsilon}}$
1	-17.5	303	0.7	D	77	268	596.2
"	"	304	1.1	"	"	269	306.2
"	"	305	2.1	"	"	271	229.6
"	"	306	0.2	"	"	239	217.9
G	77	279	174.1	"	"	272	159.5
"	"	280	143.1	"	"	238	146.1
"	"	281	162.6	"	"	274	85.5
"	"	282	102.7	"	"	270	73.3
6	108.5	323	105.1	"	"	273	58.6
"	"	324	157.2	"	"	240	50.4
"	"	325	117.3	"	"	241	0.3
"	"	326	85.5	E	108.5	246	122.3
I	77	295	131.8	"	"	248	80.6
"	"	296	125.9	"	"	251	36.1
"	"	297	92.1	F	77	275	133.2
"	"	298	136.5	"	"	276	133.1
A	-17.5	264	4.0	"	"	277	196.9
"	"	265	3.2	"	"	278	97.2
"	"	266	1.7	2	-17.5	307	2.7
"	"	267	0.8	"	"	308	1.0
B	14	262	21.8	"	"	309	2.6
"	"	255	8.0	"	"	310	1.5
"	"	256	7.5	H	77	283	181.6
"	"	257	7.0	"	"	284	205.9
"	"	258	7.0	"	"	285	76.3
"	"	254	6.8	"	"	286	139.8
"	"	261	4.1	7	108.5	327	109.3
"	"	260	0.5	"	"	328	115.1
C	45.5	242	72.3	"	"	329	104.6
"	"	244	17.6	"	"	330	76.8
"	"	243	37.4	J	77	299	144.2
"	"	247	0.2	"	"	300	95.9
				"	"	301	132.4
				"	"	302	128.9

TABLE 24 (continued)

Cell	Temp	Ser.	$\bar{\varepsilon}$
8	-17.5	331	3.0
"	"	332	2.1
"	"	333	2.4
"	"	334	3.9
K	77	287	108.5
"	"	288	148.5
"	"	289	206.7
"	"	290	203.3
3	108.5	311	218.2
"	"	312	83.8
"	"	313	159.8
"	"	314	90.0
4	-17.5	315	1.6
"	"	316	3.0
"	"	317	1.5
"	"	318	1.9
L	77	291	191.1
"	"	292	97.4
"	"	293	149.5
"	"	294	143.0
5	108.5	319	55.7
"	"	320	100.8
"	"	321	106.3
"	"	322	93.7

Cell	Temp	Ser.	$\bar{\varepsilon}$
M	140	343	357.6
"	"	345	837.5
"	"	346	458.9
N	140	371	148.1
"	"	372	180.3
"	"	373	219.6
"	"	374	126.8
P	140	339	1954.8
"	"	340	1758.8
"	"	341	1492.3
"	"	342	3059.5
Q	140	375	296.0
"	"	377	202.2
"	"	378	94.3
R	140	349	1166.0
"	"	350	4469.0
S	140	379	602.1
"	"	380	190.1
"	"	381	779.4
"	"	382	178.8
T	140	351	596.2
"	"	352	3214.7
"	"	353	635.7
U	"	355	275.4
"	"	356	2146.6
"	"	357	109.3

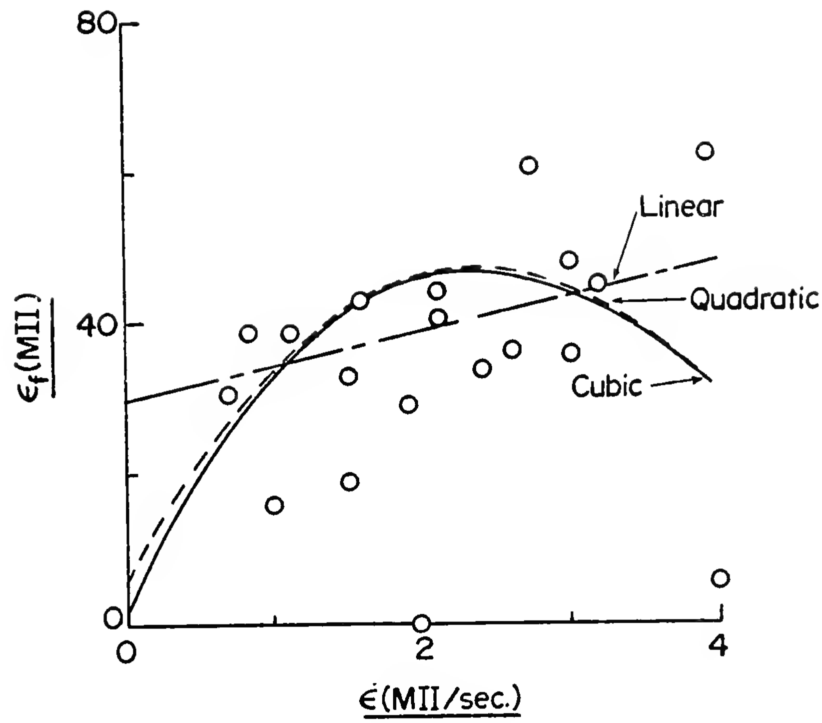

FIGURE 24 EFFECT OF STRAIN RATE (-17.5°F).

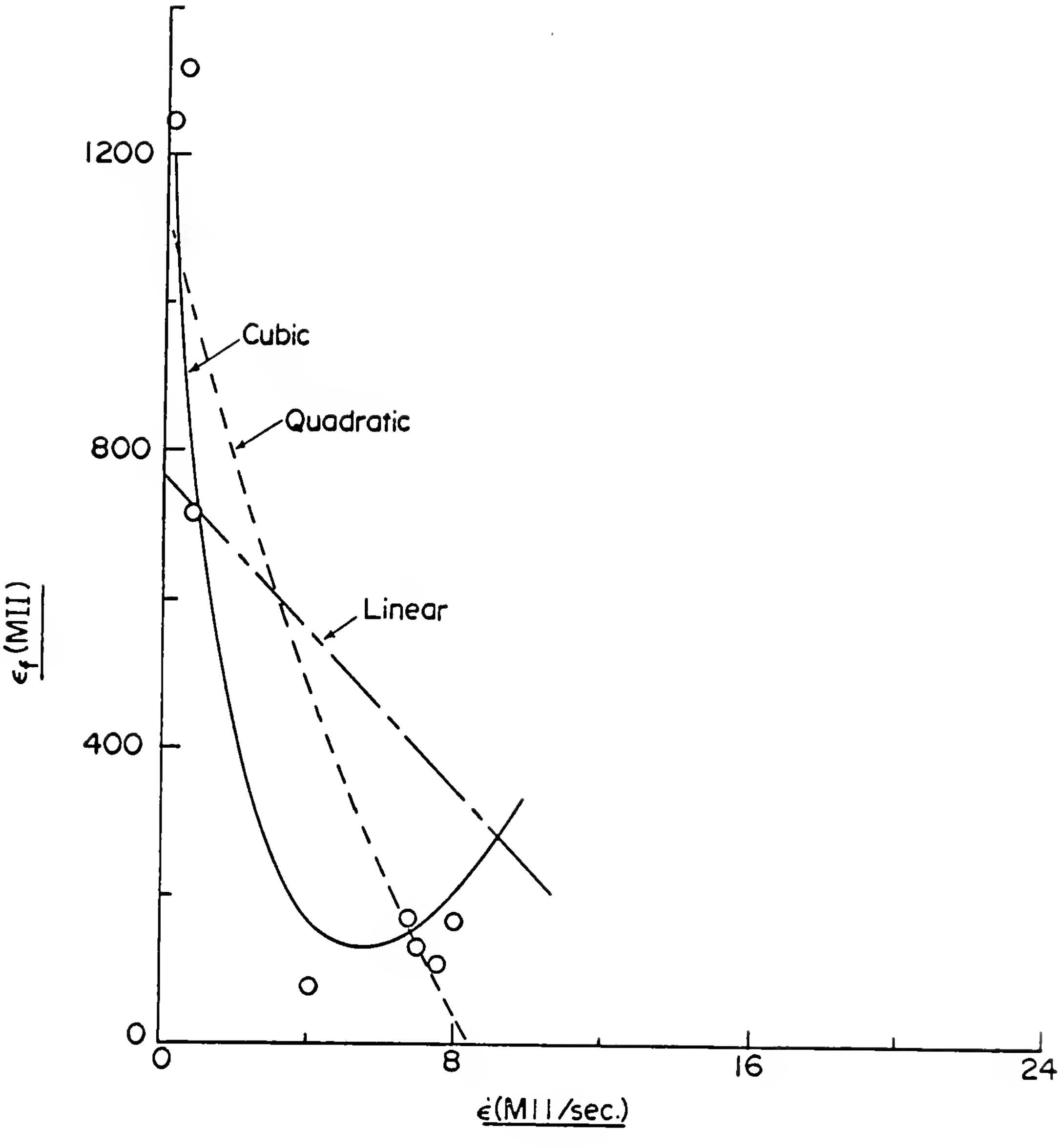

FIGURE 25 EFFECT OF STRAIN RATE (14°F).

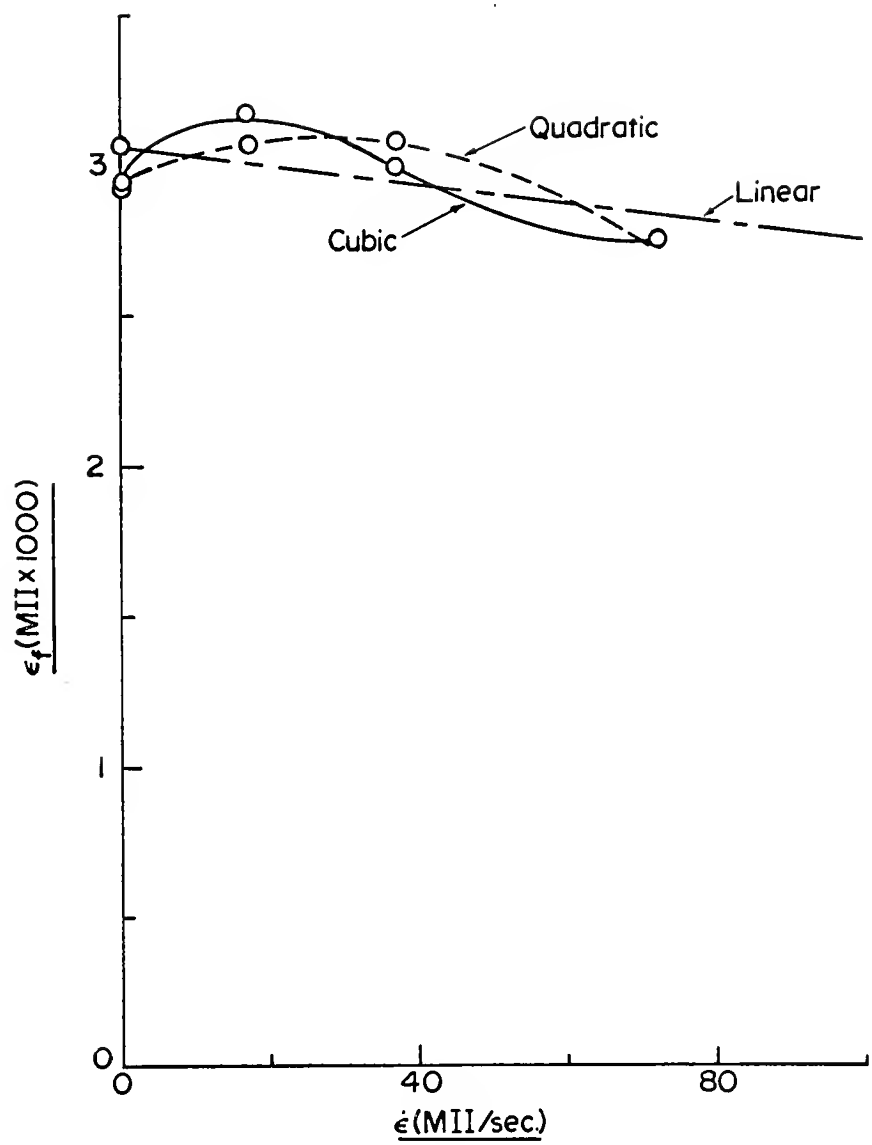

FIGURE 26 EFFECT OF STRAIN RATE (45.5°F).

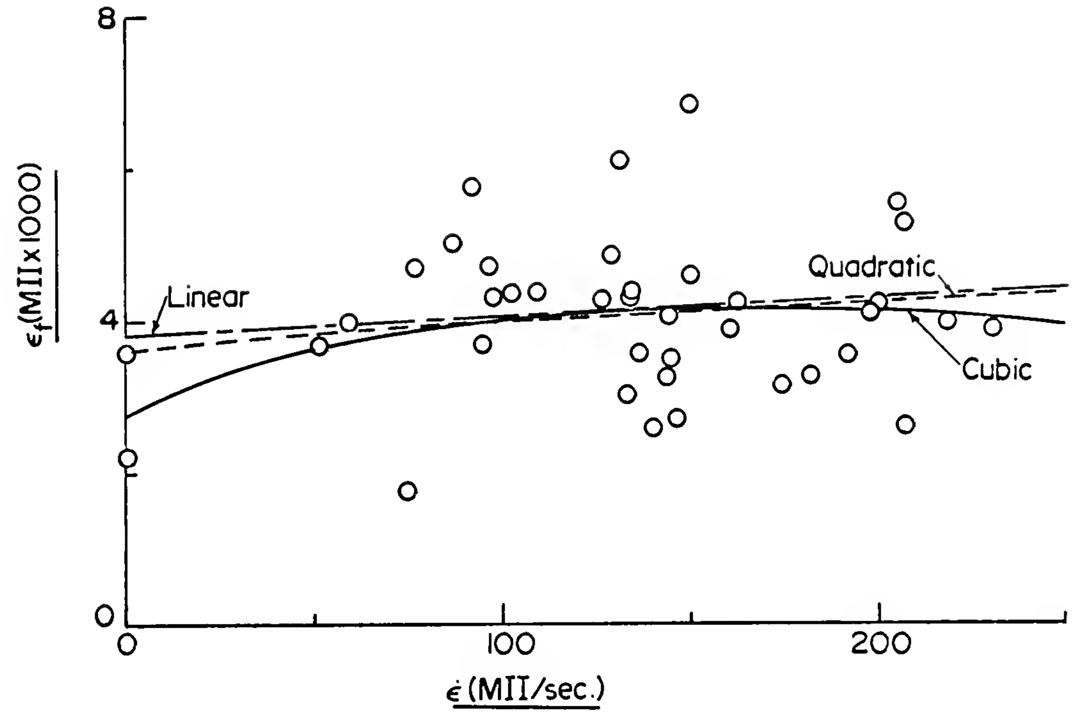

FIGURE 27 EFFCT OF STRAIN RATE (77°F).

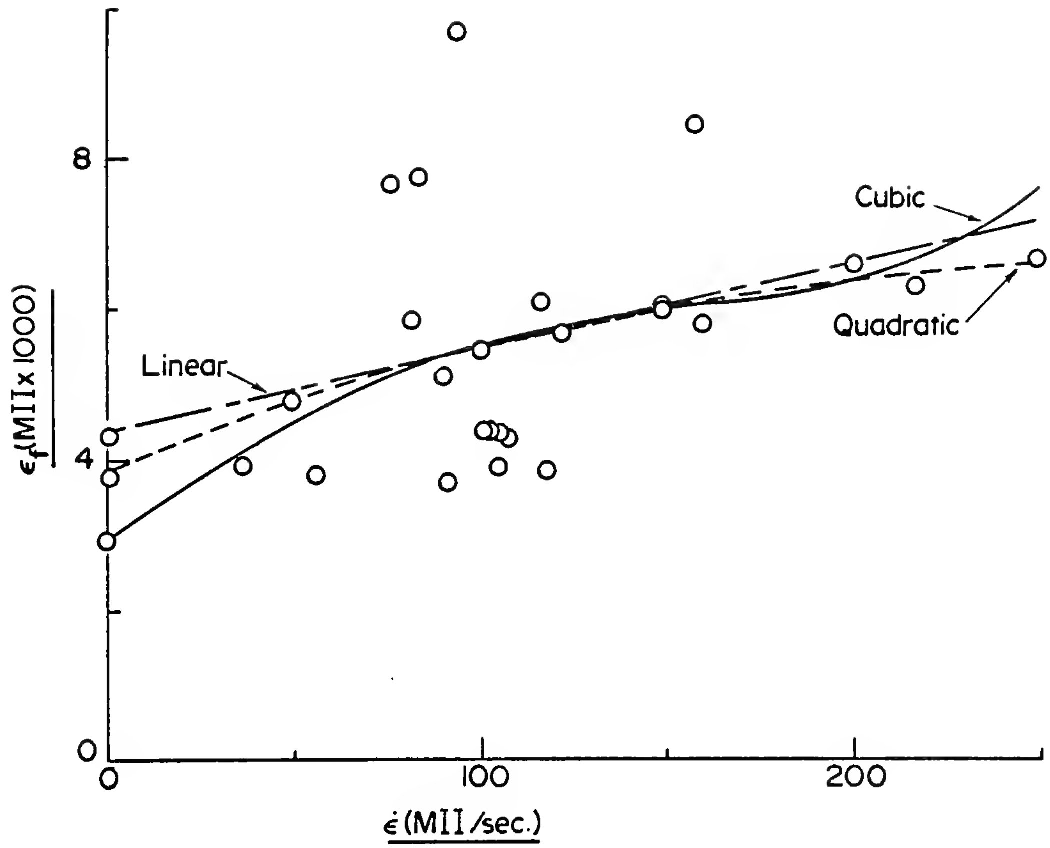

FIGURE 28 EFFECT OF STRAIN RATE (108.5°F).

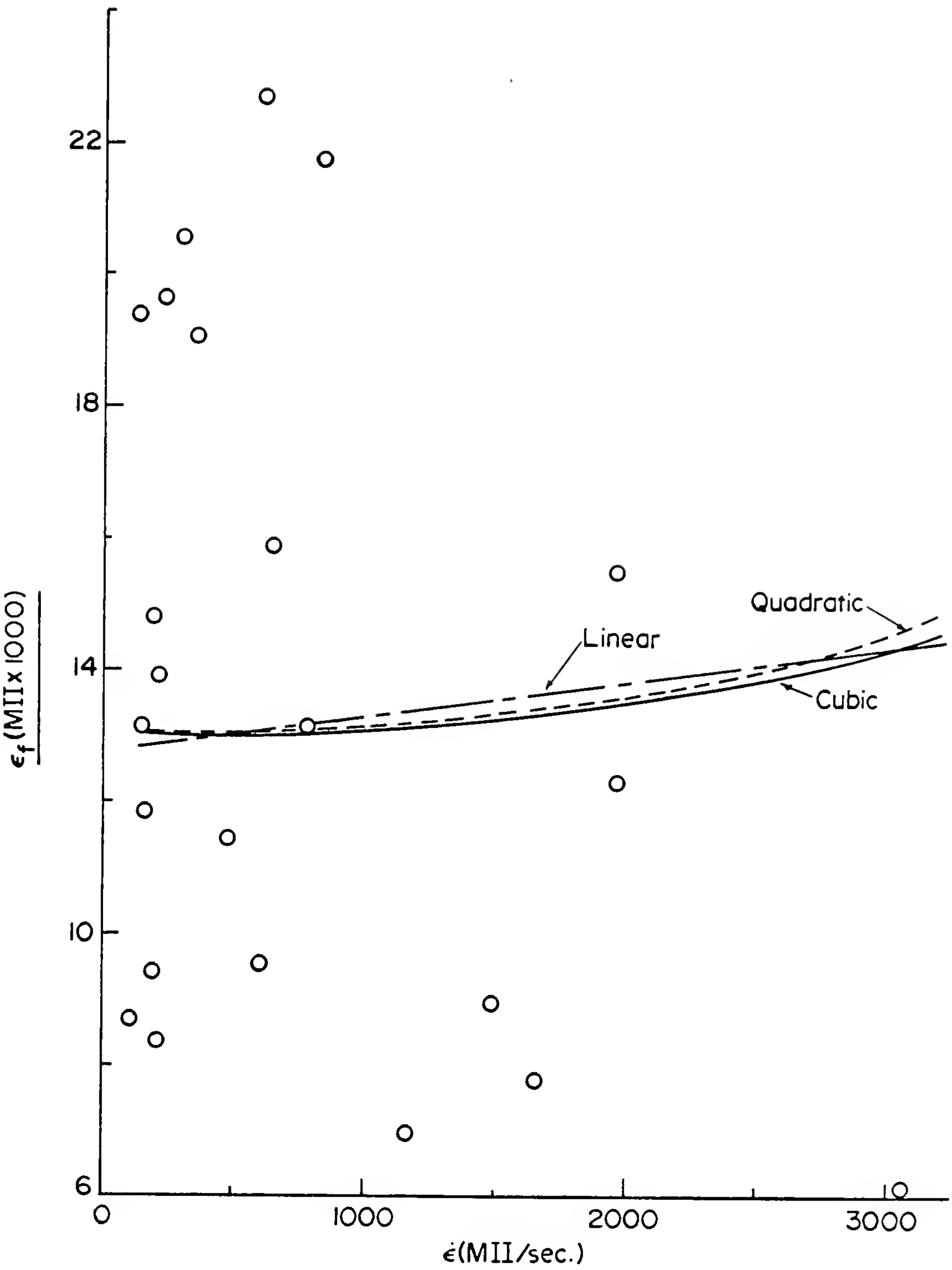

FIGURE 29 EFFECT OF STRAIN RATE (140°F).

variability. Calculations for regressions were by Purdue CDC 6500, using G2 SPSS15, REGRESSION, version 4/73. Regression equations are of the form:

$$\varepsilon_f = \beta_0 + \beta_1(\bar{\dot{\varepsilon}})^2 + \beta_2(\dot{\varepsilon})^2 + \beta_3(\bar{\dot{\varepsilon}})^3 + e$$

where ε_f = limiting strain in MII

$\bar{\dot{\varepsilon}}$ = mean strain rate in MII/Sec.

e = error term.

Coefficients and multiple R^2 values are shown in Table 25.

III. <u>Stiffness Comparison</u>

For each time increment used during an individual test a mixture stiffness value was calculated as follows:

$$S_{mix} = \frac{\sigma(t,T)}{\varepsilon(t,T)}$$

where $\sigma(t,T)$ = tensile stress as a function of time of loading (t), and temperature (T).

$\varepsilon(t,T)$ = tensile strain as a function of time of loading (t), and temperature (T).

These values were compared with theoretical stiffness which is calculated as follows:

$$\frac{S_{mix}}{S_{bit}} = \left(1 + \frac{2.5}{n}\,\frac{C_v}{1 - C_v}\right)^n$$

where S_{bit} = bitumen stiffness which is obtained from Van der Poel's nomograph and is a function of time of loading, temperature and penetration index of the bitumen.

$$n = 0.83\left(\log_{10}\frac{4(10)^5}{S_{bit}}\right).$$

TABLE 25

Regression Coefficients for Effect of Strain Rate on Limiting Strain

Temp (°F)	Fit	β_0	β_1	β_2	β_3	Mult. R^2
-17.5	Cubic	3.176	41.96	-11.55	0.7076	0.45
"	Quad.	5.655	34.85	-7.200	0	0.45
"	Linear	29.55	4.6092	0	0	0.21
14	Cubic	1206	-418.2	47.18	-1.390	0.95
"	Quad.	1125	-190.6	6.636	0	0.92
"	Linear	751-1	-51.12	0	0	0.64
45.5	Cubic	2894	33.01	-1.160	0.0094	1.00
"	Quad.	2940	10.25	-0.1812	0	0.90
"	Linear	3058	-3.295	0	0	0.34
77	Cubic	2787	19.78	-0.0835	0.0001	0.27
"	Quad.	3532	4.374	-0.0042	0	0.19
"	Linear	3764	1.966	0	0	0.17
108.5	Cubic	2929	49.35	-0.3083	0.0007	0.25
"	Quad.	3868	19.51	-0.0354	0	0.25
"	Linear	4352	10.80	0	0	0.24
140	Cubic	12,970	0.4974	-0.0003	0	0.13
"	Quad.	13,167	-0.3144	0.0002	0	0.13
"	Linear	12,800	0.6171	0	0	0.12

C_v = volume concentration of aggregate and is defined as

$$= \frac{\text{Volume of Compacted Aggregate}}{\text{Volume of (Aggregate + Asphalt)}}$$

Results of comparing 426 points on 90 specimen stress-strain curves are shown in Table 26. Comparison of theoretical and calculated values are reasonably good considering that Van der Poel considers the bitumen stiffness nomograph to be accurate within a factor of 2. Also, the bitumen to mixture conversion assumes a void content of three per cent whereas mixtures for this study contain slightly more than four per cent voids. Volume concentration of aggregates for this study is approximately 0.9 whereas the theoretical values are based on a range of 0.7 to 0.9 [69].

IV. Exploratory Experiment

To examine the effect of mixture type, test results were examined for tests that were run at 77°F and which included eight mixture types in cells G, I, D, F, H, J, K and L. In the case of cell D, four values were selected at random; these values are 4770, 4591, 3814 and 3919.

In this analysis and those to follow, homogeneity of variance was checked prior to making calculations for analysis of variance. Validity of the assumption of homogeneity was tested by the q-test of Burr and Foster [52] and the guidelines of Anderson and McLean [52] were followed in accepting or rejecting homogeneity of the raw data. In

TABLE 26

Comparison of Measured (S_C) and Theoretical (S_T) Mixture Stiffness

Mix	Temp (°F)	No. Specimens	No. Points	Avg. S_C/S_T
8LD	108.5	3	13	0.9
"	77	11	59	2.2
"	45.5	4	25	2.7
"	14	8	42	1.8
"	-17.5	4	13	1.3
8LF	108.5	4	21	0.6
"	77	4	26	3.8
"	-17.5	4	16	1.9
8LC	108.5	4	5	0.2
"	77	4	24	2.2
"	-17.5	4	22	2.1
8HD	77	4	25	2.8
6LD	108.5	4	4	4.2
"	77	4	24	3.6
"	-17.5	4	15	3.5
6HD	77	4	22	1.3
12LD	108.5	4	4	2.6
"	77	4	23	2.1
"	-17.5	4	18	5.3
12HD	77	4	25	1.4
Totals		90	426	
Avg.				2.3

cases where variance of the data was not accepted as homogeneous, appropriate transformations were applied before making the analysis of variance.

The q-test for homogeneity of variance of the raw data gives a value of 0.191 as compared with critical values of 0.325 for $\alpha = 0.01$ and 0.411 for $\alpha = 0.001$. Therefore, analysis of variance was performed on the data. Results are shown in Table 27.

TABLE 27

Exploratory Experiment

ANOVA

Source	df	SS	MS	F
Mix	7	1.317 E07	1.881 E06	2.96
Error	24	1.528 E07	6.366 E05	
Total	31	2.844 E07		

$F_{0.05} = 2.42$

$F_{0.01} = 3.50$

From this analysis, mixture type is determined to be significant at the 5 per cent level but not at the 1 per cent level. Further examination of these data by use of a Newman-Keuls test on the means shows no significant differences at the 1 per cent level. At the 5 per cent level only one pair was significant. The mean for 8LF (cell K) was greater than 12LD (cell H).

It should be noted that mixture type includes all asphalts of both high and low viscosity and all gradations, but not all of the possible combinations. It was reasoned that the trend of values for limiting strain would be the same for the fine and coarse gradations using the various asphalts as were measured for the dense gradation. It is concluded that asphalt viscosity and penetration have no significant effect at a test temperature of 77°F.

To further examine the effect of mixture type, with the viscosity parameter eliminated, tests were run at -17.5°F and 108.5°F and these data were analyzed with those from the 77°F runs. The cells included in this analysis are shown in Table 28.

TABLE 28

Cells for Effect of Mixture Type and Temperature

Temp / Mix	-17.5	77	108.5
6LD	1	G	6
8LD	A	D	E
12LD	2	H	7
8LF	8	K	3
8LC	4	L	5

Square root transformation of the data yields a q value of 0.152 while critical values of q for α's of 0.01 and

0.001 are 0.155 and 0.190, respectively. Two-way analysis of variance of the transformed data was run on the Purdue CDC 6500 using G4 UNEQUAL version 6/72 with weights proportional to the number of observations per cell. Results are given in Table 29.

TABLE 29

Effect of Mixture Type and Temperature

ANOVA

Source	df	SS	MS	F
Mix	4	616.7	154.2	2.20
Temp.	2	50,453.0	25,226.5	359.27
Mix×Temp	8	301.8	50.2	0.72
Error	51	3,581.0	70.2	

Critical F values are:

Source	df	df	$\alpha = 0.05$	$\alpha = 0.01$
Mix	4	51	2.57	3.73
Temp	2	51	3.19	5.07
Mix×Temp	8	51	2.14	2.90

This analysis shows that the only significant factor of this experiment is temperature and that it is highly significant. Mixture type is shown to have no significant effect.

V. Final Experiment

Examination of the mixture composition of the above experiment shows three dense-graded and two non-dense graded aggregates. Because of the possibility of a significant effect due to gradation, as shown by the exploratory one-way classification, it was decided to perform an analysis of the data based on gradation alone and to include a set of tests at 140°F. The cells shown in Table 30 are included in this analysis.

TABLE 30

Cells for Effect of Gradation

Temp / Mix	-17.5	77	108.5	140
8LD	A	D	E	P
8LF	8	K	3	T
8LC	4	L	5	4

Cube root transformation of the data yields a q value of 0.189 while critical values of q for α's of 0.01 and 0.001 are 0.200 and 0.249, respectively. Two-way analysis of variance of the transformed data using G4 UNEQUAL with weights proportional to the number of observations per cell provides the results given in Table 31.

TABLE 31

Effect of Gradation and Temperature

ANOVA

Source	df	SS	MS	F
Mix	2	44.18	22.09	5.24
Temp	3	2034.15	678.05	160.86
Mix×Temp	6	54.20	9.03	2.14
Error	40	168.61	4.22	

Critical F values are:

Source	df = 1	df = 2	α = 0.05	α = 0.01
Mix	2	40	3.23	5.18
Temp	3	40	2.84	4.31
Mix×Temp	6	40	2.34	3.29

Cell means for the transformed data are given in Table 32.

TABLE 32

Transformed Cell Means,
Effect of Gradation

Temp / Mix	-17.5	77	108.5	140
8LD	3.40	15.18	17.13	20.87
8LF	6.50	17.54	18.27	25.44
8LC	3.35	15.94	17.33	18.22

Analysis of variance shows that gradation is significant at the 1 per cent level and cell means of the transformed data show that the fine-graded mixtures have larger values of limiting strain than do the dense- and coarse-graded materials.

The final analysis is made on the cells shown in Table 33.

TABLE 33

Cells for Final Analysis

Temp / Mix	-17.5	77	108.5	140
6LD	1	G	6	M
8LD	A	D	E	P
12LD	2	H	7	R
8LF	8	K	3	T
8LC	4	L	5	4

The reason that all the data taken and shown in Table 23 are not included in this analysis is that the computer program G4 UNEQUAL, which was the only appropriate program available during the study, will not run if empty cells exist.

Fourth root transformation of the data yields a q value of 0.117 while critical values of q for α's of 0.01 and 0.001 are 0.119 and 0.145, respectively. Two-way

analysis of variance of the transformed data using G4 UNEQUAL with weights proportional to the number of observations per cell provides the values given in Table 34.

TABLE 34

Final Analysis

ANOVA

Source	df	SS	MS	F
Mix	4	5.9	1.5	2.79
Temp	3	624.3	208.1	390.71
Mix×Temp	12	12.7	1.1	1.98
Error	61	32.5	0.5	

Critical F values are:

Source	df = 1	df = 2	α = 0.05	α = 0.01
Mix	4	61	2.53	3.65
Temp	3	61	2.76	4.16
Mix×Temp	12	61	1.92	2.50

This analysis shows that the temperature effect is very highly significant and that mixture type is significant at the 5 per cent level but not at the 1 per cent level.

VI. Cell Means and Limits of the Means

Statistical limits were placed on the mean of limiting strain for each test temperature. These limits reflect the variability of the experiment. They can be used directly

to predict the level of probability of a limiting strain value for a given temperature and can also be used to select temperature ranges for application of the predictive equations that are presented in the next section.

Upper and lower limits of transformed limiting strains were calculated for each temperature according to the following equation:

$$\left.\begin{matrix} U' \\ L' \end{matrix}\right\} = \bar{y}_B \pm t(\nu, 0.025)\ S_{\bar{y}}$$

where $\bar{y}_B$ is the mean transformed limiting strain for a given temperature.

$t(\nu,0.025)$ is the t-statistic for 95% confidence limits with error degrees of freedom from a one-way analysis of variance, 110 in this case. A value of 1.980 is used for this analysis.

$$S_{\bar{y}} = \sqrt{\frac{\text{MS Error}}{n}}$$

n = number of observations in the cell.

U' = upper limit of transformed limiting strain means.

L' = lower limit of transformed limiting strain means.

Eighth root transformation of the data yields a q value of 0.203 while critical values of q for α's of 0.01 and 0.001 are 0.213 and 0.233, respectively. Transformed limits are inverted back to raw data by raising them to the eighth power. Upper and lower values of limiting strain at the 95% confidence level for each test temperature are shown in Table 35.

TABLE 35

Upper and Lower Values of Limiting Strain (U and L) in MII at 95% Confidence Level

Temp.	No. Obs.	L	U
-17.5	20	22	45
14	8	109	262
45.5	4	1883	4511
77	39	3437	4501
108.5	19	4378	6353
140	26	10,501	13,990

VII. Regression Equations

1. General

In order to estimate limiting strain value as is generally necessary for analytical solutions, it was considered desirable to generate regression equations to provide these estimators. Several regressions relating various functions of limiting strain to temperature and strain rate (approximately 20 combinations) were evaluated. The most reliable predictors, seven cases, are reported and discussed in the following sections. Predictive capability of each equation was judged on the basis of cumulative R^2 as well as by super-imposing a plot of the equation on a plot of the statistical limits of limiting strain for each temperature.

2. Regression Equations Without Strain Rate

Calculation of regression coefficients was by Purdue CDC 6500 using G2 SPSS 15 REGRESSION, version 4173.

A. Case I uses the following model:

$$\hat{\varepsilon}_f = \beta_0 + \beta_1(T_F') + \beta_2(T_F')^2 + \beta_3(T_F')^3 + e \qquad \text{(Case I)}$$

where $\hat{\varepsilon}_f$ = estimated limiting strain in MII.

T_F' = shifted temperature in degrees Fahrenheit and is calculated as $T_F' = T_F + 20.0$ where T_F is the actual test temperature. The reason for this shift is that the computer cannot extract a square root of a negative number (-17.5°F).

β_i = regression coefficient.

e = error term.

Three fits were made with this model. A "cubic" fit uses all terms of the model, a "quadratic" fit uses β_0, β_1 and β_2, and a "linear" fit uses only β_0 and β_1. Calculated coefficients, multiple R and cumulative R^2 values for each of these equations are shown in Table 36.

TABLE 36

Regression Coefficients for Case I

Fit	B_0	B_1	B_2	B_3	Mult. R	Cumul. R^2
Cubic	-439.4	104.5	-1.470	0.0084	0.83	0.70
Quadratic	369.1	-33.52	0.6923	0	0.83	0.68
Linear	-1981	78.05	0	0	0.76	0.57

Plots of these equations along with the 95% confidence limits of the means are shown on Figure 30.

B. Case II

In order to improve R^2 above that of Case I, the data of the experiment were fitted to the following model:

$$\sqrt[4]{\varepsilon_f} = \beta_0 + \beta_1(T'_F) + \beta_2(T'_F)^2 + \beta_3(T'_F)^3 \quad \text{(Case II)}$$

As for case I, three fits were also made with this model. A "cubic" fit uses all terms of the model, a "quadratic" fit uses β_0, β_1 and β_2, and a "linear" fit uses only β_0 and β_1. Calculated coefficients, multiple R and cumulative R^2 values for each of these equations are shown in Table 37.

TABLE 37

Regression Coefficients for Case II

Fit	B_0	B_1	B_2	B_3	Mult. R	Cumul. R^2
Cubic	2.049	0.0887	-0.0004	0	0.95	0.91
Quadratic	2.176	0.0675	-0.0001	0	0.95	0.91
Linear	2.511	0.0511	0	0	0.95	0.90

Plots of the cubic and quadratic equations along with the 95% confidence limits of the means are shown on Figure 31.

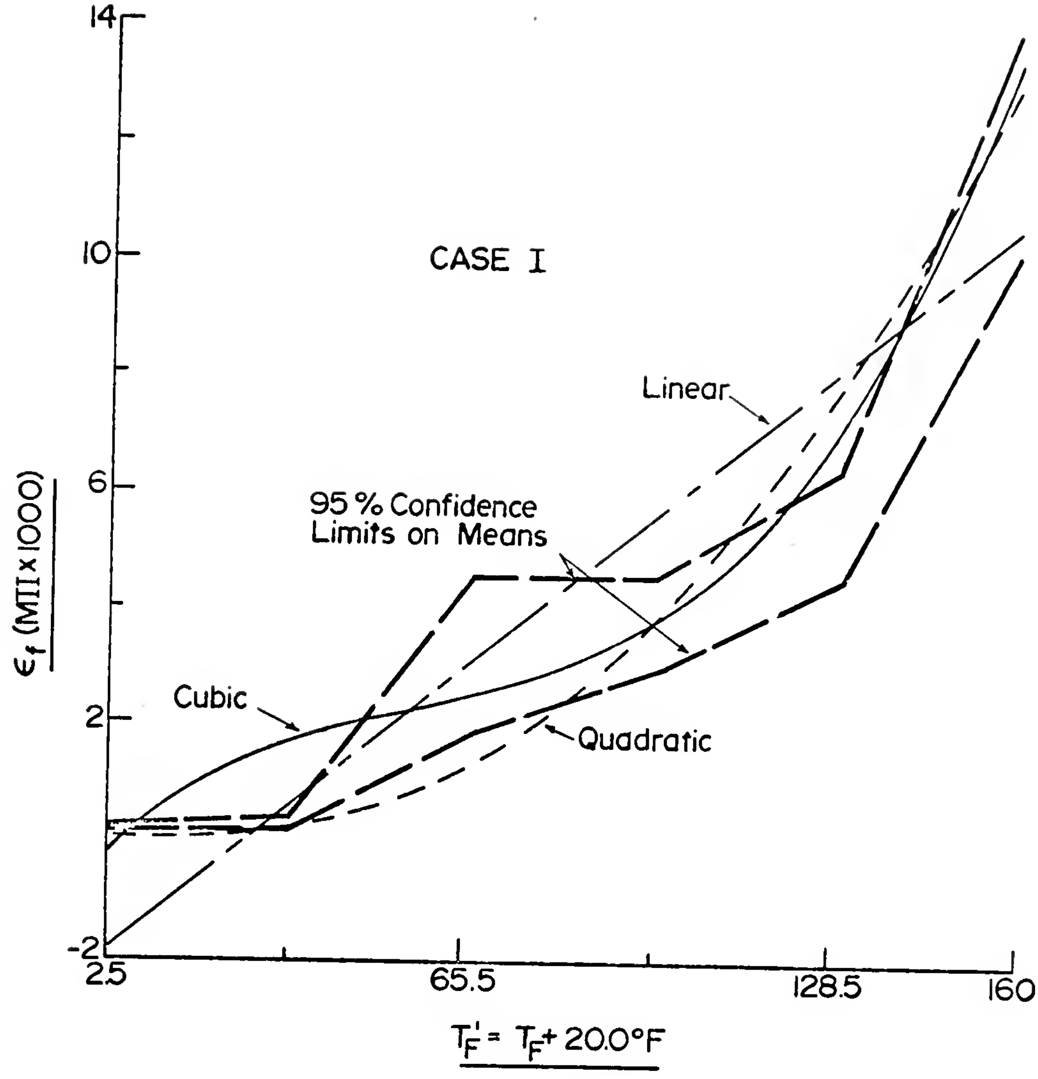

FIGURE 30 LINEAR REGRESSION FITS AND 95% CONFIDENCE LIMITS ON MEANS.

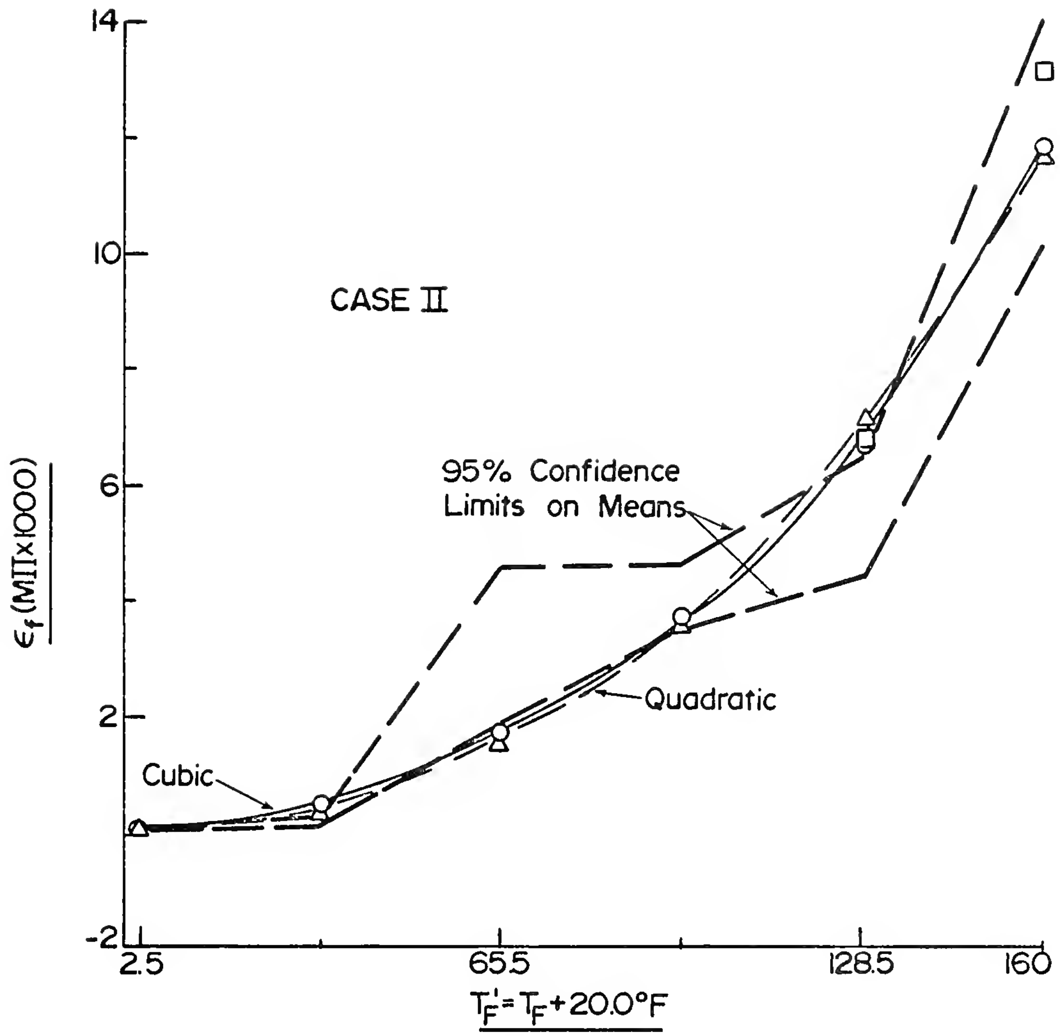

FIGURE 31 LINEAR REGRESSION FITS AND 95% CONFIDENCE LIMITS ON MEANS.

It should be noted that using the fourth root of limiting strain produces a sizable increase in R^2 over case I. The plotted equations for this case also lie in the envelope of the statistical limits of the means much better than do the curves produced in case I.

3. Regression Equations that Include Strain Rate

In order to aid in assessing the effect of strain rate and to include strain rate as an independent variable if necessary for future calculations, two more models were included.

A. Cases III and IV use the following models:

$$\begin{aligned}\hat{\varepsilon}_f = {} & \beta_0 + \beta_1\dot{\varepsilon} + \beta_2\dot{\varepsilon}^2 + \beta_3\dot{\varepsilon}^3 \\ & + \beta_4 T'_F + \beta_5 T'^2_F + \beta_6 T'^3_F \\ & + \beta_7\dot{\varepsilon}T'_F + \beta_8[\dot{\varepsilon}T'_F]^2 + \beta_9[\dot{\varepsilon}T'_F]^3 + e \qquad \text{(Case III)}\end{aligned}$$

$$\begin{aligned}\sqrt[4]{\hat{\varepsilon}_f} = {} & \beta_0 + \beta_1\dot{\varepsilon} + \beta_2\dot{\varepsilon}^2 + \beta_3\dot{\varepsilon}^3 \\ & + \beta_4 T'_F + \beta_5 T'^2_F + \beta_6 T'^3_F \\ & + \beta_7\dot{\varepsilon}T'_F + \beta_8[\dot{\varepsilon}T'_F]^2 + \beta_9[\dot{\varepsilon}T'_F]^3 + e \qquad \text{(Case IV)}\end{aligned}$$

where $\hat{\varepsilon}_f$ = limiting strain in MII.

$\dot{\varepsilon}$ = mean strain rate during the test in MII per second.

T'_F = shifted temperature in degrees Fahrenheit and is equal to $T_F + 20.0$ where T_F is the test temperature.

e = error.

Calculated coefficients, multiple R and cumulative R^2 values for each of these equations are shown in Table 38.

TABLE 38

Regression Coefficients for Cases III and IV

	Case III	Case IV
β_0	-414.5	2.059
β_1	75.04	0.0316
β_2	-0.1745	-0.0001
β_3	0.0002	0
β_4	72.21	0.0748
β_5	-1.421	-0.0004
β_6	0.0092	0
β_7	-0.4604	-0.0002
β_8	0.0001	0
β_9	0	0
Mult. R	0.83	0.96
Cumul. R^2	0.71	0.91

Comparing case III with the "cubic" fit of case I, it is seen that no significant increase in R^2 is effected by introducing strain rate into the regression. Likewise, when considering the fourth root function of limiting strain, and comparing cumulative R^2 values for case IV with case II values, it is seen that no significant increase in cumulative R^2 is effected by introducing strain rate.

This is not to imply, however, that strain rate has no effect. This effect can only be evaluated by a controlled experiment that requires equipment that was not available at the time of this study.

4. Non-Linear Regressions

Several non-linear models were tried using G2 SPSS 21 NONLINEAR.

A. Case V ("Cubic-Quadratic")

$$\varepsilon_f = B_0 + B_1(T_F') + B_3(T_F')^2 + B_4(T_F')^3 \qquad \text{(Case V)}$$

Note that this is the same type equation that appears for the linear case except that this program allows limits to be set on the coefficients and thus force the curve into a given region of the data spectrum. Results of this fit are as follows:

$B_0 = 83.22$, $B_1 = -1.213$, $B_2 = 0.007534$, $B_3 = 253.3$

B. Case VI (Portion of Normal Curve)

$$\varepsilon_f = \frac{\text{Exp}[\tfrac{1}{2}(T_F' - B_1)^2 \div B_2]}{\sqrt{2\pi\ B_3}}. \qquad \text{(Case VI)}$$

$B_1 = -124.6$, $B_2 = 8480$, $F_3 = 1.198$ E-05

C. Case VII (Modified Normal)

$$\varepsilon_f = \frac{[B_1(T_F' - B_2)^2 \div B_3]}{\sqrt{\pi\ B_4}} \qquad \text{(Case VII)}$$

$B_1 = 40.12$, $B_2 = 24.45$, $B_3 = 14.73$, $B_4 = 4.920$

Plots of these equations along with the 95% confidence limits of the means are shown on Figure 32.

5. Conclusions Regarding the Use of Developed Predictive Equations

A. Many regression equations involving various functions of limiting strain, temperature and strain rates were developed as part of this analysis. Predictive capability of each equation was judged on the basis of cumulative R^2 as well as by superimposing a plot of the equation on a plot of the statistical limits of limiting strain for each temperature. Only those solutions that appeared to have the best predictive capability or reliability are included herein.

B. When comparing cumulative R^2 values for the seven cases that are included the following is observed:

a. Using the fourth root of limiting strain (case II) improves predictive reliability as indicated by higher values of R^2 over the equation that uses limiting strain directly (case I).

b. The addition of strain rate does not greatly increase values of R^2 above those for the cases where strain rate is not included.

c. When superimposing any of the three sets of regression equations on a plot of statistical limits of limiting strain versus temperature,

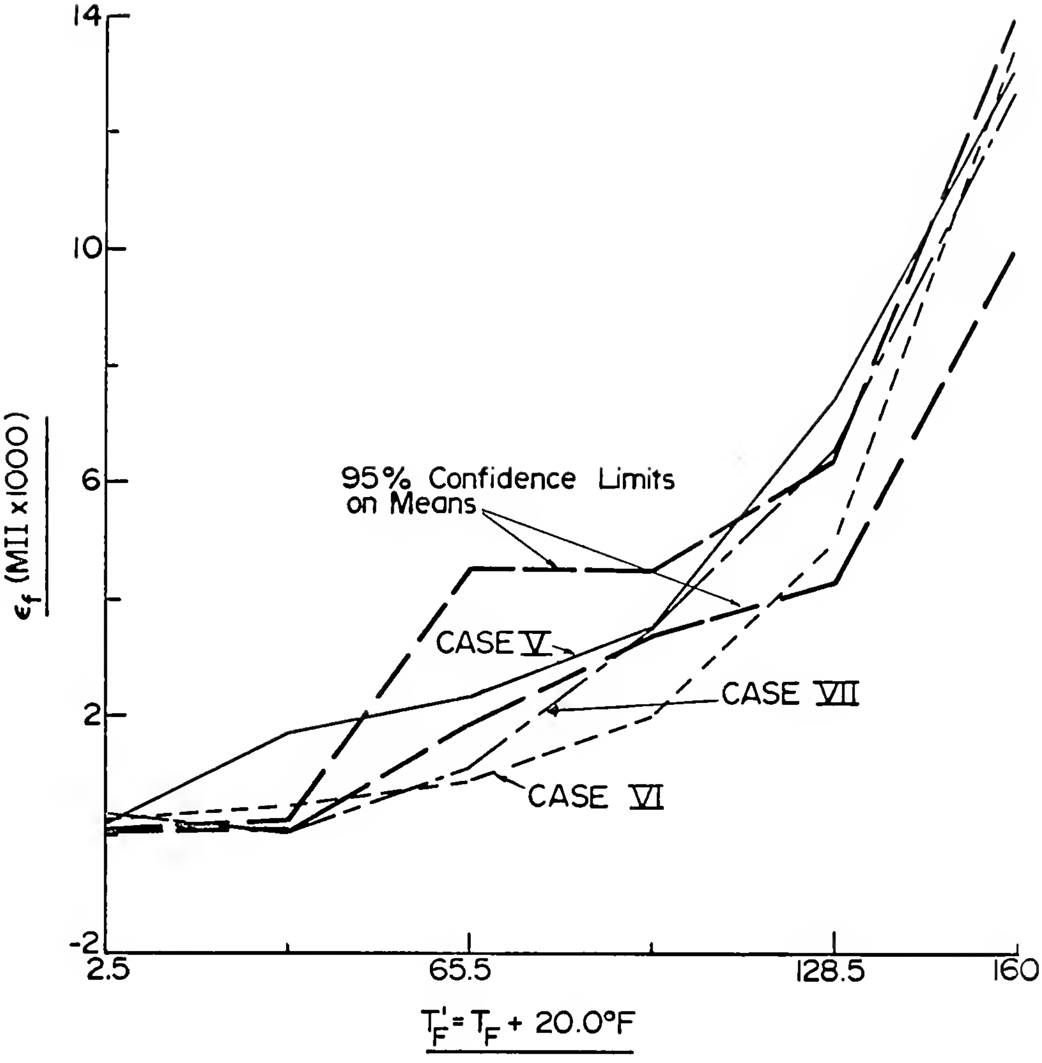

FIGURE 32 NON-LINEAR FITS AND 95% CONFIDENCE LIMITS ON MEANS.

it is observed that none of the methods provide curves that lie entirely within the statistical envelope throughout the entire temperature range of the experiment. From this point of view, it is clear that predictive reliability can be greatly increased by approximating the function between test temperatures by simple straight-line proportioning between cell means.

SUMMARY OF RESULTS AND CONCLUSIONS

I. Acoustic Emissions Techniques for Crack Detection

Based on reasonably extensive experiments conducted on portland cement concrete and somewhat limited experiments conducted on asphalt concrete, it is concluded that acoustic emission techniques are a viable method of detecting and monitoring crack initiation and propagation in brittle particulate materials.

In the case of asphalt concretes, detection of acoustic emission signals at temperatures above room temperature is difficult at best. It is possible that, at these temperatures, asphalt binder attenuates the waves generated by aggregate fracture and that signal amplification with background noise filtering was not adequate with the equipment being used. It is also possible that the failure mechanism at these higher temperatures does not involve aggregate fracture and that failure is due to excessive viscous flow of the binder. If viscous flow is the mechanism, bond breaking that generates elastic waves to activate transducers does not occur and hence there should be no emission signals.

The Kaiser or memory effect is quite pronounced in both portland cement and asphalt concretes. This effect is

produced when a load below that necessary for failure causes some microcracking that is recordable. If this load is released, and microcracks remain after this load release, subsequent loading will not cause additional cracking and hence acoustic emissions will not occur until loading exceeds the load that was previously applied.

II. Tension Test Results

Limiting strain values (strain at ultimate load) of asphalt concretes in direct tension were measured and reported. Regression equations that relate limiting strain to temperature and strain rate were developed. Parameters in the experiment included a single aggregate of 100 per cent crushed limestone at three gradations, six asphalt types, six temperatures and variable strain rate. Based on these tests, the following results and conclusions are presented:

Temperature is, by far, the most significant factor of the parameters studied affecting failure strain. Limiting strain at 140°F (60°C) is approximately 300 to 500 times as great as that at -17.5°F (-27.5°C).

Strain rate, as should be expected for a viscoelastic material has an effect on limiting strain. However, the effect of strain rate, resulting from contractions due to reasonable temperature change and ordinary vehicular loadings, is equivalent to the effect of only a few degrees of temperature change. That is, a small increase in

temperature increases the value of limiting strain much more than does a change in strain rate caused by a relatively fast moving vehicular load to that caused by a long-term temperature change.

Fine-graded mixtures have a somewhat greater value of limiting strain for a given temperature and strain rate than the coarser graded mixtures. Fine-graded mixtures have considerably more aggregate surface area and hence thinner binder films at the design asphalt content than do dense and coarse-graded mixtures. It is also quite possible that the increased filler concentrations in these thinner films provides a strengthening mechanism somewhat analogous to composite reinforcement of other organic polymers.

This study utilized asphalts of penetration grades within the range normally employed for bituminous concrete in the continental United States. Within this context, findings with regards to asphalt type may not be as one would expect. It has been contended for some time that, softer penetration grades of asphalt should be used for pavements in regions that experience lower ambient temperatures, presumably to eliminate or to at least reduce brittle cracking, and that harder grades should be used in regions of higher ambient temperatures to provide increased stability and less deformation from wheel loads at these higher temperatures. Findings of this study are

that, within the range investigated, asphalt type has no effect on limiting strain as measured by direct tension testing.

Type of asphalt as described herein refers to a combination of penetration and viscosity at standard conditions. Types for this study included a high and low viscosity material within nominal penetration grades of 60-70, 85-100 and 120-150. Because asphalt type was not a significant factor in this experiment does not preclude the possibility that type will be significant under other conditions. Situations do occur in practice where much softer materials than those used for this study are utilized. Northern regions of the continent that experience very low temperatures for extended periods of time use these softer materials and evidence suggests that such materials may have limiting strain values at a given temperature that exceed values determined by this study.

Although the test asphalts included the normal ranges of penetration and viscosity grades generally used in the United States, they did not include the full range of penetration indices available. No air-blown or chemically altered asphalts were included.

Finally, stiffness values that relate stress to strain for a given asphalt, temperature, loading time and aggregate volume as determined by the Van der Poel nomograph and modified for aggregate content were reasonably well verified.

It is possible to use these stiffness values in theoretical solutions to predict working strain for a given loading and environmental condition. Limiting strain values, for mixtures with properties similar to those used for this study, suitably reduced with appropriate safety factors for variability and fatigue can be used as working strains in rational procedures to determine design thickness or to study remaining pavement life.

RECOMMENDATIONS FOR FURTHER RESEARCH

I. Other Test Techniques

In view of the complexity of direct tension testing and the large quantities of materials necessary to perform these tests, it is recommended that an indirect method of obtaining limiting strain be considered.

At the present time the most promising test appears to be the use of the so-called splitting tension or dimetral compression test. Some preliminary work has been done that indicates strain at failure can be calculated from measurements obtained by this technique. Splitting tension tests can be performed on mixtures with the same components and properties as those used for this study in order to determine if a correlation exists. Since splitting tension testing places portions of the specimen in direct tension, measurements of strain in the failure zone should compare directly with values of limiting strain obtained in this study.

Whatever testing technique is used, acoustic emission data should be obtained to better define the temperature region where aggregate fracture no longer occurs and the failure mode becomes one of viscous flow. These data will become valuable for later fundamental studies of failure mechanisms in bituminous mixtures.

II. Mixture Parameters

Limiting strain should be evaluated for mixture parameters that were not included in this study. Effects of the following parameters should be investigated:

1. Aggregate type

This study was limited to 100 per cent crushed limestone of a single source. Other studies should include: pit run sand and gravel to find the effect of rounded rather than crushed particles; other crushed materials that are non-carbonate to determine if mineralogical characteristics have an effect; and high absorption limestones to determine if these materials, which are now considered as marginal for paving uses, have better asphalt adhesion and hence greater limiting strain values.

2. Type and amount of filler

Fillers with different mineralogical characteristics and various amounts of filler should be studied to find if a film strengthening action exists as a result of incorporating these materials into mixtures.

3. Other bituminous materials

While limiting strain was not affected by asphalt types used in this study other bituminous materials should be examined. These might include air-blown and chemically altered asphalts, asphalt emulsions and natural asphalt blended with petroleum asphalts.

4. Other parameters

Mixture properties vary due to construction practice and field exposure. Two variations that commonly occur in the field are asphalt content and degree of compaction. The effect of both of these properties should be investigated in order to more realistically determine what tolerances can be accommodated. Measurements should be made to determine the effect of age hardening of bituminous binders on limiting strain as an indicator of durability and remaining pavement life.

III. Field Verification

A pilot study should be initiated that includes several pavement thicknesses determined by theoretical design procedures and include working strain values obtained from this study. Both new pavements and overlays of existing rigid pavements should be included. Field measurements of strains at failure can be used to test the assumption that direct tension tests are a valid representation of field stress conditions. Modifications, if necessary, can be made to provide adequate safety factors for the application of limiting strain as a failure criterion for bituminous concretes.

REFERENCES

REFERENCES

1. Shields, B. P. and Anderson, K. O., "Some Aspects of Transverse Cracking in Asphalt Pavements," Proc., Canadian Technical Asphalt Association, 1964.

2. Anderson, K. O., Shields, B. P., and Dacyszyn, J. M., Proc. AAPT, 35, 1966.

3. Culley, R. W., "Transverse Cracking of Flexible Pavements in Sakatchewan," Sakatchewan Department of Highways, Technical Report 3, 1966.

4. Lamb, D. R., Pavlovich, R. D., and Scott, W. G., "Roadway Failure Study No. 1, Final Report," Highway Engineering Research Publication H-15, Natural Resources Research Institute, University of Wyoming, 1968.

5. Breen, J. J., and Stevens, J. E., "Fatigue and Tensile Characteristics of Bituminous Pavements at Low Temperatures," Report No. J.H.K. 66-3, School of Engineering, University of Connecticut, 1966.

6. Haas, R. C. G., "Thermal Shrinkage Cracking of Some Ontario Pavements," Ontario Joint Highway Research Programme, D. H. O. Report No. RR161.

7. Symposium on Non-Traffic Load Associated Cracking of Asphalt Pavements, Proc. AAPT, 35, 1966.

8. Western Summer Meeting, HRB, Denver, Colorado, 1968.

9. Young, F. D., Deme, I., Burgess, R. A., and Kopnillem, "A Field Study of Transverse Crack Development in Asphalt Pavements," The Canadian Technical Asphalt Association, 1969.

10. Van der Poel, C., "Presentation of Rheological Properties of Bitumen Over a Wide Range of Temperatures and Loading Times," Proc. Second International Conference on Rheology, 1954.

11. Van der Poel, C., "A General System Describing the Visco-Elastic Properties of Bitumens and its Relation to Routine Test Data," Journal of Applied Chemistry, May 1954.

12. Monismith, C. L., Secor, G. A., and Secor, K. E., "Temperature Induced Stresses and Deformations in Asphalt Concrete," Proc. AAPT 34, 1965.

13. Ashton, J. E. and Moavenzadeh, F., "Analysis of Stresses and Displacements in a Three-Layered Viscoelastic System," Second International Conference on the Structural Design of Asphalt Pavements, Ann Arbor Conference, 1967.

14. Perloff, W. H. and Moavenzadeh, F., "Deflection of Viscoelastic Medium Due to a Moving Load," Ann Arbor Conference, 1967.

15. Barksdale, R. D. and Leonards, G. A., "Predicting Performance of Bituminous Surfaced Pavements," Ann Arbor Conference, 1967.

16. Dunegan, H. L. and Harris, D. O., "Acoustic Emission - A New Nondestructive Testing Tool," Ultrasonics, July, 1969.

17. Dunegan, H. L., Harris, D. O. and Tatro, C. A., "Fracture Analysis by Use of Acoustic Emission," National Symposium on Fracture Mechanics, Lehigh University, 1967.

18. Ledus, F. L., "Preliminary Report on Investigation into Causes of Cracking in Sheet Asphalt," Ninth Annual Asphalt Paving Conference, 1930.

19. Rader, L. F., "Investigations of the Physical Properties of Asphaltic Mixtures at Low Temperatures," Proc. AAPT, 6, 1935.

20. Brown, J. D. and Steinbaugh, V. B., Proc. AAPT, 9, 1937.

21. Abson, G., in a discussion of a paper by Skidmore, H. W., "Basic Criteria for the Design and Control of Asphalt Paving Mixtures," Proc. AAPT, 18, 1949.

22. Hughes, E. C. and Faris, R. B., "Low Temperature Maximum Deformability of Asphalts," Proc. AAPT, 19, 1950.

23. Vallerga, B. A., "On Asphalt Pavement Performance," Proc. AAPT, 24, 1955.

24. Chipperfield, E. H. and Welch, T. K., "Studies on the Relationship Between the Properties of Road Bitumens and Their Service Performance," Proc. AAPT, 36, 1967.

25. Tuckett, G. M., Jones, G. M. and Littlefield, G., "The Effects of Mixture Variables on Thermally Induced Stresses in Asphaltic Concrete," Proc. AAPT, 39, 1970.

26. Saal, K. N. J. and Pell, P. S., "Fatigue of Bituminous Road Mixes," Kolloid-Zeitschrift (Colloid Journal), Vol. 171, 1960.

27. Pell, P. S., "Fatigue of Asphalt Paving Mixes," Ann Arbor Conference, 1967.

28. Anderson, D. A. and Goetz, W. H., "Mechanical Behavior and Reinforcement of Mineral Filler-Asphalt Mixtures," Proc. AAPT, 42, 1973.

29. Ferry, J. D., "Viscoelastic Properties of Polymers," John Wiley and Sons, 1970.

30. Heukelom, W. and Klomp, J. G., "Road Design and Dynamic Loading," Proc. AAPT, 33, 1964.

31. Heukelom, W., "Observations on the Rheology and Fracture of Bitumens and Asphalt Mixes," Proc. AAPT, 35, 1965.

32. Van Draat, W. E. F. and Sommer, P., "Ein Gerat zue Bestimung der Dynamischen Elastizitatt-smoduln von Asphalt," Strasse und Autobohn, Vol. 35, 1966. (An Instrument for Determination of the Dynamic Modulii of Elasticity of Asphalt).

33. Lockhart, C., "Indiana Aggregate Sources and Bituminous Mixing Plants for State Highway Use," a map from the Indiana State Highway Commission, January, 1969, revised January 1970.

34. "Index of Aggregate Producers for Aggregate Source Map," Indiana State Highway Commission, January, 1970.

35. Ault, C. H. and Carr, D. C., "Directory of Crushed Stone, Ground Limestone, Cement, and Lime Producers in Indiana," Indiana Geological Survey, 1970.

36. French, R. R., "Crushed Stone Resources of the Devonian and Silurian Carbonate Rocks of Indiana." Department of Natural Resources Geological Survey Bulletin 37, 1967.

37. Carr, D. D., French, R. R. and Ault, C. H., "Crushed Stone Aggregate Resources of Indiana," Department of Natural Resources Geological Survey Bulletin 42-Id, 1971.

38. Indiana State Highway Standard Specifications, 1971. Section 903.02, Coarse Aggregates.

39. Schuster, R. L., "A Study of Chert and Shale Gravel in Concrete." Joint Highway Research Project, Purdue University and Indiana State Highway Commission, Commission, September, 1960.

40. "Specifications and Construction Methods for Asphalt Concrete and Other Plant-Mix Types." The Asphalt Institute, Specification Series No. 1, 1964.

41. Ostle, B., "Statistics in Research," second edition, p. 63. The Iowa State University Press, 1963.

42. "Asphalt Surface Treatments and Asphalt Penetration Macadam." Appendix F. "Determination of the Flakiness Index of Aggregates," The Asphalt Institute, Manual Series No. 13, 1969.

43. Krumbein, W. C. and Pettijohn, F. J., "Manual of Sedimentary Petrography." Appleton-Century-Crofts, Inc., 1938.

44. Rostler, F. S., Rostler, K. S., Halstead, W. W. and Oglio, E. R., "Fingerprinting of Highway Asphalts," Proc. AAPT 41, 1972.

45. Rostler, F. S., and Rostler, K. S., "'Fingerprinting' of Highway Asphalts—A Method for Cataloguing and Identifying Highway Asphalts," Final Report, Contract Number FH-11-7188, U. S. Department of Transportation, Federal Highway Asphalts," Final Report, Contract Number FH-11-7188, U. S. Department of Transportation, Federal Highway Administration, 1971.

46. Mandel, John, "The Statistical Analysis of Experimental Data." Chapter 11. Interscience Publishers, 1964.

47. Pfeiffer, J. P., "The Properties of Asphaltic Bitumen," Elsevier Press, Inc. Houston, Tex., 1950.

48. Schofield, B. H., "Acoustic Emission Under Applied Stress," Aeronautical Research Laboratory, Office of Aerospace Research, U. S. Air Force, Wright-Patterson AFB, Ohio, U.S.A., ARL-150, 1961.

49. Green, A. T., "Detection of Incipient Failures in Pressure Vessels by Stress-Wave Emissions," Nuclear Safety, Vol. 10, No. 1, 1969.

50. Dunegan, H. L., Harris, D. O., and Tetelman, A. S., "Detection of Fatigue Crack Growth by Acoustic Emission Techniques," Materials Evaluation, Vol. XXV 111, No. 10, 1969.

51. Bickle, L. W., Eric H. Wang Civil Engineering Research Facility, University of New Mexico, Albuquerque. Telephone conversations regarding unpublished studies. August, 1974.

52. Anderson, V. L., and McLean, R. A., "Design of Experiments," Marcel-Dekker, Inc., 1974.

53. Holliday, L., "Composite Materials," Elsevier Publishing Co., 1966. Reference is to section VIII, "Concrete Systems," by K. Newman.

54. Robinson, G. S., Unpublished Ph.D. Thesis, University of London, 1964.

55. Blakey, F. A. and Beresford, F. D., C.S.I.R.O., Melbourne, Report C2.2-1, 1953; Report C2.2-2, 1955.

56. Kaplan, M. F., Proc. Am. Concrete Inst., 55 (1959) 1193.

57. Welch, G. B., Road Research Laboratory, D.S. & R., Lab Note No. LN15981GBW, June 1964.

58. Traxler, R. N., "Asphalt, Its Composition, Properties and Uses," Reinhold Publishing Corp. 1961.

59. "Mix Design Methods for Asphalt Concrete and Other Hot Mix Types," The Asphalt Institute, Manual Series No. 2, fourth edition, March 1974.

60. Test Method No. Calif. 303-E (October 3, 1966), "Method of Test for Centrifugal Kerosene Equivalent Including K Factor," Materials Manual, Vol. I, State of California, Department of Public Works, Division of Highways.

61. "Thickness Design - Asphalt Pavement Structures for Highways and Streets," The Asphalt Institute, Manual Series No. 1, eighth edition, December, 1969.

62. "Full Depth Pavements for Air Carrier Airports," The Asphalt Institute, Manual Series No. 11, first edition, January, 1973.

63. "BISTRO" (Bitumen Structures in Roads), "Computer Program for Layered Systems under Normal Surface Loads." Courtesy of Koninklijke/Shell-Laboratorium, Amsterdam, Netherlands, (Shell Research N.V.). This program was modified to run on the Purdue CDC-6500. This program was provided for the sole use of Purdue University, Civil Engineering. All rights reserved. Use of this program by unauthorized persons is prohibited.

64. Haas, R. C. G., "A Method for Designing Asphalt Pavements to Minimize Low-Temperature Shrinkage Cracking," The Asphalt Institute, Research Report No. 73-1 (RR-73-1), January, 1973.

65. Hooks, C. C. and Goetz, W. H., "Laboratory Thermal Expansion Measuring Techniques Applied to Bituminous Concrete," Report to U. S. Army Engineers, Waterways Experiment Station, Vicksburg, Miss., by Purdue University, August, 1964.

66. Cook, N. H. and Rabinowicz, E., "Physical Measurement and Analysis," Addison-Wesley, 1963.

67. Herceg, E. E., "Handbook of Measurement and Control," Schaevitz Engineering, Pennsanken, N. J., 1972.

68. "The Asphalt Handbook," The Asphalt Institute, Manual Series No. 4, 1970.

69. Finn, F. F., "Factors Involved in the Design of Asphaltic Pavement Surfaces," NCHRP Program Report 39, Highway Research Board, 1967.

70. Readshaw, "Asphalt Specifications in British Columbia for Low Temperature Performance," Proc. AAPT, 41, 1972.

71. Fabb, "The Influence of Mix Composition, Binder Properties and Cooling Rate on Asphalt Cracking at Low Temperatures," Proc. AAPT, 43, 1974.

APPENDICES

APPENDIX A

Acoustic Emissions

Reduced Data and Calculations for Plots

(Normalized counts versus stress ratio,

portland cement concrete.)

Σ_{10} = AE counts @ σ/σ_f = 10%

$\Sigma_n = \frac{\Sigma}{\Sigma_{10}}$

W/C = 0.40
CA = 0.42

Time (Sec)	CYL. 1			CYL. 2			CYL. 3		
	Cyl 1 Σ_{10} = 6.70			2 Σ_{10} = 15.39			3 Σ_{10} = 5.52		
	σ/σ_f	AE (1000's) Σ	Σ_N	σ/σ_f	AE (1000's) Σ	Σ_N	σ/σ_f	AE (1000's) Σ	Σ_N
0	0	4.50	0.67	0	7.00	0.45	0	1.80	0.33
2.5	2	6.00	0.90	2	11.80	0.77	2	3.30	0.60
5	6	6.56	0.98	6	13.85	0.90	5	4.26	0.77
7.5	11	6.74	1.01	9	15.[illegible]4	0.98	9	5.33	0.97
10	15	7.06	1.05	13	16.14	1.05	14	6.30	1.14
12.5	20	7.15	1.07	19	16.87	1.10	18	6.96	1.26
15	25	7.24	1.08	24	17.36	1.13	23	7.36	1.33
17.5	30	7.33	1.09	29	17.93	1.17	28	7.72	1.40
20	35	7.33	1.09	35	18.46	1.20	33	8.05	1.46
22.5	40	7.46	1.11	39	18.83	1.22	37	8.40	1.52
25	45	7.46	1.11	43	19.17	1.25	43	8.82	1.60
27.5	50	7.47	1.11	49	19.42	1.26	48	9.00	1.63
30	56	7.49	1.12	53	19.63	1.28	53	9.22	1.67
32.5	60	7.51	1.12	58	20.08	1.30	58	9.36	1.70
35	66	7.52	1.12	63	20.43	1.32	64	4.48	1.72
37.5	71	7.54	1.13	69	20.70	1.35	69	9.58	1.74
40	75	7.57	1.13	74	21.05	1.37	74	9.80	1.78
42.5	80	7.64	1.14	80	21.35	1.39	79	10.36	1.88
45	86	7.71	1.15	83	21.70	1.41	84	11.24	2.04
47.5	89	7.79	1.16	90	22.37	1.45	88	11.82	2.14
50	94	7.81	1.17	93	23.09	1.50	93	12.30	2.23
52.5	98	8.20	1.22	97	24.24	1.58	97	12.90	2.34
55	100	10.00	1.49	100	26.50	1.72	100	15.00	2.72

Cyls 4, 5 & 6

W/C = 0.45
CA = 0.42

	CYL 4			CYL 5			CYL 6		
	$\Sigma_{10} = 1.75$			$\Sigma_{10} = 8.69$			$\Sigma_{10} = 4.89$		
Time (Sec)	σ_f/σ	AE (1000's)	Σ_n	σ_f/σ	AE (1000's)	Σ_n	σ_f/σ	AE (1000's)	Σ_n
0	0	1.10	0.63	0	8.55	0.98	0	0.85	0.17
2.5	2	1.50	0.86	2	8.61	0.99	1	1.90	0.39
5	6	1.65	0.94	7	8.66	1.00	4	3.95	0.81
7.5	10	1.75	1.00	11	8.70	1.00	9	4.83	0.99
10	15	1.86	1.06	20	8.72	1.00	14	5.15	1.05
12.5	19	1.90	1.09	27	8.77	1.01	21	5.40	1.10
15	24	1.91	1.09	36	8.77	1.01	25	5.59	1.14
17.5	30	1.94	1.11	43	8.78	1.01	32	5.68	1.16
20	35	1.98	1.13	52	8.86	1.02	38	5.74	1.17
22.5	41	2.00	1.14	61	8.87	1.02	45	5.87	1.20
25	47	2.01	1.15	71	8.90	1.02	50	5.88	1.20
27.5	52	2.05	1.17	80	8.94	1.03	56	5.94	1.21
30	58	2.05	1.17	87	9.30	1.07	63	5.95	1.22
32.5	63	2.06	1.18	95	10.70	1.23	67	6.03	1.23
35	69	2.07	1.18	100			72	6.09	1.25
37.5	74	2.07	1.18				78	6.12	1.25
40	79	2.09	1.19				85	6.16	1.26
42.5	86	2.09	1.19				89	6.23	1.27
45	89	2.20	1.26				94	6.36	1.30
47.5	95	2.22	1.27				99	6.55	1.34
50	98	2.33	1.33				100	7.05	1.44
52.5	100								

W/C = 0.50
CA = 0.42

TIME (Sec)	CYL 7 $\Sigma_{10} = 2.65$			CYL 8 $\Sigma_{10} = 0.27$			CYL 9 $\Sigma_{10} = 4.03$		
	σ/σ_f	AE (1000's)	Σ_N	σ/σ_f	AE (1000's)	Σ_N	σ/σ_f	AE (1000's)	Σ_N
0	0	0.50	0.19	0	0.20	0.74	0	1.40	0.35
2.5	2	1.60	0.60	5	0.25	0.93	3	2.60	0.65
5	6	2.33	0.88	10	0.27	1.00	5	3.20	0.79
7.5	11	2.73	1.03	16	0.27	1.00	9	4.00	0.99
10	18	2.89	1.09	23	0.27	1.00	17	4.20	1.04
12.5	26	3.00	1.13	32	0.27	1.00	25	4.20	1.04
15	33	3.03	1.14	40	0.27	1.00	32	4.50	1.12
17.5	42	3.05	1.15	49	0.27	1.00	40	4.70	1.17
20	51	3.07	1.16	57	0.27	1.00	49	4.70	1.17
22.5	57	3.07	1.16	64	0.27	1.00	56	4.90	1.22
25	63	3.09	1.17	72	0.27	1.00	63	5.00	1.24
27.5	71	3.10	1.17	80	0.27	1.00	72	5.00	1.24
30	77	3.10	1.17	86	0.27	1.00	80	5.00	1.24
32.5	86	3.13	1.18	93	0.27	1.00	87	5.10	1.27
35	91	3.15	1.19	99	0.29	1.07	94	5.50	1.36
37.5	96	3.33	1.26	100	0.32	1.19	98	7.40	1.84
40	99	3.54	1.34		∞	∞	100	10.00	2.48
42.5	100	4.09	1.54					∞	

W/C = 0.40
CA = 0.52

TIME (Sec)	CYL 10 $\Sigma_{10} = 28.54$ σ/σ_f	AE (1000's)	Σ_N	CYL 11 $\Sigma_{10} = 12.60$ σ/σ_f	AE (1000's)	Σ_N	CYL 12 $\Sigma_{10} = 4.05$ σ/σ_f	AE (1000's)	Σ
0	0	26.30	0.92	0	12.08	0.96	0	1.67	0.41
2.5	2	27.20	0.95	2	12.36	0.98	2	2.80	0.69
5	5	27.88	0.98	4	12.97	1.03	4	3.60	0.89
7.5	10	28.54	1.00	7	12.57	1.00	7	3.91	0.97
10	16	29.00	1.02	10	12.60	1.00	11	4.10	1.01
12.5	22	29.46	1.03	16	12.61	1.00	15	4.25	1.05
15	27	29.70	1.04	21	12.64	1.00	19	4.31	1.06
17.5	34	30.26	1.06	26	12.70	1.01	23	4.35	1.07
20	41	30.47	1.07	32	12.74	1.01	27	4.37	1.08
22.5	47	30.90	1.08	37	12.79	1.02	30	4.43	1.09
25	55	31.10	1.09	44	12.80	1.02	34	4.50	1.11
27.5	62	31.32	1.10	49	12.84	1.02	38	4.50	1.11
30	69	31.45	1.10	55	12.88	1.02	42	4.51	1.11
32.5	75	31.97	1.12	60	12.90	1.02	45	4.52	1.12
35	81	32.30	1.13	66	12.91	1.02	50	4.52	1.12
37.5	88	32.60	1.14	73	12.91	1.02	54	4.53	1.12
40	94	33.00	1.16	77	12.93	1.03	59	4.55	1.12
42.5	100	34.35	1.20	82	12.96	1.03	63	4.56	1.13
45				88	13.05	1.04	67	4.58	1.13
47.5				92	13.12	1.04	72	4.59	1.13
50				96	13.36	1.06	75	4.61	1.14
52.5				100	13.95	1.11	79	4.65	1.15

CYL 12

TIME (Sec)	$\Sigma_{10} = 4.05$		
	σ/σ_f	AE (1000's)	Σ
55	83	4.67	1.15
57.5	87	4.80	1.19
60	91	4.85	1.20
62.5	94	4.95	1.22
65	98	5.24	1.29
67.5	100	∞	∞
70			
72.5			
75			

W/C = 0.45
CA = 0.52

	CYL 13			CYL 14			CYL 15		
	$\Sigma_{10} = 7.78$			$\Sigma_{10} = 7.96$			$\Sigma_{10} = 2.01$		
TIME (Sec)	σ/σ_f	AE (1000's)	Σ_N	σ/σ_f	AE (1000's)	Σ_N	σ/σ_f	AE (1000's)	Σ_N
0	0	-	-	0	7.72	0.97	0	1.54	0.77
2.5	0	-	-	2	7.86	0.99	3	1.80	0.90
5	0	7.52	0.97	6	7.94	1.00	8	1.97	0.98
7.5	1	7.59	0.98	11	7.96	1.00	13	2.08	1.03
10	4	7.68	0.99	18	7.98	1.00	18	2.10	1.04
12.5	9	7.76	1.00	26	8.00	1.01	24	2.17	1.08
15	16	7.87	1.01	33	8.00	1.01	29	2.18	1.08
17.5	23	7.93	1.02	39	8.03	1.01	35	2.19	1.09
20	28	8.03	1.03	47	8.03	1.01	41	2.20	1.09
22.5	34	8.09	1.04	56	8.04	1.01	47	2.20	1.09
25	42	8.15	1.05	64	8.05	1.01	53	2.21	1.10
27.5	47	8.30	1.07	72	8.11	1.02	59	2.21	1.10
30	54	8.38	1.08	79	8.12	1.02	65	2.26	1.12
32.5	60	8.53	1.10	85	8.17	1.03	70	2.28	1.13
35	68	8.72	1.12	92	8.26	1.04	76	2.33	1.16
37.5	75	9.00	1.16	96	8.74	1.10	82	2.38	1.18
40	80	9.28	1.19	100	∞	∞	86	2.42	1.20
42.5	88	9.53	1.22				92	2.49	1.24
45	93	10.18	1.31				97	2.53	1.26
47.5	97	11.00	1.41				100	2.65	1.32
50	100	∞	∞						

W/C = 0.50
CA = 0.52

	CYL 16			CYL 17			CYL 18		
	Σ_{10} = 2.70			Σ_{10} = 7.43			Σ_{10} = 10.59		
TIME (Sec)	σ/σ_f	AE (1000's)	Σ_N	σ/σ_f	AE (1000's)	Σ_N	σ/σ_f	AE (1000's)	Σ_N
0	0	1.52	0.56	0	7.00	0.94	0	9.00	0.85
2.5	2	2.30	0.85	2	7.26	0.98	3	9.80	0.93
5	5	2.57	0.95	5	7.40	1.00	5	10.40	0.98
7.5	11	2.72	1.01	13	7.45	1.00	13	10.70	1.01
10	18	2.77	1.03	23	7.50	1.01	17	10.90	1.03
12.5	26	2.80	1.04	29	7.52	1.01	26	11.10	1.05
15	34	2.81	1.04	40	7.56	1.02	32	11.35	1.07
17.5	43	2.82	1.04	48	7.56	1.02	40	11.65	1.10
20	54	2.82	1.04	58	7.58	1.02	49	11.86	1.12
22.5	61	2.85	1.06	67	7.60	1.02	56	12.15	1.15
25	68	2.86	1.06	76	7.68	1.03	66	12.42	1.17
27.5	77	2.91	1.08	85	7.71	1.04	73	12.78	1.21
30	85	3.00	1.11	93	7.78	1.05	81	13.18	1.24
32.5	89	3.08	1.14	99	8.00	1.08	90	13.60	1.28
35	96	3.25	1.20	100	9.70	1.31	96	14.20	1.34
37.5	100	3.94	1.46				100	14.95	1.41

W/C = 0.40
CA = 0.62

TIME (Sec)	CYL 19 Σ_{10} = 1.75			CYL 20 Σ_{10} = 1.24			CYL 21 Σ_{10} = 4.45		
	σ/σ_f	AE (1000's)	Σ_N	σ/σ_f	AE (1000's)	Σ_N	σ/σ_f	AE (1000's)	Σ_N
0	0	1.10	0.63	0	0.62	0.50	0	1.95	0.44
2.5	3	1.47	0.84	2	1.04	0.84	1	3.14	0.71
5	5	1.65	0.94	6	1.17	0.94	3	3.80	0.85
7.5	10	1.75	1.00	9	1.23	0.99	7	4.26	0.96
10	14	1.83	1.05	13	1.27	1.02	11	4.50	1.01
12.5	18	1.87	1.07	17	1.30	1.05	15	4.71	1.06
15	23	1.91	1.09	22	1.35	1.09	20	4.90	1.10
17.5	28	1.96	1.12	26	1.35	1.09	24	4.96	1.11
20	32	2.00	1.14	31	1.36	1.10	27	5.13	1.15
22.5	36	2.06	1.18	35	1.37	1.10	32	5.20	1.17
25	41	2.08	1.19	40	1.37	1.10	37	5.25	1.18
27.5	46	2.10	1.20	44	1.37	1.10	41	5.30	1.19
30	50	2.11	1.21	49	1.38	1.11	46	5.36	1.20
32.5	55	2.15	1.23	55	1.39	1.12	50	5.40	1.21
35	61	2.20	1.26	59	1.40	1.13	54	5.47	1.23
37.5	65	2.21	1.26	63	1.40	1.13	60	5.56	1.25
40	70	2.31	1.32	69	1.40	1.13	65	5.62	1.26
42.5	75	2.40	1.37	73	1.46	1.18	69	5.80	1.30
45	79	2.57	1.47	77	1.47	1.19	74	6.01	1.35
47.5	84	2.75	1.57	82	1.50	1.21	78	6.13	1.38
50	88	3.00	1.71	85	1.50	1.21	82	6.45	1.45
52.5	92	3.22	1.84	90	1.62	1.31	87	6.55	1.47
55	96	3.75	2.14	94	1.70	1.37	91	6.77	1.52
57.5	100	4.65	2.66	98	1.88	1.52	95	7.17	1.61
60				100	2.90	2.34	97	7.76	1.74
62.5							100	∞	

W/C = 0.45
CA = 0.62

TIME (Sec)	CYL 22 $\Sigma_{10} = 1.33$ σ/σ_f	AE (1000's)	Σ_N	CYL 23 $\Sigma_{10} = 1.22$ σ/σ_f	AE (1000's)	Σ_N	CYL 24 $\Sigma_{10} = 0.88$ σ/σ_f	AE (1000's)	Σ_N
0	0	0.94	0.71	0	0.70	0.57	0	0.47	0.53
2.5	2	1.13	0.85	4	1.04	0.85	1	0.68	0.77
5	5	1.28	0.96	7	1.18	0.97	4	0.84	0.95
7.5	8	1.32	0.99	12	1.28	1.05	9	0.87	0.99
10	15	1.37	1.03	19	1.33	1.09	15	0.90	1.02
12.5	19	1.41	1.06	26	1.36	1.11	21	0.90	1.02
15	25	1.41	1.06	35	1.38	1.13	25	0.95	1.08
17.5	30	1.41	1.06	41	1.40	1.15	32	0.97	1.10
20	35	1.41	1.06	49	1.41	1.16	37	0.97	1.10
22.5	41	1.41	1.06	57	1.43	1.17	43	1.01	1.15
25	47	1.43	1.08	64	1.44	1.18	48	1.02	1.16
27.5	52	1.44	1.08	73	1.45	1.19	54	1.04	1.18
30	58	1.44	1.08	80	1.46	1.20	60	1.08	1.23
32.5	64	1.44	1.08	87	1.61	1.32	67	1.08	1.23
35	70	1.44	1.08	93	1.80	1.48	72	1.22	1.39
37.5	76	1.44	1.08	99	2.40	1.97	78	1.27	1.44
40	81	1.45	1.09	100	∞	∞	83	1.35	1.53
42.5	86	1.46	1.10				89	1.42	1.61
45	91	1.50	1.13				94	1.59	1.81
47.5	95	1.60	1.20				99	1.86	2.11
50	100	1.76	1.32				100	2.50	2.84

W/C = 0.50
CA = 0.62

	CYL 25			CYL 26			CYL 27		
	Σ_{10} = 2.63			Σ_{10} = 2.87			Σ_{10} = 14.94		
TIME (Sec)	σ/σ_f	AE (1000's)	Σ_N	σ/σ_f	AE (1000's)	Σ_N	σ/σ_f	AE (1000's)	Σ_N
0	0	2.50	0.95	0	0.40	0.14	0	14.15	0.95
2.5	1	2.57	0.98	2	1.70	0.59	4	14.55	0.97
5	2	2.61	0.99	5	2.57	0.90	8	14.87	1.00
7.5	5	2.63	1.00	10	2.87	1.00	16	15.15	1.01
10	9	2.63	1.00	16	3.05	1.06	27	15.38	1.03
12.5	16	2.66	1.01	22	3.16	1.10	43	15.57	1.04
15	21	2.67	1.02	29	3.28	1.14	57	15.63	1.05
17.5	29	2.67	1.02	35	3.36	1.17	71	15.74	1.05
20	36	2.67	1.02	42	3.40	1.18	84	16.20	1.08
22.5	44	2.67	1.02	49	3.42	1.19	100	17.82	1.19
25	52	2.70	1.03	56	3.46	1.21			
27.5	60	2.70	1.03	63	3.48	1.21			
30	67	2.70	1.03	69	3.51	1.22			
32.5	78	2.70	1.03	77	3.52	1.23			
35	83	2.71	1.03	82	3.55	1.24			
37.5	89	2.77	1.05	88	3.58	1.25			
40	95	2.84	1.08	96	3.65	1.27			
42.5	100	∞	∞	100	3.76	1.31			

$\dot{C} = \frac{\Delta\Sigma}{2.5 \text{ Sec}}$ = Count rate

Time (Sec)	CYL 1: Cyl 1 $\Sigma_{10} = 6.70$		CYL 2: 2 $\Sigma_{10} = 15.39$		CYL 3: 3 $\Sigma_{10} = 5.52$	
	σ/σ_f	Σ_N	σ/σ_f	Σ_N	σ/σ_f	Σ_N
0	1	600	1	1920	1	600
2.5	4	224	4	820	3.5	384
5	8.5	72	7.5	516	7	428
7.5	13	128	11	400	11.5	388
10	17.5	36	16	292	16	264
12.5	22.5	36	21.5	196	20.5	160
15	27.5	36	26.5	228	25.5	144
17.5	32.5	0	32	212	30.5	132
20	37.5	52	37	148	35	140
22.5	42.5	0	41	136	39.5	168
25	47.5	4	46	100	45.5	72
27.5	53	8	51	84	50.5	88
30	58	8	55.5	180	55.5	56
32.5	63	4	60.5	140	61	48
35	68.5	8	66	108	66.5	40
37.5	73	12	71.5	140	71.5	88
40	77.5	28	77	120	76.5	224
42.5	83	28	81.5	140	81.5	352
45	87.5	32	86.5	268	86	232
47.5	91.5	81	91.5	288	90.5	192
50	96	156	95	460	95	240
52.5	99	720	98.5	904	98.5	840
55						

$\dot{C}$

TIME (Sec)	CYL 4 σ/σ_f	CYL 4 AE (1000's)	CYL 5 σ/σ_f	CYL 5 AE (1000's)	CYL 6 σ/σ_f	CYL 6 AE (1000's)
0	1	160	1	24	0.5	420
2.5	4	60	4.5	20	2.5	120
5	8	40	9	16	6.5	353
7.5	12.5	44	15.5	8	11.5	128
10	17	16	23.5	20	17.5	100
12.5	21.5	4	31.5	0	23	76
15	27	12	40.5	4	26.5	36
17.5	32.5	16	47.5	32	35	24
20	38	8	56.5	4	41.5	52
22.5	44	4	66	12	47.5	4
25	49.5	16	75.5	16	53	24
27.5	55	0	83.5	144	59.5	4
30	60.5	4	91	560	65	32
32.5	66	4	97.5		69.5	24
35	71.5	0			75	12
37.5	76.5	8			81.5	16
40	82.5	0			87	28
42.5	87.5	44			91.5	52
45	92	8			96.5	76
47.5	96.5	44			99.5	200
50	99					

	CYL 7		CYL 8		CYL 9	
TIME (Sec)	σ/σ_f	AE (1000's)	σ/σ_f	AE (1000's)	σ/σ_f	AE (1000's)
0	1	440	2.5	20	1.5	480
2.5	4	292	7.5	8	4	240
5	8.5	160	13	0	7	320
7.5	14.5	64	19.5	0	13	80
10	22	44	27.5	0	21	0
12.5	29.5	12	36	0	29.5	120
15	37.5	8	44.5	0	36	160
17.5	46.5	8	53	0	44.5	0
20	54	0	60.5	0	53.5	80
22.5	60	8	68	0	60.5	40
25	67	4	76	0	67.5	0
27.5	74	0	83	0	76	0
30	81.5	12	90.5	0	83.5	40
32.5	88.5	8	96	8	90.5	160
35	93.5	72	99.5	12	96	760
37.5	97.5	84			99	1040
40	99.5	220				
42.5						

TIME (Sec)	CYL 10 $\Sigma_{10} = 28.54$ σ/σ_f	AE (1000's)	CYL 11 $\Sigma_{10} = 12.60$ σ/σ_f	AE (1000's)	CYL 12 $\Sigma_{10} = 4.05$ σ/σ_f	AE (1000's)
0	1	360	1	356	1	452
2.5	3.5	272	3	244	3	320
5	7.5	264	5.5	160	5.5	124
7.5	14	184	8.5	12	9	76
10	19	184	13	4	13	60
12.5	24.5	96	18.5	12	17	24
15	30.5	224	23.5	24	21	16
17.5	37.5	84	29	16	25	8
20	44	172	34.5	20	28.5	24
22.5	51	80	40.5	4	32	28
25	58.5	88	46.5	16	36	0
27.5	65.5	52	52	16	40	4
30	72	208	57.5	8	43.5	4
32.5	78	132	63	4	47.5	0
35	84.5	120	69.5	0	52	4
37.5	91	160	75	8	56.5	8
40	97	500	79.5	12	61	4
42.5			85	36	65	8
45			90	28	69.5	4
47.5			94	96	73.5	8
50			98	236	77	16
52.5					82	8
55					85	52
57.5					89.5	20
60					92.5	40
62.5					96	116
65					99	
67.5						

W/C = 0.45
CA = 0.52

TIME (Sec.)	CYL 13 $\Sigma_{10} = 7.78$ σ/σ_f	CYL 13 AE (1000's)	CYL 14 $\Sigma_{10} = 7.96$ σ/σ_f	CYL 14 AE (1000's)	CYL 15 $\Sigma_{10} = 2.01$ σ/σ_f	CYL 15 AE (1000's)
0			1	56	1.5	116
2.5			4	32	5.5	68
5	0.5	28	8.5	8	10.5	44
7.5	2.5	36	14.5	8	15.5	8
10	6.5	32	22	8	21	28
12.5	12.5	44	29.5	0	26.5	4
15	19.5	24	36	12	32	4
17.5	25.5	40	43	0	38	4
20	31	24	51.5	4	44	0
22.5	38	24	60	4	50	4
25	44.5	60	68	24	56	0
27.5	50.5	32	75.5	4	62	20
30	57	60	82	20	67.5	8
32.5	64	76	88.5	36	73	20
35	71.5	112	94	192	79	20
37.5	77.5	112	98		84	16
40	84	100			89	28
42.5	90.5	260			94.5	16
45	95	328			98.5	48
47.5	98.5					
50						
52.5						

W/C = 0.50
CA = 0.52

TIME (Sec)	CYL 16 $\Sigma_{10} = 2.70$ σ/σ_f	CYL 16 AE (1000's)	CYL 17 $\Sigma_{10} = 7.43$ σ/σ_f	CYL 17 AE (1000's)	CYL 18 $\Sigma_{10} = 10.59$ σ/σ_f	CYL 18 AE (1000's)
0	1	312	1	104	1.5	320
2.5	3.5	108	3.5	56	4.5	240
5	8	60	9	20	9	120
7.5	14.5	20	18	20	15	80
10	22	12	26	8	21.5	80
12.5	30	4	34.5	16	29	100
15	38.5	4	44	0	36	120
17.5	48.5	0	53	8	44.5	84
20	57.5	12	62.5	8	52.5	116
22.5	64.5	4	71.5	32	61	108
25	72.5	20	80.5	12	69.5	144
27.5	81	36	89	28	77	160
30	87	32	96	88	85.5	168
32.5	92.5	68	99.5	680	93	240
35	98	276			98	300
37.5						

W/C = 0.40
CA = 0.62

TIME (Sec)	CYL 19 $\Sigma_{10} = 1.75$ σ/σ_f	CYL 19 AE (1000's)	CYL 20 $\Sigma_{10} = 1.24$ σ/σ_f	CYL 20 AE (1000's)	CYL 21 $\Sigma_{10} = 4.45$ σ/σ_f	CYL 21 AE (1000's)
0	1.5	148	1	168	0.5	476
2.5	4	72	4	52	2	264
5	7.5	40	7.5	24	5	184
7.5	12	32	11	16	9.5	96
10	16	16	15	12	13	84
12.5	20.5	16	19.5	20	17.5	76
15	25.5	20	24	0	22	24
17.5	30	16	28.5	4	25.5	68
20	34	24	33	4	29.5	28
22.5	38.5	8	37.5	0	34.5	20
25	43.5	8	42	0	39	20
27.5	48	4	46.5	4	43.5	24
30	52.5	16	52	4	48	16
32.5	58	20	57	4	52	28
35	63	4	61	0	57	36
37.5	67.5	40	66	0	62.5	24
40	72.5	36	71	24	67	72
42.5	77	68	75	4	71.5	84
45	81.5	72	79.5	12	76	48
47.5	86	100	84.5	0	80	128
50	90	88	87.5	48	84.5	40
52.5	94	212	92	32	89	88
55	98	360	96	72	93	160
57.5			99	408	96	236
60					98.5	
62.5						

W/C = 0.45
CA = 0.62

TIME (Sec)	CYL 22 $\Sigma_{10} = 1.33$ σ/σ_f	CYL 22 AE (1000's)	CYL 23 $\Sigma_{10} = 1.22$ σ/σ_f	CYL 23 AE (1000's)	CYL 24 $\Sigma_{10} = 0.88$ σ/σ_f	CYL 24 AE (1000's)
0	1	76	2	136	0.5	84
2.5	3.5	60	5.5	56	2.5	64
5	6.5	16	9.5	40	6.5	12
7.5	11.5	20	15.5	20	12	12
10	17	16	22.5	12	18	0
12.5	22	0	30.5	8	23	20
15	27.5	0	38	8	28.5	8
17.5	32.5	0	45	4	34.5	0
20	38	0	53	8	40	16
22.5	44	8	60.5	4	45.5	4
25	49.5	4	68.5	4	51	8
27.5	55	0	76.5	4	57	16
30	61	0	83.5	60	63.5	0
32.5	67	0	90	76	69.5	56
35	73	0	96	240	75	20
37.5	78.5	4	99.5		80.5	32
40	83.5	4			86	28
42.5	88.5	16			91.5	68
45	93	40			96.5	108
47.5	97.5	64			99.5	256
50						

W/C = 0.50
CA = 0.62

	CYL 25		CYL 26		CYL 27	
	Σ_{10} = 2.63		Σ_{10} = 2.87		Σ_{10} = 14.94	
TIME (Sec)	σ/σ_f	AE (1000's)	σ/σ_f	AE (1000's)	σ/σ_f	AE (1000's)
0	0.5	28	1	520	2	160
2.5	1.5	16	3.5	348	6	128
5	3.5	8	7.5	120	12	112
7.5	7	0	13	72	19.5	92
10	12.5	12	19	44	35	76
12.5	18.5	4	25.5	48	50	24
15	25	0	32	32	64	44
17.5	32.5	0	38.5	16	77.50	184
20	40	0	45.5	8	92	648
22.5	48	12	52.5	16		
25	56	0	59.5	8		
27.5	63.5	0	66	12		
30	72.5	0	73	4		
32.5	80.5	4	79.5	12		
35	86	24	85	12		
37.5	92	28	92	28		
40	97.5		98	44		
42.5						

APPENDIX B

Acoustic Emissions Plots

1. Normalized counts versus stress ratio, portland cement concrete.
2. Count rate versus stress ratio, portland cement concrete.

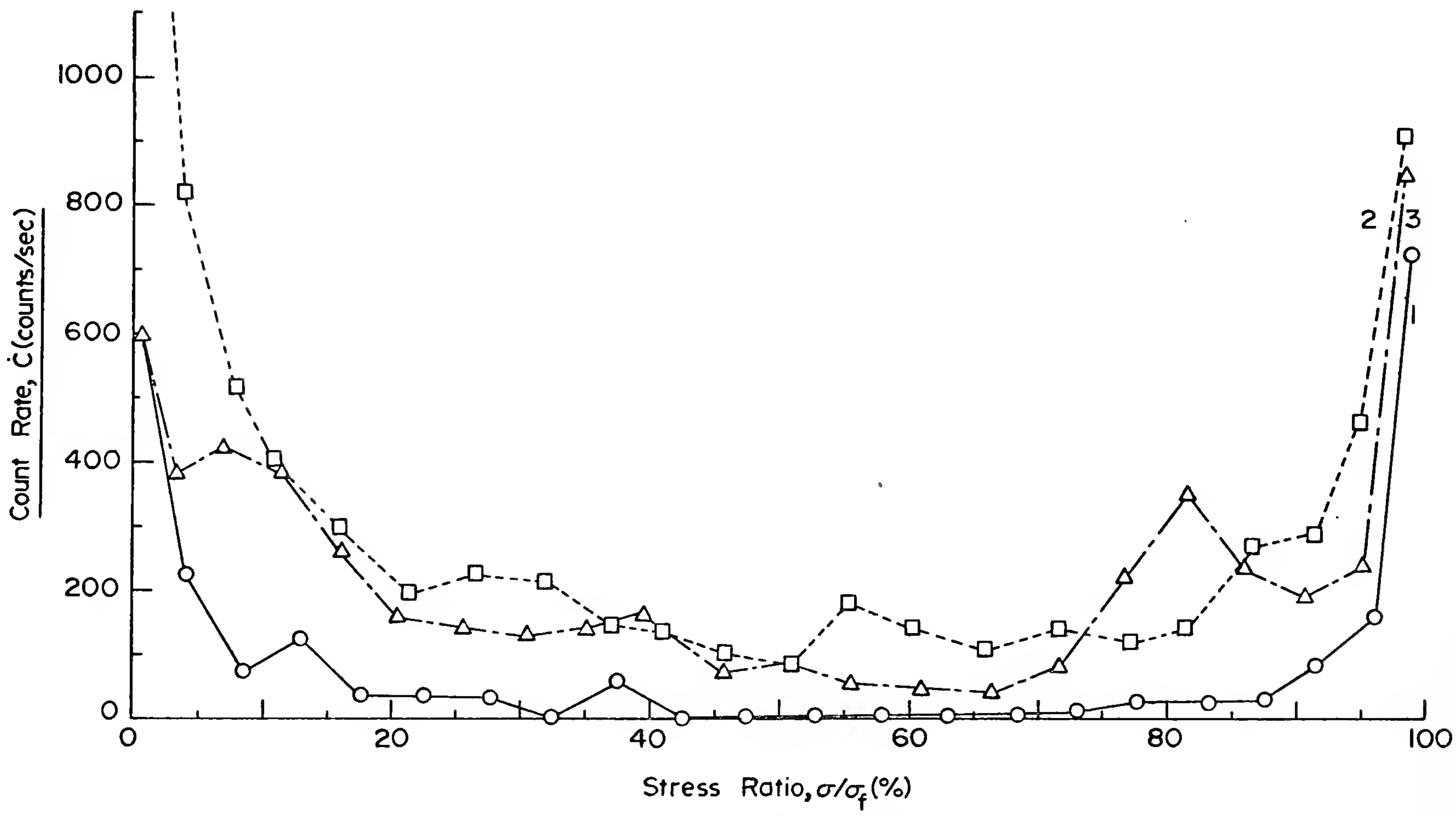

FIGURE BI COUNT RATE VS. STRESS RATIO, CYLINDERS 1, 2 AND 3, W/C=0.40, CA=0.42.

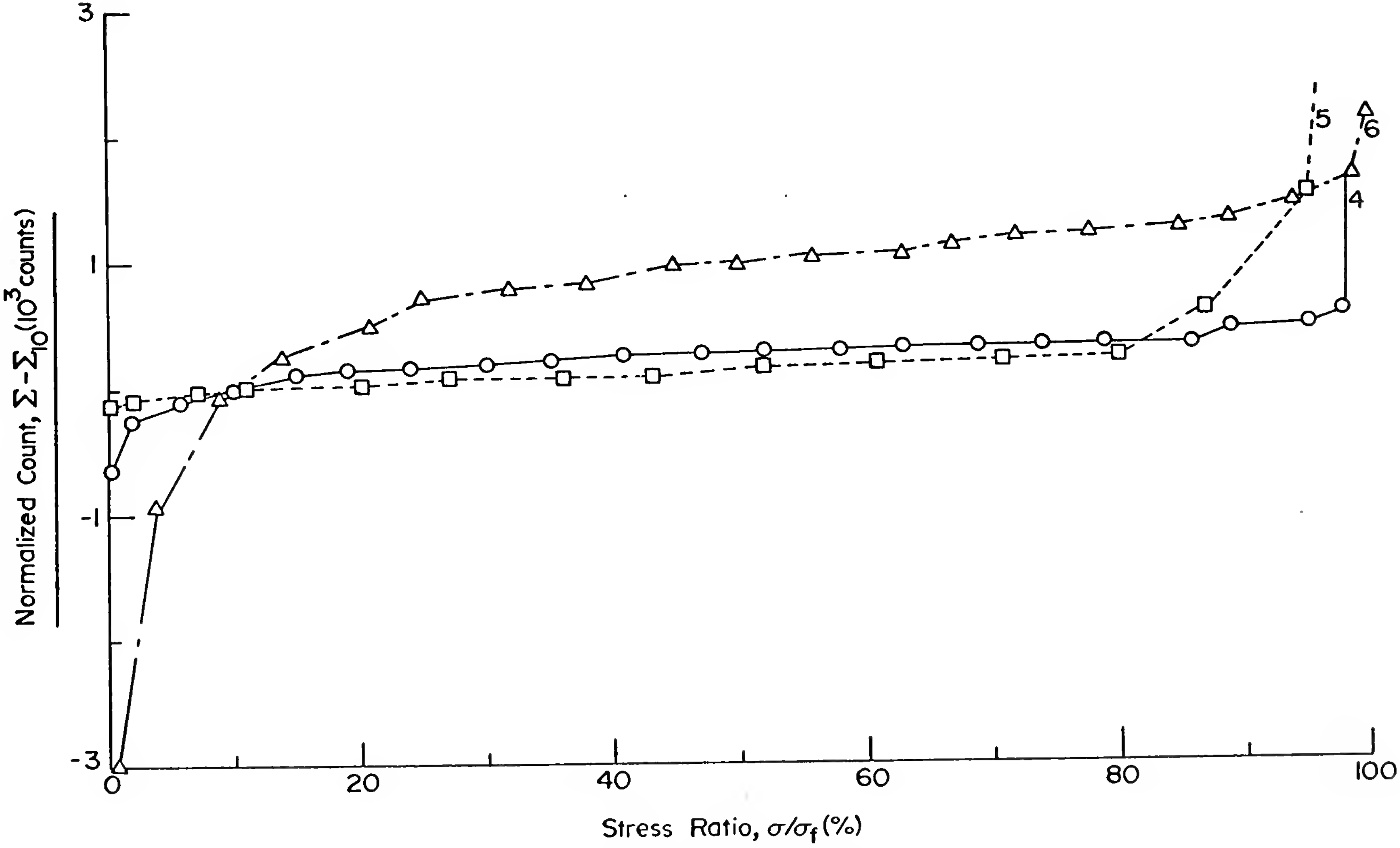

FIGURE B2 · NORMALIZED COUNTS VS. STRESS RATIO, CYLIDERS 4, 5 AND 6, W/C=0.45, CA=0.42.

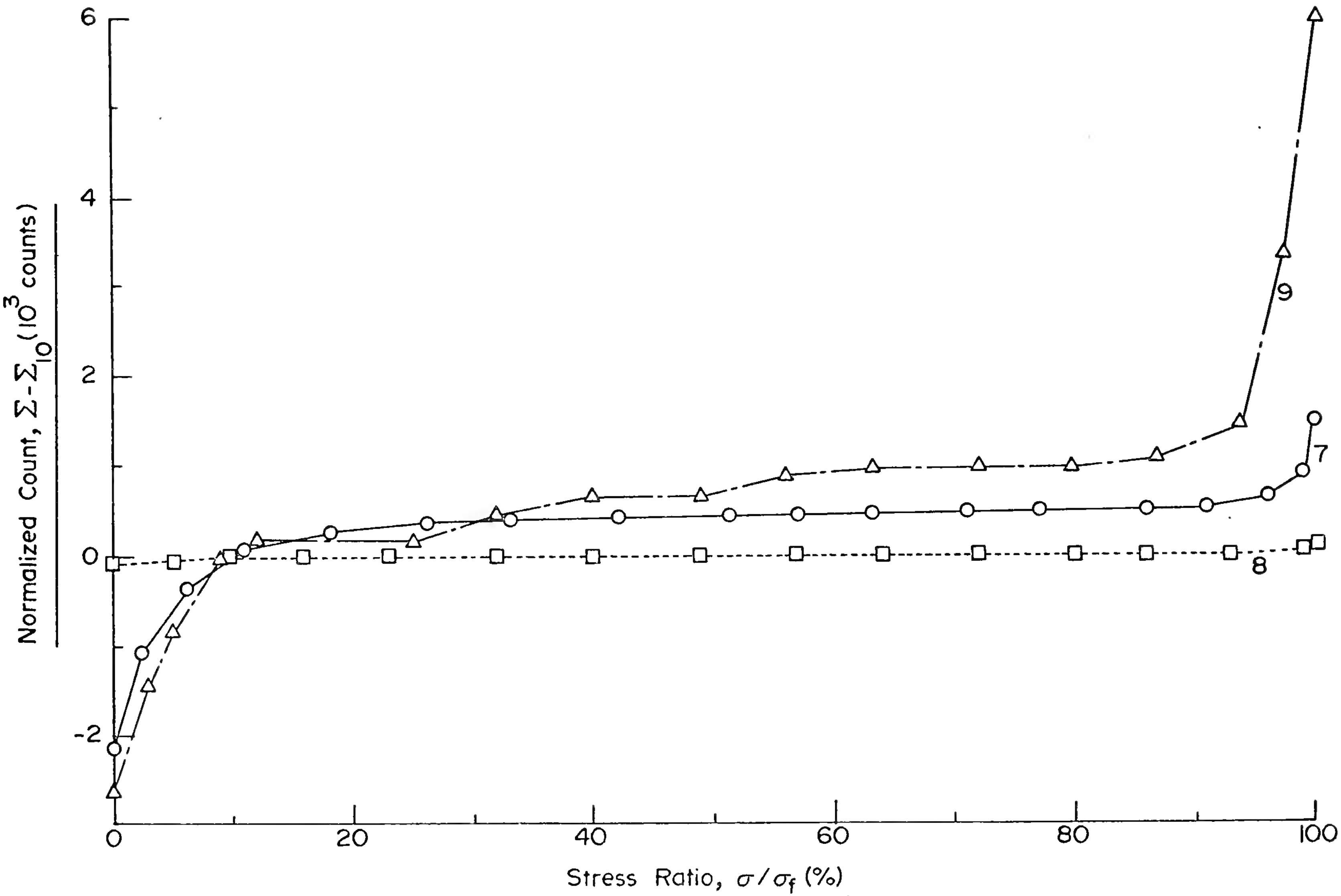

FIGURE B3 NORMALIZED COUNTS VS. STRESS RATIO CYLINDERS 7, 8 AND 9, W/C=0.50, CA=0.42.

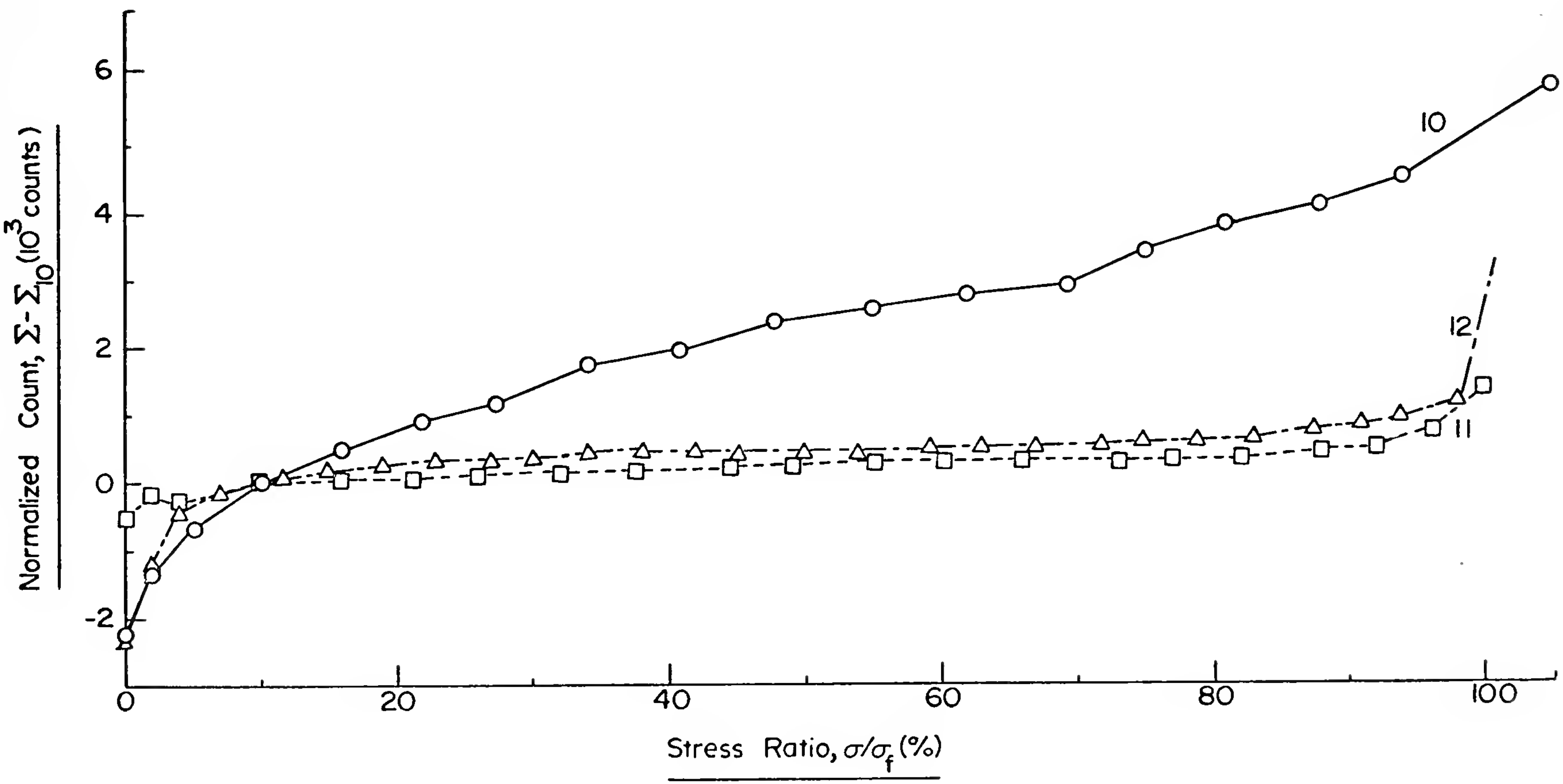

FIGURE B4 NORMALIZED COUNT VS. STRESS RATIO, CYLINDERS 10, 11 AND 12, W/C=0.40, CA=0.52.

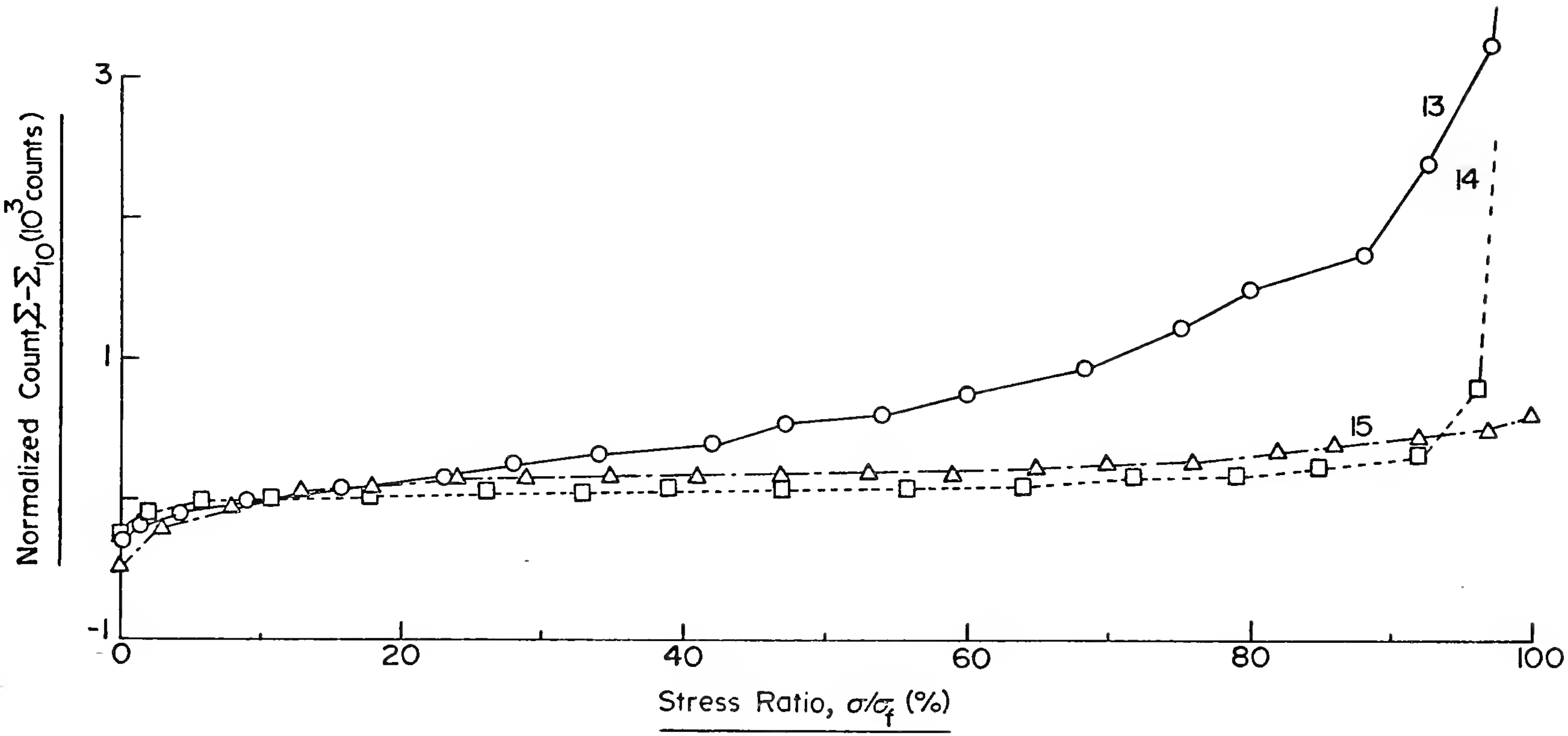

FIGURE B5 NORMALIZED COUNTS VS. STRESS RATIO, CYLINDERS 13, 14 AND 15, W/C=0.45, CA=0.52.

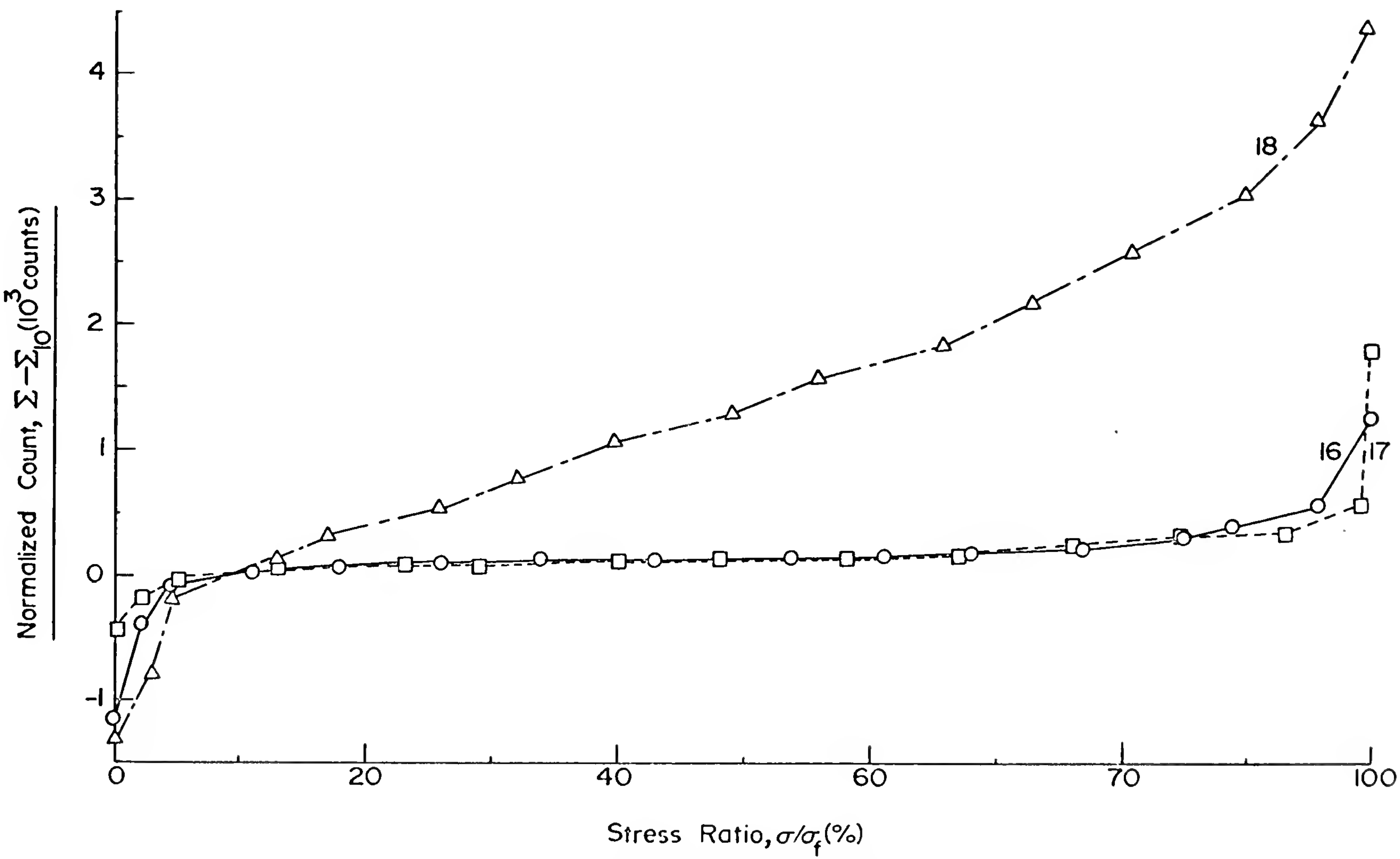

FIGURE B6 NORMALIZED COUNTS VS. STRESS RATIO, CYLINDERS 16, 17 AND 18, W/C=0.50, CA=0.52.

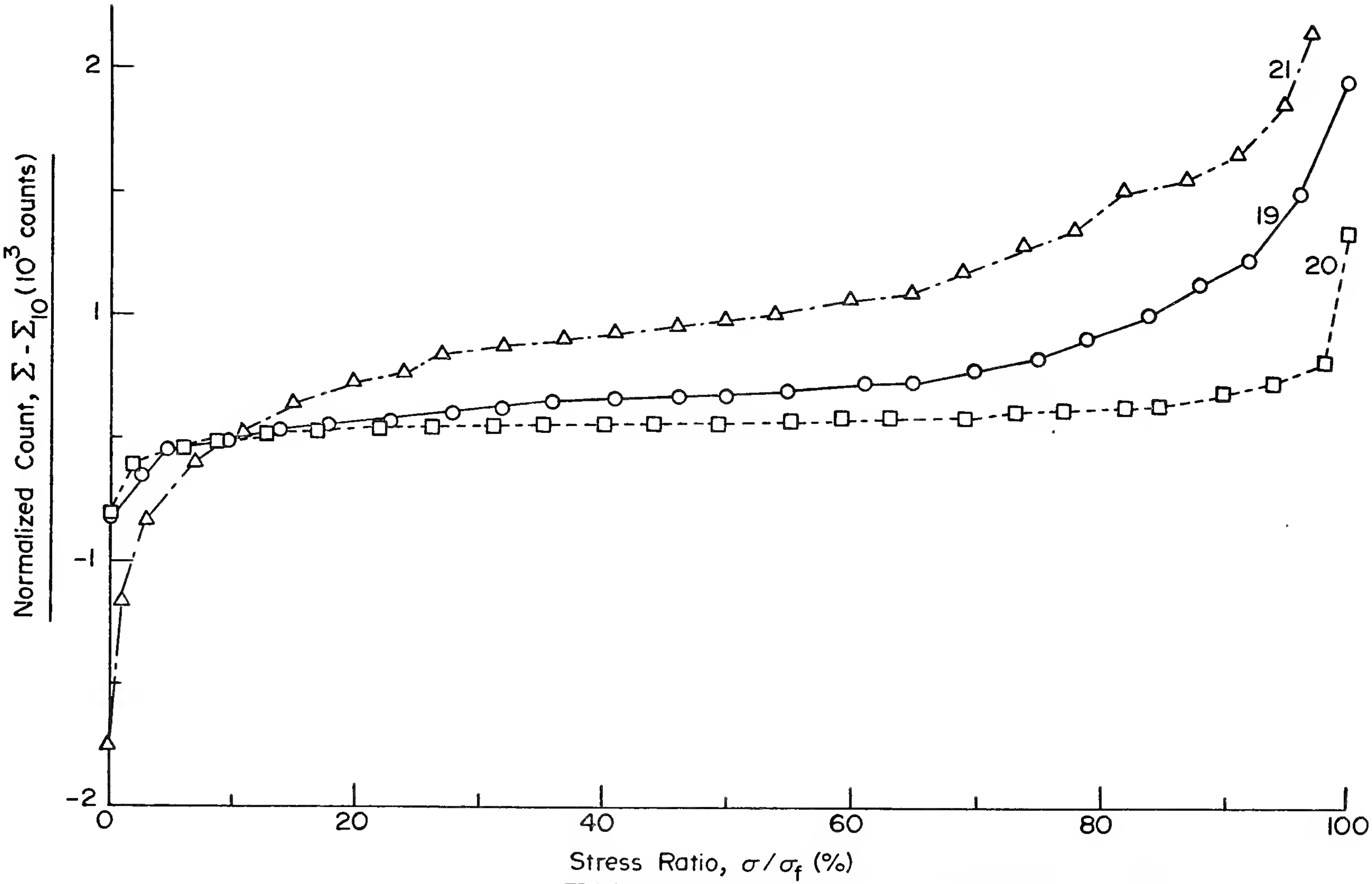

FIGURE B7 NORMALIZED COUNTS VS. STRESS RATIO, CYLINDERS 19, 20 AND 21, W/C = 0.40, CA = 0.62.

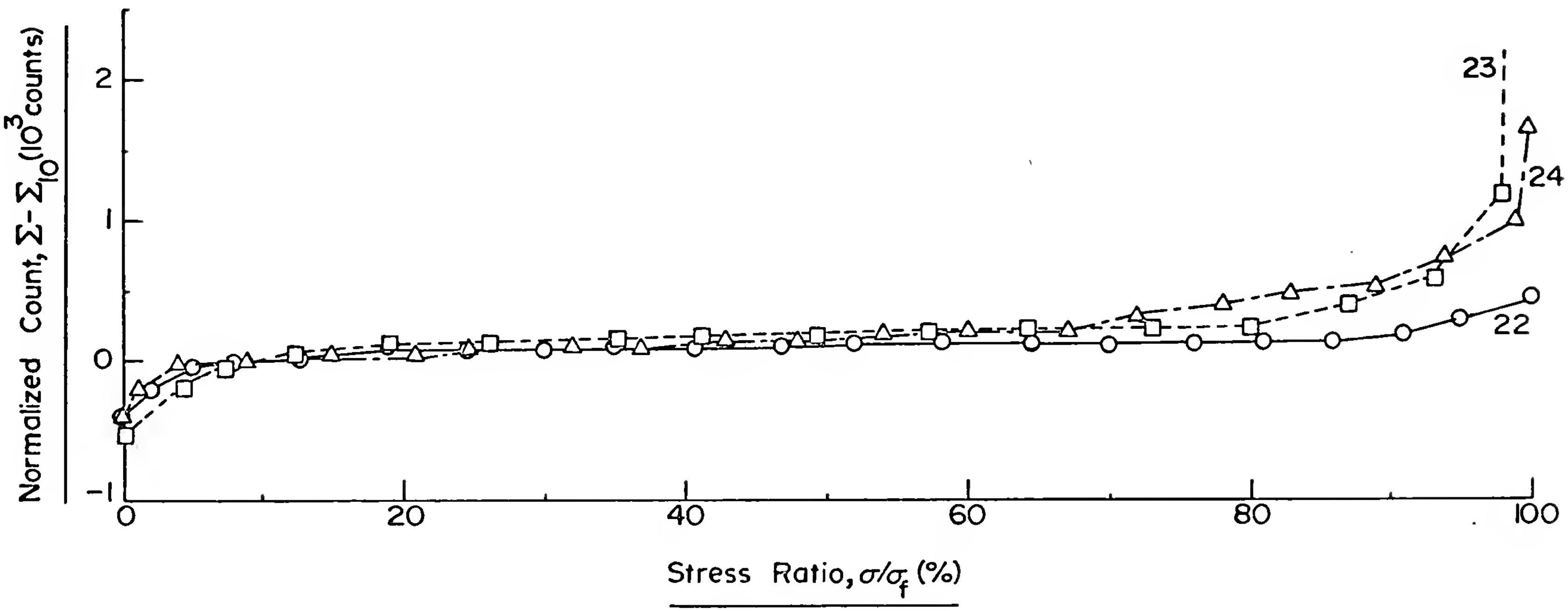

FIGURE B8 NORMALIZED COUNTS VS. STRESS RATIO, CYLINDERS 22, 23 AND 24, W/C=0.45 CA=0.62.

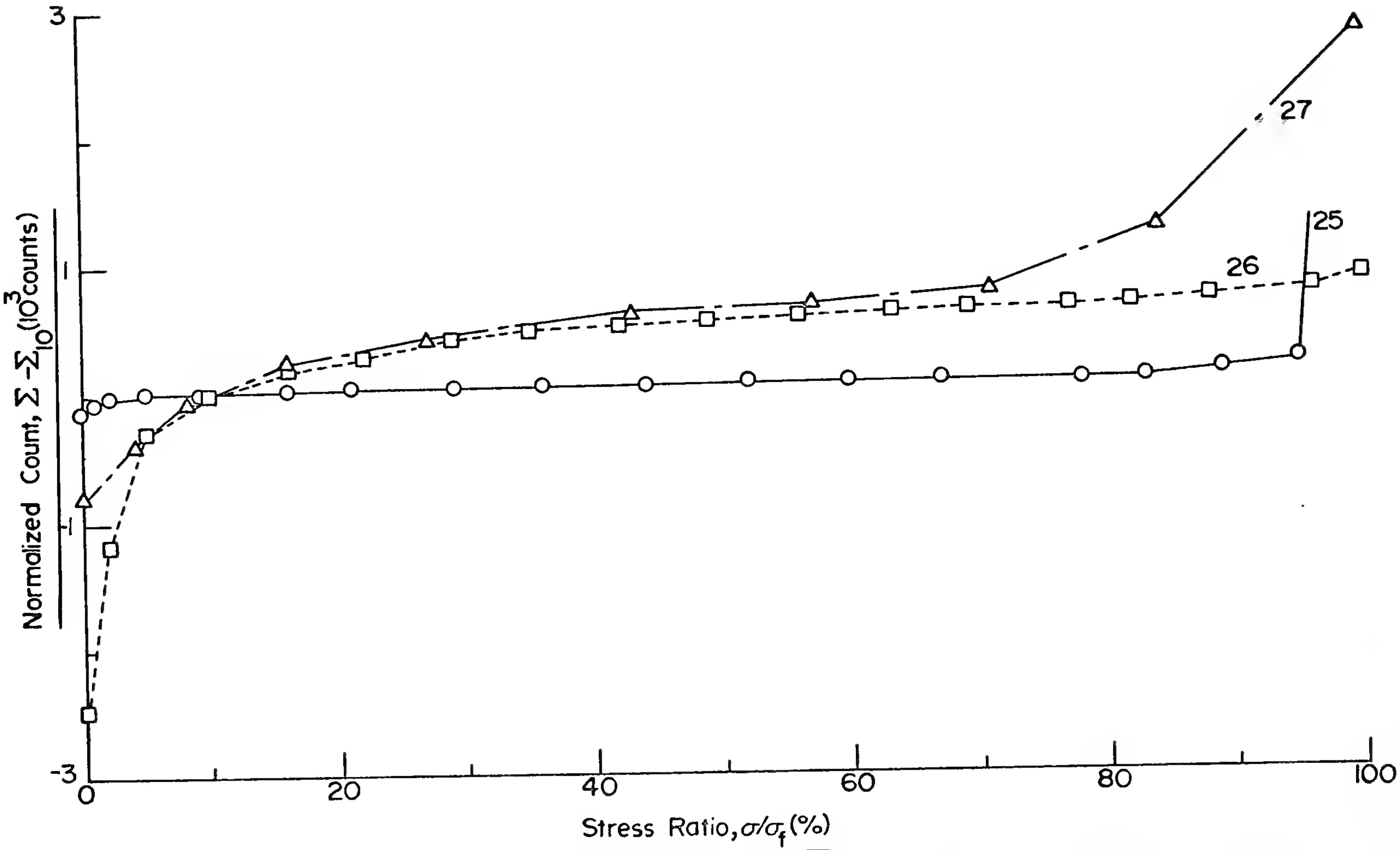

FIGURE B9 NORMALIZED COUNTS VS. STRESS RATIO CYLINDERS 25, 26 AND 27, W/C=0.50 CA=0.62.

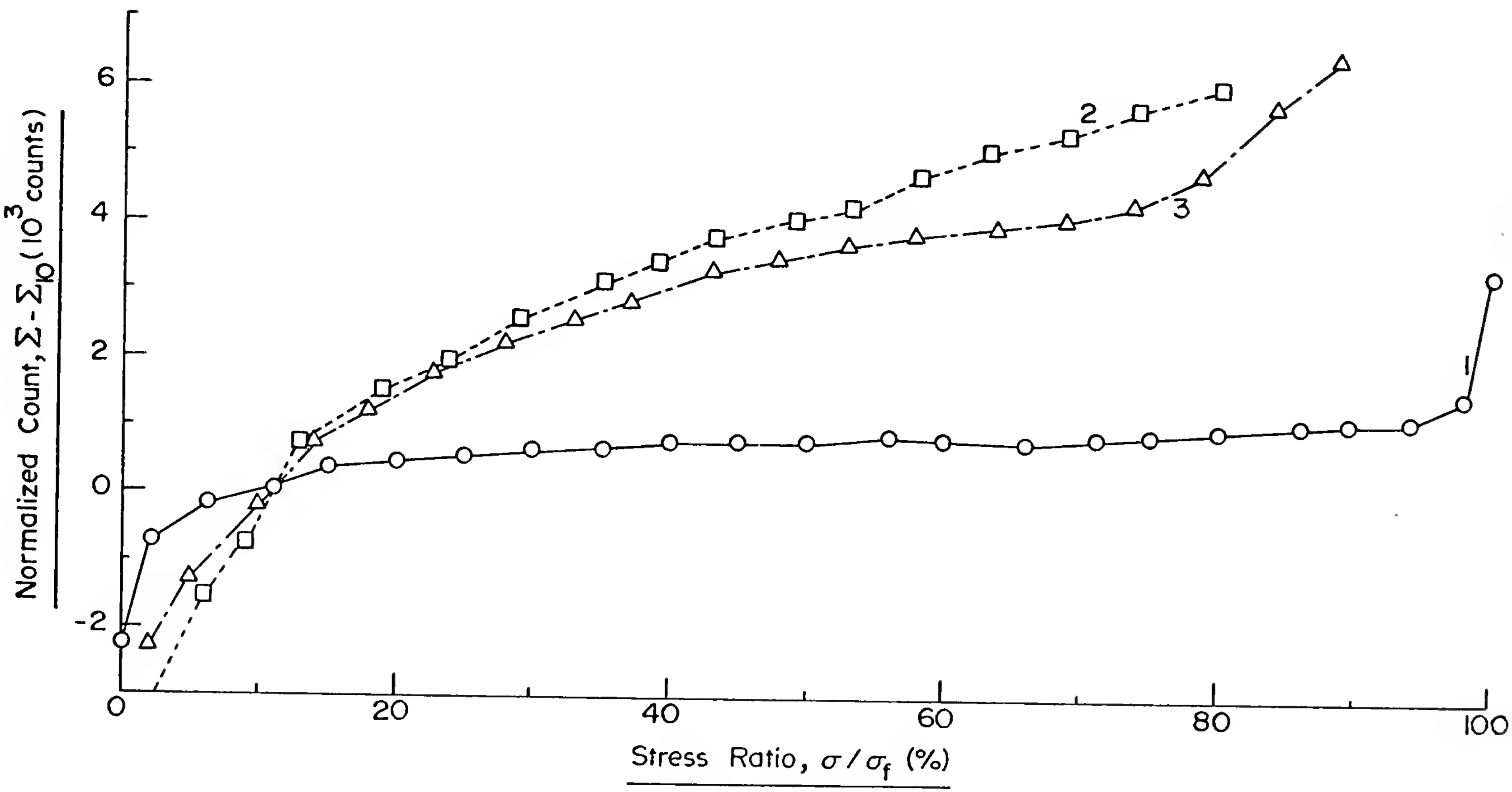

FIGURE B10 NORMALIZED COUNTS VS. STRESS RATIO CYLINDERS 1, 2 AND 3, W/C=0.40, CA=0.42.

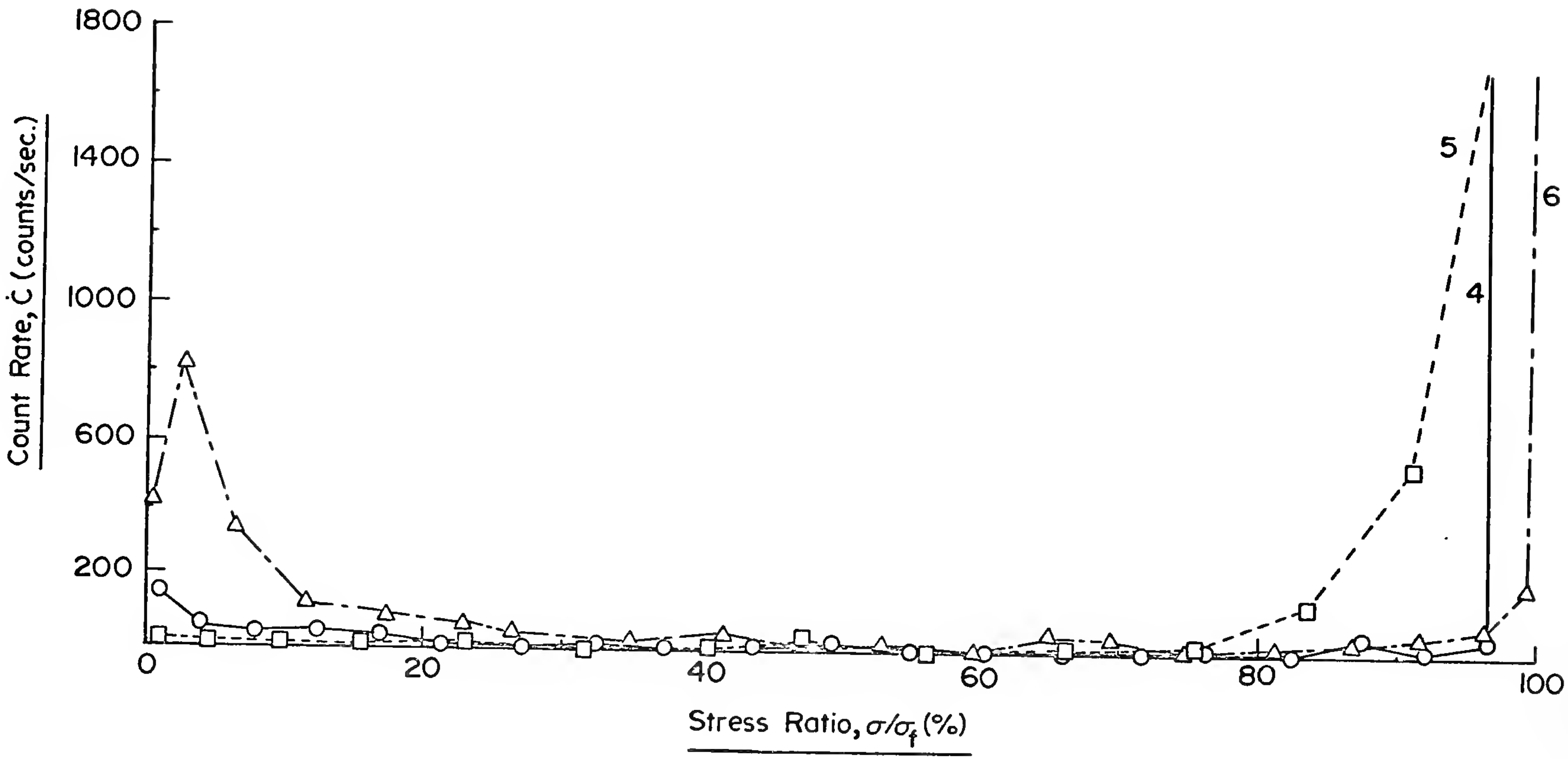

FIGURE B11 COUNT RATE VS. STRESS RATIO, CYLINDERS 4, 5 AND 6, W/C=0.45, CA=0.42.

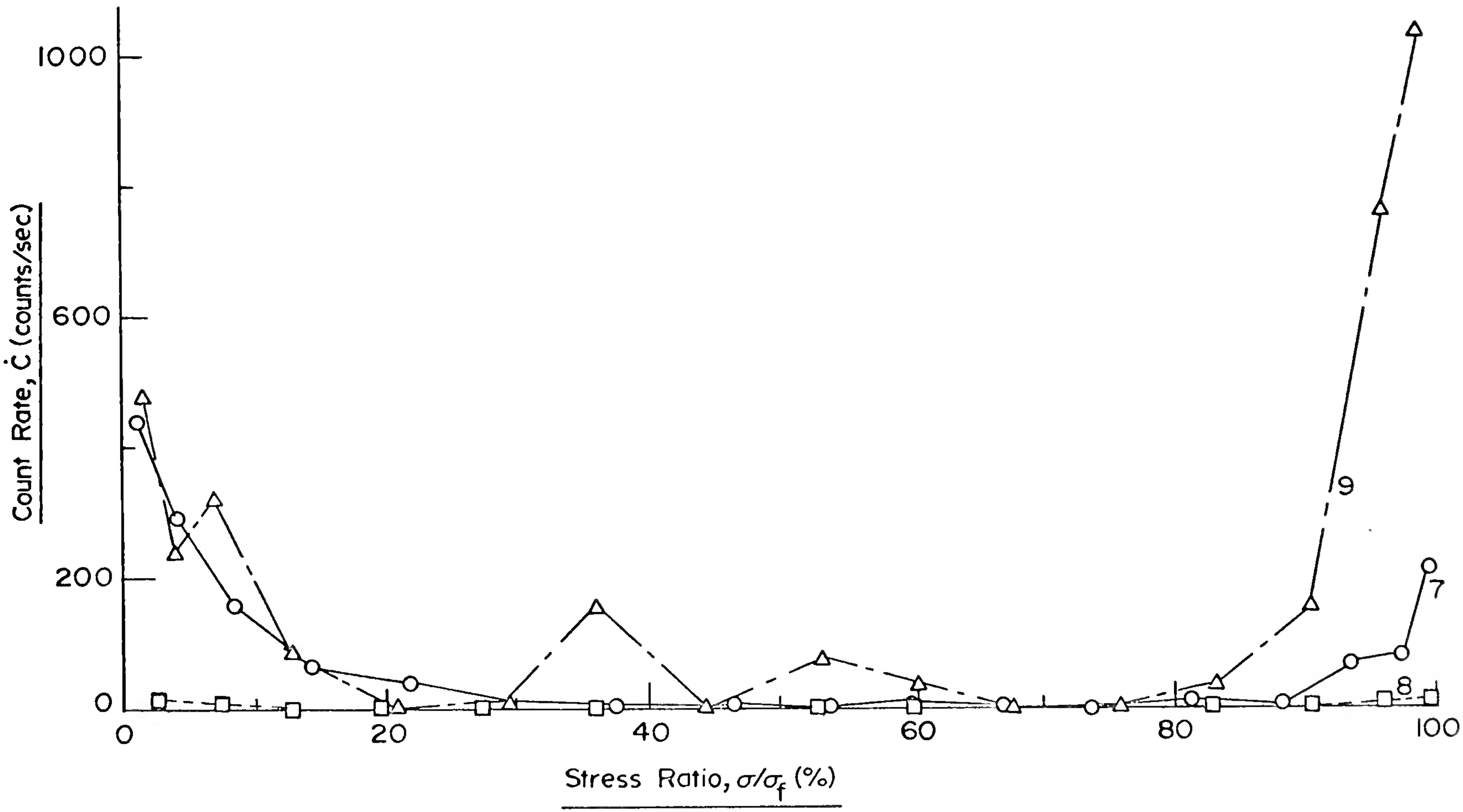

FIGURE B12 COUNT RATE VS. STRESS RATIO, CYLINDERS 7, 8 AND 9, W/C=0.50, CA=0.42.

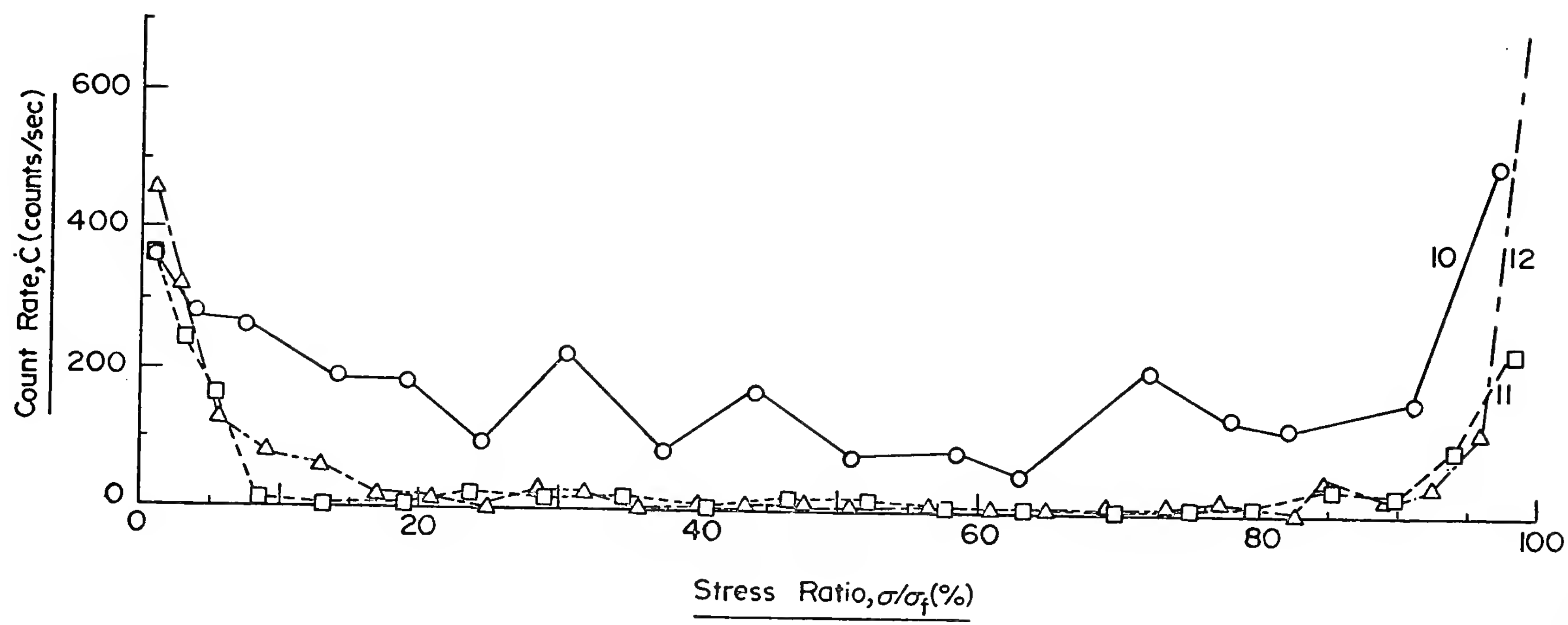

FIGURE B13 COUNT RATE VS. STRESS RATIO, CYLIDERS 10, 11 AND 12, W/C=0.40, CA=0.52.

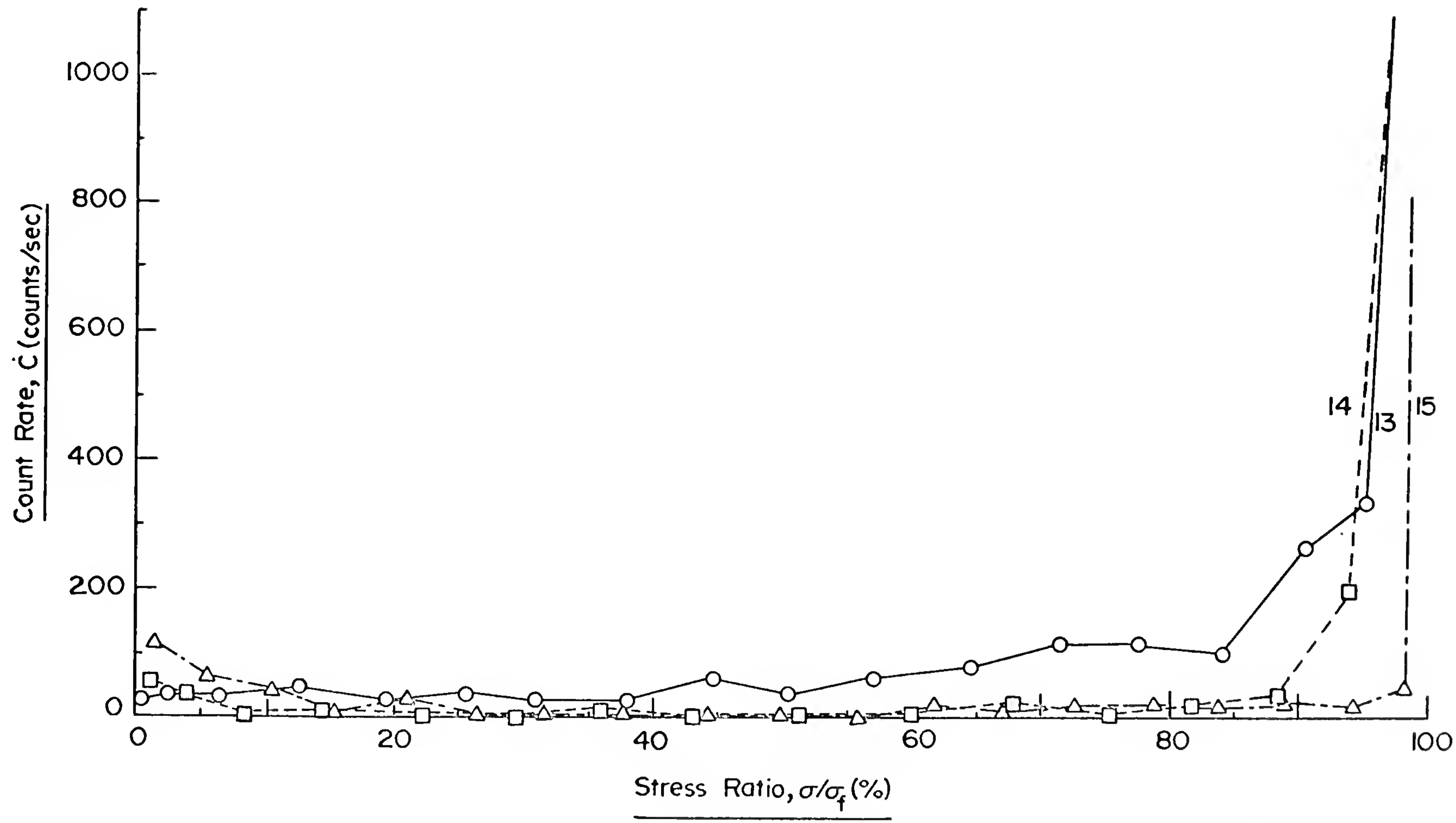

FIGURE B14 COUNT RATE VS. STRESS RATIO, CYLINDERS 13, 14 AND 15, W/C=0.45, CA=0.52.

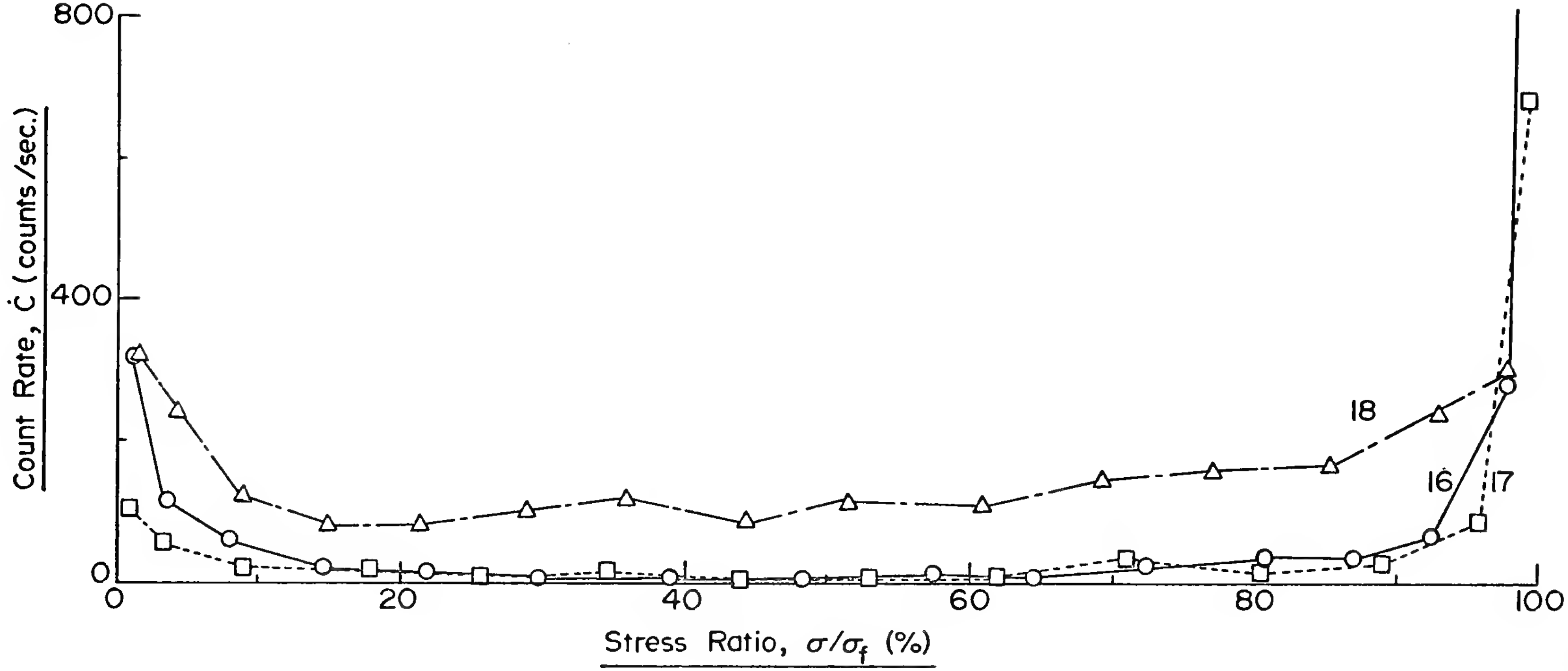

FIGURE B15 COUNT RATE VS. STRESS RATIO, CYLINDERS 16, 17 AND 18, W/C = 0.50, CA = 0.52.

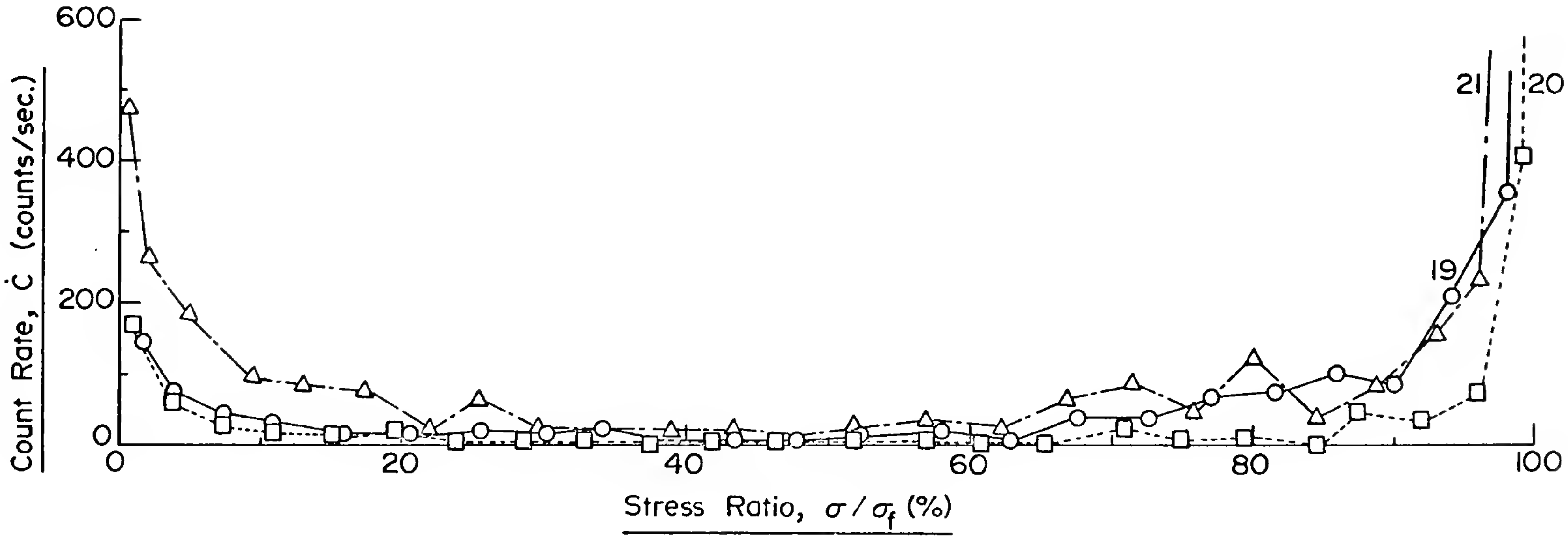

FIGURE B16 COUNT RATE VS. STRESS RATIO, CYLINDERS 19,20 AND 21, W/C=0.50, CA=0.62.

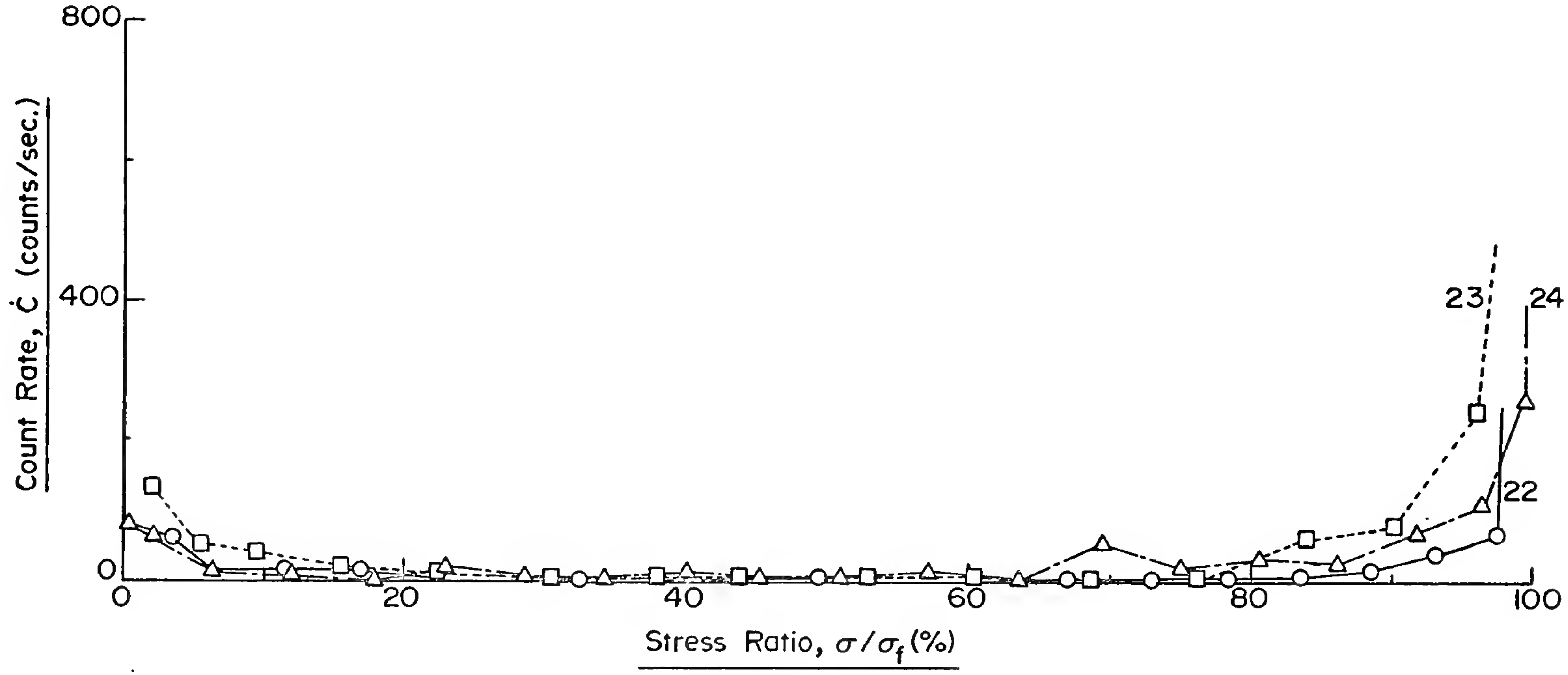

FIGURE B17 COUNT RATE VS. STRESS RATIO, CYLINDERS 22, 23 AND 24, W/C=0.45, CA=0.62.

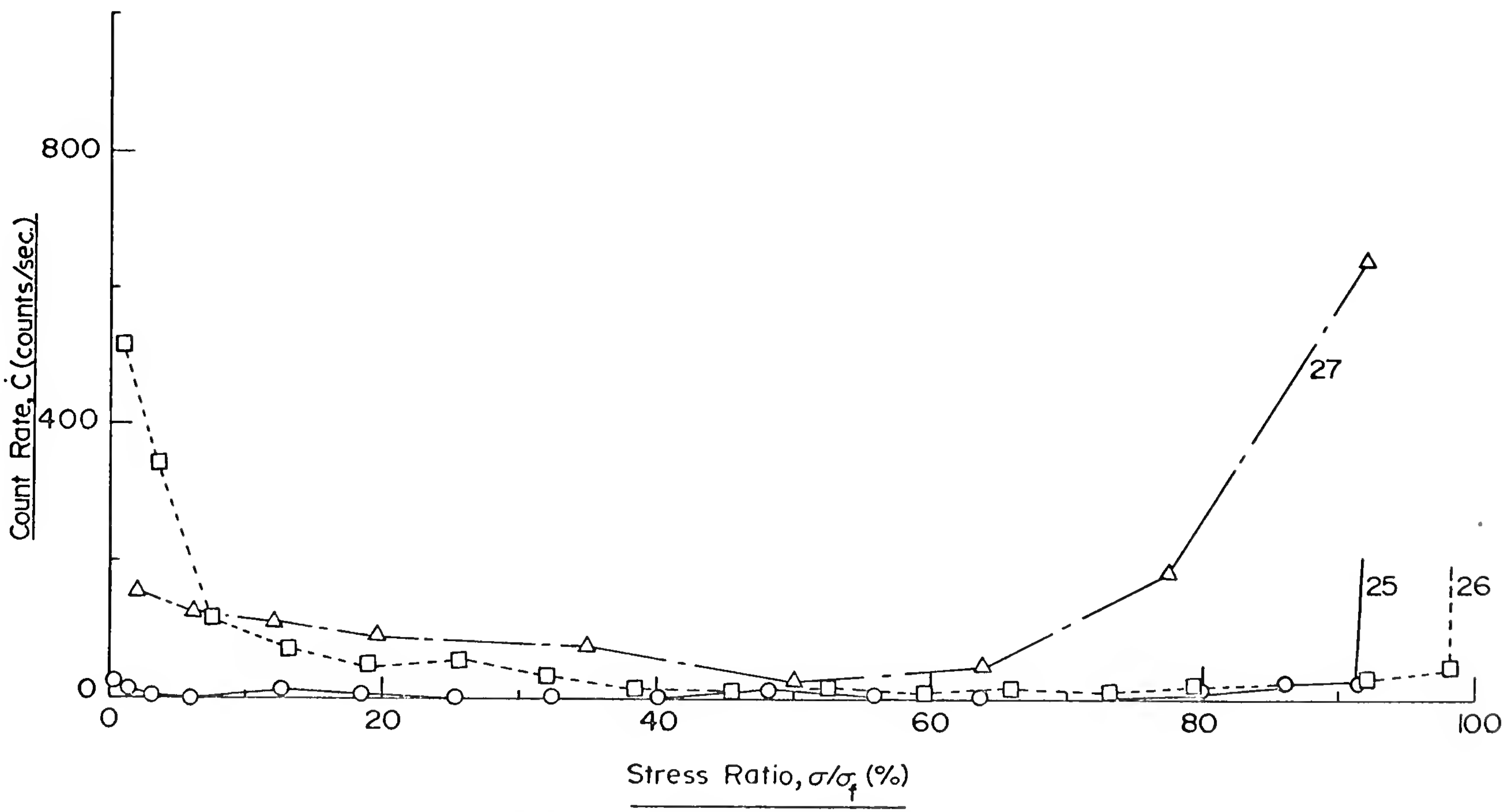

FIGURE B18 COUNT RATE VS. STRESS RATIO, CYLINDERS 25, 26 AND 27, W/C=0.50, CA=0.62.

APPENDIX C

Asphalt Concrete Tension Specimens

Specimen bulk specific gravities and specimen percentage of Hveem bulk specific gravity

SPECIMEN BULK
Specific Gravities

t Values from ASTM E178

DENSE GRADATION: t (.99) = 3.01 t (.95) = 3.21

Ser.	G_{mb}	t	% Hveem
215	2.348	-0.30	98.8
216	2.351	-0.04	99.0
217	2.336	-1.34	98.3
218	2.353	0.13	99.0
219	2.346	-0.47	98.7
220	2.360	0.73	99.3
221	2.355	0.30	99.1
222	2.352	0.04	99.0
223	2.363	0.99	99.5
224	2.364	1.08	99.5
225	2.352	0.04	99.0
226	2.358	0.56	99.2
227	2.349	-0.21	98.9
228	2.353	0.13	99.0
229	2.358	0.56	99.2
230	2.347	-0.39	98.8
231	2.356	0.39	99.2
232	2.353	0.13	99.0
233	2.342	-0.82	98.6
234	2.358	0.56	99.2
235	2.348	-0.30	98.8
236	2.324	-2.37	97.8
237	2.340	-0.99	98.5
238	2.342	-0.82	98.6
239	2.350	-0.13	98.9
240	2.342	-0.82	98.6
241	2.339	-1.08	98.4
242	2.346	-0.47	98.7
243	2.350	-0.13	98.9
244	2.333	-1.59	98.2
245	2.340	-0.99	98.5
246	2.345	-0.56	98.7

Ser.	G_{mb}	t	% Hveem
247	2.339	-1.08	98.4
248	2.347	-0.39	98.8
249	2.343	-0.73	98.6
250	2.344	-0.65	98.7
251	2.350	-0.13	98.9
252	2.344	-0.65	98.7
253	2.352	0.04	99.0
254	2.342	-0.82	98.6
255	2.345	-0.56	98.7
256	2.335	-1.42	98.3
257	2.338	-1.16	98.4
258	2.348	-0.30	98.8
259	2.356	0.39	99.2
260	2.348	-0.30	98.8
261	2.342	-0.82	98.6
262	2.344	-0.65	98.7
263	2.361	0.82	99.4
264	2.348	-0.30	98.8
265	2.350	-0.13	98.9
266	2.353	0.13	99.0
267	2.342	-0.82	98.6
268	2.334	-1.51	98.2
269	2.333	-1.59	98.2
270	2.336	-1.34	98.3
271	2.353	0.13	99.0
272	2.350	-0.13	98.9
273	2.343	-0.73	98.6
274	2.347	-0.39	98.8
275	2.345	-0.56	98.7
276	2.353	0.13	99.0
277	2.347	-0.39	98.8
278	2.352	0.04	99.0

Ser.	G_{mb}	t	% Hveem
279	2.341	-0.90	98.5
280	2.396	3 8.84	100.8
281	2.351	-0.04	99.0
282	2.343	-0.73	98.6
283	2.339	-0.08	98.4
284	2.348	-0.30	98.8
285	2.342	-0.82	98.6
286	2.344	-0.65	98.7
295	2.353	0.13	99.0
296	2.357	0.48	99.2
297	2.357	0.48	99.2
298	2.365	1.17	99.5
299	2.354	0.22	99.1
300	2.354	0.22	99.1
301	2.349	-0.21	98.9
302	2.349	-0.21	98.9
303	2.344	-0.65	98.7
304	2.344	-0.65	98.7
305	2.344	-0.65	98.7
306	2.349	-0.21	98.9
307	2.337	-1.25	98.4
308	2.331	-1.77	98.1
309	2.338	-1.16	98.4
310	2.342	-0.82	98.6
323	2.342	-0.82	98.6
324	2.341	-0.90	98.5
325	2.340	-0.99	98.5
326	2.338	-1.16	98.4
327	2.354	0.22	99.1
328	2.350	-0.13	98.9
329	2.341	-0.90	98.5
330	2.339	-1.08	98.4

Ser.	G_{mb}	t	% Hveem
339	2.342	-0.82	98.6
340	2.343	-0.73	98.6
341	2.346	-0.47	98.7
342	2.346	-0.47	98.7
343	2.367	1.34	99.6
344	2 1.368	1.42	99.7
345	2.365	1.17	99.5
346	2.355	0.30	99.1
347	2.360	0.73	99.3
348	2.367	1.34	99.6
349	2.352	0.04	99.0
350	2.372	1.77	99.8
359	2.363	0.99	99.5
360	2.377	2.20	100.0
361	2.355	0.30	99.1
362	2.365	1.17	99.5
363	2.362	0.91	99.4
364	2.357	0.48	99.2
365	2.364	1.08	99.5
366	2.364	1.08	99.5
367	2.369	1.51	99.7
368	2.371	1.68	99.8
369	2.358	0.56	99.2
370	2.368	1.42	99.7
371	2.367	1.34	99.6
372	2.368	1.42	99.7
373	2.368	1.42	99.7
374	2.385	2.89	100.4
375	2.359	0.65	99.3
376	2.362	0.91	99.4
377	2.373	1.86	99.9
378	2.349	-0.21	98.9
379	2.371	1.68	99.8
380	2.364	1.08	99.5
381	2.369	1.51	99.7
382	2.372	1.77	99.8

COARSE GRADATION:

Ser.	G_{mb}	t	% Hveem
291	2.376	0.68	99.0
292	2.370	0.03	98.7
293	2.373	0.37	98.8
294	2.372	0.25	98.8
319	2.369	-0.08	98.7
320	2.376	0.70	99.0
321	2.378	0.93	99.0
322	2.364	-0.65	98.5
355	2.377	0.82	99.0
356	2.369	-0.08	98.7
357	2.372	0.25	98.8
358	2.384	1.60	99.3
315	2.350	-2.22	97.9
316	2.369	-0.08	98.7
317	2.365	-0.53	98.5
318	2.352	-2.00	98.0

t(.99) = 2.75
t(.95) = 2.44

FINE GRADATION:

Ser.	G_{mb}	t	% Hveem
287	2.350	-0.17	98.3
288	2.348	-0.37	98.2
289	2.351	-0.07	98.4
290	2.355	0.34	98.5
311	2.352	0.04	98.4
312	2.349	-0.27	98.3
313	2.348	-0.37	98.2
314	2.347	-0.47	98.2
331	2.351	-0.07	98.4
332	2.355	0.34	98.4
333	2.349	-0.27	98.3
334	2.346	-0.57	98.2
335	2.341	-1.08	98.0
336	2.336	-1.59	97.7
337	2.339	-1.28	97.9
338	2.344	-0.78	98.1
351	2.373	2.16	99.3
352	2.372	2.06	99.2
353	2.363	1.15	98.9
354	2.364	1.25	98.9

t(.99) = 2.88
t(.95) = 2.56

APPENDIX D

Asphalt Concrete Tension Test Data

SERIAL 238 ;MIX 8LD;TEMP 77 ;GAGE LENGTH (In.)4.3362;REMKS

TIME (Sec.)	LVDT DISPLACEMENT (Microinches) L	R	Ave.	STRAIN (MII)	STRESS (PSI)	STIFF-NESS (PSI)	STRAIN RATE ($\dot{\varepsilon}$) (MII/Sec)
2	150	444	297	68	6	8.31 E04	
4	592	1328	960	221	11	4.96 E04	76.5
6	1219	2535	1877	433	16	3.61 E04	106.0
8	2069	3972	3020	697	18	2.62 E04	132.0
10	2993	5220	4257	982	21	2.13 E04	142.5
12	4006	7219	5613	1294	23	1.79 E04	156.0
14	5063	9029	7046	1625	25	1.53 E04	165.5
16	6192	10817	8504	1961	27	1.36 E04	168.0
18	7363	12690	10026	2312	29	1.25 E04	175.5
20	8641	14759	11700	2698	30	1.10 E04	193.0
22	9963	16797	13380	3086	29		
24	11245	18815	15030	3466	30		

SERIAL 239;MIX 8LD;TEMP 77 ;GAGE LENGTH (In.)4.6020;REMKS

TIME (Sec.)	LVDT DISPLACEMENT (Microinches) L	R	Ave.	STRAIN (MII)	STRESS (PSI)	STIFF-NESS (PSI)	STRAIN RATE ($\dot{\varepsilon}$) (MII/Sec)
2	220	228	224	49	4	8.22 E04	
4	419	505	462	100	8	7.96 E04	25.5
6	1191	1451	1321	287	16	5.68 E04	93.5
8	2451	2920	2685	584	23	4.01 E04	148.5
10	4249	4878	4563	992	29	2.93 E04	204.0
12	6356	7213	6784	1474	34	2.28 E04	241.0
14	8900	9748	9324	2026	37	1.82 E04	276.0
16	11892	12347	12120	2634	39	1.48 E04	304.0
18	13490	13719	13604	2956	39	1.33 E04	161.0
20	18574	17977	18275	3971	40	1.01 E04	507.5
22	22274	20853	21563	4686	40		
24	26049	23681	24865	5403	39		

SERIAL 240;MIX 8LD;TEMP 77 ;GAGE LENGTH (In.)4.6082;REMKS Sht 1/2

TIME (Sec.)	LVDT DISPLACEMENT (Microinches) L	R	Ave.	STRAIN (MII)	STRESS (PSI)	STIFF-NESS (PSI)	STRAIN RATE ($\dot{\varepsilon}$) (MII/Sec)
2	44	26	35	8	-	3.71 E04	-
4	83	73	78	17	1	3.03 E04	4.5
6	166	131	148	32	1	2.62 E04	7.5
8	202	204	203	44	1	2.84 E04	6.0
10	289	283	286	62	2	3.08 E04	9.0
12	429	428	428	93	3	3.42 E04	15.5
14	621	636	629	136	4	2.91 E04	21.5
16	843	878	861	187	5	2.91 E04	25.5
18	1132	1168	1150	250	6	2.46 E04	31.5
20	1480	1499	1489	323	7	2.31 E04	36.5
22	1784	1851	1817	394	8	2.00 E04	35.5
24	2182	2244	2213	480	9	1.90 E04	43.0
26	2621	2646	2633	571	10	1.68 E04	45.5
28	3213	3076	3145	682	11	1.59 E04	55.5
30	3688	3514	3601	782	11	1.39 E04	50.0
32	4202	3966	4084	886	12	1.35 E04	52.0
34	4744	4442	4593	997	12	1.23 E04	55.5
36	5274	4922	5098	1106	13	1.18 E04	54.5
38	5941	5423	5682	1233	14	1.09 E04	63.5
40	6570	5923	6246	1355	14	1.03 E04	61.0
42	7237	6434	6836	1483	15	9.80 E03	64.0
44	7937	6944	7440	1615	15	9.14 E03	66.0
46	8637	7459	8048	1746	16	8.90 E03	65.5
48	9286	7978	8632	1873	15	8.15 E03	63.5
50	10103	8500	9301	2018	16	7.95 E03	72.5
52	10891	9019	9955	2160	16	7.22 E03	71.0
54	11680	9534	10607	2302	16	7.10 E03	71.0
56	12495	10062	11278	2447	16	6.44 E03	72.5
58	13282	10585	11933	2590	16	6.33 E03	71.5
60	14103	11120	12611	2737	16	5.90 E03	73.5

SERIAL 240 ;MIX____;TEMP____;GAGE LENGTH (In.) ______;REMKS Sht 2/2

TIME (Sec.)	LVDT DISPLACEMENT (Microinches) L	R	Ave.	STRAIN (MII)	STRESS (PSI)	STIFF-NESS (PSI)	STRAIN RATE ($\dot{\varepsilon}$) (MII/Sec)
62	14940	11643	13292	2884	17	5.76 E03	73.5
64	15745	12185	13965	3030	16	5.43 E03	73.0
66	16594	12702	14648	3179	16	5.18 E03	74.5
68	17419	13255	15337	3328	17	4.98 E03	74.5
70	18274	13689	15982	3468	16	4.70 E03	70.0
72	19138	14341	16739	3632	17	4.59 E03	82.0
74	19951	14888	17419	3780	16		
76	20802	15445	18124	3933	17		

SERIAL 241;MIX 8LD;TEMP 77 ;GAGE LENGTH (In.) 4.5918;REMKS

TIME (Sec.)	LVDT DISPLACEMENT (Microinches) L	R	Ave.	STRAIN (MII)	STRESS (PSI)	STIFF-NESS (PSI)	STRAIN RATE ($\dot{\varepsilon}$) (MII/Sec)
900	673	319	496	108	-	4.78 E02	0.12
1800	2077	359	1218	265	-	1.66 E03	0.17
2700	3656	603	2129	464	1	1.18 E03	0.22
3600	5082	1643	3362	732	-	5.48 E02	0.30
4500	6845	2684	4764	1038	1	6.52 E02	0.34
5400	8946	3970	6458	1406	1	4.84 E02	0.41
6300	11318	4599	7958	1733	1	3.56 E02	0.36
7200	13166	6151	9659	2103	1	3.67 E02	0.41
8100	13807	6581	10194	2220	1		
9000	15999	8204	12102	2636	1		

SERIAL 242 ;MIX 8LD;TEMP45.5;GAGE LENGTH (In.) 4.5915;REMKS

TIME (Sec.)	LVDT DISPLACEMENT (Microinches) L	R	Ave.	STRAIN (MII)	STRESS (PSI)	STIFF-NESS (PSI)	STRAIN RATE ($\dot{\varepsilon}$) (MII/Sec)
2	14	63	39	8	11	1.30 E06	4.0
4	2	210	106	23	24	1.05 E06	7.5
6	24	452	238	52	39	7.45 E05	14.5
8	61	755	408	89	54	6.04 E05	18.5
10	121	1132	627	136	71	5.17 E05	23.5
12	194	1621	908	198	86	4.37 E05	31.0
14	340	2178	1259	274	104	3.79 E05	38.0
16	475	2819	1647	359	120	3.35 E05	42.5
18	645	3586	2115	461	137	2.98 E05	51.0
20	954	4418	2686	585	152	2.59 E05	62.0
22	1296	5352	3324	724	167	2.31 E05	69.5
24	1697	6373	4035	879	181	2.06 E05	77.5
26	2184	7507	4845	1055	195	1.85 E05	88.0
28	2431	8171	5301	1154	201	1.74 E05	49.5
30	3203	10494	6848	1492	217	1.45 E05	169.0
32	3707	12379	8043	1752	226	1.29 E05	130.0
34	4190	14563	9377	2042	235	1.15 E05	145.0
36	4580	17196	10888	2371	239	1.01 E05	164.5
38	4801	20431	12616	2748	244	8.86 E04	188.5
40	4803	25005			241		
42							

SERIAL 243;MIX____;TEMP_____;GAGE LENGTH (In.) ______;REMKS Sht 2/2

TIME (Sec.)	LVDT DISPLACEMENT (Microinches) L	R	Ave.	STRAIN (MII)	STRESS (PSI)	STIFF-NESS (PSI)	STRAIN RATE ($\dot{\varepsilon}$) (MII/Sec)
62	6707	5840	6274	1394	197	1.41 E05	61.5
64	7371	6385	6878	1529	202	1.32 E05	67.5
66	8072	6983	7528	1673	207	1.24 E05	72.0
68	8811	7614	8212	1825	212	1.16 E05	76.0
70	9599	8313	8956	1991	216	1.08 E05	83.0
72	10444	9074	9759	2169	219	1.01 E05	89.0
74	11304	9893	10599	2356	222	9.42 E04	93.5
76	12220	10777	11499	2556	224	8.77 E04	100.0
78	13168	11760	12464	2770	226	8.14 E04	107.0
80	14107	12845	13476	2995	226	7.55 E04	112.5
82	15039	12845	13942	3099	225		

SERIAL 243;MIX 8LD;TEMP45.5;GAGE LENGTH (In.) 4.4992;REMKS Sht 1/2

TIME (Sec.)	LVDT DISPLACEMENT (Microinches) L	R	Ave.	STRAIN (MII)	STRESS (PSI)	STIFF-NESS (PSI)	STRAIN RATE ($\dot{\varepsilon}$) (MII/Sec)
2	6	4	5	1	3	2.79 E06	0.5
4	10	4	7	2	4	2.61 E06	0.5
6	16	4	10	2	6	2.88 E06	0
8	26	8	17	4	9	2.26 E06	1.0
10	38	4	21	5	12	2.62 E06	0.5
12	59	10	34	8	17	2.21 E06	1.5
14	91	14	52	12	22	1.88 E06	2.0
16	131	22	77	17	28	1.64 E06	2.5
18	174	36	105	23	34	1.48 E06	3.0
20	237	46	141	31	41	1.31 E06	4.0
22	313	69	191	43	48	1.14 E06	6.0
24	392	111	252	56	56	1.00 E06	6.5
26	508	258	383	85	64	7.48 E05	14.5
28	647	412	530	118	71	6.07 E05	16.5
30	797	549	673	150	79	5.30 E05	16.0
32	965	692	828	184	87	4.75 E05	17.0
34	1157	850	1004	223	95	4.28 E05	19.5
36	1379	1011	1195	266	103	3.90 E05	21.5
38	1636	1215	1426	317	112	3.52 E05	25.5
40	1927	1528	1728	384	120	3.11 E05	33.5
42	2224	1808	2016	448	128	2.85 E05	32.0
44	2542	2099	2320	516	135	2.62 E05	34.0
46	2880	2428	2654	590	143	2.43 E05	37.0
48	3242	2785	3013	670	150	2.25 E05	40.0
50	3632	3160	3396	755	158	2.09 E05	42.5
52	4050	3552	3801	845	165	1.95 E05	45.0
54	4507	3956	4232	941	172	1.83 E05	48.0
56	5003	4391	4697	1044	183	1.75 E05	51.5
58	5531	4850	5191	1154	185	1.61 E05	55.0
60	6103	5330	5716	1271	191	1.50 E05	58.5

SERIAL 244;MIX 8LD;TEMP 45.5;GAGE LENGTH (In.) 4.3560;REMKS Sht 1/2

TIME (Sec.)	LVDT DISPLACEMENT (Microinches) L	R	Ave.	STRAIN (MII)	STRESS (PSI)	STIFF-NESS (PSI)	STRAIN RATE ($\dot{\varepsilon}$) (MII/Sec)
2	6	2	4	1	-	2.54 E05	0.5
4	6	12	9	2	2	8.57 E05	0.5
6	10	12	11	3	3	1.10 E06	0.5
8	6	20	13	3	3	1.15 E06	0
10	18	26	22	5	5	1.08 E06	1.0
15	49	38	43	10	9	9.14 E05	1.0
20	75	63	69	16	12	7.70 E05	1.2
25	142	89	115	26	16	6.07 E05	2.0
30	245	135	190	44	21	4.76 E05	3.6
35	386	186	286	66	25	3.76 E05	4.4
40	566	258	412	95	31	3.31 E05	5.8
45	787	343	565	130	36	2.80 E05	7.0
50	1029	430	730	168	43	2.57 E05	7.6
55	1316	531	924	212	49	2.31 E05	8.8
60	1616	644	1130	259	54	2.08 E05	9.4
65	1978	761	1369	314	60	1.91 E05	11.0
70	2374	860	1617	371	66	1.79 E05	11.4
75	2827	985	1906	438	73	1.66 E05	13.4
80	3280	1060	2170	498	78	1.56 E05	12.0
85	3854	1215	2535	582	83	1.43 E05	16.8
90	4467	1350	2908	668	89	1.33 E05	17.2
95	5126	1463	3295	756	95	1.26 E05	17.6
100	5876	1576	3726	855	99	1.16 E05	19.8
105	6720	1679	4199	964	105	1.09 E05	21.8
110	7613	1764	4689	1076	110	1.02 E05	22.4
115	8606	1828	5217	1198	113	9.50 E04	24.4
120	9710	1859	5785	1328	119	8.90 E04	26.0

SERIAL 244;MIX ____;TEMP _____;GAGE LENGTH (In.) ______;REMKS Sht 2/2

TIME (Sec.)	LVDT DISPLACEMENT (Microinches) L	R	Ave.	STRAIN (MII)	STRESS (PSI)	STIFF-NESS (PSI)	STRAIN RATE ($\dot{\varepsilon}$) (MII/Sec)
125	10934	1877	6405	1470	123	8.40 E04	28.4
130	12258	1889	7074	1624	126	7.80 E04	30.8
135	13745	1879	7812	1793	131	7.30 E04	33.8
140	15370	1825	8598	1974	133	6.80 E04	36.2
145	17269	1645	9457	2171	136	6.30 E05	39.4
150	19437	1318	10377	2382	141	5.90 E05	42.2
155	21995	819	11407	2619	140	5.30 E05	47.4
160	24968	95	12531	2877	141	4.90 E05	51.6
165	28535	-930	13802	3167	142	4.50 E05	58.0
170	32898	-2373	15263	3504	140		
175	38524	-4478	17023	3908	136		

Shut off before
SERIAL 245;MIX 8LD;TEMP 45.5;GAGE LENGTH (In.)4.4720;REMKSfailure-rerun.

SERIAL 246;MIX 8LD;TEMP 108.5;GAGE LENGTH (In.)4.4018;REMKS

TIME (Sec.)	LVDT DISPLACEMENT (Microinches) L	R	Ave.	STRAIN (MII)	STRESS (PSI)	STIFF-NESS (PSI)	STRAIN RATE ($\dot{\varepsilon}$) (MII/Sec)
2	15561	15253	15407	3500	1.7	4.77 E02	-
4	16001	15255	15628	3550	1.9	5.41 E02	25.0
6	17142	15273	16207	3682	2.2	5.88 E02	91.0
8	18818	15310	17064	3877	2.4	6.13 E02	97.5
10	21000	15370	18185	4131	2.6	6.24 E02	127.0
12	22435	15429	19432	4415	2.7	6.05 E02	142.0
14	25993	15469	20731	4710	2.7	5.73 E02	147.5
16	28531	15427	21979	4993	2.8	5.52 E02	141.5
18	30369	15540	22955	5215	2.6	4.97 E02	111.0
20	34203	15554	24879	5652	2.9	5.12 E02	218.5
22					2.7		
24					2.5		
26					2.6		

SERIAL 247 MIX 8LD;TEMP 45.5;GAGE LENGTH (In.) 4.5548:REMKS

TIME (Sec.)	LVDT DISPLACEMENT (Microinches) L	R	Ave.	STRAIN (MII)	STRESS (PSI)	STIFF-NESS (PSI)	STRAIN RATE ($\dot{\varepsilon}$) (MII/Sec)
900	10	2	6	1	1	1.04 E06	0
1800	77	202	140	31	4	1.41 E05	0.03
2700	317	678	498	109	6	5.04 E04	0.09
3600	580	1076	828	182	6	3.46 E04	0.08
4500	890	1552	1221	268	8	2.95 E04	0.10
5400	1254	2127	1690	371	9	2.43 E04	0.11
6300	1602	3312	2457	539	11	2.00 E04	0.19
7200	2115	3508	2812	617	12	1.91 E04	0.09
8100	2639	4339	3489	766	13	1.69 E04	0.17
9000	3165	5243	4204	923	14	1.52 E04	0.17
9900	3796	6282	5039	1106	15	1.33 E04	0.20
10800	4420	7344	5882	1291	15	1.18 E04	0.21
11700	4590	8517	6554	1439	17	1.15 E04	0.16
12600	5822	9838	7830	1719	17	1.00 E04	0.31
13500	6612	11184	8898	1954	18	8.97 E03	0.26
14400	7411	12583	9997	2195	18	8.05 E03	0.27
15300	8277	14008	11142	2446	17	7.04 E03	0.28
16200	8995	15320	12157	2669	18	6.60 E03	0.25
17100	9735	16888	13211	2901	18	6.10 E03	0.26

SERIAL 248;MIX 8LD;TEMP 108.5; GAGE LENGTH (In.)4.5465;REMKS

TIME (Sec.)	LVDT DISPLACEMENT (Microinches) L	R	Ave.	STRAIN (MII)	STRESS (PSI)	STIFF-NESS (PSI)	STRAIN RATE ($\dot{\varepsilon}$) (MII/Sec)
2	15561	15253	15407	3389	1.7	4.93 E02	-
4	16228	15257	15742	3462	1.7	4.83 E02	36.5
6	16927	15255	16091	3539	1.7	4.78 E02	38.5
8	17627	15245	16436	3615	1.8	4.85 E02	38.0
10	18414	15255	16834	3703	1.8	4.84 E02	44.0
12	19516	15255	17385	3824	1.9	4.87 E02	60.5
14	20887	15247	18067	3974	1.8	4.55 E02	75.0
16	22353	15231	18792	4133	1.9	4.53 E02	79.5
18	23910	15207	19559	4302	1.9	4.45 E02	84.5
20	25617	15146	20381	4483	1.9	4.27 E02	90.5
22	27463	15039	21251	4674	1.9	4.09 E02	95.5
24	29451	14890	22170	4876	1.9	3.97 E02	101.0
26	31653	14639	23146	5091	1.9	3.81 E02	107.5
28	34113	14204	24159	5314	1.9	3.66 E02	111.5
30	36912	13594	25253	5554	1.9	3.48 E02	120.0
32	39980	12831	26405	5808	1.9	3.35 E02	127.0
34					1.9		
36					1.9		

SERIAL 249 ;MIX 8LD;TEMP 108.5 ;GAGE LENGTH(Inc.) 4.5430;REMKS Failed during rigging

SERIAL 250;MIX 8LD;TEMP 108.5;GAGE LENGTH (In.)4.5098;REMKS Failed above LVDT Yoke

SERIAL 251;MIX 8LD;TEMP 108.5;GAGE LENGTH (In.)4.6502;REMKS

TIME (Sec.)	LVDT DISPLACEMENT (Microinches) L	R	Ave.	STRAIN (MII)	STRESS (PSI)	STIFF-NESS (PSI)	STRAIN RATE ($\dot{\varepsilon}$) (MII/Sec)
4	6344	135	3239	697	1.5	2.14 E03	-
10	7559	127	3843	826	1.5	1.85 E03	21.5
14	8457	165	4311	927	1.7	1.79 E03	25.2
20	10040	236	5138	1105	1.6	1.44 E03	29.7
30	12323	180	6252	1344	1.6	1.19 E03	23.9
40	15083	165	7624	1639	1.8	1.08 E03	29.5
50	18307	143	9225	1984	1.7	8.79 E02	34.5
60	21591	-10	10790	2320	1.7	7.25 E02	33.6
70	25255	-268	12494	2687	1.8	6.62 E02	36.7
80	29386	5352	17369	3735	1.8	4.91 E02	104.8
90	34571	-1376	16598	3569	1.8	5.13 E02	-16.6
92	35776	-1566	17105	3678	1.9	5.09 E02	54.5
96	38277	-2008	18135	3900	1.9	4.87 E02	55.5

SERIAL 252;MIX 8LD;TEMP 14;GAGE LENGTH (In.) 4.5895;REMKS Scanner not functioning

Failed above
SERIAL 253;MIX 8LD;TEMP 14;GAGE LENGTH (In.) 4.6002;REMKS LVDT yoke

SERIAL 254;MIX 8LD; TEMP 14;GAGE LENGTH (In.) 4.5730;REMKS

TIME (Sec.)	LVDT DISPLACEMENT (Microinches) L	R	Ave.	STRAIN (MII)	STRESS (PSI)	STIFF-NESS (PSI)	STRAIN RATE ($\dot{\varepsilon}$) (MII/Sec)
2	22	4	13	3	49	3.74 E06	1.5
4	53	14	33	7	74	1.01 E07	2.0
6	93	30	61	13	101	7.52 E06	3.0
8	142	56	99	22	131	6.07 E06	4.5
10	204	89	147	32	162	5.04 E06	5.0
12	285	141	213	47	194	4.16 E06	7.5
14	372	192	282	62	226	3.67 E06	7.5
16	471	264	367	80	259	3.23 E06	9.0
18	566	337	452	99	292	2.96 E06	9.5
20	681	426	554	121	325	2.68 E06	11.0
22	809	551	680	149	355	2.39 E06	14.0
23	853	642	748	164	369	2.26 E06	7.5

SERIAL 255;MIX 8LD;TEMP 14; GAGE LENGTH (In.)4.3992:REMKS

TIME (Sec.)	LVDT DISPLACEMENT (Microinches) L	R	Ave.	STRAIN (MII)	STRESS (PSI)	STIFF-NESS (PSI)	STRAIN RATE ($\dot{\varepsilon}$) (MII/Sec)
2	34	33	34	8	26	3.34 E06	4.0
4	83	67	75	17	54	3.17 E06	4.5
6	133	107	120	27	84	3.09 E06	5.0
8	202	155	178	41	116	2.87 E06	7.0
10	279	204	242	55	149	2.72 E06	7.0
12	364	262	313	71	183	2.57 E06	8.0
14	445	321	383	87	216	2.48 E06	8.0
16	552	390	471	107	249	2.32 E06	10.0
18	643	466	554	126	281	2.23 E06	9.5
20	777	551	664	151	311	2.06 E06	12.5
21	849	591	720	164	325	1.99 E06	13.0

SERIAL 256;MIX 8LD;TEMP 14: GAGE LENGTH (In.)4.4325;REMKS

TIME (Sec.)	LVDT DISPLACEMENT (Microinches) L	R	Ave.	STRAIN (MII)	STRESS (PSI)	STIFF-NESS (PSI)	STRAIN RATE ($\dot{\varepsilon}$) (MII/Sec)
2	-6	0	-3	-	0.1	-	-
4	-2	-4	-3	-	0.1	-	-
6	4	2	3	1	13	1.95 E07	-
8	57	30	43	10	47	4.78 E06	4.5
10	129	56	92	21	83	3.99 E06	5.5
12	212	87	150	34	124	3.66 E06	6.5
14	326	127	226	51	166	3.24 E06	8.5
16	453	190	322	73	208	2.87 E06	11.0
18	611	220	415	94	252	2.69 E06	10.5
19	712	226	469	106	273	2.58 E06	6.0

SERIAL 257;MIX 8LD;TEMP 14 ;GAGE LENGTH (In.)4.4682;REMKS

TIME (Sec.)	LVDT DISPLACEMENT (Microinches) L	R	Ave.	STRAIN (MII)	STRESS (PSI)	STIFF-NESS (PSI)	STRAIN RATE ($\dot{\varepsilon}$) (MII/Sec)
2	4	0	2	1	2	3.91 E06	0.25
4	2	-6	-2	-	6	-	-
6	12	-8	2	1	18	3.80 E07	0.45
8	22	-2	10	2	37	1.65 E07	0.75
10	47	4	25	6	58	1.03 E07	2.0
12	79	12	45	10	84	8.27 E06	2.0
14	113	38	75	17	113	6.71 E06	3.5
16	168	61	115	26	145	5.65 E06	4.5
18	224	79	152	34	178	5.23 E06	4.0
20	279	113	196	44	212	4.82 E06	5.0
22	356	153	254	57	246	4.32 E06	6.5
24	459	200	330	74	280	3.79 E06	8.5
26	564	254	409	92	313	3.42 E06	9.0
28	686	327	506	113	346	3.05 E06	10.5
29	744	387	565	127	361	2.86 E06	7.0

SERIAL 258;MIX 8LD;TEMP 14 ;GAGE LENGTH (In.)4.4682;REMKS

TIME (Sec.)	LVDT DISPLACEMENT (Microinches) L	R	Ave.	STRAIN (MII)	STRESS (PSI)	STIFF-NESS (PSI)	STRAIN RATE ($\dot{\varepsilon}$) (MII/Sec)
2	-6	10	2	-	1	1.44 E06	0.2
4	18	44	31	7	1	1.92 E05	3.3
6	30	56	43	10	3	3.10 E05	1.5
8	127	131	129	29	3	1.20 E05	9.5
10	28	46	37	8	7	8.27 E05	10.5
12	168	230	199	45	12	2.76 E05	18.5
14	259	317	288	64	22	3.43 E05	9.5
16	229	270	249	56	38	6.79 E05	4.0
18	121	145	133	30	55	1.85 E05	13.0
20	-60	-6	-32	-7	75	-	-
22	-101	6	-48	-11	95	-	-
24	-99	28	-37	-8	116	-	-
26	-51	121	35	8	139	1.76 E07	8.0
28	-16	168	76	17	161	9.46 E06	4.5
30	6	216	111	25	184	7.42 E06	4.0
32	26	274	150	34	208	6.19 E06	4.5
34	73	345	209	47	231	4.95 E06	6.5
36	93	381	237	53	254	4.80 E06	3.0
38	144	416	280	63	278	4.43 E06	5.0
40	289	462	376	84	301	3.58 E06	10.5
42	374	500	437	98	322	3.30 E06	7.0
44	453	549	501	112	343	3.06 E06	7.0
46	542	607	574	129	362	2.82 E06	8.5

Failed during
SERIAL 259;MIX 8LD; TEMP 108.5; GAGE LENGTH (In.)4.5312;REMKS hook-up.

SERIAL 260;MIX 8LD;TEMP 14 ;GAGE LENGTH (In.)4.5950;REMKS Sht 1/2

TIME (Sec.)	LVDT DISPLACEMENT (Microinches) L	R	Ave.	STRAIN (MII)	STRESS (PSI)	STIFF-NESS (PSI)	STRAIN RATE ($\dot{\varepsilon}$) (MII/Sec)
900	651	357	504	110	2	1.54 E04	0.12
1800	202	-8	97	21	4	1.71 E05	0.10
2700	524	244	384	84	7	8.04 E04	0.07
3600	384	125	255	55	10	1.75 E05	0.03
4500	570	278	424	92	9	9.54 E04	0.04
5400	402	145	273	60	9	1.43 E05	0.04
6300	601	297	449	98	9	8.92 E04	0.04
7200	601	297	449	98	9	8.96 E04	0
8100	623	317	470	102	8	8.29 E04	0
9000	819	468	643	140	9	6.08 E04	0.04
9900	880	517	698	152	9	5.87 E04	0.01
10800	872	515	693	151	9	5.90 E04	0
11700	916	547	732	159	9	5.94 E04	0.01
12600	978	595	787	171	10	6.05 E04	0.01
13500	1167	763	965	210	11	5.20 E04	0.04
14400	1199	775	987	215	11	5.26 E04	0.01
15300	1231	797	1014	220	12	5.64 E04	0.01
16200	1276	821	1048	228	12	5.39 E04	0.01
17100	1308	858	1083	236	12	5.26 E04	0.01
18000	1326	866	1096	239	13	5.46 E04	0
18900	1335	864	1099	239	14	5.80 E04	0
19800	1359	872	1116	243	20	8.22 E04	0
20700	1411	902	1157	252	30	1.21 E05	0.01
21600	1488	938	1213	264	42	1.58 E05	0.01
22500	1502	926	1214	264	54	2.05 E05	0
23640	1723	1072	1398	304	69	2.28 E05	0.04
24600	1870	1173	1522	331	88	2.65 E05	0.03

SERIAL 260;MIX 8LD;TEMP 14 ;GAGE LENGTH (In.)4.5950;REMKS Sht 2/2

TIME (Sec.)	LVDT DISPLACEMENT (Microinches) L	R	Ave.	STRAIN (MII)	STRESS (PSI)	STIFF-NESS (PSI)	STRAIN RATE ($\dot{\varepsilon}$) (MII/Sec)
25500	2052	1304	1678	365	108	2.97 E05	0.04
26400	2257	1421	1839	400	129	3.23 E05	0.04
27240	2495	1568	2032	442	150	3.39 E05	0.05
28140	2524	1508	2016	439	171	3.90 E05	0
29100	3106	1885	2496	543	192	3.54 E05	0.12
30000	3692	2176	2934	639	213	3.34 E05	0.11
30840	4048	2206	3127	681	232	3.41 E05	0.05
31740	5274	2787	4030	877	251	2.86 E05	0.22
32700	6906	3312	5109	1112	265	2.38 E05	0.26
33300	8635	3465	6050	1317	272	2.06 E05	0.23
33600	10293	3334	6813	1483	271		
33660	10934	3140	7037	1531	270		

SERIAL 261;MIX 8LD;TEMP 14 ;GAGE LENGTH (In.) 4.5792;REMKS

TIME (Sec.)	LVDT DISPLACEMENT (Microinches) L	R	Ave.	STRAIN (MII)	STRESS (PSI)	STIFF-NESS (PSI)	STRAIN RATE ($\dot{\epsilon}$) (MII/Sec)
2	2	14	8	2	3	1.48 E06	1.0
4	10	26	18	4	8	2.00 E06	1.0
6	10	36	23	5	14	2.84 E06	0.5
8	8	56	32	7	18	2.55 E06	1.0
10	2	65	34	7	22	2.95 E06	0
12	0	83	42	9	26	2.86 E06	1.0
14	-6	95	45	10	31	3.19 E06	0.5
16	-2	109	53	12	37	3.18 E06	1.0
18	-8	115	53	12	44	3.81 E06	0
20	-36	119	41	9	52	5.82 E06	1.5
22	-44	135	45	10	61	6.21 E06	0.5
24	-51	145	47	10	72	7.05 E06	0
26	-59	174	58	13	86	6.83 E06	1.5
28	-129	129	0	0	104	-	6.5
30	-152	158	3	-	127	-	-
32	-168	208	-	-	156	-	-
34	-190	264	-	-	190	-	-
36	-218	331	274	60	227	-	7.5
38	-249	416	84	18	270	1.48 E07	21.0
40	-263	545	141	31	313	1.02 E07	6.5
42	-77	765	344	75	355	4.73 E06	22.0
44	138	991	564	123	97		

SERIAL 262;MIX 8LD; TEMP 14: GAGE LENGTH (In.) 4.4700;REMKS

TIME (Sec.)	LVDT DISPLACEMENT (Microinches) L	R	Ave.	STRAIN (MII)	STRESS (PSI)	STIFF-NESS (PSI)	STRAIN RATE ($\dot{\varepsilon}$) (MII/Sec)
1	8	18	13	3	21	7.40 E06	3.0
2	28	52	40	9	83	9.25 E06	6.0
3	83	149	116	26	153	5.92 E06	17.0
4	243	315	279	62	232	3.72 E06	36.0
5	443	527	485	109	313	2.88 E06	47.0
6	706	827	766	171	-		

Failed during
SERIAL 263;MIX 8LD;TEMP 108.5;GAGE LENGTH (In.)4.6535:REMKS hook-up.

SERIAL 264;MIX 8LD;TEMP -17.5; GAGE LENGTH (In.)4.5598;REMKS

TIME (Sec.)	LVDT DISPLACEMENT (Microinches) L	R	Ave.	STRAIN (MII)	STRESS (PSI)	STIFF-NESS (PSI)	STRAIN RATE ($\dot{\varepsilon}$) (MII/Sec)
1	-	-	-	-	-	-	
2	0	32	16	4	152	2.19 E07	

SERIAL 265;MIX 8LD;TEMP -17.5; GAGE LENGTH (In.)4.6158;REMKS

TIME (Sec.)	LVDT DISPLACEMENT (Microinches) L	R	Ave.	STRAIN (MII)	STRESS (PSI)	STIFF-NESS (PSI)	STRAIN RATE ($\dot{\varepsilon}$) (MII/Sec)
2	6	6	6	1	15	1.17 E07	0.5
4	18	14	16	3	32	9.24 E06	1.0
6	32	28	30	7	62	9.45 E06	2.0
8	57	46	51	11	85	7.70 E06	2.0
10	77	67	72	16	122	7.83 E06	2.5
12	111	109	110	24	181	7.60 E06	4.0
14	186	226	206	45	276	6.19 E06	10.5

SERIAL 266;MIX 8LD;TEMP -17.5;GAGE LENGTH (In.)4.5898;REMKS

TIME (Sec.)	LVDT DISPLACEMENT (Microinches) L	R	Ave.	STRAIN (MII)	STRESS (PSI)	STIFF-NESS (PSI)	STRAIN RATE ($\dot{\varepsilon}$) (MII/Sec)
5	10	8	9	2	7	3.76 E06	0.4
10	24	12	18	4	17	4.27 E06	0.4
15	44	22	33	7	28	3.94 E06	0.6
20	67	32	49	11	38	3.51 E06	0.8
25	87	36	61	13	42	3.15 E06	0.4
30	105	52	78	17	52	3.04 E06	0.8
35	140	63	101	22	65	2.93 E06	1.0
40	168	73	121	26	79	3.01 E06	0.8
45	200	83	142	31	95	3.09 E06	1.0
50	237	109	173	38	115	3.06 E06	1.4
55	281	121	201	44	133	3.04 E06	1.2
60	320	139	229	50	155	3.11 E06	1.2
65	370	161	265	58	177	3.06 E06	1.6
70	417	188	302	66	197	2.99 E06	1.6
75	471	208	340	74	219	2.96 E06	1.6
80	528	238	383	83	242	2.90 E06	1.8
81	542	242	392	85	244	2.86 E06	2.0
82	552	250	401	87	252	2.88 E06	2.0
83	570	260	415	90	255	2.82 E06	3.0
84	578	268	423	92	260	2.82 E06	2.0
85	599	271	435	95	265	2.80 E06	3.0
86	611	283	447	97	268	2.75 E06	2.0
87	623	283	453	99	275	2.78 E06	2.0
88	639	291	465	101	278	2.75 E06	2.0
89	653	301	477	104	282	2.71 E06	3.0
90	671	311	491	107	288	2.69 E06	3.0
91	683	315	499	109	290	2.67 E06	2.0
92	698	319	508	111	298	2.69 E06	2.0
93	726	331	528	115	298	2.59 E06	4.0

SERIAL 267;MIX 8LD;TEMP -17.5;GAGE LENGTH (In.)4.5172;REMKS

TIME (Sec.)	LVDT DISPLACEMENT (Microinches) L	R	Ave.	STRAIN (MII)	STRESS (PSI)	STIFF-NESS (PSI)	STRAIN RATE ($\dot{\epsilon}$) (MII/Sec)
5	4	4	4	1	14	1.60 E07	0.2
10	12	12	12	3	34	1.29 E07	0.4
15	10	26	18	4	53	1.33 E07	0.2
20	16	44	30	7	75	1.14 E07	0.6
25	18	69	44	10	95	9.80 E06	0.6
30	28	95	62	14	119	8.73 E06	0.8
35	24	121	73	16	141	8.78 E06	0.4
40	36	151	94	21	165	7.98 E06	1.0
45	44	174	109	24	189	7.80 E06	0.6
50	57	220	138	31	211	6.89 E06	1.4
51	61	222	141	31	220	7.04 E06	0
52	65	228	146	32	224	6.93 E06	1.0
53	67	236	151	33	226	6.74 E06	1.0
54	65	240	152	34	232	6.88 E06	1.0
55	73	248	160	35	238	6.70 E06	1.0
56	77	256	166	37	241	6.54 E06	2.0
57	75	264	169	37	245	6.54 E06	0
58	81	270	175	39	252	6.50 E06	2.0
59	83	272	177	39	255	6.51 E06	0

SERIAL 268;MIX 8LD;TEMP 77 ;GAGE LENGTH (In.)4.5360;REMKS

TIME (Sec.)	LVDT DISPLACEMENT (Microinches) L	R	Ave.	STRAIN (MII)	STRESS (PSI)	STIFF-NESS (PSI)	STRAIN RATE ($\dot{\varepsilon}$) (MII/Sec)
1	10	364	187	41	3	6.68 E04	41.0
2	34	1118	576	127	7	5.70 E04	86.0
3	506	2529	1517	334	18	5.31 E04	207.0
4	2172	5467	3819	842	28	3.37 E04	508.0
5	4418	9437	6928	1527	33	2.17 E04	685.0
6	8123	14841	11482	2531	39	1.56 E94	1004.0
7	11609	20922	16266	3586	43	1.21 E04	1055.0
8	15522	27751	21636	4770	44	9.30 E03	1184.0
9	20207	35077	27642	6094			

SERIAL 269;MIX 8LD;TEMP 77; GAGE LENGTH (In.)4.6135; REMKS

TIME (Sec.)	LVDT DISPLACEMENT (Microinches) L	R	Ave.	STRAIN (MII)	STRESS (PSI)	STIFF-NESS (PSI)	STRAIN RATE ($\dot{\varepsilon}$) (MII/Sec)
1	12	0	6	1	-	4.54 E04	1.0
2	20	-20	0	0	-	-	1.0
3	32	18	25	5	1	1.97 E05	5.0
4	99	172	136	29	3	9.90 E04	24.0
5	287	355	321	70	3	4.25 E04	41.0
6	427	626	527	114	7	6.09 E04	44.0
7	841	1152	996	216	9	4.33 E04	102.0
8	1335	1845	1590	345	15	4.38 E04	129.0
9	2208	3675	2942	638	26	4.03 E04	293.0
10	4129	6131	5130	1112	25	2.20 E04	474.0
11	5692	8014	6853	1485	24	1.63 E04	373.0
12	7126	10040	8583	1860	31	1.67 E04	375.0
13	9088	13820	11454	2483	41	1.65 E04	623.0
14	12133	19431	15782	3421	47	1.38 E04	938.0
15	16226	26135	21181	4591	49	1.07 E04	1170.0
16	21051	33471	27261	5909	49		
17	112139	41180	76659	16616	47		

SERIAL 270;MIX 8LD;TEMP 77;GAGE LENGTH (In.)4.5440;REMKS

TIME (Sec.)	LVDT DISPLACEMENT (Microinches) L	R	Ave.	STRAIN (MII)	STRESS (PSI)	STIFF-NESS (PSI)	STRAIN RATE ($\dot{\varepsilon}$) (MII/Sec)
2	10	-2	4	1	-	4.00 E04	0.5
4	47	8	27	6	1	1.06 E05	2.5
6	111	30	70	16	1	5.98 E04	5.0
8	204	73	139	31	2	4.96 E04	7.5
10	346	262	304	67	3	3.91 E04	18.0
12	607	924	765	168	7	3.88 E04	50.5
14	1169	2073	1621	357	10	2.88 E04	94.5
16	2109	3804	2956	651	15	2.26 E04	147.0
18	3428	5994	4711	1037	18	1.73 E04	193.0
20	4977	8434	6705	1476	20	1.37 E04	219.5
21	5812	9754	7783	1713	21	1.25 E04	237.0
22	6685	11023	8854	1949	19		
23					20		

SERIAL 271;MIX 8LD;TEMP 77;GAGE LENGTH (In.)4.5850; REMKS

TIME (Sec.)	LVDT DISPLACEMENT (Microinches) L	R	Ave.	STRAIN (MII)	STRESS (PSI)	STIFF-NESS (PSI)	STRAIN RATE ($\dot{\varepsilon}$) (MII/Sec)
2	79	115	97	21	6	2.64 E05	10.5
4	1231	1223	1227	268	13	4.98 E04	123.5
6	3179	2981	3080	672	18	2.72 E04	202.0
8	5549	5076	5313	1159	21	1.84 E04	243.5
10	8218	7356	7787	1698	23	1.38 E04	269.5
12	11132	9693	10412	2271	25	1.08 E04	286.5
14	14246	12070	13158	2870	25	8.88 E03	299.5
16	17566	14490	16028	3496	26	7.45 E03	313.0
17	19283	15693	17488	3814	27	6.97 E03	318.0
18	21039	16886	18962	4136	26		
21					26		
22					26		
23					25		

SERIAL 272;MIX 8LD;TEMP 77: GAGE LENGTH (In.) 4.6010; REMKS

TIME (Sec.)	LVDT DISPLACEMENT (Microinches) L	R	Ave.	STRAIN (MII)	STRESS (PSI)	STIFF-NESS (PSI)	STRAIN RATE ($\dot{\varepsilon}$) (MII/Sec)
2	8	4	6	1	-	2.16 E05	0.5
4	89	85	87	19	2	1.02 E05	9.0
6	364	349	356	77	4	5.53 E04	29.0
8	1060	918	989	215	9	4.23 E04	69.0
10	2528	1931	2229	484	15	3.04 E04	134.5
12	4554	3110	3832	833	17	2.06 E04	174.5
14	6766	4395	5580	1213	21	1.72 E04	190.0
16	9296	5814	7555	1642	23	1.39 E04	214.5
18	12230	7413	9822	2135	24	1.12 E04	246.5
20	15423	9112	12268	2666	25	9.24 E03	265.5
22	18891	10835	14863	3230	26	8.17 E03	282.0
24	22537	12694	17615	3829	27	6.95 E03	299.5
26	26353	14573	20463	4447	26		

SERIAL 273;MIX 8LD;TEMP 77;GAGE LENGTH (In.)4.5950;REMKS

TIME (Sec.)	LVDT DISPLACEMENT (Microinches) L	R	Ave.	STRAIN (MII)	STRESS (PSI)	STIFF-NESS (PSI)	STRAIN RATE ($\dot{\varepsilon}$) (MII/Sec)
2	30	54	42	9	1	9.42 E04	4.5
4	212	242	227	49	3	5.61 E04	20.0
6	550	605	577	126	3	2.52 E04	38.5
8	926	1029	977	213	5	2.16 E04	43.5
10	1409	1475	1442	314	6	1.97 E04	50.5
12	1931	1982	1957	426	6	1.48 E04	56.0
14	2451	2533	2492	542	7	1.29 E04	58.0
16	3039	3066	3053	664	8	1.24 E04	61.0
18	3654	3643	3649	794	9	1.09 E04	65.0
20	4249	4252	4250	925	9	9.35 E03	65.5
22	4885	4835	4860	1058	10	9.20 E03	66.5
24	5565	5465	5515	1200	11	8.79 E03	71.0
28	6863	6694	6779	1475	11	7.23 E03	68.8
30	7573	7308	7441	1619	11	7.06 E03	72.0
35	9255	8852	9054	1970	12	5.89 E03	70.2
41	11737	11071	11404	2482	12	5.02 E03	85.3
48	13943	12983	13463	2830	13	4.32 E03	49.7
55	16551	15245	15898	3460	13	3.71 E03	90.0
61	18806	17213	18009	3919	13	3.31 E03	76.5
67	21014	19174	20094	4373	13		

SERIAL 274;MIX 8LD;TEMP 77;GAGE LENGTH (In.)4.4875:REMKS

TIME (Sec.)	LVDT DISPLACEMENT (Microinches) L	R	Ave.	STRAIN (MII)	STRESS (PSI)	STIFF-NESS (PSI)	STRAIN RATE ($\dot{\varepsilon}$) (MII/Sec)
2	53	44	48	11	-	1.45 E04	5.5
4	73	0	36	8	-	5.25 E04	-1.5
6	127	6	67	15	1	3.88 E04	3.5
8	202	10	106	24	1	3.69 E04	4.5
10	297	54	175	39	1	2.93 E04	7.5
12	461	32	246	55	2	3.20 E04	8.0
14	637	50	343	76	3	3.57 E04	10.5
16	993	141	567	126	5	3.64 E04	25.0
18	1664	589	1126	251	8	3.31 E04	62.5
20	2712	1156	1934	431	10	2.42 E04	90.0
22	4099	1837	2968	661	14	2.04 E04	115.0
24	5719	2599	4159	927	15	1.65 E04	133.0
26	7375	3340	5357	1194	15	1.27 E04	133.5
28	8976	4121	6549	1459	17	1.15 E04	132.5
30	10673	4936	7804	1739	18	1.01 E04	140.0
33	13302	6270	9786	2181	19	8.60 E03	147.3
37	16990	8299	12645	2818	20	7.21 E03	159.2
40	19866	10022	14944	3330	21	6.34 E03	170.7
43	22792	11895	17343	3865	21	5.52 E03	178.3
46	25714	13927	19820	4417	22	4.95 E03	184.0
49	28703	16117	22410	4994	22	4.39 E03	-
52	31689	18478	25084	5590	22		

SERIAL 275;MIX 8HD;TEMP 77; GAGE LENGTH (In.) 4.4382;REMKS

TIME (Sec.)	LVDT DISPLACEMENT (Microinches) L	R	Ave.	STRAIN (MII)	STRESS (PSI)	STIFF-NESS (PSI)	STRAIN RATE ($\dot{\varepsilon}$) (MII/Sec)
2	30	20	25	6	1	1.40 E05	3.0
4	142	109	125	28	1	4.05 E04	11.0
6	267	224	245	55	2	3.04 E04	13.5
8	451	402	427	96	3	3.08 E04	20.5
10	821	767	794	179	5	2.94 E04	41.5
12	1442	1388	1415	319	9	2.68 E04	70.0
14	2477	2414	2446	551	13	2.29 E04	116.0
16	3925	3899	3912	881	16	1.83 E04	165.0
18	5531	5606	5568	1255	19	1.48 E04	187.0
20	7382	7522	7425	1673	21	1.23 E04	209.0
22	9199	9526	9363	2110	21	9.98 E03	218.5
24	11102	11604	11353	2558	22	8.71 E03	224.0
26	13041	13826	13433	3027	23	7.71 E03	234.5
28	15033	16062	15547	3503	24	6.74 E03	238.0
31	18040	19630	18835	4244	24	5.58 E03	247.0
33					24		
35					23		

SERIAL 276;MIX 8HD;TEMP 77; GAGE LENGTH (In.) 4.5305;REMKS

TIME (Sec.)	LVDT DISPLACEMENT (Microinches) L	R	Ave.	STRAIN (MII)	STRESS (PSI)	STIFF-NESS (PSI)	STRAIN RATE ($\dot{\varepsilon}$) (MII/Sec)
2	6	14	10	2	-	6.15 E04	1.0
4	8	59	34	7	1	9.02 E04	2.5
6	16	155	85	19	1	7.11 E04	6.0
8	30	509	270	60	3	5.54 E04	20.5
10	59	856	457	101	5	4.46 E04	20.5
12	123	1465	794	175	7	3.80 E04	37.0
14	720	2389	1554	343	10	2.95 E04	84.0
16	1508	3592	2550	563	14	2.43 E04	110.0
18	2552	5132	3842	848	17	1.98 E04	142.5
20	3798	7007	5402	1192	20	1.65 E04	172.0
22	5247	9043	7145	1577	22	1.38 E04	192.5
24	6881	11229	9055	1999	24	1.19 E04	211.0
26	8733	13552	11143	2460	25	1.01 E04	230.5
28	10780	15921	13351	2947	26	8.71 E03	243.5
30	13037	18296	15666	3458	26	7.56 E03	255.5
32	15461	20647	18054	3985	26	6.59 E03	263.5
33	16754	21798	19276	4255	26	6.21 E03	270.0
35							

SERIAL 277;MIX 8HD;TEMP 77; GAGE LENGTH (In.)4.4905;REMKS

TIME (Sec.)	LVDT DISPLACEMENT (Microinches) L	R	Ave.	STRAIN (MII)	STRESS (PSI)	STIFF-NESS (PSI)	STRAIN RATE ($\dot{\varepsilon}$) (MII/Sec)
2	4	-2	1	-	1	2.65 E06	-
4	188	174	181	40	7	1.71 E05	20.0
6	1573	1013	1293	288	13	4.55 E04	124.0
8	3490	1980	2735	609	18	2.90 E04	160.5
10	5660	3132	4396	979	22	2.20 E04	185.0
12	8046	4480	6263	1395	24	1.74 E04	208.0
14	10507	6002	8255	1838	27	1.44 E04	221.5
16	12978	7695	10337	2302	28	1.22 E04	232.0
18	15504	9507	12505	2785	29	1.05 E04	241.5
20	18108	11435	14772	3290	30	9.01 E03	252.5
22	20757	13398	17078	3803	30	7.83 E03	256.5
23	22082	14444	18263	4067	30	7.34 E03	264.0
24	23409	15540	19474	4337	30		
25							

SERIAL 278;MIX 8HD;TEMP 77; GAGE LENGTH (In.) 4.5558;REMKS

TIME (Sec.)	LVDT DISPLACEMENT (Microinches) L	R	Ave.	STRAIN (MII)	STRESS (PSI)	STIFF-NESS (PSI)	STRAIN RATE ($\dot{\varepsilon}$) (MII/Sec)
2	26	50	38	8	-	3.49 E04	4.0
4	95	153	124	27	1	4.55 E04	9.5
6	263	406	335	73	4	5.75 E04	23.0
8	841	1203	1022	224	8	3.76 E04	75.5
10	1879	2258	2068	454	7	1.62 E04	115.0
12	2164	2509	2337	513	7	1.29 E04	29.5
14	2394	2759	2577	566	6	1.08 E04	26.5
16	2625	3078	2851	626	6	1.00 E04	30.0
18	2898	3340	3119	685	7	1.03 E04	29.5
20	3193	3675	3434	754	7	9.62 E03	34.5
22	3496	4052	3774	828	8	9.24 E03	37.0
24	3885	4557	4221	926	11	1.15 E04	49.0
26	4657	5491	5074	1114	14	1.26 E04	94.0
28	5682	6831	6256	1373	17	1.26 E04	129.5
30	7039	8627	7833	1719	22	1.27 E04	173.0
32	8730	10807	9768	2144	25	1.17 E04	212.5
34	10667	13265	11966	2627	27	1.03 E04	241.5
36	12788	15881	14335	3147	28	9.06 E04	260.0
38	15095	18553	16824	3693	30	8.13 E03	273.0
40	15573	21253	19413	4261	30		

SERIAL 279;MIX 6LD;TEMP 77; GAGE LENGTH (In.) 4.4542;REMKS

TIME (Sec.)	LVDT DISPLACEMENT (Microinches) L	R	Ave.	STRAIN (MII)	STRESS (PSI)	STIFF-NESS (PSI)	STRAIN RATE ($\dot{\varepsilon}$) (MII/Sec)
2	20	63	42	9	6	6.56 E05	4.5
4	497	731	614	138	17	1.21 E05	64.5
6	1478	1950	1714	385	25	6.61 E04	123.5
8	2871	3711	3291	739	32	4.33 E04	177.0
10	4445	5578	5011	1125	37	3.28 E04	193.0
12	6208	7804	7006	1573	40	2.52 E04	224.0
14	8143	10139	9141	2052	44	2.12 E04	239.5
16	10321	12698	11510	2584	44	1.72 E04	266.0
18	12554	15362	13958	3134	46	1.47 E04	275.0
19					46		
22					46		
27					45		

SERIAL 280;MIX 6LD;TEMP 77; GAGE LENGTH (In.) 4.5338; REMKS

TIME (Sec.)	LVDT DISPLACEMENT (Microinches) L	R	Ave.	STRAIN (MII)	STRESS (PSI)	STIFF-NESS (PSI)	STRAIN RATE ($\dot{\varepsilon}$) (MII/Sec)
2	14	32	23	5	5	1.00 E06	2.5
4	198	385	291	64	15	2.37 E05	29.5
6	595	1035	815	180	27	1.48 E05	58.0
8	1191	2058	1624	358	36	1.00 E05	89.0
10	1982	3536	2759	609	46	7.50 E04	125.5
12	2894	5255	4074	899	53	5.95 E04	145.0
14	3905	7219	5562	1227	60	4.93 E04	164.0
16	5007	9481	7244	1598	66	4.14 E04	185.5
18	6157	12016	9087	2004	71	3.52 E04	203.0
20	7367	14849	11108	2450	75	3.04 E04	223.0
22	8667	17879	13273	2928	76	2.58 E04	239.0
24	9994	21140	15567	3434	78	2.26 E04	253.0
26					77		
28					76		
30					74		

SERIAL 281;MIX 6LD;TEMP 77; GAGE LENGTH (In.) 4.5000;REMKS

TIME (Sec.)	LVDT DISPLACEMENT (Microinches) L	R	Ave.	STRAIN (MII)	STRESS (PSI)	STIFF-NESS (PSI)	STRAIN RATE ($\dot{\varepsilon}$) (MII/Sec)
2	10	4	7	2	-	1.53 E04	1.0
4	12	8	10	2	1	3.48 E05	0
6	103	276	189	42	9	2.04 E05	20.0
8	514	1310	912	203	18	8.74 E04	80.5
10	1179	2926	2052	456	25	5.57 E04	126.5
12	2097	5076	3587	797	32	4.07 E04	170.5
14	3248	7604	5426	1206	39	3.21 E04	204.5
16	4588	10458	7523	1672	43	2.55 E04	233.0
18	6010	13693	9851	2189	45	2.07 E04	258.5
20	7411	17239	12325	2739	48	1.77 E04	275.0
22	8786	21013	14900	3311	50	1.50 E04	286.0
24	10117	25124	17621	3916	50	1.27 E04	302.5
25	10770	27285	19027	4228	50	1.19 E04	156.0
28					50		
31					49		

SERIAL 282;MIX 6LD;TEMP 77; GAGE LENGTH (In.) 4.4562;REMKS

TIME (Sec.)	LVDT DISPLACEMENT (Microinches) L	R	Ave.	STRAIN (MII)	STRESS (PSI)	STIFF-NESS (PSI)	STRAIN RATE ($\dot{\varepsilon}$) (MII/Sec)
2	·16	12	14	3	1	2.31 E05	1.5
4	18	32	25	6	2	2.77 E05	1.5
6	30	65	48	11	4	3.53 E05	2.5
8	44	163	104	23	5	2.04 E05	6.0
10	131	438	285	64	10	1.54 E05	20.5
12	615	890	752	169	10	6.03 E04	52.5
14	855	1300	1078	242	14	5.63 E04	36.5
16	1276	1738	1507	338	16	4.84 E04	48.0
18	1761	2280	2020	453	15	3.40 E04	57.5
20	2257	2926	2591	581	20	3.49 E04	64.0
22	3132	3691	3412	766	23	3.01 E04	92.5
24	3943	4650	4297	964	27	2.78 E04	99.0
26	4829	5604	5216	1171	29	2.50 E04	103.5
28	5967	6866	6417	1440	33	2.32 E04	134.5
30	7385	8482	7933	1780	36	2.01 E04	170.0
32	8988	10133	9561	2145	39	1.83 E04	182.5
34	10285	12078	11181	2509	42	1.67 E04	182.0
36	12093	14357	13225	2968	45	1.51 E04	229.5
38	14003	16920	15462	3470	46	1.33 E04	251.0
40	16062	19772	17917	4021	47	1.18 E04	275.5
41	17170	21265	19218	4312	48	1.11 E04	145.5
43					47		
45					47		
48					46		

SERIAL 283;MIX 12LD;TEMP 77;GAGE LENGTH (In.) 4.4805;REMKS

TIME (Sec.)	LVDT DISPLACEMENT (Microinches) L	R	Ave.	STRAIN (MII)	STRESS (PSI)	STIFF-NESS (PSI)	STRAIN RATE ($\dot{\varepsilon}$) (MII/Sec)
2	14	22	18	4	-	6.64 E04	2.0
4	40	141	91	20	3	1.28 E05	8.0
6	712	1393	1053	235	9	3.66 E04	107.5
8	2038	3623	2831	632	12	1.93 E04	198.5
10	3694	6355	5025	1121	15	1.35 E04	244.5
12	5531	9201	7366	1644	16	9.95 E03	261.5
14	7826	11941	9883	2206	18	8.14 E03	281.0
16	9502	14714	12108	2702	18	6.56 E03	248.0
18	11761	17536	14649	3269	19	5.77 E03	283.5
20					18		
22					18		
24					18		

SERIAL 284;MIX 12LD;TEMP 77; GAGE LENGTH (In.) 4.5435;REMKS

TIME (Sec.)	LVDT DISPLACEMENT (Microinches) L	R	Ave.	STRAIN (MII)	STRESS (PSI)	STIFF-NESS (PSI)	STRAIN RATE ($\dot{\varepsilon}$) (MII/Sec)
2	552	36	294	65	6	9.92 E04	32.5
4	2546	759	1653	364	11	3.02 E04	149.5
6	5215	1847	3531	777	14	1.74 E04	206.5
8	8424	2944	5684	1251	16	1.24 E04	237.0
10	12135	3934	8034	1768	16	9.26 E03	258.5
12	16317	4737	10527	2317	17	7.41 E03	274.5
13	18557	5070	11814	2600	18	6.79 E03	283.0
14					17		
17					18		
19					16		

SERIAL 285;MIX 12LD;TEMP 77; GAGE LENGTH (In.) 4.4865; REMKS Sht 1/2

TIME (Sec.)	LVDT DISPLACEMENT (Microinches) L	R	Ave.	STRAIN (MII)	STRESS (PSI)	STIFF-NESS (PSI)	STRAIN RATE ($\dot{\varepsilon}$) (MII/Sec)
2	4	57	31	7	-	4.41 E04	3.5
4	10	151	80	18	-	2.18 E04	5.5
6	22	248	135	30	1	1.75 E04	6.0
8	18	371	194	43	1	1.79 E04	6.5
10	36	521	279	62	1	1.59 E04	9.5
12	61	682	371	83	1	1.34 E04	10.5
14	81	829	455	101	1	1.14 E04	9.0
16	101	977	539	120	1	1.05 E04	9.5
18	121	1128	625	139	1	9.09 E03	9.5
20	146	1284	715	159	1	9.06 E03	10.0
22	178	1457	817	182	2	8.54 E03	11.5
24	218	1653	936	209	2	8.51 E03	13.5
26	281	1879	1080	241	2	8.63 E03	16.0
28	366	2145	1255	280	2	8.65 E03	19.5
30	475	2458	1467	327	3	8.59 E03	23.5
32	609	2840	1725	384	4	1.00 E04	28.5
34	963	3738	2350	524	7	1.33 E04	70.0
35	1288	4355	2822	629	8	1.30 E04	105.0
38	1913	5465	3689	822	8	9.65 E03	64.3
39	2164	6010	4087	911	9	9.81 E03	89.0
41	2880	7556	5218	1163	11	9.76 E03	84.0
43	3775	9419	6597	1470	13	8.80 E03	102.3
44	4255	10442	7348	1638	14	8.34 E03	168.0
46	5199	12335	8767	1954	13	6.89 E03	158.0
48	6123	14323	10223	2279	14	6.24 E03	162.5
50	7110	16440	11775	2625	15	5.63 E03	173.0
52	8157	18680	13419	2991	15	5.11 E03	183.0

SERIAL 285;MIX____;TEMP____;GAGE LENGTH (In.)______;REMKS Sht 2/2

TIME (Sec.)	LVDT DISPLACEMENT (Microinches)			STRAIN (MII)	STRESS (PSI)	STIFF-NESS (PSI)	STRAIN RATE ($\dot{\varepsilon}$) (MII/Sec)
		R	Ave.				
54	9245	21009	15127	3372	16	4.60 E03	190.5
56	10396	23439	16918	3771	16	4.20 E03	199.5
58	11603	25975	18789	4188	16	3.81 E03	208.5
60	12871	28583	20727	4620	16	3.50 E03	216.0
61	13548	29923	21736	4845	16	3.34 E03	
64							
67					16		
70					16		

SERIAL 286;MIX 12LD;TEMP 77;GAGE LENGTH (In.) 4.4968;REMKS

TIME (Sec.)	LVDT DISPLACEMENT (Microinches) L	R	Ave.	STRAIN (MII)	STRESS (PSI)	STIFF-NESS (PSI)	STRAIN RATE ($\dot{\varepsilon}$) (MII/Sec)
2	4	6	5	1	-	7.16 E04	0.5
4	32	121	77	17	3	1.68 E05	8.0
6	506	934	720	160	9	5.58 E04	71.5
8	1624	2456	2040	454	13	2.96 E04	147.0
10	3153	4355	3754	835	17	2.00 E04	190.5
12	4958	6472	5715	1271	19	1.47 E04	218.0
14	6978	8745	7862	1748	20	1.14 E04	238.5
16	9122	11170	10146	2256	21	9.10 E03	254.0
17	10222	12416	11319	2517	21	8.27 E03	130.5
18					21		
20					20		
22					20		

SERIAL 287;MIX 8LF;TEMP 77;GAGE LENGTH (In.) 4.5890;REMKS

TIME (Sec.)	LVDT DISPLACEMENT (icroinches) L	R	Ave.	STRAIN (MII)	STRESS (PSI)	STIFF-NESS (PSI)	STRAIN RATE ($\dot{\varepsilon}$) (MII/Sec)
2	32	6	19	4	-	1.33 E04	2.0
4	6	28	17	4	-	6.59 E04	0
6	20	67	44	10	1	1.25 E05	3.0
8	182	513	348	76	5	6.31 E04	33.0
10	566	1459	1013	221	7	3.39 E04	72.5
12	1149	2803	1976	431	10	2.32 E04	105.0
14	1856	4533	3195	696	12	1.73 E04	132.5
16	2657	6587	4622	1007	14	1.41 E04	155.5
18	3320	8099	5710	1244	7	5.63 E03	118.5
20	3300	8270	5785	1261	6	4.49 E03	8.5
22	3328	8627	5977	1303	7	5.27 E03	21.0
24	3478	9445	6462	1408	8	6.01 E03	52.5
26	3676	10317	6997	1525	8	5.43 E03	58.5
28	3893	11505	7699	1678	12	7.16 E03	76.5
30	4511	13679	9095	1982	16	8.21 E03	152.0
32	5409	16448	10929	2382	19	8.11 E03	200.0
34	6459	19535	12997	2832	22	7.61 E03	225.0
36	7599	22793	15196	3311	23	7.01 E03	239.5
38	8849	26189	17519	3818	25	6.44 E03	253.5
40	10173	29664	19919	4340	25	5.77 E03	261.0
42					23		
45					24		
47					24		

SERIAL 288;MIX 8LF;TEMP 77;GAGE LENGTH (In.) 4.6158;REMKS

TIME (Sec.)	LVDT DISPLACEMENT (Microinches) L	R	Ave.	STRAIN (MII)	STRESS (PSI)	STIFF-NESS (PSI)	STRAIN RATE ($\dot{\varepsilon}$) (MII/Sec)
2	8	28	18	4	1	2.23 E05	2.0
4	224	468	346	75	4	5.36 E04	35.5
6	609	1154	881	191	5	2.80 E04	58.0
8	1064	2050	1557	337	8	2.34 E04	73.0
10	1678	3223	2451	531	9	1.78 E04	97.0
12	2376	4692	3534	766	12	1.55 E04	117.5
14	3288	6456	4872	1056	13	1.22 E04	145.0
16	4091	7968	6030	1306	13	1.03 E04	125.0
18	4881	9511	7196	1559	14	9.30 E03	126.5
20	5723	11126	8424	1825	15	8.06 E03	133.0
22	6574	12757	9666	2094	16	7.55 E03	134.5
24	7553	14508	11030	2390	17	7.06 E03	148.0
26	8590	16375	12483	2704	18	6.53 E03	157.0
28	9696	18373	14035	3041	19	6.16 E03	168.5
30	10908	20534	15721	3406	20	5.85 E03	182.5
32	12252	22894	17573	3807	21	5.55 E03	200.5
34	13710	25447	19579	4242	22	5.25 E03	217.5
36	15259	28187	21723	4706	24	5.00 E03	232.0
38	16853	31081	23967	5192	24	4.66 E03	243.0
40	18481	34183	26332	5705	25	4.37 E03	256.5
42	20179	37410	28795	6238	26	4.09 E03	266.5
44	21932	40829	31381	6799	26	3.82 E03	284.0
46					26		
48					26		

SERIAL 289;MIX 8LF;TEMP 77; GAGE LENGTH (In.) 4.5790; REMKS

TIME (Sec.)	LVDT DISPLACEMENT (Microinches) L	R	Ave.	STRAIN (MII)	STRESS (PSI)	STIFF-NESS (PSI)	STRAIN RATE ($\dot{\varepsilon}$) (MII/Sec)
2	26	14	20	4	-	1.45 E04	2.0
4	174	262	218	48	6	1.28 E04	22.0
6	1524	1334	1429	312	13	4.15 E04	132.0
8	3749	2753	3251	710	18	2.47 E04	199.0
10	6392	4341	5367	1172	21	1.79 E04	231.0
12	9225	6032	7628	1666	23	1.41 E04	247.0
14	12177	7804	9991	2182	25	1.15 E04	258.0
16	15235	9612	12423	2713	26	9.70 E03	265.5
18	18436	11465	14951	3265	27	8.42 E03	276.0
20	21629	13328	17479	3817	28	7.32 E03	276.0
23	26523	16218	21370	4667	29	6.26 E03	283.3
25	29801	18236	24018	5245	29	5.61 E03	289.0
27					29		
29					29		
32					29		

SERIAL 290;MIX 8LF;TEMP 77; GAGE LENGTH (In.) 4.5760; REMKS

TIME (Sec.)	LVDT DISPLACEMENT (Microinches) L	R	Ave.	STRAIN (MII)	STRESS (PSI)	STIFF-NESS (PSI)	STRAIN RATE ($\dot{\varepsilon}$) (MII/Sec)
2	18	2	10	2	-	7.58 E04	1.0
4	154	30	92	20	5	2.64 E05	9.0
6	1432	698	1065	233	13	5.40 E04	106.5
8	3539	1869	2704	591	18	2.99 E04	179.0
10	6089	3249	4669	1020	21	2.06 E04	214.5
12	8948	4672	6810	1488	24	1.64 E04	234.0
14	12030	6198	9114	1992	27	1.34 E04	252.0
16	15247	7758	11503	2514	28	1.13 E04	261.0
18	18596	9314	13955	3050	30	9.73 E03	268.0
20	22058	10864	16461	3597	31	8.56 E03	273.5
22	25631	12407	19019	4156	31	7.54 E03	279.5
25	31012	14744	22878	4999	32	6.46 E03	281.0
27	34662	16300	25481	5568	33	5.86 E03	284.5
29	38368	17850	28109	6143	33		
31					32		

SERIAL 291;MIX 8LC;TEMP 77; GAGE LENGTH (In.) 4.4208; REMKS

TIME (Sec.)	LVDT DISPLACEMENT (Microinches) L	R	Ave.	STRAIN (MII)	STRESS (PSI)	STIFF-NESS (PSI)	STRAIN RATE ($\dot{\varepsilon}$) (MII/Sec)
2	18	6	12	3	-	1.78 E05	1.5
4	220	54	137	31	7	2.30 E05	14.0
6	1393	953	1173	265	14	5.43 E04	117.0
8	3128	2464	2796	632	20	3.18 E04	183.5
10	5296	4143	4719	1068	24	2.29 E04	218.0
12	7781	5947	6864	1553	28	1.78 E04	242.5
14	10537	7840	9189	2078	30	1.42 E04	262.5
16	13524	9741	11632	2631	31	1.16 E04	276.5
18	16768	11655	14212	3215	31	9.61 E03	292.0
19	18501	12613	15557	3519	31	8.83 E03	304.0
21					31		
23					31		
25					30		

SERIAL 292;MIX 8LC;TEMP 77; GAGE LENGTH (In.) 4.5152; REMKS

TIME (Sec.)	LVDT DISPLACEMENT (Microinches) L	R	Ave.	STRAIN (MII)	STRESS (PSI)	STIFF-NESS (PSI)	STRAIN RATE ($\dot{\varepsilon}$) (MII/Sec)
2	-2	14	6	1	-	3.03 E04	0.5
4	6	38	22	5	-	7.40 E04	2.0
6	2	91	47	10	1	1.17 E05	2.5
8	6	244	125	28	2	6.66 E04	9.0
10	16	458	237	52	3	5.82 E04	12.0
12	42	696	369	82	3	4.26 E04	15.0
14	71	969	520	115	4	3.89 E04	16.5
16	140	1328	734	163	5	3.31 E04	24.0
18	451	1641	1046	232	6	2.67 E04	34.5
20	908	2135	1521	337	10	2.89 E04	52.5
22	1626	2882	2254	499	13	2.53 E04	81.0
24	2580	3885	3233	716	17	2.32 E04	108.5
26	3709	5088	4398	974	19	1.93 E04	129.0
28	4938	6496	5717	1266	21	1.66 E04	146.0
30	6259	8103	7181	1590	24	1.48 E04	162.0
32	7731	9798	8764	1941	25	1.26 E04	175.5
34	9316	11550	10433	2311	26	1.14 E04	185.0
36	10964	13277	12120	2684	26	9.76 E03	186.5
38	12689	15019	13854	3068	27	8.76 E03	192.0
40	14503	16757	15630	3462	27	7.94 E03	197.0
42	16434	18500	17467	3868	27	6.97 E03	203.0
44	18454	20248	19351	4286	28	6.52 E03	209.0
49					27		
50					27		
54					27		

SERIAL 293;MIX 8LC;TEMP 77; GAGE LENGTH (In.) 4.5015; REMKS

TIME (Sec.)	LVDT DISPLACEMENT (Microinches) L	R	Ave.	STRAIN (MII)	STRESS (PSI)	STIFF-NESS (PSI)	STRAIN RATE ($\dot{\varepsilon}$) (MII/Sec)
2	6	38	22	5	2	3.14 E05	2.5
4	36	498	267	59	7	1.15 E05	27.0
6	237	1556	896	199	11	5.36 E04	24.0
8	708	2874	1791	398	15	3.77 E04	99.5
10	1405	4456	2931	651	19	2.85 E04	126.5
12	2107	5770	3939	875	16	1.81 E04	112.0
14	2639	7074	4857	1079	21	1.93 E04	102.0
16	3533	8971	6252	1389	24	1.71 E04	155.0
18	4590	11197	7894	1754	27	1.54 E04	182.5
20	5783	13651	9717	2159	30	1.37 E04	202.5
22	7102	16294	11698	2599	30	1.16 E04	220.0
24	8536	19041	13788	3063	32	1.03 E04	232.0
26	10020	21887	15954	3544	32	8.97 E03	240.5
28	11561	24930	18245	4053	32	7.78 E03	254.5
30	13148	28068	20608	4578	32	7.07 E03	262.5
32					32		
34					31		
36					30		

SERIAL 294;MIX 8LC;TEMP 77; GAGE LENGTH (In.) 4.4792;REMKS

TIME (Sec.)	LVDT DISPLACEMENT (Microinches) L	R	Ave.	STRAIN (MII)	STRESS (PSI)	STIFF-NESS (PSI)	STRAIN RATE ($\dot{\varepsilon}$) (MII/Sec)
2	6	0	3	1	-	5.29 E04	0.5
4	59	71	65	15	2	1.70 E05	7.0
6	479	373	426	95	6	6.21 E04	40.0
8	1076	864	970	217	10	4.69 E04	61.0
10	2075	1697	1886	421	14	3.38 E04	102.0
12	3371	2755	3063	684	18	2.60 E04	131.5
14	4837	3958	4398	982	21	2.11 E04	149.0
16	6649	5352	6000	1340	24	1.79 E04	179.0
18	8693	6805	7749	1730	26	1.53 E04	195.0
20	11005	8262	9633	2151	27	1.26 E04	210.5
22	13538	9655	11597	2589	29	1.12 E04	219.0
24	16240	10997	13619	3040	29	9.61 E03	225.5
26	19152	12331	15742	3514	29	8.36 E03	237.0
28	22209	13669	17939	4005	30	7.57 E03	245.5
30					29		
32					29		
34					29		

SERIAL 295;MIX 6HD;TEMP 77; GAGE LENGTH (In.) 4.6670;REMKS

TIME (Sec.)	LVDT DISPLACEMENT (Microinches) L	R	Ave.	STRAIN (MII)	STRESS (PSI)	STIFF-NESS (PSI)	STRAIN RATE ($\dot{\varepsilon}$) (MII/Sec)
2	-4	4	0	0	-	-	0
4	77	83	80	17	2	8.91 E04	8.5
6	235	262	248	53	4	7.58 E04	18.0
8	556	565	561	120	6	4.76 E04	33.5
10	1033	1136	1085	232	10	4.13 E04	56.0
12	1565	1742	1654	354	11	3.02 E04	61.0
14	2164	2628	2396	513	15	2.84 E04	79.5
16	2932	3740	3336	715	18	2.49 E04	101.0
18	3903	5152	4527	970	22	2.29 E04	127.5
20	5043	6942	5992	1284	26	2.00 E04	157.0
22	6164	8327	7245	1552	25	1.61 E04	134.0
24	7260	9800	8530	1828	26	1.40 E04	138.0
26	8380	11263	9821	2104	28	1.32 E04	138.0
28	9686	12944	11315	2424	30	1.24 E04	160.0
30	11100	16820	13960	2991	31	1.03 E04	283.5
32	12634	16438	14536	3115	32	1.02 E04	62.0
34	14452	18325	16389	3512	34	9.57 E03	198.5
36	16377	20345	18361	3934	35	9.02 E03	211.0
38	18392	22540	20466	4385	36	8.22 E03	225.5
40	20424	24861	22642	4852	36	7.38 E03	233.5
42	22485	27307	24882	5332	36	6.70 E03	240.0
44	24454	29848	27151	5818	36	6.21 E03	243.0
45	25434	31134	28286	6061	36	5.96 E03	121.5

SERIAL 296;MIX 6HD;TEMP 77; GAGE LENGTH (In.) 4.6142; REMKS

TIME (Sec.)	LVDT DISPLACEMENT (Microinches) L	R	Ave.	STRAIN (MII)	STRESS (PSI)	STIFF-NESS (PSI)	STRAIN RATE ($\dot{\varepsilon}$) (MII/Sec)
2	6	10	8	2	-	2.30 E04	1.0
4	6	22	14	3	-	1.17 E04	0.5
6	14	63	39	8	2	1.79 E05	2.5
8	89	416	253	55	6	1.06 E05	23.5
10	528	1267	897	194	12	6.21 E04	69.5
12	1225	2545	1885	409	18	4.37 E04	107.5
14	2052	4046	3049	661	22	3.37 E04	126.0
16	3072	5715	4393	952	26	2.71 E04	145.5
18	4214	7497	5855	1269	29	2.25 E04	158.5
20	5456	9368	7412	1606	30	1.89 E04	168.5
22	6807	11356	9081	1968	32	1.65 E04	181.0
24	8240	13481	10861	2354	34	1.46 E04	193.0
26	9718	15715	12717	2756	36	1.31 E04	201.0
28	11221	18030	14626	3170	37	1.15 E04	207.0
30	12709	20429	16569	3591	37	1.02 E04	210.5
33	14901	24280	19591	4246	37	8.80 E03	218.3
35							
37							

SERIAL 297;MIX 6HD;TEMP 77: GAGE LENGTH (In.) 4.7455;REMKS

TIME (Sec.)	LVDT DISPLACEMENT (Microinches) L	R	Ave.	STRAIN (MII)	STRESS (PSI)	STIFF-NESS (PSI)	STRAIN RATE ($\dot{\varepsilon}$) (MII/Sec)
5	26	20	23	5	-	5.71 E04	1.0
10	127	149	138	30	2	4.59 E04	5.0
15	532	612	572	123	7	5.31 E04	18.6
20	1832	1929	1880	403	12	3.06 E04	56.0
25	3355	3298	3327	714	16	2.18 E04	62.2
30	5090	4791	4940	1060	19	1.78 E04	69.2
35	7233	6093	6663	1430	20	1.43 E04	74.0
40	9644	8339	8991	1929	24	1.25 E04	99.8
45	12291	10444	11367	2439	26	1.05 E04	102.0
50	15180	12805	13993	3002	27	9.00 E03	112.6
55	18396	15431	16913	3629	28	7.77 E03	125.4
60	22784	18199	20492	4397	30	6.93 E03	153.6
63	25186	20736	22961	4926	31	6.25 E03	176.3
65	26874	20022	24448	5246	31	5.86 E03	160.0
68	29548	23998	26773	5744	31	5.43 E03	166.0
73					31		
76					31		
79					30		

SERIAL 298;MIX 6HD;TEMP 77; GAGE LENGTH (In.) 4.6608;REMKS

TIME (Sec.)	LVDT DISPLACEMENT (Microinches) L	R	Ave.	STRAIN (MII)	STRESS (PSI)	STIFF-NESS (PSI)	STRAIN RATE ($\dot{\varepsilon}$) (MII/Sec)
2	51	178	114	24	5	2.06 E05	12.0
4	568	892	730	154	10	6.59 E04	65.0
6	1019	1861	1440	303	16	5.17 E04	74.5
8	1830	3118	2474	521	21	3.95 E04	109.0
10	2981	4686	3833	808	24	2.98 E04	143.5
12	3931	6244	5087	1072	27	2.47 E04	132.0
14	5096	7959	6527	1375	30	2.15 E04	151.5
16	6388	9939	8163	1720	32	1.88 E04	172.5
18	7632	11891	9761	2057	34	1.66 E04	168.5
20	8922	13925	11423	2407	35	1.44 E04	175.0
22	10291	16155	13223	2786	35	1.27 E04	189.5
24	11577	18436	15007	3162	37	1.17 E04	188.0
26	12841	20841	16841	3549	38	1.06 E04	193.5
29					38		
34					37		
39					36		

SERIAL 299;MIX 12HD;TEMP 77; GAGE LENGTH (In.) 4.5012; REMKS

TIME (Sec.)	LVDT DISPLACEMENT (Microinches) L	R	Ave.	STRAIN (MII)	STRESS (PSI)	STIFF-NESS (PSI)	STRAIN RATE ($\dot{\varepsilon}$) (MII/Sec)
2	12	8	10	2	-	4.82 E04	1.0
4	408	248	328	73	5	6.56 E04	35.5
6	1877	864	1370	304	9	2.81 E04	115.5
8	3737	1602	2669	593	11	1.82 E04	144.5
10	5783	2400	4092	909	12	1.36 E04	158.0
12	7977	3237	5607	1246	15	1.17 E04	168.5
14	10305	4097	7201	1600	16	1.01 E04	177.0
16	12705	4942	8823	1960	16	8.38 E03	180.0
18	15099	5727	10413	2313	17	7.13 E03	176.5
20	17668	6529	12098	2688	17	6.41 E03	187.5
22	20339	7310	13825	3071	18	5.86 E03	191.5
24	23089	8058	15573	3460	18	5.30 E03	194.5
27					18		
29					18		
32					17		

SERIAL 300;MIX 12HD;TEMP 77; GAGE LENGTH (In.) 4.4918;REMKS

TIME (Sec.)	LVDT DISPLACEMENT (Microinches) L	R	Ave.	STRAIN (MII)	STRESS (PSI)	STIFF-NESS (PSI)	STRAIN RATE ($\dot{\varepsilon}$) (MII/Sec)
2	6	20	13	3	-	4.14 E03	1.5
4	6	42	24	5	-	1.50 E04	1.0
6	10	65	38	8	-	4.59 E04	1.5
8	42	153	98	22	1	2.80 E04	7.0
10	83	264	173	39	1	2.34 E04	8.5
12	154	396	275	61	1	2.05 E04	11.0
14	269	573	421	94	2	1.80 E04	16.5
16	568	838	703	157	3	1.68 E04	31.5
18	706	1219	962	214	4	1.81 E04	28.5
20	1039	1719	1379	307	5	1.77 E04	46.5
22	1541	2511	2026	451	8	1.73 E04	72.0
24	2295	3651	2973	662	10	1.48 E04	105.5
26	3181	5003	4092	911	11	1.23 E04	124.5
28	4071	6643	5307	1181	12	1.05 E04	135.0
30	4926	8297	6612	1472	13	9.11 E03	145.5
32	5717	10105	7911	1761	15	8.33 E03	144.5
34	6538	12081	9310	2073	16	7.60 E03	156.0
36	7353	14147	10750	2393	16	6.78 E03	160.0
38	8182	16220	12201	2716	16	6.01 E03	161.5
40	9063	18385	13724	3055	16	5.35 E03	169.5
42	9959	20664	15312	3409	16	4.74 E03	177.0
44	10918	22890	16904	3763	16	4.31 E03	177.0
46	11927	25190	18558	4132	17	4.06 E03	184.5
48	12940	27533	20236	4505	17	3.83 E03	186.5
49	13451	28718	21085	4694	17	3.70 E03	144.0
52							
54							

SERIAL 301;MIX 12HD;TEMP 77; GAGE LENGTH (In.) 4.5802;REMKS ______

TIME (Sec.)	LVDT DISPLACEMENT (Microinches) L	R	Ave.	STRAIN (MII)	STRESS (PSI)	STIFF-NESS (PSI)	STRAIN RATE ($\dot{\varepsilon}$) (MII/Sec)
2	55	93	74	16	2	1.24 E05	8.0
4	675	706	691	151	6	4.03 E04	67.5
6	1703	1586	1644	359	9	2.60 E04	104.0
8	2902	2591	2746	600	12	2.05 E04	120.5
10	4287	3703	3995	872	14	1.61 E04	136.0
12	5779	4844	5312	1160	15	1.33 E04	144.0
14	7379	6099	6739	1471	16	1.11 E04	155.5
16	9067	7400	8233	1798	17	9.47 E03	163.5
18	10839	8702	9770	2133	18	8.45 E03	167.5
20	12685	9998	11342	2476	19	7.71 E03	171.5
22	14576	11306	12941	2825	20	6.90 E03	174.5
23	15530	11965	13747	3001	20	6.53 E03	176.0
24					20		
26					19		
34					18		

SERIAL 302;MIX 12HD;TEMP 77; GAGE LENGTH (In.) 4.5570;REMKS

TIME (Sec.)	LVDT DISPLACEMENT (Microinches) L	R	Ave.	STRAIN (MII)	STRESS (PSI)	STIFF-NESS (PSI)	STRAIN RATE ($\dot{\varepsilon}$) (MII/Sec)
2	0	14	7	2	-	2.35 E04	1.0
4	16	52	34	7	-	9.64 E03	2.5
6	26	83	55	12	-	1.79 E04	2.5
8	59	157	108	24	1	3.52 E04	26.5
10	324	593	458	101	4	4.29 E04	38.5
12	1213	1540	1377	302	8	2.54 E04	100.5
14	2358	2716	2537	557	10	1.79 E04	127.5
16	3610	4083	3846	844	12	1.38 E04	143.5
18	4294	5633	5279	1158	13	1.12 E04	157.0
20	6212	7364	6788	1490	14	9.30 E03	166.0
22	7454	9251	8352	1833	15	8.21 E03	171.5
24	8651	11326	9989	2192	16	7.47 E03	179.5
26	9775	13528	11652	2557	17	6.71 E03	182.5
28	10819	15854	13336	2927	17	5.89 E03	185.0
30	11795	18288	15041	3301	17	5.21 E03	187.0
32	12703	20861	16782	3683	17	4.62 E03	191.0
34	13548	23576	18562	4073	17	4.12 E03	195.0
36	14295	26385	20340	4463	17	3.83 E03	195.0
38	14966	29299	22132	4857	18	3.61 E03	197.0
40					17		
42					17		

SERIAL 303;MIX 6LD;TEMP -17.5;GAGE LENGTH (In.) 4.6580;REMKS

TIME (Sec.)	LVDT DISPLACEMENT (Microinches) L	R	Ave.	STRAIN (MII)	STRESS (PSI)	STIFF-NESS (PSI)	STRAIN RATE ($\dot{\varepsilon}$) (MII/Sec)
5	4	4	4	1	-1	-	0.2
10	12	12	12	3	3	1.01 E06	0.4
15	18	18	18	4	7	1.90 E06	0.2
20	16	28	22	5	13	2.86 E06	0.2
25	22	44	33	7	22	3.14 E06	0.4
30	28	54	41	9	32	3.69 E06	0.4
35	28	71	50	11	47	4.40 E06	0.4
40	42	105	74	16	93	5.87 E06	1.0
45	93	192	143	31	160	5.24 E06	3.0
47					13		

SERIAL 304;MIX 6LD;TEMP -17.5 GAGE LENGTH (In.) 4.6278;REMKS

TIME (Sec.)	LVDT DISPLACEMENT (Microinches) L	R	Ave.	STRAIN (MII)	STRESS (PSI)	STIFF-NESS (PSI)	STRAIN RATE ($\dot{\varepsilon}$) (MII/Sec)
5	16	2	9	2	3	1.32 E06	0.4
10	22	8	15	3	8	2.37 E06	0.2
15	40	20	30	7	23	3.48 E06	0.8
20	57	28	42	9	20	2.19 E06	0.4
25	67	28	47	10	23	2.28 E06	0.2
30	109	75	92	20	86	4.29 E06	2.0
35	184	172	178	39	178	4.63 E06	3.8
36							

SERIAL 305;MIX 6LD;TEMP -17.5; GAGE LENGTH (In.) 4.6750;REMKS

TIME (Sec.)	LVDT DISPLACEMENT (Microinches) L	R	Ave.	STRAIN (MII)	STRESS (PSI)	STIFF-NESS (PSI)	STRAIN RATE ($\dot{\varepsilon}$) (MII/Sec)
2	4	0	2	-	-	4.60 E05	-
4	2	2	2	-	2	3.70 E06	-
6	10	4	7	2	6	3.89 E06	1.0
8	16	6	11	2	17	7.20 E06	0
10	20	16	18	4	33	8.49 E06	1.0
12	34	18	26	6	51	9.12 E06	1.0
14	47	30	38	8	72	8.82 E06	1.0
16	69	46	57	12	95	7.76 E06	2.0
18	95	63	79	17	119	7.04 E06	2.5
20	127	87	107	23	145	6.30 E06	3.0
22	154	99	126	27	170	6.30 E06	2.0
24	196	139	167	36	196	5.47 E06	4.5
25	220	159	189	41	209	5.14 E06	5.0

SERIAL 306;MIX 6LD;TEMP -17.5;GAGE LENGTH (In.) 4.7245;REMKS see note

TIME (Sec.)	LVDT DISPLACEMENT (Microinches) L	R	Ave.	STRAIN (MII)	STRESS (PSI)	STIFF-NESS (PSI)	STRAIN RATE ($\dot{\varepsilon}$) (MII/Sec)
2	-2	4	1	-	5	2.36 E07	-
4	2	-2	0	-	22	5.13 E09	-
6	0	-2	-1	-	43	-	-
8	4	4	4	1	67	7.88 E07	0.5
10	2	2	2	-	93	2.19 E08	-0.5
12	8	8	8	2	122	7.18 E07	1.0
14	4	12	8	2	152	9.00 E07	0
16	2	14	8	2	183	1.09 E08	0
17	-2	20	9	2	198	1.05 E08	0

Note: LVDT cores may have frozen into housing and thus not responding. However, when E178 is run with 303-304-305-306, this specimen is not significant as an outliner at the 5% or 1% level.

304 sawed and

SERIAL 304A;MIX 6LD;TEMP -17.5;GAGE LENGTH (In.) 2.6110;REMKS retested

TIME (Sec.)	LVDT DISPLACEMENT (Microinches) L	R	Ave.	STRAIN (MII)	STRESS (PSI)	STIFF-NESS (PSI)	STRAIN RATE ($\dot{\varepsilon}$) (MII/Sec)
2	0	6	3	1	21	1.82 E07	0.5
4	0	4	2	1	43	5.65 E07	0
6	-2	18	8	3	67	2.20 E07	1.0
8	-4	26	11	4	90	2.17 E07	0.5
10	8	38	23	9	116	1.33 E07	2.5
12	47	61	54	21	142	6.88 E06	6.0
14	77	95	86	33	167	5.08 E06	6.0
16	109	133	121	46	194	4.20 E06	6.5
18	162	180	171	66	220	3.36 E06	10.0
19					-		

305 sawed

SERIAL 305A;MIX 6LD;TEMP -17.5;GAGE LENGTH (In.) 2.7232;REMKS & retested

TIME (Sec.)	LVDT DISPLACEMENT (Microinches) L	R	Ave.	STRAIN (MII)	STRESS (PSI)	STIFF-NESS (PSI)	STRAIN RATE ($\dot{\varepsilon}$) (MII/Sec)
10	26	4	15	6	-	6.59 E04	0.6
20	10	6	8	3	1	2.27 E05	-0.3
30	34	42	38	14	2	1.36 E05	1.1
40	81	105	93	34	12	3.43 E05	2.0
50	65	153	109	40	23	5.81 E05	0.6
60	111	200	156	57	39	6.34 E05	1.7
70	57	244	150	55	69	1.26 E06	-0.2
80	97	329	213	78	138	1.76 E06	2.3
90	156	474	315	116	236	2.04 E06	3.8
94	198	571	385	141	279	1.97 E06	6.2
95							

SERIAL 306A; MIX 6LD; TEMP -17.5; GAGE LENGTH (In.) 2.6172; REMKS 306 sawed and retested.

TIME (Sec.)	LVDT DISPLACEMENT (Microinches) L	R	Ave.	STRAIN (MII)	STRESS (PSI)	STIFF-NESS (PSI)	STRAIN RATE ($\dot{\varepsilon}$) (MII/Sec)
2	0	6	3	1	-	3.50 E04	0.5
4	-4	12	4	1	3	1.81 E06	0
6	6	14	10	4	17	4.44 E06	1.5
8	20	18	19	7	36	4.93 E06	1.5
10	38	26	32	12	57	4.65 E06	2.5
12	59	30	44	17	80	4.72 E06	2.5
14	65	36	50	19	105	5.46 E06	1.0
16	85	42	63	24	131	5.41 E06	2.5
18	99	50	74	28	158	5.56 E06	2.0
20	109	52	80	31	186	6.04 E06	1.5
22	121	61	91	35	213	6.11 E06	2.0
24	121	69	95	36	242	6.63 E06	0.5
26	113	79	96	37	268	7.29 E06	0.5
27					-		

SERIAL 307;MIX 12LD ;TEMP -17.5;GAGE LENGTH (In.) 4.5815;REMKS

TIME (Sec.)	LVDT DISPLACEMENT (Microinches) L	R	Ave.	STRAIN (MII)	STRESS (PSI)	STIFF-NESS (PSI)	STRAIN RATE ($\dot{\varepsilon}$) (MII/Sec)
2	8	2	5	-	15	3.77 E07	0
4	10	6	8	2	23	1.30 E07	1.0
6	0	10	5	1	36	3.36 E07	-0.5
10	47	12	29	6	72	1.13 E07	1.25
12	71	22	46	10	95	9.44 E06	2.0
14	89	30	59	13	121	9.33 E06	1.5
16	115	44	79	17	148	8.51 E06	2.0
18	150	36	93	20	177	8.76 E06	1.5
20	190	103	147	32	169	5.27 E06	6.0
22	235	151	193	42	241	5.74 E06	5.0
24	283	210	247	54	274	5.08 E06	6.0
25	315	246	281	61	289	4.73 E06	7.0

SERIAL 308;MIX 12LD;TEMP -17.5; GAGE LENGTH (In.) 4.5520;REMKS

TIME (Sec.)	LVDT DISPLACEMENT (Microinches) L	R	Ave.	STRAIN (MII)	STRESS (PSI)	STIFF-NESS (PSI)	STRAIN RATE ($\dot{\varepsilon}$) (MII/Sec)
2	6	-2	2	-	19	4.33 E07	0
4	6	-8	-1	-	43	-	0
6	16	-8	4	1	70	7.72 E07	0.5
8	30	-8	11	2	101	4.09 E07	0.5
10	42	-4	19	4	132	3.12 E07	1.0
12	61	-2	29	6	171	2.66 E07	1.0
14	95	10	52	12	209	1.81 E07	3.0
16	123	22	73	16	248	1.55 E07	2.0
17					0		

SERIAL 309;MIX 12LD;TEMP -17.5;GAGE LENGTH (In.) 4.5540;REMKS

TIME (Sec.)	LVDT DISPLACEMENT (Microinches) L	R	Ave.	STRAIN (MII)	STRESS (PSI)	STIFF-NESS (PSI)	STRAIN RATE ($\dot{\varepsilon}$) (MII/Sec)
2	0	8	4	1	6	7.12 E06	0.5
4	16	14	15	3	27	8.32 E06	1.0
6	30	32	31	7	58	8.52 E06	2.0
8	44	56	50	11	92	8.37 E06	2.0
10	61	85	73	16	127	7.96 E06	2.5
12	87	133	110	24	165	6.83 E06	4.0
14	117	208	163	36	203	5.69 E06	6.0
15					0		

SERIAL 310;MIX 12LD;TEMP -17.5;GAGE LENGTH (In.) 4.5408;REMKS

TIME (Sec.)	LVDT DISPLACEMENT (Microinches) L	R	Ave.	STRAIN (MII)	STRESS (PSI)	STIFF-NESS (PSI)	STRAIN RATE ($\dot{\varepsilon}$) (MII/Sec)
2	6	-6	0	0	25	-	
4	10	-10	0	0	54	2.47 E09	0
6	18	-6	6	1	88	6.51 E07	0.5
8	16	-16	0	0	124	3.51 E09	0
10	30	-4	13	3	161	5.55 E07	1.5
12	42	20	31	7	200	2.92 E07	2.0
14	75	63	69	15	240	1.58 E07	4.0
15	85	91	88	19	259	1.34 E07	4.0
16					0		

SERIAL 311;MIX 8LF;TEMP 108.5;GAGE LENGTH (In.) 4.7700;REMKS

TIME (Sec.)	LVDT DISPLACEMENT (Microinches) L	R	Ave.	STRAIN (MII)	STRESS (PSI)	STIFF-NESS (PSI)	STRAIN RATE ($\dot{\varepsilon}$) (MII/Sec)
0	8827	16912	12869	2698	1.7	6.24 E02	
2	10738	17574	14156	2968	1.8	6.19 E02	135.0
4	11108	18650	14879	3119	1.9	5.94 E02	75.5
6	11625	19856	15741	3300	2.0	6.20 E02	90.5
8	12627	21862	17014	3567	2.3	6.53 E02	133.0
10	13468	25134	19301	4046	2.6	6.52 E02	239.5
12	15004	28732	21868	4585	2.6	5.78 E02	269.5
14	16349	33006	24677	5173	2.8	5.49 E02	294.0
16	18278	37921	28100	5891	2.9	4.90 E02	359.0
17	19190	40520	29855	6259	2.9	4.62 E02	368.0
18					2.9		
19					2.8		
20					2.7		

SERIAL 312;MIX 8LF;TEMP 108.5; GAGE LENGTH (In.) 4.7260;REMKS

TIME (Sec.)	LVDT DISPLACEMENT (Microinches) L	R	Ave.	STRAIN (MII)	STRESS (PSI)	STIFF-NESS (PSI)	STRAIN RATE ($\dot{\varepsilon}$) (MII/Sec)
0	50433	5287	27860	5895	1.7	2.80 E02	
2	51209	5310	28260	5980	1.7	2.80 E02	42.5
4	52050	5334	28692	6071	1.7	2.77 E02	45.5
6	52888	5350	29119	6161	1.7	2.73 E02	45.0
8	53757	5358	29557	6254	1.7	2.70 E02	46.5
10	54679	5378	30028	6354	1.7	2.71 E02	50.5
12	55585	5405	30495	6453	1.7	2.69 E02	49.5
14	56697	5461	31079	6576	1.8	2.78 E02	61.5
16	58452	5380	31916	6753	2.0	2.92 E02	88.5
18	61017	5788	33402	7068	2.1	2.97 E02	157.5
20	63955	5966	34961	7398	2.1	2.89 E02	165.0
22	67010	6141	36576	7739	2.1	2.77 E02	170.5
24					2.1		
26					2.1		
28					2.1		

SERIAL 313; MIX 8LF; TEMP 108.5; GAGE LENGTH (In.) 4.7280; REMKS

TIME (Sec.)	LVDT DISPLACEMENT (Microinches) L	R	Ave.	STRAIN (MII)	STRESS (PSI)	STIFF-NESS (PSI)	STRAIN RATE ($\dot{\varepsilon}$) (MII/Sec)
0	14883	18294	16588	3509	1.7	4.77 E02	
2	15083	18613	16848	3563	1.7	4.69 E02	27.0
4	15362	18950	17156	3629	1.7	4.65 E02	33.0
6	15989	19836	17913	3789	2.3	6.07 E02	80.0
8	18313	22214	20264	4286	2.7	6.21 E02	248.5
10	21146	24809	22977	4860	2.7	5.64 E02	287.0
12	24100	27404	25752	5447	2.8	5.10 E02	293.5
13	25643	28680	27162	5746	2.8	4.88 E02	149.5
14					2.8		
16					2.8		
18					2.7		

SERIAL 314;MIX 8LF;TEMP 108.5; GAGE LENGTH (In.) 4.7698;REMKS

TIME (Sec.)	LVDT DISPLACEMENT (Microinches) L	R	Ave.	STRAIN (MII)	STRESS (PSI)	STIFF-NESS (PSI)	STRAIN RATE ($\dot{\varepsilon}$) (MII/Sec)
0	31714	1051	16382	3435	1.7	4.84 E02	
2	32280	1047	16663	3493	1.7	4.79 E02	29.0
4	32684	1051	16867	3536	1.7	4.87 E02	21.5
6	33230	1049	17139	3593	1.7	4.85 E02	28.5
8	33916	1051	17483	3665	1.8	4.97 E02	36.0
10	35000	1074	18037	3781	2.2	5.72 E02	58.0
12	38029	1116	19572	4103	2.4	5.93 E02	161.0
14	41531	1158	21344	4475	2.6	5.90 E02	186.0
16	45153	1189	23171	4858	2.6	5.41 E02	191.5
17	47027	1197	24112	5055	2.7	5.27 E02	98.5
18					2.5		
20					2.7		
22					2.6		

SERIAL 315;MIX 8LC;TEMP -17.5; GAGE LENGTH (In.) 4.6232:REMKS

TIME (Sec.)	LVDT DISPLACEMENT (Microinches) L	R	Ave	STRAIN (MII)	STRESS (PSI)	STIFF-NESS (PSI)	STRAIN RATE ($\dot{\varepsilon}$) (MII/Sec)
2	18	10	14	3	1	2.54 E05	1.5
4	20	12	16	3	12	3.60 E06	0
6	10	6	8	2	22	1.27 E07	-0.5
8	18	10	14	3	19	6.32 E06	0.5
10	30	22	26	6	21	3.80 E06	1.5
12	34	16	25	5	24	4.42 E06	0.5
14	24	-4	10	2	33	1.51 E07	-1.5
16	8	0	4	1	53	6.08 E06	-0.5
18	24	20	22	5	80	1.69 E07	2.0
20	65	56	60	13	112	8.58 E06	4.0
22	81	71	76	16	147	8.92 E06	1.5
24	115	129	122	26	184	6.98 E06	5.0
26	160	172	166	36	223	6.21 E06	5.0
27	188	206	197	43	243	5.69 E06	3.5
28					0		

SERIAL 316;MIX 8LC;TEMP -17.5; GAGE LENGTH (In.) 4.6000;REMKS

TIME (Sec.)	LVDT DISPLACEMENT (Microinches) L	R	Ave.	STRAIN (MII)	STRESS (PSI)	STIFF-NESS (PSI)	STRAIN RATE ($\dot{\varepsilon}$) (MII/Sec)
2	0	10	5	1	13	1.20 E07	0.5
4	6	24	15	3	43	1.34 E07	1.0
6	18	48	33	7	76	1.06 E07	2.0
8	32	71	52	11	110	9.76 E06	2.0
10	65	101	83	18	146	8.10 E06	3.5
12	103	137	120	26	183	7.03 E06	4.0
14	150	180	165	36	221	6.17 E06	5.0
16	208	230	219	48	258	5.42 E06	6.0
18					0		

SERIAL 317;MIX 8LC;TEMP -17.5; GAGE LENGTH (In.) 4.6348;REMKS

TIME (Sec.)	LVDT DISPLACEMENT (Microinches) L	R	Ave.	STRAIN (MII)	STRESS (PSI)	STIFF-NESS (PSI)	STRAIN RATE ($\dot{\varepsilon}$) (MII/Sec)
2	2	6	4	1	4	4.80 E06	0.5
4	10	6	8	2	14	8.36 E06	0.5
6	10	2	6	1	28	2.16 E07	-0.5
8	18	8	13	3	48	1.71 E07	1.0
10	32	16	24	5	74	1.42 E07	1.0
12	47	32	39	8	102	1.21 E07	1.5
14	65	40	52	11	133	1.18 E07	1.5
16	93	65	79	17	166	9.71 E06	3.0
18	121	95	108	23	200	8.58 E06	3.0
20	138	127	132	29	237	8.31 E06	3.0
21	154	149	151	33	255	7.83 E06	2.0
22					0		

SERIAL 318;MIX 8LC;TEMP -17.5; GAGE LENGTH (In.) 4.5200;REMKS

TIME (Sec.)	LVDT DISPLACEMENT (Microinches) L	R	Ave.	STRAIN (MII)	STRESS (PSI)	STIFF-NESS (PSI)	STRAIN RATE ($\dot{\varepsilon}$) (MII/Sec)
2	4	-2	1	-	9	3.89 E07	-
4	10	-2	4	1	25	2.82 E07	0.5
6	12	-6	3	1	46	6.71 E07	0
8	30	-4	13	3	69	2.38 E07	1.0
10	53	12	32	7	99	1.38 E07	2.0
12	67	8	37	8	132	1.60 E07	0.5
14	91	16	53	12	167	1.41 E07	2.0
16	127	36	82	18	204	1.13 E07	3.0
18	160	57	109	24	242	1.01 E07	3.0
19	182	77	130	29	261	9.09 E06	5.0
20					2		

SERIAL 319;MIX 8LC;TEMP 108.5;GAGE LENGTH (In.) 4.5952;REMKS

TIME (Sec.)	LVDT DISPLACEMENT (Microinches) L	R	Ave.	STRAIN (MII)	STRESS (PSI)	STIFF-NESS (PSI)	STRAIN RATE ($\dot{\varepsilon}$) (MII/Sec)
50	6701	2672	4687	1020	1.7	1.63 E03	12.0
100	9211	4426	6819	1484	1.7	1.14 E03	8.6
150	11363	5836	8599	1871	1.6	8.78 E02	7.3
200	13860	7396	10628	2313	1.8	7.76 E02	8.8
202	14086	7590	10838	2359	1.9	8.22 E02	23.0
204	14471	7937	11204	2438	2.1	8.71 E02	39.5
206	15231	8607	11919	2594	2.5	9.76 E02	78.0
208	16493	9695	13094	2849	2.9	1.03 E03	127.5
210	18058	10977	14518	3159	3.1	9.91 E02	155.0
212	19593	12284	15938	3468	3.3	9.54 E02	154.5
214	21152	13754	17453	3798	3.5	9.32 E02	165.0
216					3.5		
218					3.5		
220					3.5		

SERIAL 320;MIX 8LC;TEMP 108.5; GAGE LENGTH (In.) 4.5678;REMKS

TIME (Sec.)	LVDT DISPLACEMENT (Microinches) L	R	Ave.	STRAIN (MII)	STRESS (PSI)	STIFF-NESS (PSI)	STRAIN RATE ($\dot{\varepsilon}$) (MII/Sec)
50	1078	9784	5431	1189	1.7	1.40 E03	23.8
100	1511	13818	7664	1678	1.7	9.96 E02	9.8
150	1923	17293	9608	2103	1.6	7.68 E02	8.5
166	2079	18383	10231	2240	1.8	7.98 E02	8.6
168	2156	19217	10687	2340	2.3	9.86 E02	50.0
170	2732	20664	11698	2561	2.7	1.07 E02	110.5
172	4635	22264	13449	2845	3.1	1.09 E03	142.0
174	5005	24205	14605	3197	3.3	1.03 E03	176.0
176	6333	26268	16301	3569	3.6	1.01 E03	186.0
178	7628	28510	18069	3956	3.7	9.30 E02	193.5
180	8966	30839	19903	4357	3.9	9.00 E02	200.5
182					3.8		
184					3.8		
186					3.9		

SERIAL 321;MIX 8LC;TEMP 108.5;GAGE LENGTH (In.) 4.6095;REMKS

TIME (Sec.)	LVDT DISPLACEMENT (Microinches) L	R	Ave.	STRAIN (MII)	STRESS (PSI)	STIFF-NESS (PSI)	STRAIN RATE ($\dot{\varepsilon}$) (MII/Sec)
50	11166	1150	6158	1336	1.6	1.18 E03	26.7
100	15609	1330	8470	1837	1.7	9.27 E02	10.0
102	15793	1340	8567	1858	1.7	9.29 E02	10.5
104	15981	1354	8667	1880	1.8	9.40 E02	11.0
106	16246	1417	8832	1916	2.0	1.03 E03	18.0
108	17249	1800	9524	2066	2.5	1.20 E03	75.0
110	18571	2369	10470	2271	2.9	1.29 E03	102.5
112	20464	3312	11888	2579	3.3	1.28 E03	154.0
114	22735	4321	13528	2935	3.5	1.19 E03	178.0
116	25187	5400	15294	3318	3.6	1.10 E03	191.5
118	27669	6563	17116	3713	3.7	1.01 E03	197.5
120	30094	7737	18915	4104	3.8	9.29 E02	195.5
121	31418	8375	19897	4316	3.8	8.90 E02	212.0
123					3.8		
125					3.8		

SERIAL 322; MIX 8LC; TEMP 108.5; GAGE LENGTH (In.) 4.5995; REMKS

TIME (Sec.)	LVDT DISPLACEMENT (Microinches) L	R	Ave.	STRAIN (MII)	STRESS (PSI)	STIFF-NESS (PSI)	STRAIN RATE ($\dot{\varepsilon}$) (MII/Sec)
50	36775	36219	36497	7935	1.7	2.12 E02	158.7
100	36823	39136	37980	8257	1.7	2.07 E02	6.4
106	36749	39450	38099	8283	1.7	2.05 E02	4.3
110	36743	39693	38218	8309	1.7	2.08 E02	6.5
112	36773	40978	38875	8452	2.9	3.47 E02	71.5
114	36785	43398	40091	8717	3.4	3.84 E02	132.5
116	36801	45874	41338	8987	3.5	3.87 E02	135.0
118	36828	48322	42575	9256	3.8	4.07 E02	134.5
120	36755	50946	43881	9540	3.9	4.09 E02	142.0
121	36832	52274	44553	9686	4.1	4.20 E02	146.0
122					4.0		
123					4.0		
124					4.0		

SERIAL 323;MIX 6LD;TEMP 108.5; GAGE LENGTH (In.)4.6108;REMKS

TIME (Sec.)	LVDT DISPLACEMENT (Microinches) L	R	Ave.	STRAIN (MII)	STRESS (PSI)	STIFF-NESS (PSI)	STRAIN RATE ($\dot{\varepsilon}$) (MII/Sec)
50	1252	-278	487	106	1.7	1.57 E04	2.1
100	3341	4327	3834	832	1.7	2.02 E03	14.5
140	4704	8375	6539	1418	1.8	1.28 E03	14.6
142	4815	8706	6760	1466	1.9	1.29 E03	24.0
144	4983	9098	7040	1527	2.0	1.29 E03	30.5
146	5239	9544	7392	1603	2.1	1.28 E03	38.0
148	5630	10089	7860	1705	2.2	1.29 E03	51.0
150	6186	10999	8592	1864	2.7	1.46 E03	79.5
152	7365	12870	10118	2194	3.4	1.53 E03	165.0
154	8938	15382	12160	2637	3.6	1.38 E03	221.5
156	10608	18107	14358	3114	3.8	1.23 E03	238.5
158	12084	21168	16626	3606	3.9	1.07 E03	246.0
159	12752	22724	17738	3847	3.9	1.01 E03	241.0
160					3.9		
162					3.8		
164					3.8		

SERIAL 324;MIX 6LD;TEMP 108.5;GAGE LENGTH (In.) 4.6500;REMKS

TIME (Sec.)	LVDT DISPLACEMENT (Microinches) L	R	Ave.	STRAIN (MII)	STRESS (PSI)	STIFF-NESS (PSI)	STRAIN RATE ($\dot{\varepsilon}$) (MII/Sec)
1	-1343	12600	5629	1211	1.6	1.31 E03	
50	-1001	30496	14748	3172	1.5	4.78 E02	40.0
75	-1058	37018	17980	3867	1.6	4.06 E02	27.8
85	-991	38839	18294	4070	1.6	3.86 E02	20.3
86	-983	39037	19027	4092	1.6	3.83 E02	22.0
88	-985	39773	19394	4171	2.2	5.28 E02	39.5
90	-928	42128	20560	4430	2.8	6.41 E02	129.5
92	-659	45297	22319	4800	3.2	6.69 E02	185.0
94	-368	48996	24314	5229	3.5	6.75 E02	214.5
96	382	52933	26657	5733	3.7	6.44 E02	252.0
98	2123	56540	29332	6308	3.8	6.06 E02	287.5
100	3373	60618	31995	6881	3.8	5.59 E02	286.5
102	4788	64887	34838	7492	3.9	5.17 E02	305.5
104	5294	68721	37007	7959	3.9	4.89 E02	233.5
106	6071	72467	39629	8445	4.0		
108					3.8		
110					3.8		
112					3.7		

SERIAL 325;MIX 6LD;TEMP 108.5; GAGE LENGTH (In.) 4.6400;REMKS

TIME (Sec.)	LVDT DISPLACEMENT (Microinches) L	R	Ave.	STRAIN (MII)	STRESS (PSI)	STIFF-NESS (PSI)	STRAIN RATE ($\dot{\varepsilon}$) (MII/Sec)
1	1913	1126	1519	327	1.3	3.91 E03	
50	-3753	8151	2199	474	1.3	2.72 E03	3.0
75	-3798	9893	3043	656	1.3	1.91 E03	7.3
90	-3365	10799	3717	801	1.5	1.83 E03	9.7
92	-3138	11013	3937	849	1.5	1.80 E03	24.0
94	-2928	11334	4203	906	1.6	1.78 E03	28.5
96	-2479	12024	4772	1029	1.6	1.53 E03	61.5
98	-1240	13509	6135	1322	2.8	2.12 E03	146.5
100	431	15269	7850	1692	3.1	1.84 E03	185.0
102	2366	17037	9701	2091	3.3	1.56 E03	199.5
104	4368	18884	11626	2506	3.3	1.33 E03	207.5
106	6416	20730	13573	2925	3.4	1.15 E03	209.5
108	8685	22651	15668	3377	3.4	1.00 E03	226.0
110	10782	24575	17679	3810	3.4	9.00 E02	216.5
112					3.3		
114					3.3		
116					3.2		

SERIAL 326;MIX 6LD;TEMP 108.5; GAGE LENGTH (In.) 4.6475;REMKS

TIME (Sec.)	LVDT DISPLACEMENT (Microinches) L	R	Ave.	STRAIN (MII)	STRESS (PSI)	STIFF-NESS (PSI)	STRAIN RATE ($\dot{\varepsilon}$) (MII/Sec)
50	5488	1263	3375	726	1.7	2.36 E03	14.5
100	9104	1269	5186	1116	1.7	1.54 E03	7.8
150	12297	1241	6769	1456	1.7	1.17 E03	6.8
160	13164	1235	7200	1549	1.9	1.24 E03	9.3
162	13520	1237	7379	1588	2.1	1.29 E03	19.5
164	14109	1243	7676	1652	2.4	1.46 E03	32.0
166	15492	1257	8374	1802	2.8	1.57 E03	75.0
168	17619	1271	9445	2032	3.3	1.60 E03	115.0
170	20254	1271	10762	2316	3.5	1.52 E03	142.0
172	23237	1279	12258	2637	3.7	1.42 E03	160.5
174	26399	1282	13841	2978	3.8	1.29 E03	170.5
176	29706	1286	15496	3334	3.9	1.16 E03	178.0
178	33091	1259	17175	3695	3.9	1.06 E03	180.5
180					3.9		
182					3.9		
184					3.8		

SERIAL 327;MIX 12LD ;TEMP 108.5; GAGE LENGTH (In.) 4.6410;REMKS

TIME (Sec.)	LVDT DISPLACEMENT (Microinches) L	R	Ave.	STRAIN (MII)	STRESS (PSI)	STIFF-NESS (PSI)	STRAIN RATE ($\dot{\varepsilon}$) (MII/Sec)
1	18602	8910	13756	2964	1.6	5.54 E02	-
25	5450	1350	3400	733	1.7	2.28 E03	29.3
30	5498	1968	3733	804	1.6	2.04 E03	14.2
32	5484	2293	3889	838	1.6	1.96 E03	17.0
34	5468	2733	4101	884	1.8	2.06 E03	23.0
36	5523	3610	4566	984	1.9	1.92 E03	50.0
38	5575	4556	5116	1102	2.1	1.87 E03	59.0
40	5688	6250	5969	1286	2.3	1.79 E03	92.0
42	6052	8133	7093	1528	2.5	1.60 E03	121.0
44	6643	9867	8255	1779	2.5	1.41 E03	125.5
46	7205	11836	9520	2051	2.6	1.29 E03	136.0
48	7971	14068	11019	2374	2.7	1.13 E03	161.5
50	8934	16206	12570	2709	2.8	1.03 E03	167.5
52	9789	18423	14106	3039	2.8	9.28 E02	165.0
54	10883	20561	15722	3388	2.9	8.47 E02	174.5
56	12004	22730	17367	3742	2.9	7.70 E02	177.0
58	13075	24924	19000	4094	2.9	7.11 E02	176.0
59	13573	25993	19783	4263	2.9	6.85 E02	169.0
60					2.9		
62					2.9		
64					2.9		

SERIAL 328;MIX 12LD;TEMP 108.5; GAGE LENGTH (In.) 4.6330;REMKS

TIME (Sec.)	LVDT DISPLACEMENT (Microinches) L	R	Ave.	STRAIN (MII)	STRESS (PSI)	STIFF-NESS (PSI)	STRAIN RATE ($\dot{\varepsilon}$) (MII/Sec)
50	15087	13344	14216	3068	1.6	5.21 E02	61.4
95	19560	21202	20381	4399	1.6	3.53 E02	29.6
96	19676	21404	20540	4433	1.6	3.52 E02	17.0
98	19947	21832	20889	4509	1.6	3.50 E02	38.0
100	20855	23259	22057	4761	2.1	4.33 E02	126.0
102	22565	25299	23932	5166	2.2	4.25 E02	202.5
104	24454	27507	25980	5608	2.3	4.06 E02	221.0
106	26415	29727	28071	6059	2.3	3.80 E02	225.5
107					2.3		
109					2.3		
111					2.2		

SERIAL 329;MIX 12LD;TEMP 108.5; GAGE LENGTH (In.) 4.6155;REMKS

TIME (Sec.)	LVDT DISPLACEMENT (Microinches) L	R	Ave.	STRAIN (MII)	STRESS (PSI)	STIFF-NESS (PSI)	STRAIN RATE ($\dot{\varepsilon}$) (MII/Sec)
25	5771	-1859	1956	424	1.5	3.55 E03	17.0
50	11439	787	6113	1324	1.7	1.30 E03	36.0
75	11848	4948	8398	1819	1.7	9.56 E02	19.8
76	11872	5144	8508	1843	1.8	9.54 E02	24.0
78	11959	5641	8800	1907	1.8	9.43 E02	32.0
80	12097	6290	9193	1992	1.9	9.31 E02	42.5
82	12517	7528	10023	2172	2.2	1.00 E03	90.0
84	13429	9677	11553	2503	2.3	9.08 E02	165.5
86	14333	11986	13160	2851	2.3	8.04 E02	174.0
88	14867	14595	14731	3192	2.4	7.37 E02	170.5
90	15536	17307	16421	3558	2.4	6.63 E02	183.0
92	16090	20367	18229	3949	2.4	5.99 E02	195.5
94	16547	23788	20168	4370	2.4	5.49 E02	210.5
96					2.4		
98					2.3		
100					2.3		

SERIAL 330;MIX 12LD;TEMP 108.5; GAGE LENGTH (In.) 4.7030;REMKS Never carried ram load.

TIME (Sec.)	LVDT DISPLACEMENT (Microinches) L	R	Ave.	STRAIN (MII)	STRESS (PSI)	STIFF-NESS (PSI)	STRAIN RATE ($\dot{\varepsilon}$) (MII/Sec)
25	14388	15388	14888	3166	1.6	5.14 E02	126.6
50	17852	25232	21541	4580	1.6	3.54 E02	56.6
75	23477	32042	27760	5903	1.6	2.77 E02	52.9
100	34419	37806	36113	7679	1.6	2.08 E02	71.0
125	77153	34280	55717	11847	-		

SERIAL 331;MIX 8LF;TEMP -17.5; GAGE LENGTH (In.) 4.6705;REMKS

TIME (Sec.)	LVDT DISPLACEMENT (Microinches) L	R	Ave.	STRAIN (MII)	STRESS (PSI)	STIFF-NESS (PSI)	STRAIN RATE ($\dot{\varepsilon}$) (MII/Sec)
2	12	2	7	2	23	1.53 E07	1.0
4	26	6	16	3	49	1.42 E07	0.5
6	38	22	30	6	80	1.24 E07	1.5
8	57	54	55	12	115	9.79 E06	3.0
10	95	87	91	20	153	7.82 E06	4.0
12	146	135	140	30	191	6.35 E06	5.0
13	174	165	169	36	208	5.75 E06	6.0

SERIAL 332;MIX 8LF;TEMP -17.5; GAGE LENGTH (In.) 4.5152;REMKS

TIME (Sec.)	LVDT DISPLACEMENT (Microinches) L	R	Ave.	STRAIN (MII)	STRESS (PSI)	STIFF-NESS (PSI)	STRAIN RATE ($\dot{\varepsilon}$) (MII/Sec)
2	6	2	4	1	4	4.02 E06	0.5
4	12	8	10	2	16	7.15 E06	0.5
6	18	4	11	2	29	1.18 E07	0
8	22	8	15	3	39	1.16 E07	0.5
10	30	16	23	5	52	1.01 E07	1.0
12	42	24	33	7	66	8.98 E06	1.0
14	51	36	43	10	86	9.04 E06	1.5
16	77	56	66	15	114	7.76 E06	2.5
18	105	81	93	21	144	7.00 E06	3.0
20	138	111	124	28	178	6.46 E06	3.5
22	186	157	171	38	213	5.61 E06	5.0
23	214	184	199	44	231	5.23 E06	6.0

SERIAL 333;MIX 8LF;TEMP -17.5; GAGE LENGTH (In.) 4.5738;REMKS

TIME (Sec.)	LVDT DISPLACEMENT (Microinches) L	R	Ave.	STRAIN (MII)	STRESS (PSI)	STIFF-NESS (PSI)	STRAIN RATE ($\dot{\varepsilon}$) (MII/Sec)
2	-2	6	2	-	22	-	
4	10	20	15	3	44	1.35 E07	1.5
6	12	36	24	5	71	1.35 E07	1.0
8	20	57	39	8	101	1.19 E07	1.5
10	44	81	62	14	134	9.78 E06	3.0
12	65	115	90	20	156	7.92 E06	3.0
14	105	161	133	29	207	7.13 E06	4.5
15	127	184	156	34	225	6.60 E06	2.5

SERIAL 334;MIX 8LF;TEMP -17.5; GAGE LENGTH (In.) 4.6815;REMKS

TIME (Sec.)	LVDT DISPLACEMENT (Microinches) L	R	Ave.	STRAIN (MII)	STRESS (PSI)	STIFF-NESS (PSI)	STRAIN RATE ($\dot{\varepsilon}$) (MII/Sec)
2	2	4	3	1	5	8.23 E06	0.5
4	6	8	7	2	25	1.69 E07	0.5
6	18	22	20	4	51	1.19 E06	1.0
8	49	44	46	10	80	8.11 E06	3.0
10	89	85	87	19	113	6.06 E06	4.5
12	138	135	136	29	148	5.09 E06	5.0
14	210	206	208	44	185	4.16 E06	7.5
16	289	287	288	62	223	3.62 E06	9.0

SERIAL 335; MIX 6LF; TEMP 140; GAGE LENGTH (In.) 4.6718; REMKS

TIME (Sec.)	LVDT DISPLACEMENT (Microinches) L	R	Ave.	STRAIN (MII)	STRESS (PSI)	STIFF-NESS (PSI)	STRAIN RATE ($\dot{\varepsilon}$) (MII/Sec.)
2	39776	2777	21276	4554	1.6	3.12 E03	2277.0
4	47776	747	24261	5193	1.6	3.00 E03	319.5
6	52736	1671	27303	5823	1.6	2.69 E02	315.0
8	57437	2151	29794	6377	1.6	2.49 E02	277.0
10	60402	3949	32175	6887	1.5	2.18 E02	255.0
12	63431	5784	34608	7408	1.5	2.02 E02	260.5
14	65168	8789	36979	7915	1.5	1.94 E02	253.5
16	68945	10995	39970	8556	1.5	1.76 E02	320.5
18	72375	13877	43126	9231	1.6	1.72 E02	337.5
20	73884	17582	45733	9789	1.6	1.61 E02	279.0
22	76607	20103	48355	10351	1.6	1.53 E02	281.0
24	79432	23396	51414	11005	1.6	1.46 E02	327.0
26	83179	26980	55080	11790	1.6	1.35 E02	392.5
28	89515	29572	59544	12745	1.6	1.22 E02	477.5
30	93610	37783	65696	14062	1.5	1.08 E02	658.5
32	95743	50502	73123	15652	1.6	1.01 E02	795.0
34	95072	73876	84474	18082	1.6	8.91 E01	1215.0
36	86203	142437	114170	24438	1.6	6.51 E01	3178.0

SERIAL 336;MIX 6LF;TEMP 140; GAGE LENGTH (In.) 4.6982; REMKS______

TIME (Sec.)	LVDT DISPLACEMENT (Microinches) L	R	Ave.	STRAIN (MII)	STRESS (PSI)	STIFF-NESS (PSI)	STRAIN RATE ($\dot{\varepsilon}$) (MII/Sec.)
2	9316	10179	9747	2075	1.3	6.08 E02	1037.5
4	11537	21860	16723	3559	1.4	3.82 E02	742.0
6	-3078	29592	13257	2822	1.4	4.84 E02	-368.5
8	8026	50381	29204	6216	1.6	2.61 E02	1697.0
10	29590	47129	38359	8165	1.7	2.05 E02	974.5
12	42488	44134	43311	9218	1.7	1.81 E02	526.5
14	49604	52439	51021	10860	1.6	4.43 E02	821.0
16	54902	59050	56976	12127	1.6	1.32 E02	633.5
18					0.6		

SERIAL 337;MIX 6LF;TEMP 140; GAGE LENGTH (In.) 4.7015;REMKS

TIME (Sec.)	LVDT DISPLACEMENT (Microinches) L	R	Ave.	STRAIN (MII)	STRESS (PSI)	STIFF-NESS (PSI)	STRAIN RATE ($\dot{\varepsilon}$) (MII/Sec)
2	89883	6359	48121	10235	1.4	1.40 E02	5117.5
4	45523	11804	28663	6097	3.8	6.32 E02	-2069.0
6	53177	16199	34688	7378	1.7	2.29 E02	640.5
8	62428	18874	40651	8646	1.7	1.98 E02	634.0
10	70543	20938	45740	9729	1.7	1.74 E02	541.5
12	83074	21650	52362	11137	1.6	1.46 E02	704.0
14	101274	20536	60905	12954	1.7	1.29 E02	908.5
16	131499	15063	73281	15587	1.7	1.08 E02	1316.5
18					1.6		

SERIAL 338;MIX 6LF;TEMP 140; GAGE LENGTH (In.) 4.6620;REMKS

TIME (Sec.)	LVDT DISPLACEMENT (Microinches) L	R	Ave.	STRAIN (MII)	STRESS (PSI)	STIFF-NESS (PSI)	STRAIN RATE ($\dot{\varepsilon}$) (MII/Sec)
2	32045	28930	30488	6540	1.6	2.46 E02	3270.0
4	33194	37582	35388	7591	1.6	2.10 E02	525.0
6	39673	46940	43307	9289	1.6	1.69 E02	849.0
7					0.5		

SERIAL 339;MIX 8LD;TEMP 140; GAGE LENGTH (In.) 4.6250;REMKS

TIME (Sec.)	LVDT DISPLACEMENT (Microinches) L	R	Ave.	STRAIN (MII)	STRESS (PSI)	STIFF-NESS (PSI)	STRAIN RATE ($\dot{\varepsilon}$) (MII/Sec)
1	20226	-176	10025	2167	-	-	2167.0
2	60920	13479	37199	8043	0.6	6.88 E01	5876.0
4	47705	32120	39912	8630	1.6	1.87 E02	293.5
6	48910	43438	46174	9984	1.6	1.62 E02	677.0
8	53183	56421	54802	11849	1.6	1.37 E02	932.5
10	59910	82669	71290	15414	1.6	1.03 E02	1782.5
11					1.6		

SERIAL 340;MIX 8LD;TEMP 140; GAGE LENGTH (In.) 4.6115;REMKS

TIME (Sec.)	LVDT DISPLACEMENT (Microinches) L	R	Ave.	STRAIN (MII)	STRESS (PSI)	STIFF-NESS (PSI)	STRAIN RATE ($\dot{\varepsilon}$) (MII/Sec)
2	-1739	80184	39222	8505	1.0	1.14 E02	4252.5
4	14640	57018	35829	7770	1.6	2.10 E02	-735.0
6					1.6		

SERIAL 341;MIX 8LD;TEMP 140; GAGE LENGTH (In.) 4.6650; REMKS

TIME (Sec.)	LVDT DISPLACEMENT (Microinches) L	R	Ave.	STRAIN (MII)	STRESS (PSI)	STIFF-NESS (PSI)	STRAIN RATE ($\dot{\varepsilon}$) (MII/Sec)
2	22169	26657	26413	5662	0.8	1.32 E02	2831.0
4	23957	21911	22934	4916	1.6	3.22 E02	-373.0
6	32771	50722	41772	8954	1.6	1.84 E02	2019.0
8					1.6		

SERIAL 342;MIX 8LD;TEMP 140; GAGE LENGTH (In.) 4.7080;REMKS Failed above top yoke, no data.

TIME (Sec.)	LVDT DISPLACEMENT (Microinches) L	R	Ave.	STRAIN (MII)	STRESS (PSI)	STIFF-NESS (PSI)	STRAIN RATE ($\dot{\varepsilon}$) (MII/Sec)

SERIAL 343;MIX 6LD;TEMP 140; GAGE LENGTH (In.) 4.6050;REMKS Load cell not functioning. No load data. Fail @ 40 Sec.

TIME (Sec.)	LVDT DISPLACEMENT (Microinches) L	R	Ave.	STRAIN (MII)	STRESS (PSI)	STIFF-NESS (PSI)	STRAIN RATE ($\dot{\varepsilon}$) (MII/Sec)
5	39256	8686	23971	5205			1041.0
10	42148	14080	28114	6105			180.0
15	43430	19810	31620	6866			152.2
20	45418	25987	35702	7753			177.4
25	46562	33501	40032	8693			188.0
30	47812	42893	45353'	9848			231.0
35	50398	55349	52874	11482			326.8
40	59023	72715	65869	14304			564.4
45	130756	80642	105698	22953			

SERIAL 344;MIX 6LD;TEMP 140;GAGE LENGTH (In.) 4.6398;REMKS Fail at 60 sec.

TIME (Sec.)	LVDT DISPLACEMENT (Microinches) L	R	Ave.	STRAIN (MII)	STRESS (PSI)	STIFF-NESS (PSI)	STRAIN RATE ($\dot{\varepsilon}$) (MII/Sec)
5	32706	30090	31398	6767	1.7	2.47 E02	1353.4
10	17552	21402	19477	4198	1.7	3.98 E02	-513.8
15	17496	22934	20215	4357	1.7	3.89 E02	31.8
20	17494	25338	21416	4616	1.7	3.67 E02	51.8
25	17546	28417	22982	4953	1.7	3.45 E02	67.4
30	17350	32300	24825	5351	1.7	3.18 E02	79.6
35	17300	36254	26777	5771	1.7	2.96 E02	84.0
40	17342	37087	27214	5866	1.7	2.88 E02	19.0
45	17433	46829	32131	6925	1.7	2.51 E02	211.8
50	17417	54429	35923	7742	1.7	2.14 E02	163.4
55	17312	66053	41682	8984	1.7	1.82 E02	248.4
60	15069	93893	54481	11742	1.7	1.46 E02	551.6
63	6667	169932	88299	19031	1.7	8.84 E01	2429.7
65					0.8		

SERIAL 345;MIX 6LD;TEMP 140;GAGE LENGTH (In.) 4.6502; REMKS

TIME (Sec.)	LVDT DISPLACEMENT (Microinches) L	R	Ave.	STRAIN (MII)	STRESS (PSI)	STIFF-NESS (PSI)	STRAIN RATE ($\dot{\varepsilon}$) (MII/Sec)
5	35489	-5988	14750	3172	1.6	5.16 E02	634.4
10	42164	-7822	17171	3693	1.7	4.56 E02	104.2
15	50855	-9447	20704	4452	1.7	3.75 E02	151.8
20	62282	-9519	26382	5673	1.7	2.94 E02	244.2
25	83800	-9023	37389	8040	1.7	2.09 E02	473.4
29	200113	1792	100952	21709	1.8	8.21 E01	3417.2
31					1.0		

SERIAL 346; MIX 6LD; TEMP 140; GAGE LENGTH (In.) 4.6355; REMKS Fail at 25 sec.

TIME (Sec.)	LVDT DISPLACEMENT (Microinches) L	R	Ave.	STRAIN (MII)	STRESS (PSI)	STIFF-NESS (PSI)	STRAIN RATE ($\dot{\varepsilon}$) (MII/Sec)
5	22899	21055	21977	4741	1.6	3.42 E02	948.2
10	24875	31006	27940	6027	1.6	2.66 E02	257.2
15	28583	38457	33520	7231	1.6	2.24 E02	240.8
20	35133	46106	40619	8763	1.6	1.87 E02	306.4
25	52681	53684	53183	11473	1.6	1.43 E02	542.0
30	163930	50086	107008	23085	1.6	7.00 E01	10765.0
32					0.8		

SERIAL 347; MIX 12LD; TEMP 140; GAGE LENGTH (In.) 4.6205; REMKS Scanner not operating properly. No data.

SERIAL 348; MIX 12LD; TEMP 140; GAGE LENGTH (In.) - ; REMKS Failed during rigging. No data.

SERIAL 349;MIX 12LD;TEMP 140;GAGE LENGTH (In.) 4.6168;REMKS

TIME (Sec.)	LVDT DISPLACEMENT (Microinches) L	R	Ave.	STRAIN (MII)	STRESS (PSI)	STIFF-NESS (PSI)	STRAIN RATE ($\dot{\varepsilon}$) (MII/Sec)
2	40437	-22333	9052	1961	1.6	8.32 E02	980.5
4	47043	-18407	14318	3101	1.6	5.20 E02	570.0
6	91242	-26645	32299	6996	1.6	2.28 E02	1947.5
7					0.8		

SERIAL 350;MIX 12LD;TEMP 140;GAGE LENGTH (In.) 4.6442;REMKS

TIME (Sec.)	LVDT DISPLACEMENT (Microinches) L	R	Ave.	STRAIN (MII)	STRESS (PSI)	STIFF-NESS (PSI)	STRAIN RATE ($\dot{\varepsilon}$) (MII/Sec)
2	151146	9185	80166	17261	1.6	9.27 E01	8630.5
4	39739	25029	32384	6973	1.6	2.31 E02	-5144.0
6	42902	35717	39310	8464	1.6	1.91 E02	745.5
8	74007	66955	70481	15176	1.6	1.07 E02	3356.0
9					0.9		

SERIAL 351;MIX 8LF;TEMP 140;GAGE LENGTH (In.)4.5111;REMKS

TIME (Sec.)	LVDT DISPLACEMENT (Microinches) L	R	Ave.	STRAIN (MII)	STRESS (PSI)	STIFF-NESS (PSI)	STRAIN RATE ($\dot{\varepsilon}$) (MII/Sec)
2	91950	33509	62729	13906	1.6	1.13 E02	6953.0
4	19759	29697	24728	5482	1.6	2.93 E02	-4212.0
6	21868	29786	25827	5725	1.6	2.80 E02	121.5
8	26498	30219	28358	6287	1.6	2.50 E02	281.0
10	31345	31420	31383	6957	1.6	2.28 E02	335.0
12	36821	32492	34657	7683	1.6	2.06 E02	363.0
14	43046	33596	38321	8495	1.6	1.88 E02	406.0
16	49978	36080	43029	9540	1.6	1.66 E02	522.5
17					0.7		

SERIAL 352;MIX 8LF;TEMP 140;GAGE LENGTH (In.) 4.4880;REMKS

TIME (Sec.)	LVDT DISPLACEMENT (Microinches) L	R	Ave.	STRAIN (MII)	STRESS (PSI)	STIFF-NESS (PSI)	STRAIN RATE ($\dot{\varepsilon}$) (MII/Sec)
5	67198	-11188	28005	6240	1.6	2.60 E02	1248.0
10	71186	-3409	33888	7551	1.5	2.03 E02	262.2
15	76895	2246	39570	8817	1.6	1.78 E02	253.2
20	89699	12224	50962	11355	1.6	1.40 E02	507.6
22	98275	25005	61640	13734	1.6	1.14 E02	53339.0
24	138043	109623	123833	27592	1.6	5.68 E01	11678.0
25					0.8		

SERIAL 353;MIX 8LF;TEMP 140;GAGE LENGTH (In.) 4.4928;REMKS

TIME (Sec.)	LVDT DISPLACEMENT (Microinches) L	R	Ave.	STRAIN (MII)	STRESS (PSI)	STIFF-NESS (PSI)	STRAIN RATE ($\dot{\varepsilon}$) (MII/Sec)
5	24474	2539	13507	3006	1.7	5.51 E02	601.2
10	38504	3068	20786	4627	1.7	3.58 E02	324.2
15	55423	3019	29221	6504	1.7	2.54 E02	375.4
20	82712	2571	42642	9491	1.7	1.74 E02	597.4
25	146469	-3663	71403	15893	1.7	1.05 E02	1280.4
27					1.6		

SERIAL 354;MIX 8LF;TEMP 140;GAGE LENGTH (In.) 4.4455;REMKS Failed above top yoke, LVDT did not read displ. No data.

SERIAL 355;MIX 8LC;TEMP 140;GAGE LENGTH (In.) 4.4852;REMKS

TIME (Sec.)	LVDT DISPLACEMENT (Microinches) L	R	Ave.	STRAIN (MII)	STRESS (PSI)	STIFF-NESS (PSI)	STRAIN RATE ($\dot{\varepsilon}$) (MII/Sec)
5	-4900	5245	173	38	1.7	4.32 E04	7.6
10	-5013	8327	1657	369	1.6	4.42 E03	66.2
15	-4896	11402	3253	725	1.7	2.28 E03	71.2
20	-4813	13953	4570	1019	1.7	1.64 E03	58.8
25	-4748	16684	5968	1331	1.6	1.23 E03	62.4
30	-4493	21467	8487	1892	1.6	8.62 E03	503.8
35	-12703	40132	13714	3058	1.7	5.41 E03	233.2
37	-23150	72114	24482	5458	1.6	2.94 E03	1200.0
38					0.9		

SERIAL 356;MIX 8LC;TEMP 140;GAGE LENGTH (In.) 4.4892;REMKS

TIME (Sec.)	LVDT DISPLACEMENT (Microinches) L	R	Ave.	STRAIN (MII)	STRESS (PSI)	STIFF-NESS (PSI)	STRAIN RATE ($\dot{\varepsilon}$) (MII/Sec)
5	14167	916	7542	1680	1.6	9.50 E02	336.0
10	14185	3074	8630	1922	1.6	8.18 E02	48.4
15	14444	5063	9753	2173	1.6	7.12 E02	50.2
20	17494	7342	12418	2766	1.6	5.70 E02	118.6
25	26215	11923	19069	4248	1.6	3.72 E02	296.4
28	65174	45147	55160	12287	1.5	1.21 E02	12030.3
29					0.9		

SERIAL 357;MIX 8LC;TEMP 140;GAGE LENGTH (In.) 4.4798;REMKS

TIME (Sec.)	LVDT DISPLACEMENT (Microinches) L	R	Ave.	STRAIN (MII)	STRESS (PSI)	STIFF-NESS (PSI)	STRAIN RATE ($\dot{\varepsilon}$) (MII/Sec)
5	-5698	6624	463	103	1.6	1.53 E04	20.6
10	-4030	10512	3241	723	1.6	2.18 E03	124.0
15	-3391	14530	5569	1243	1.6	1.28 E03	104.0
20	-3343	20131	8394	1874	1.6	8.37 E02	126.2
25	-12368	36732	12182	2719	1.5	5.63 E02	169.0
26	-28243	53607	12682	2831	1.5	5.43 E02	112.0
27					0.8		

SERIAL 358;MIX 8LC;TEMP 140;GAGE LENGTH (In.) 4.4512;REMKS Failed above top yoke. LVDT did not read displ. No data.

SERIAL 359;MIX 8LD;TEMP 14; GAGE LENGTH (In.) 4.5270;REMKS

TIME (Sec)	LVDT DISPLACEMENT (Microinches) L	R	Ave.	STRAIN (MII)	STRESS (PSI)	STIFF-NESS (PSI)	STRAIN RATE ($\dot{\varepsilon}$) (MII/Sec)
900	1234	1015	1124	248	7	2.78 E04	* 0.28
7267	2469	2107	2288	505	31	6.18 E04	0.38
10842	643	622	633	140	77	5.50 E05	-0.34
14471	952	735	844	186	149	8.00 E05	0.04
18108	2048	1782	1915	423	234	1.00 E06	0.05
20716	3122	4676	3899	861	286	3.32 E05	0.04

* Strain rates calculated from times 15 min. prior to these readings.

SERIAL 360;MIX 8LD;TEMP 14; GAGE LENGTH (In.) 4.5222;REMKS

TIME (Sec.)	LVDT DISPLACEMENT (Microinches) L	R	Ave.	STRAIN (MII)	STRESS (PSI)	STIFF-NESS (PSI)	STRAIN RATE ($\dot{\varepsilon}$) (MII/Sec)
972	975	357	666	147	18	1.23 E05	* 0.15
2730	2030	1104	1567	347	50	1.44 E05	0.08
6366	1600	204	902	199	128	6.43 E05	-0.28
9985	3597	1070	2334	516	215	4.16 E05	0.09
13622	8637	2644	5640	1247	289	2.32 E05	0.43

* See note on Serial 359

SERIAL 361;MIX 8LD;TEMP 14; GAGE LENGTH (In.) - REMKS AE exp.

SERIAL 362;MIX 8LD;TEMP 42; GAGE LENGTH (In.) - ;REMKS AE exp.

SERIAL 363; MIX 8HD; TEMP 140; GAGE LENGTH (In.) 4.5658; REMKS ______

TIME (Sec.)	LVDT DISPLACEMENT (Microinches) L	R	Ave.	STRAIN (MII)	STRESS (PSI)	STIFF-NESS (PSI)	STRAIN RATE ($\dot{\varepsilon}$) (MII/Sec)
10	3484	13370	8427	1846	1.6	8.90 E02	184.6
20	6451	16407	11429	2503	1.6	6.45 E02	65.7
30	10843	18617	14730	3226	1.7	5.17 E02	72.3
40	13368	21261	17315	3792	1.6	4.25 E02	56.6
50	16766	24203	20484	4486	1.7	3.75 E02	69.4
60	21811	28561	25186	5516	1.6	2.99 E02	103.0
70	71833	49813	60823	13322	1.7	1.28 E02	780.6
71	88811	66699	77755	17030	1.7	9.86 E02	3708.0
72					0.9		

SERIAL 364; MIX 8HD; TEMP 140; GAGE LENGTH (In.) 4.5610; REMKS ______

TIME (Sec.)	LVDT DISPLACEMENT (Microinches) L	R	Ave.	STRAIN (MII)	STRESS (PSI)	STIFF-NESS (PSI)	STRAIN RATE ($\dot{\varepsilon}$) (MII/Sec)
10	69781	-1072	34354	7532	1.6	2.17 E02	753.2
20	75926	1883	38905	8530	1.7	1.95 E02	99.8
30	80429	5273	42851	9395	1.7	1.79 E02	86.5
40	84825	9610	47251	10352	1.7	1.61 E02	95.7
50	93424	15485	54459	11940	1.7	1.44 E02	158.8
60	137507	20450	78978	-	-		

SERIAL 365; MIX 8HD; TEMP 140; GAGE LENGTH (In.) 4.6230; REMKS

TIME (Sec.)	LVDT DISPLACEMENT (Microinches) L	R	Ave	STRAIN (MII)	STRESS (PSI)	STIFF-NESS (PSI)	STRAIN RATE ($\dot{\varepsilon}$) (MII/Sec)
10	13245	7366	10305	2229	1.8	7.84 E02	222.9
20	16454	8995	12275	2752	1.8	6.37 E02	52.3
30	18588	10194	14391	3113	1.8	5.68 E02	36.1
40	20618	11154	15886	3436	1.8	5.18 E02	32.3
50	22840	12022	17431	3771	1.8	4.74 E02	33.5
60	25427	12928	19177	4148	1.7	4.16 E02	37.7
70	28549	13828	21188	4583	1.7	3.80 E02	43.5
80	33283	14415	23849	5159	1.8	3.48 E02	57.6
85	38955	14278	26616	5757	1.7	2.99 E02	119.6
86					1.4		

SERIAL 366; MIX 8HD; TEMP 140; GAGE LENGTH (In.) 4.6090; REMKS

TIME (Sec.)	LVDT DISPLACEMENT (Microinches) L	R	Ave.	STRAIN (MII)	STRESS (PSI)	STIFF-NESS (PSI)	STRAIN RATE ($\dot{\varepsilon}$) (MII/Sec)
20	19866	7830	13848	3004	1.7	5.60 E02	150.2
40	24161	9762	16962	3680	1.7	4.57 E02	33.8
60	29166	11174	20170	4376	1.7	3.91 E02	34.8
80	36645	12020	23832	5171	1.6	3.17 E02	39.8
100	45579	12351	28965	6284	1.7	2.75 E02	55.6
120	63433	12563	37998	8244	1.8	2.12 E02	98.0
139					1.7		

SERIAL 367;MIX 12HD;TEMP 14; GAGE LENGTH (In.) - ;REMKS AE exp.

SERIAL 368;MIX 12HD;TEMP 30; GAGE LENGTH (In.) - ;REMKS AE exp.

SERIAL 369;MIX 12HD;TEMP - ; GAGE LENGTH (In.) - ; REMKS AE exp.

SERIAL 370;MIX 12HD;TEMP - ; GAGE LENGTH (In.) - ; REMKS AE exp.

SERIAL 371; MIX 6HD; TEMP 140; GAGE LENGTH (In.) 4.6472; REMKS

TIME (Sec.)	LVDT DISPLACEMENT (Microinches) L	R	Ave.	STRAIN (MII)	STRESS (PSI)	STIFF-NESS (PSI)	STRAIN RATE ($\dot{\varepsilon}$) (MII/Sec)
10	33604	2511	18058	3886	1.6	4.03 E02	388.6
20	46231	3590	24910	5360	1.6	3.03 E02	147.4
30	51330	5838	28584	6151	1.6	2.60 E02	79.1
40	56948	7972	32460	6985	1.8	2.52 E02	83.4
50	63033	10603	36818	7922	1.7	2.19 E02	93.7
60	70881	14230	42555	9157	1.7	1.90 E02	123.5
70	76508	21911	49210	10589	1.8	1.67 E02	143.2
80	62193	47949	55071	11850	1.8	1.56 E02	126.1
86					1.8		

SERIAL 372; MIX 6HD; TEMP 140; GAGE LENGTH (In.) 4.6368; REMKS

TIME (Sec.)	LVDT DISPLACEMENT (Microinches) L	R	Ave.	STRAIN (MII)	STRESS (PSI)	STIFF-NESS (PSI)	STRAIN RATE ($\dot{\varepsilon}$) (MII/Sec)
20	-7771	10636	1433	309	1.6	5.13 E03	15.4
40	-9365	9519	77	17	1.7	9.97 E04	-14.6
60	-8869	8995	63	14	1.7	1.26 E05	-0.2
80	-4331	8353	2011	434	1.6	3.73 E03	21.0
100	11571	7846	9708	2094	1.7	7.91 E02	83.0
113	141274	-4050	68612	14797	1.6	1.06 E02	977.1
115					0.7		

SERIAL 373; MIX 6HD; TEMP 140; GAGE LENGTH (In.) 4.6488; REMKS

TIME (Sec.)	LVDT DISPLACEMENT (Microinches) L	R	Ave.	STRAIN (MII)	STRESS (PSI)	STIFF-NESS (PSI)	STRAIN RATE ($\dot{\varepsilon}$) (MII/Sec)
20	34543	-551	16996	3656	1.7	4.77 E02	182.8
40	51098	-664	25217	5424	1.8	3.32 E02	88.7
60	72494	-920	35787	7698	1.8	2.31 E02	113.7
80	94774	1667	48221	10373	1.8	1.76 E02	133.8
96	192085	-9526	91279	19635	1.8	9.44 E01	578.9
99					1.1		

SERIAL 374; MIX 6HD; TEMP 140; GAGE LENGTH (In.) 4.6368; REMKS

TIME (Sec.)	LVDT DISPLACEMENT (Microinches) L	R	Ave.	STRAIN (MII)	STRESS (PSI)	STIFF-NESS (PSI)	STRAIN RATE ($\dot{\varepsilon}$) (MII/Sec)
25	44330	-2289	21020	4533	1.7	3.80 E02	181.3
50	56572	-3174	26699	5758	1.7	2.96 E02	49.0
75	72179	-4817	33681	7264	1.8	2.43 E02	60.2
100	83450	-5790	38830	8374	1.6	1.96 E02	44.4
125	95515	-6575	44470	9591	1.7	1.78 E02	48.7
150	110481	-7790	51345	11074	1.8	1.62 E02	59.3
175	133139	-10785	61177	13194	1.7	1.30 E02	84.8
200	175022	-16571	79225	17086	1.7	9.92 E01	155.7
* 205	198358	-18668	89845	19377	1.7	8.87 E01	458.2
213					0.9		

* Exceeded linear range of LVDT; call 205 sec. failure.

SERIAL 375; MIX 8HD; TEMP 140; GAGE LENGTH (In.) 4.4592; REMKS

TIME (Sec.)	LVDT DISPLACEMENT (Microinches) L	R	Ave.	STRAIN (MII)	STRESS (PSI)	STIFF-NESS (PSI)	STRAIN RATE ($\dot{\varepsilon}$) (MII/Sec)
25	10034	9620	9827	2204	1.6	7.08 E02	88.2
50	18062	11463	14762	3311	1.8	5.54 E02	44.3
75	31479	11844	21661	4858	1.8	3.80 E02	61.9
100	49705	10753	30229	6779	1.8	2.61 E02	76.8
125	88797	5057	46927	10523	1.8	1.69 E02	149.8
140	172318	-9037	81641	18308	1.8	9.65 E01	519.0
142	193527	10056	91735	20572	1.8	8.80 E01	1132.0
143					1.8		

SERIAL 376; MIX 8HD; TEMP 140; GAGE LENGTH (In.) 4.5060; REMKS Failed above top yoke. No data

SERIAL 377; MIX 8HD; TEMP 140; GAGE LENGTH (In.) 4.5122; REMKS

TIME (Sec.)	LVDT DISPLACEMENT (Microinches) L	R	Ave.	STRAIN (MII)	STRESS (PSI)	STIFF-NESS (PSI)	STRAIN RATE ($\dot{\varepsilon}$) (MII/Sec)
50	20808	-9519	5645	1251	1.7	1.32 E03	25.0
100	28781	-8472	10155	2250	1.7	7.74 E02	20.0
150	36866	-8627	14120	3129	1.8	5.59 E02	17.6
200	39022	-8900	15061	3338	1.7	5.22 E02	4.2
250	41527	-9312	16107	3570	1.7	4.85 E02	4.6
300	38567	29549	34058	7548	1.7	2.22 E02	79.6
305	58996	66213	62590	13871	1.7	1.20 E02	1264.6
306					0.9		

SERIAL 378;MIX 8HD;TEMP 140; GAGE LENGTH (In.) 4.5085; REMKS

TIME (Sec.)	LVDT DISPLACEMENT (Microinches) L	R	Ave.	STRAIN (MII)	STRESS (PSI)	STIFF-NESS (PSI)	STRAIN RATE ($\dot{\varepsilon}$) (MII/Sec)
25	4079	7411	5745	1274	1.6	1.26 E03	51.0
50	6944	9689	8317	1845	1.6	8.89 E02	22.8
75	11935	13154	12544	2782	1.7	6.13 E02	37.5
100	15605	20466	18036	4000	1.7	4.23 E02	48.7
115	16365	61815	39090	8670	1.7	1.96 E02	311.3
116					1.0		

SERIAL 379;MIX 12HD;TEMP 140; GAGE LENGTH (In.) 4.6092; REMKS

TIME (Sec.)	LVDT DISPLACEMENT (Microinches) L	R	Ave.	STRAIN (MII)	STRESS (PSI)	STIFF-NESS (PSI)	STRAIN RATE ($\dot{\varepsilon}$) (MII/Sec)
5	56066	-6597	24704	5360	1.7	3.10 E02	1072.0
10	76480	-7471	34505	7486	1.7	2.25 E02	425.2
15	87549	-5096	41227	8944	1.7	1.87 E02	291.6
20	99842	-3007	48418	10504	1.6	1.57 E02	312.0
25	109724	2248	55986	12146	1.7	1.40 E02	328.4
30	122642	8177	65409	14191	1.7	1.18 E02	409.0
35	145021	12232	78627	17058	1.6	9.68 E01	573.4
39	202119	6946	104532	22679	1.7	7.53 E01	1405.2
42					0.9		

SERIAL 380; MIX 12HD; TEMP 140; GAGE LENGTH (In.) 4.6222; REMKS

TIME (Sec.)	LVDT DISPLACEMENT (Microinches) L	R	Ave.	STRAIN (MII)	STRESS (PSI)	STIFF-NESS (PSI)	STRAIN RATE ($\dot{\varepsilon}$) (MII/Sec)
10	35816	4791	20304	4393	1.8	3.98 E02	439.3
20	36199	8942	22570	4883	1.8	3.63 E02	49.0
30	38761	13079	25920	5608	1.8	3.27 E02	72.5
40	43460	26811	35136	7601	1.8	2.35 E02	199.3
44	5088	72217	38653	8362	1.7	2.07 E02	190.2
45					1.0		

SERIAL 381; MIX 12HD; TEMP 140; GAGE LENGTH (In.) 4.6378; REMKS

TIME (Sec.)	LVDT DISPLACEMENT (Microinches) L	R	Ave.	STRAIN (MII)	STRESS (PSI)	STIFF-NESS (PSI)	STRAIN RATE ($\dot{\varepsilon}$) (MII/Sec)
10	17116	11578	14347	3093	1.8	5.76 E02	309.3
20	25237	16446	20841	4494	1.8	3.98 E02	140.1
30	25975	26429	26202	5650	1.8	3.18 E02	115.6
40	26555	35243	30899	6663	1.9	2.84 E02	101.3
45	46433	43807	45120	9729	2.0	2.00 E02	613.2
46	68317	53432	60874	13126	2.0	1.52 E02	3397.0
47					1.1		

SERIAL 382;MIX 12HD;TEMP 140; GAGE LENGTH (In.) 4.6438; REMKS

TIME (Sec.)	LVDT DISPLACEMENT (Microinches) L	R	Ave.	STRAIN (MII)	STRESS (PSI)	STIFF-NESS (PSI)	STRAIN RATE ($\dot{\varepsilon}$) (MII/Sec)
10	8331	7582	7957	1410	1.7	1.22 E03	141.0
20	10556	8183	9369	1660	1.8	1.09 E03	25.0
30	15502	8940	12221	2165	1.7	7.85 E02	50.5
40	22027	10048	16038	2842	1.7	6.12 E02	67.7
50	36049	11685	23867	4229	1.8	4.32 E02	138.7
58	89422	16974	53198	9426	1.8	1.92 E02	649.6
59					1.0		

APPENDIX E

Asphalt Concrete Tension Specimen Failure Surfaces

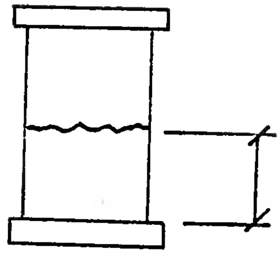

A denotes above top yoke

B denotes below bottom yoke

FAILURE SURFACES

Temp	Cell	Serial	H	Remarks
-17.5	1	303	B	
"	"	304	B	
"	"	305	B	
"	"	306	B	
-17.5	A	264	B	
"	"	265	B	
"	"	266	B	
"	"	267	B	
-17.5	2	307	B	
"	"	308	B	
"	"	309	B	
"	"	310	B	
-17.5	8	331	B	
"	"	332	B	
"	"	333	B	
"	"	334	B	
-17.5	4	315	B	
"	"	316	B	
"	"	317	1	
"	"	318	B	
14.0	B	262	B	
"	"	255	$3\frac{1}{4}$	
"	"	256	$2\frac{1}{2}$	
"	"	257	$1\frac{1}{2}$	
"	"	258	-	At top yoke
"	"	254	A	
"	"	261	A	
"	"	260	2	
45.5	C	242	$2\frac{1}{2}$	
"	"	244	$2\frac{1}{2}$	
"	"	243	$2\frac{1}{2}$	
"	"	243	1	
"	"	247	-	

Temp	Cell	Serial	H	Remarks
77.0	G	279	3	
"	"	280	-	At bott yoke
"	"	281	2	
"	"	282	2	
77.0	I	295	2	
"	"	296	2	
"	"	297	2½	
"	"	298	2¼	
77.0	D	268	3	
"	"	269	2	
"	"	271	2	
"	"	239	2½	
"	"	272	2	
"	"	238	1	
"	"	274	2	
"	"	270	2	
"	"	273	2	
"	"	240	B	
"	"	241	2½	
77.0	F	275	2½	
"	"	276	2 3/4	
"	"	277	3 1/4	
"	"	278	B	
77.0	H	283	2½	
"	"	284	-	At bott yoke
"	"	285	2	
"	"	286	2½	
77.0	J	299	2	
"	"	300	1½ - 2¼	
"	"	301	2¼	
"	"	302	3½	
77.0	K	287	2	
"	"	288	2	
"	"	289	2	
"	"	290	B	
77.0	L	291	2¼	
"	"	292	2½	
"	"	293	13/4 - 3	
"	"	294	2	

Temp	Cell	Serial	H	Remarks
108.5	6	323	2	
"	"	324	2½	
"	"	325	2½	
"	"	326	2	
108.5	E	246	2½	
"	"	248	2½	
"	"	251	A	
108.5	7	327	2 - 2½	
"	"	328	2½	
"	"	329	2	
"	"	330	2½	
108.5	3	311	1/2	
"	"	312	5	
"	"	313	2 & ½	
"	"	314	-	At bott yoke
108.5	5	319	2	
"	"	320	3½	
"	"	321	½	
"	"	322	1	

VITA

VITA

Raymond Doran Pavlovich was born July 14, 1934 near Rocky Point, Wyoming. He attended elementary schools at Lead, South Dakota, Edgemont, South Dakota, and Gillette, Wyoming, and completed High School at Gillette, Wyoming.

After graduation from High School in 1952, he served with the United States Marine Corps in Korea and received an honorable discharge.

He entered the University of Wyoming and received the Bachelor of Science, with honors in Civil Engineering in 1959 and began work with consulting engineering firms practicing throughout the Rocky Mountain States. He returned to the University of Wyoming as a research associate in highway pavements and completed the requirements for a Master's degree in 1965.

In February of 1967, the author came to Purdue University to pursue his studies toward the Ph.D. in civil engineering materials.

He has several published papers and engineering reports to his credit that have been presented to road conferences and to engineering clients.

The author is currently registered as a professional engineer in Indiana and as a professional engineer and land

surveyor in Wyoming and presently is a member of the American Society for Testing and Materials and the Transportation Research Board.

He is married and has three children.

COVER DESIGN BY ALDO GIORGINI